2024

Identifying and quantifying pelagic organisms around seamounts, atolls, and islands in the Chagos Archipelago in relation to local oceanographic processes

Eager, Dannielle Sophie

UNIVERSITY OF
PLYMOUTH

Identifying and quantifying pelagic organisms around seamounts, atolls, and islands in the Chagos Archipelago in relation to local oceanographic processes

by

Dannielle Sophie Eager

A thesis submitted to the University of Plymouth

in partial fulfilment for the degree of

DOCTOR OF PHILOSOPHY

School of Biological and Marine Sciences

September 2023

Acknowledgments

The past 4 years working on this thesis have sped by. Without the wonderful support of my supervisors, colleagues, friends, and family I would not have been able to complete this thesis. My words here will never convey my true gratitude to all that have helped me on this journey but I'm going to give it a try.

Firstly, my biggest thank you is to my Director of Studies, Dr Clare Embling. Clare you somehow believed in me back when I was completing my undergraduate dissertation and have helped me continue my studies throughout this degree. You are a wonderful force of nature with your multitudes of projects and scale of knowledge, but your continued support, encouragement and mentorship makes you the kindest and understanding supervisor anyone could have ever wished for.

To Dr Phil Hosegood, thank you for all your support and guidance on the cruises where I had no idea what was going on sometimes. Your leadership and perseverance during unpredictable and testing times at sea were greatly appreciated and without you this project and dataset would not exist. I remember back in your taught OS201 lectures videos of Chagos and your talks of your earlier cruises, I feel incredible grateful to have experienced Chagos and all your oceanographic knowledge, thank you!

It took traveling to the USA to finally meet in person for more than a few hours, but I couldn't have done this without you Dr Benjamin Williamson. Thank you for putting up with dodgy zoom connections and long emails from me trying to figure out all my technical troubles. Your support and advice throughout this project has been invaluable and one day I will get up to Thurso to see you!

Without the funding from the Bertarelli Foundation and Garfield Weston Foundation this project would not have existed- thank you for funding this work package and the overall project.

Thank you to Ted, Joanna and Clara- you have all been an immense support helping with the cruises, discussing ideas and drinking cocktails. Ted- as Clare phrased it, thank you for being the oceanographic glue that holds us all together, you have the patience of a saint! To everyone in the office who has kept morale up through this project Kat, Isha, Harvey, and everyone else, thank you I owe you all a lot of chocolate! Thank you to everyone who helped in any way, shape, or form- Nicola, Adam, Tom, Peter, Elaine, Jenny, the crew of the Tethys Supporter and all the colleagues I have been fortunate enough to meet.

I could not have done any of this without the support of my friends and family. I am 90% sure you still don't fully know what I do but I am grateful for your questions, engagement with my work and support of my career, it means the world to me. To my parents Chris and Julie and my sisters Amy and Kayleigh (Kaos) thank you for your endless distractions and entertainment. To my Grandparents Jean, Laurie, Gina and John, thank you for all your love and care- I know I would be told off if I didn't include your names so there you go!

Finally, my biggest thanks and appreciation must go to my wonderful partner Louis who has been by my side throughout this whole process. Your unwavering love and support has sometimes been the only thing driving me to continue throughout this PhD and I could not have completed it without you. Thank you for every dinner, every hug, every adventure, and everything you have done for me that I may not have noticed. Now let's have a holiday!

Author's Declaration

At no time during the registration for the degree of Doctor of Philosophy has the author been registered for any other University award without prior agreement of the Doctoral College Quality Sub-Committee.

Work submitted for this research degree at the University of Plymouth has not formed part of any other degree either at the University of Plymouth or at another establishment.

This study was financed with the aid of a studentship from the Garfield Weston Foundation and carried out in collaboration and funding from the Bertarelli Foundation, University of the Highlands and Islands and Zoological Society of London.

The identification of plankton samples presented in Chapter 4 using the FlowCam was completed by Jennifer Devaney, a masters student at the University of Plymouth and was supervised by Elaine Fileman from Plymouth Marine Laboratory.

The collection of oceanographic data and the initial import and cleaning of the data was conducted by Edward Robinson, a PhD student studying the oceanographic regime in the Chagos Archipelago.

Multibeam bathymetry presented in all Chapters was collected and processed by Adam Bolton.

The work conducted on the MITgcm model to produce the values and figure of modelled vertical velocities in Chapter 3 was completed by Natalyia Stashchuk.

Relevant scientific conferences and meetings were regularly attended, at which work was presented and work is currently underway to prepare scientific papers from Chapters 2-4.

Taught modules attended:

- MAR513 Research Skills and Methods: 79.74 %
- MAR514 Marine Science: 70.4 %
- Species Distribution Modelling using R (PR Statistics) February 2022

Cruise participation:

- MV Tethys Supporter, Chagos Archipelago. March-April 2020, cruise ref: MV Tethys Supporter, GWF-BF Cruise No. 2.
- MV Tethys Supporter, Chagos Archipelago. March- April 2022, cruise ref: MV Tethys Supporter, GWF-BF Cruise No. 3.

Publications and cruise reports:

- Hays, G.C., Koldewey, H.J., Andrzejaczek, S., […], **Eager, D.S**., *et al*. (2020) 'A review of a decade of lessons from one of the world's largest MPAs: conservation gains and key challenges', *Mar Biol,* 167(159). Available at: https://doi.org/10.1007/s00227-020-03776-w (Accessed: 19 November 2020).
- Hosegood. P., Arber, P., Diaz. C., **Eager, D.,** Foster, N.L., Harris, J., Murray, P. and Robinson, E. (2020) *Cruise Report: MV Tethys Supporter, GWF-BF Cruise No. 2, Gan –Victoria, 5th–22ndMarch 2020, Conservation Strategies for Biodiversity Hotspots and Safe Havens in a Changing Climate: Oceanographic Drivers of Ecosystem Variability in the Chagos Archipelago.* Available on request.

Oral presentations at conferences:

- **Eager D.S,** Robinson, E., Hosegood, P., Williamson, B.J. and Embling, C.B. (2023) 'Fish responses to regional and sub-mesoscale flow-topographic interactions

over a tropical seamount, *ICES Fisheries and Plankton Acoustic Symposium.* Maine (USA), 27-30 March.

- **Eager D.S,** Robinson, E., Stashchuk, N., Vlasenko, V., Hosegood, P., Williamson, B.J. and Embling, C.B. (2022) 'Fine-scale oceanographic drivers of pelagic biomass around a tropical coral atoll within the Chagos Archipelago Marine Protected Area', *ICES Annual Science Conference.* Dublin (Ireland), 19-22 September.
- **Eager D.S,** Robinson, E., Hosegood, P., Williamson, B.J. and Embling, C.B. (2022) 'Changes in fish aggregations in relation to oceanographic processes around a tropical seamount', *Challenger Society Conference.* London (UK), 6-8 September.
- **Eager, D.S.,** Robinson, E., Harris, J. and Diaz, C. (2021) 'Biodiversity hotspots: a multidisciplinary study of a protected tropical marine ecosystem', *Ocean Decade: Virtual Early Career Ocean Professional Day.* 1 June.
- **Eager, D.S.,** Robinson, E., Hosegood, P., Williamson, B. and Embling, C.B. (2021) 'Oceanographic drivers of fish behaviour around Sandes seamount within the Chagos Archipelago', *MBA 17th Annual Postgraduate conference.* Virtual conference at Exeter (UK), 12-14 April.

Conference posters:

- **Eager D.S,** Diaz, C., Harris, J., Robinson, E., Foster, N., Embling, C.B., Stevens, G., Howell, K., Williamson, B.J. and Hosegood., P. (2022) 'Biodiversity hotspots: a multidisciplinary study of a protected tropical ecosystem, *Challenger Society Conference.* London (UK), 6-8 September.
- **Eager D.S,** Robinson, E., Hosegood, P., Williamson, B.J. and Embling, C.B. (2021) 'Seamounts as refuges: A case study of climate driven oceanographic events and

the effects on fish in the Indian Ocean', *PlymSEF Climate Conference.* Plymouth (UK), 27 October.

Awards and grants:

- Best Overall Presentation at the ICES ASC 2022. *Press release: https://www.ices.dk/news-and-events/news-archive/news/Pages/ASCaward22.aspx*
- PlymSEF Travel Grant 2022 £400
- Marine Biological Association 17th Annual Postgraduate conference 2021 - Best Overall Presentation, Best Session Presentation and Audience Award
- Winner of ASL Environmental Sciences 5th annual early career researcher AZFP contest 2020. *Press Release: https://aslenv.com/assets/files/ASL-AZFP-Award-Winner-2020.pdf*

Word count of main body of thesis: ~ 38,400

Signed .....

Date 29/09/2023.....

Abstract

Identifying and quantifying pelagic biomass around seamounts, atolls, and islands in the Chagos Archipelago in relation to local oceanographic processes

Dannielle S. Eager

Topographic features, such as seamounts and atolls, are commonly identified as biodiversity hotspots that are key areas of productivity in an otherwise oligotrophic Indian Ocean. Whilst these sites of increased biomass are frequently identified, the oceanographic drivers that underpin the spatiotemporal distributions of biomass are not. If effective conservation measures are to be continued and implemented in regions such as the Chagos Archipelago Marine Protected Area (MPA) then the spatial variability of biomass and the physical drivers must be elucidated. This study presents case studies at Sandes seamount and Egmont atoll in the Chagos Archipelago identifying the distributions and behavioural responses of pelagic biota to oceanographic processes. Multifrequency fisheries acoustics data was combined with synoptically collected oceanographic sensor data to determine the oceanographic drivers of pelagic biota. In-situ sampling was also conducted to determine the composition of species over topographic features. Both regional and fine-scale physical processes were identified driving the distribution of biological aggregations over the different topographic features in the Chagos Archipelago. Around Sandes seamount, a joint climatic-oceanographic event, the Indian Ocean Dipole (IOD), affected sea surface temperatures and current velocities causing the deepening of the thermocline. This dramatically reduced the number of schooling fish over the summit of Sandes seamount re-distributing schools into deeper water around the flanks of the seamount. Analysis of the plankton distributions at Sandes seamount also highlighted the role of the thermocline in

aggregating biota. At Egmont atoll, flow-topography interactions dictated the spatial distribution of schooling fish, with canyons and lagoons influencing fish behaviour. This research emphasises the biological importance of seamounts and atolls in the Chagos Archipelago. Understanding the spatial variability of biota around topographic features is vital to improve the efficiency and efficacy of marine spatial plans. By recognizing the behavioural responses of pelagic fish and plankton to oceanographic processes in the Chagos Archipelago this work can contribute to a wider understanding of biophysical interactions around topographic features globally.

Table of Contents

List of figures

List of tables

Chapter 1: A review of oceanographic drivers and the detection of biological aggregations in the Chagos Archipelago

1.1 Introduction

The pelagic realm is a vast environment harbouring a diverse array of organisms that adopt a range of behaviours that can be influenced by local and regional oceanographic processes. Behaviours can change based on a range of biological needs such as reproduction, foraging and predator avoidance. Biological behavioural mechanisms such as schooling, diel vertical migration and swimming movements are employed by pelagic species as survival strategies (Castro and Huber, 2010). When coupled with oceanographic processes, pelagic organisms change their foraging behaviour to exploit turbulent flow movements (Liao, 2007), flow-topographic interactions (Genin, 2004; Pitcher and Bulman, 2007) and oceanic flows (Pineda, 1994). These interactions have been identified globally in a range of environments including around islands in the Atlantic Ocean (Hernández-Léon *et al.,* 2001), banks in the Celtic Sea (Embling *et al.,* 2013) and seamounts in the Chagos Archipelago (Hosegood *et al.,* 2019).

This review considers pelagic fish and plankton behaviour within the Chagos Archipelago, in the central Indian Ocean. The Chagos Archipelago is a 640,000 km^2 marine protected area (MPA) that is home to a variety of threatened and endangered species (Figure 1.1; Koldewey *et al.*, 2010; Sheppard *et al.,* 2013). Situated in the central Indian Ocean it undergoes a variety of tidal, wind and current variations over multiple timescales (Sheppard *et al.,* 1999). This region is of particular interest due to its pristine nature allowing natural processes to be investigated in an area relatively free of anthropogenic impacts (Readman *et al*., 2013). Combining knowledge of the regional and local oceanographic processes with pelagic biota behaviour, allows the drivers of

biological aggregations and distributions to be investigated. These links allow specific conservation plans to be implemented globally using knowledge of the oceanographic properties that drive biological aggregations. Furthermore, by developing a baseline understanding of oceanographic measurements in a region, effects of climate change can be measured, especially in areas with climate-driven oceanography.

This review will explore research conducted on pelagic biota behaviour and oceanography, focussing on how these mechanisms occur in the Chagos Archipelago. A significant body of work already exists in this region with particular focus on corals (Sheppard *et al.,* 1999; Sheppard *et al.,* 2013; Hays *et al.,*2020), turtles (Hays *et al.,* 2014; Esteban *et al.,* 2018) and sharks (Tickler *et al.,* 2017; Hosegood, *et al*., 2019; Jacoby *et al.,* 2020). Looking to draw on these conclusions and apply them to a more diverse range of pelagic species this assessment will link them to oceanographic processes measured for the first time in the region in 2015 (Hosegood *et al.,* 2019). The review is structured with an introduction into the pelagic realm and global biota behaviours before looking at the geographical region of the Chagos Archipelago. Considerations of both the regional and mesoscale processes that occur around the Archipelago are made before identifying flow-topographic interactions within it. Further thought is then given on the detection of biological and physical processes using acoustic tools. This review continues with a detailed discussion of the gaps in the field of knowledge of the oceanographic drivers of pelagic biota distributions and behaviours in the Chagos Archipelago and its

global implications. Finally, an overview of the aims of this thesis are presented along with the structure of the following chapters.

Figure 1.1: Map of the Chagos Archipelago in the context of the Indian Ocean (Dunne *et al.,* 2014; Google, 2019).

1.2 The pelagic realm

Oceans form 70% of the planet with the pelagic realm consisting of the whole water column where water is not constrained by the seafloor or a coastal region (Castro and Huber, 2010). These huge bodies of water play a significant role in global climate, food, and processes such as the carbon and nitrogen cycles (Castro and Huber, 2010; Pauly *et al.,* 2002). With different physical and chemical properties, the pelagic realm can be divided into different depth regions which support a range of different organisms. The

most biologically abundant and smallest region is the epipelagic zone, defined as the surface to 200m depth (Miller and Wheeler, 2012). Within this region is the photic zone which is the maximum depth light can penetrate where photosynthetic organisms thrive. Over the continental shelf the upper 200 m of the water column is referred to as the neritic zone whereas over the continental slope and abyssal plain it is the oceanic epipelagic region (Castro and Huber, 2010); here is where this research is focussed.

1.2.1 Pelagic organisms

Within the pelagic realm locating food can be difficult for organisms due to the vast open environment. For phytoplankton it is vital they remain in the photic zone for photosynthesis and for zooplankton, epipelagic fish, and larger organisms they must be able to relocate depending on the availability of food sources. To achieve this, pelagic organisms must be able to control their buoyancy with organisms using a variety of techniques to stay afloat. Depending on the species, body shape, lipids, floats, and spines can be ultilised for buoyancy (Castro and Huber, 2010). The storage of lipids can increase the buoyancy of an organism as is seen in some cartilaginous fish (Phleger, 1998). These types of fish and many other active species, such as tuna, have under-developed or no swimbladder (Rasmussen and Arnason, 1999). Swimbladders are typically found in most osteichthyes and are a gas filled bladder that aids the buoyancy of a fish (Rasmussen and Arnason, 1999). The swimbladder must be regulated by the individual as it moves throughout the water column due to the expansion and reduction of gas under pressure (Boyle's law; West, 1999). Other methods to achieve buoyancy for both plankton and fish species is through swimming or propulsion techniques and by controlling the internal ion composition of bodily fluids (Castro and Huber, 2010).

To balance the need to forage and avoid predation, some species undergo diel vertical migration (DVM) which is the vertical mass movement of most fish, cephalopods, and crustaceans in the micronekton community (2-10 cm) and zooplankton at specific times (Neilson and Perry, 1990; Brodeur *et al.*, 2005a). The micronekton community are an important link between plankton and apex predators within the food web (Annasawmy *et al.,* 2020). They can vertically migrate 100's of metres from depth (300-500m) to the surface waters (Badcock and Merrett, 1967; Cascão *et al.*, 2019). Drivers of DVM include foraging for prey, thermoregulation, navigation and avoidance of hypoxic conditions and predators (Campana *et al.,* 2011). Micronekton and zooplankton can undertake any of the three forms of DVM which are nocturnal (Yang *et al.,* 2013), reversed (Hutchinson, 1967) and twilight (Valle-Levinson *et al.*, 2014). Nocturnal DVM is the most common form having been observed worldwide and is thought to be triggered by light. As dusk occurs the reduction in light reduces the chances of being visually observed by predators making it safer for micronekton to migrate to the upper surface layers (Brierley, 2014). This theory of predator avoidance has been tested using copepods caged off and integrated with their natural fish predators in an open environment (Bollens and Frost, 1989). Open water copepods underwent nocturnal DVM movements, unlike their caged counterparts who showed no specific vertical movements suggesting copepod behavioural responses are due to visual predator avoidance stimuli (Bollens and Frost, 1989). Further support for the predator avoidance theory is the increase in descent speeds of the sound scattering layer suggesting that as light increases organisms must vertically migrate downwards quicker to avoid predation in the surface waters (Bianchi and Mislan, 2015; Yang *et al.*, 2019).

Predator-avoidance, however, is not the only reason to undertake DVM with fish shown to detect and actively avoid hypoxic conditions (Howell and Simpson, 1994; Wannamaker and Rice, 2000; Zhang *et al.,* 2009). With increased oxygen levels usually observed in shallower pelagic regions biota may have to migrate out of deeper oxygen deficient waters for respiration (Klevjer *et al.*, 2016; Annasawmy *et al.,* 2018). In-situ measurements around a seamount in the Chagos Archipelago measured the depth of the deep chlorophyll maximum to be between 60 and 70 m correlating with the depth of the pycnocline, where dissolved oxygen concentrations were reduced (Hosegood *et al*., 2019). This led to the hypothesis that zooplankton must vertically migrate above the seamount summit to not only feed on phytoplankton in the surface waters during the night, but also to benefit from the increased oxygen concentrations in the surface waters (Hosegood *et al*., 2019).

The pelagic environment can be challenging for individual fish due to predation, foraging and swimming against strong currents. However, many fish species benefit from turbulent flows: defined as chaotic velocity fluctuations that cause mixing in the water column (Warhaft, 1997; Liao, 2007). There are three mechanisms that individual fish can employ to benefit from turbulent flows: station holding, selective locomotion and enhanced predation. Station holding occurs when fish actively exploit the velocity vortices produced by increased turbulence to provide momentum when swimming (Webb, 1989). With the additional momentum from turbulence and reduced muscle activity it can enhance the feeding success rate of fish by improving their locomotion (Liao, 2007). If turbulence is too high the locomotive ability of fish can be overwhelmed as tested with herring larvae (Utne-Palm and Stiansen, 2001). When turbulence of over $8x10^{-6}$ Wkg^{-1} occurred, attack rates on prey were reduced (Utne-Palm and Stiansen,

2001). However, it must be noted that both larval size and light also had significant effects on reducing the attack rate of larvae along with turbulence (Utne-Palm and Stiansen, 2001). Alternatively, in turbulent flows fish can hold station and allow the advection of nutrients and prey brought with the currents to travel towards them, reducing their energy expenditure (Porteiro and Sutton, 2007).

Another advantageous behaviour for fish is to aggregate. This can occur for a variety of reasons such as defence against predators, foraging, shelter, and reproduction (Robert *et al.,* 2013). Fish can group in two different ways: shoaling and schooling. Social bonds usually hold shoaling fish together in an uncoordinated manner (Pitcher, 1998), whereas schooling fish swim as a compact group with coordinated movements and similar sized individuals (Pitcher, 1983). There are two mechanisms that contribute to the aggregation of fish: attraction and retention (Robert *et al.,* 2013). Attraction is where there is a sudden increase in individuals over a short period of time whereas retention is the constant influx of a few fish over a long period (Ame *et al.,* 2006; Girard *et al.,* 2004; Robert *et al.,* 2013). Both processes can be caused by a mutual attraction between individuals or an environmental stimulus (Robert *et al.,* 2013). Although shoals can provide protection from predators, the tight, organised nature of schools optimise foraging, hydrodynamic activity, and protection from predators (Noda *et al.,* 2016). This forms the basis of the hydrodynamic hypothesis, which states that fish may increase their locomotive efficiency by swimming in schools (Belyaev and Zuev, 1969). The shape of schools causes a reduction in the drag wake when swimming, so fish require less energy and can swim for longer durations in turbulent environments (Liao, 2007). Although seemingly beneficial for fish to school, there are some drawbacks. If schooling fish are not all the same size, then smaller fish may have to expend more energy to keep

up with the movements of larger individuals (Noda *et al.,* 2016). In addition, position in a school can also affect the energy expenditure of individuals (Fish *et al*., 1991; Noda *et al.,* 2016).

Aggregations can also be seen in large marine vertebrates who work together to locate groups of prey and share foraging approaches to enhance their success rates which was observed at the mesoscale level (10-100 km; Scales *et al.,* 2014*).* Several studies within the Chagos Archipelago have looked at the submesoscale level, observing both sharks and reef manta rays (*Mobula alfredi*) aggregating around specific atolls and seamounts where an increased abundance of fish and plankton were found due to oceanographic currents (Letessier *et al.,* 2016; Hosegood *et al.,* 2019; Harris *et al.,* 2021). These topographic structures in vast oligotrophic waters can become a refuge for pelagic organisms, providing shelter, increased nutrients, and enhanced foraging grounds. However, an understanding of the oceanographic regimes that directly affect organisms and the distribution of prey and nutrients is required to recognise the mechanisms that drive these interactions and aggregations.

1.3 Chagos Archipelago

The tropical Indian Ocean is similar to most tropical oligotrophic seas where oceanographic processes interact with topographic features such as seamounts, atolls and islands, promoting highly productive oceanic waters (Ryther *et al.,* 1966; Braga *et al.,* 2018). Located at the end of the Chagos-Laccadive ridge in the centre of the Indian Ocean, the Chagos Archipelago encompasses a 640,000 km^2 MPA with a 'no take' zone implemented in 2010 (Koldewey *et al.,* 2010). The Chagos Archipelago covers 50 islands and at least 86 seamounts, providing protection from fishing and other anthropogenic factors to many highly mobile migratory and pelagic species (Koldewey *et al.,* 2010;

Wood *et al.,* 2008). The MPA affords protection to 76 species on the IUCN Red List such as the hawksbill turtle (*Eretmochelys imbricata*) and bigeye tuna (*Thunnus obesus*) (Koldewey *et al.,* 2010; Sheppard *et al.,* 2013). Waters in the region are described as 'pristine' due to the amount of protection around the region however, observations have recorded an increase in plastic pollution which may counteract some of the conservation measures (Readman *et al*., 2013).

1.4 Biological influences on biota in the Chagos Archipelago

Biological drivers can affect the distributions and behaviour of biota as much as physical processes. Knowledge of biological drivers are key to obtain a full understanding of the pelagic environment. Key biological drivers such as spawning, migration, predator, and prey densities are all key to understanding the interlinking processes occurring in the pelagic environment. Until recently, research on the spatial variability of pelagic fish in the Chagos Archipelago was minimal. Research recently conducted in the region deployed GPS tags and reviewed historical fishing records with a focus on higher pelagic predators such as blue marlin, reef mantas, sailfish, silky sharks, silvertip sharks, yellowfin tuna, and bigeye tuna (Carlisle *et al.,* 2019; Curnick *et al.,* 2020b). Many of these species are classified as migratory although their movements within the Indian Ocean are unknown. From the tagging study higher than expected residency times were observed for silky sharks, sailfish and yellowfin tuna suggesting the Chagos MPA provides an optimum site for these species reducing their need to migrate (Carlisle *et al.,* 2019). The reasons behind why these species residency times are increased are currently unknown but it is suggested that optimal conditions and higher prey concentrations in the MPA are key factors although no surveys identifying the distributions and migration patterns of species in the lower trophic levels have been conducted (Carlisle *et al.,* 2019).

Spawning is known to occur around seamounts for reef associated species and jacks (e.g. trevally; Sala *et al.,* 2003; Pitcher *et al.,* 2007). Large aggregations of species such as rainbow runners and bigeye trevally (Pinheiro *et al.,* 2011; Madgett *et al.,* 2022) often occur at times of spawning which in turn leads to an increase in predators. The exact timing of spawning for pelagic fish species within the Indian Ocean is not well documented. From the lack of literature available there is clearly an urgent need to research the behavioural patterns of pelagic fish in the Indian Ocean and specifically the Chagos Archipelago to understand the role the MPA plays in the retention of fish species and whether certain seamounts are key spawning sites.

1.5 Oceanographic influences on biota in the Chagos Archipelago

1.5.1 Regional oceanographic regimes in the Chagos Archipelago

The Indian Ocean presents a challenging set of oceanographic processes, some mutually linked, connecting the ocean to atmospheric events. Confined by multiple continents, the Northern Indian Ocean undergoes multiple processes interlinking the land and ocean. This section covers the major, large scale oceanographic variables that control the Indian Ocean and look at the effects each one has on the Chagos Archipelago before focussing on the submesoscale oceanography within the MPA.

The central Indian Ocean comprises of 3 dominant water masses which underpin the seasonality and current flow of the region. These 3 bodies of water; North Equatorial current, Equatorial countercurrent, and South Equatorial current all directly affect the Chagos Archipelago which lies on the border of the latter two (Figure 1.2; Pickard and Emery, 1990). These central Indian Ocean currents undergo directional changes driven by the monsoon winds. The Northeast monsoon season occurs between November and March when north-easterly winds cause the North and South Equatorial Currents to flow

westwards while the Equatorial Countercurrent flows eastward (Pickard and Emery, 1990). In comparison, the South West monsoon season occurs between April and October when the direction of the trade winds turns eastward (Trujilo and Thurman, 2007). These stronger eastward winds cause eddies to form in the central Indian Ocean combining the North Equatorial current and the Equatorial Countercurrent (Pond and Pickard, 1983; Sheppard *et al.,* 1999: Robinson *et al.,* 2017). Therefore, during the Northeast monsoon season currents in the Chagos Archipelago move westward whereas during the Southwest monsoon they are predominantly eastward flowing (Schott and McCreary, 2001). During the transition period between the monsoons the current direction changes quickly over a period of a month. This can lead to different temporary current regimes that vary year to year (Wyrtki, 1973; Schott and McCreary, 2001; Shankar *et al.,* 2002; Talley *et al.,* 2011; Robinson *et al.,* 2017).

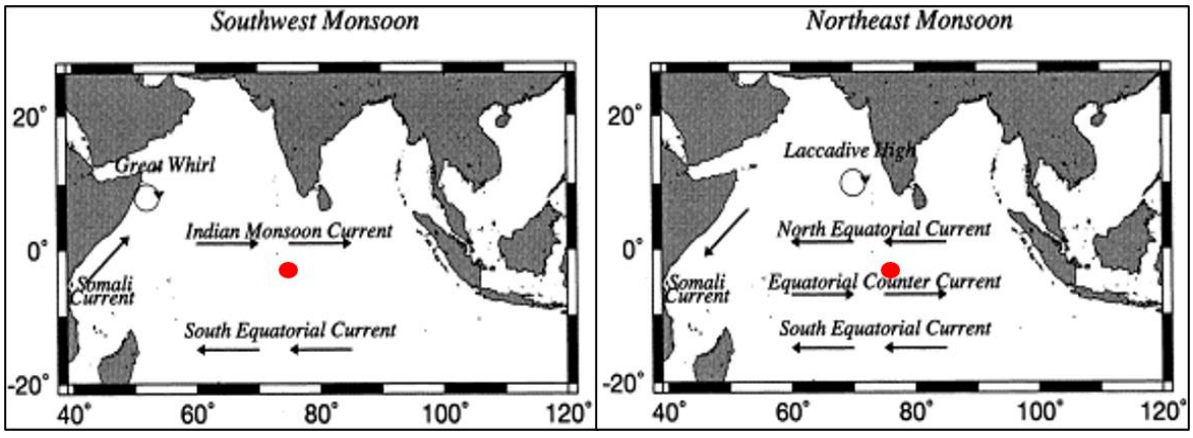

Figure 1.2: Comparison of the southwest and northeast monsoon current directions with the Chagos Archipelago indicated with the red circle (Shenoi *et al.,* 1999).

Another variable influencing the oceanography in the Chagos Archipelago is the Indian Ocean Dipole (IOD) which is a coupled ocean-atmosphere event affecting the climate and sea surface temperatures (SST) for the ocean and surrounding land masses (Saji and Yamagata, 2003a; Marchant *et al.,* 2006; Sheppard *et al.,* 2012). This climate instability occurs on an interannual basis between May and December lasting from 2 to 7 months

(Talley *et al.,* 2011). Decreased rainfall and cooler SST occur over the eastern Indian Ocean while increased rainfall and warm SST are observed in the western Indian Ocean during a positive IOD event (Marchant *et al.,* 2006). These climatic events switch during a negative IOD (Sheppard *et al.,* 2013). The Chagos Archipelago is one of the "centres of action" for the IOD bringing about changes in SST and rainfall patterns which affect the geophysical properties of corals (Saji and Yamagata, 2003a; Sheppard *et al.,* 2012). It can also influence the mean sea level of the region during positive and negative events by up to 11 cm with a time lag of 1 month between an IOD event and the increase in mean sea level occurring (Dunne *et al.,* 2012). The sea level change is thought to be caused by increased strengths in the wind field and although only a small sea level rise, when coupled with other climatic events the results can be amplified (Saji and Yamagata, 2003a; Dunne *et al.,* 2012).

Atmospheric variability over the Indian Ocean is controlled by the Madden-Julian Oscillation (MJO). With greater effects over the south-western Indian Ocean (Madden and Julian, 1972; Duvel and Vialard, 2007) the MJO propagates east at speeds of up to 5 ms^{-1} towards the Pacific Ocean over periods of 30-90 days (Zhang, 2005; Jayakumar *et al.,* 2011). During active MJO phases strong westerly surface winds build up over areas with high SST increasing evaporation and causing increased amounts of ocean mixing in a usually stratified water column (DeMott *et al.,* 2015). During intense MJO winds when cyclones form, oceanic Kelvin waves, which balance the Coriolis force, may become more energetic whilst travelling towards the eastern coast of the Indian Ocean (Zhang, 1997; Webber *et al.,* 2010; DeMott *et al.,* 2015). When they near the coast they are associated with occasional downwelling Rossby waves that occur due the Earth's rotation (Zhang, 1997; Webber *et al.,* 2010; DeMott *et al.,* 2015). The MJO plays a

significant role in dictating the climate in the Archipelago as moisture is transported across the ocean by winds controlling rainfall over land and cyclonic activity (Zhang, 2005; Sheppard *et al.,* 2013). It can also contribute to fluctuations in the SST caused by IOD and El Nino Southern Oscillation (ENSO) events (Sheppard *et al.,* 2012) and has a greater effect over regions with high SST (Kiladis *et al.,* 2005).

While the processes previously described are dominant drivers of climate and oceanography in the tropical Indian Ocean the ENSO is a major Pacific Ocean event that can also affect the Indian Ocean. ENSO is a coupled ocean-atmosphere event that leads to large scale warming of the Indian Ocean affecting the climate of East Africa and other surrounding land (Talley *et al.,* 2011). ENSO events have two SST phases: a warming El Nino and cooling La Nina phase. During the Indian Monsoon, abnormally high SST readings have been observed along the Seychelles Chagos Ridge where a shallow thermocline is located between 5°S and 12°S with a study suggesting links between the depth of the thermocline and monsoon and ENSO circulation (Hermes and Reason, 2008). A study also showed that over 34 % of interannual variability, part of which includes SST, is the result of ENSO in the Indian Ocean (Tourre and White, 1995). Links between ENSO and the IOD have been suggested for many years however, there have been conflicting arguments as to the true mechanisms of the interaction. Temporal data of sufficiently long timescales have yet to be recorded to examine the similarities and differences between the two events (Sheppard *et al.,* 2012). However, the use of coral cores to explore a period of 150 years showed a strong correlation between both events amplifying the heating and cooling effects in the Indian Ocean (Pfeiffer and Dullo, 2006). Further studies have investigated whether a correlation between the two occurs by looking at independent IOD and ENSO events and comparing the SST anomalies with

that of combined events leading to the hypothesis that joint IOD and ENSO events are stronger than independent events (Saji and Yamagata, 2003a; Meyers *et al.,* 2007; McPhaden and Nagura, 2014). An important note made during this study was that the strength of an IOD event did not change whether it was independent or joint to an ENSO event (Saji and Yamagata, 2003a). Instead, it was the ENSO event that changed strength when combined with an IOD event (Saji and Yamagata, 2003a). The occurrence of IOD and ENSO events can also influence the strength (reviewed in DeMott *et al.,* 2015) and occurrence (Jones *et al.,* 2004; Izumo *et al.,* 2010) of the MJO. When positive the IOD can supress MJO activity in the eastern Indian Ocean (DeMott *et al.,* 2015). While ENSO events can decrease the occurrence of the MJO during La Nina events (Jones *et al.,* 2004). The occurrence of joint IOD and ENSO events on the Chagos Archipelago could result in more severe climatic events and changes in the SST (Sheppard *et al.,* 2012). A devastating ENSO event in 1998 led to severe coral bleaching in Chagos with the reef taking 7 to 10 years to recover (Sheppard *et al.,* 2012; Ateweberhan *et al.,* 2013). If these concurrent events occur regularly, they could have detrimental effects on coral recovery and other biota in the oceans that rely on specific temperature ranges for biological processes. However, not all impacts are negative with the co-occurrence of these two events having a positive impact on tuna fisheries with increased yields caught in the Indian Ocean (Kumar *et al.,* 2014; Marsac and Demarcq, 2016; Baez *et al.,* 2020).

The monsoon, IOD, ENSO and MJO all contribute to undulations of the Indian Ocean surface through wind and energy fluxes. Independent of all these ocean-atmospheric events is the tidal regime of the Indian Ocean. There is little published data on tidal variability within the Chagos Archipelago, with some data showing mixed tidal patterns around atolls and seamounts (Robinson *et al.,* 2023). Data from the Indian Ocean

suggests a semi-diurnal tidal regime with a dominant principle lunar semi-diurnal (M2) constituent, with two high and low tides observed every 24 hours and 50 minutes and high tide occurring around 10 hours after the moon crosses the Greenwich Meridian (Trujilo and Thurman, 2007). The luni-solar semi-diurnal constituent is noted to have a lower forcing effect than the M2 constituent and has a period of 11.97 hours (Pond and Pickard, 1983). From three previous records the tidal range of the Chagos Archipelago has been modelled at 50 cm for an M2 tide (Accad and Pekeris, 1978), measured in situ at a 49 cm range (Dunne *et al.*, 2012) with a more in-depth study at Peros Banhos recording a 1.2 m spring and 0.2 m neap tidal range (Pugh and Rayner, 1981). Although these are small tidal ranges compared to the maximum of 12.2 m in the Bay of Fundy (NOAA, 2018), they can have a significant effect on the reef flat around the Archipelago's islands. A reduction of coral cover in shallow waters over the reef flats has been identified when left exposed to the midday sun at neap low tides during peak solar hours (Sheppard *et al.,* 1999).

Throughout this section the many large-scale events that influence the oceanography and climate in the Chagos Archipelago have been discussed. With significant monsoon seasons dictating the direction and strength of the three major water bodies in the Northern Indian Ocean, this event must be considered one of the most important with regards to the current regimes around Chagos. The IOD and ENSO also both play major roles in influencing the climate of the Ocean. Individually, both events can have minor effects on the Archipelago during short IOD events and La Nina ENSO conditions. When IOD and ENSO events combine the results can be amplified, causing large fluctuations in SST, which can have devastating effects on corals through bleaching events. These two events can also influence the strength and occurrence of the MJO influencing the

atmospheric variability over the Indian Ocean. At an intraseasonal level, the MJO has the strongest influence on wind and climate around Chagos but lasts the shortest period of the three atmospheric events. Although a less obvious oceanographic influence, tidal movements, even with small ranges, must be accounted for as they underpin the fine scale oceanography. With changing current directions, alterations in the ocean's stratification and fluctuations of the SST, all these large-scale oceanographic factors must be considered when looking at meso/submesoscale regions. The reason large basin scale processes must be considered here, is the impact they have on biota within the region. They can directly affect larger marine species such as whale sharks through seasonal upwelling (Hermes and Reason, 2008) or indirectly affect the distribution of prey due to current movements (Escalle *et al.,* 2016). With Chagos Archipelago's many islands, atolls and seamounts the effects of all these factors may be amplified due to interaction with varying topography. This will be discussed further in the following section when considering fine scale oceanography in the Chagos Archipelago.

1.4.2 Submesoscale processes affecting biota

Fine temporal and spatial scale oceanographic surveys are not common in the Chagos Archipelago so there is little known about physical dynamic processes that occur at a submesoscale level. Around varying topography, the changing of current magnitudes and their direction can cause dynamic oceanographic features. Flow topography interactions are common with internal waves identified around bank features such as Jones Bank in the Celtic Sea (Embling *et al*., 2013) and hydraulic jumps in the Strait of Bosphorus, Black Sea (Dorrell *et al.,* 2016): both of which have been observed in Chagos (Hosegood *et al.,* 2019).

Internal waves are undulations in the water column that slowly propagate at amplitudes of 5-50 m between density layers (Pond and Pickard, 1983; Hughes Clarke, 2017). Caused by flow-topography interactions, tides, and turbidity currents (rapid downhill current), internal waves stimulate turbulence in the water column through shear instabilities (Johnston and Merrifield, 2003; Trujilo and Thurman, 2007). When an internal wave interacts with a topographic feature the turbulence is dispersed into the surrounding water (Johnston and Merrifield, 2003) amplifying near-bottom current flows and causing the suspension of nutrients (Eriksen, 1982; Eriksen 1991; Mohn and Beckmann, 2002a; Mohn and Beckmann, 2002b; Genin, 2004). These additional nutrients help to sustain the phytoplankton community which are prey to zooplankton and higher trophic levels (Genin *et al.,* 1986; Genin, 2004). If these short, localised nutritional benefits are continued over an extended period, they can enhance the productivity of a region in an otherwise oligotrophic ocean (Woodson, 2018). Internal tides act in a similar way to internal waves but propagate with a tidal frequency (Johnston and Merrifield, 2003). They are generated when strong barotropic tidal regimes interact with sloping topography such as seamounts (Garrett, 2003; Pollard and Read, 2017) and can aid in the transportation and aggregation of nutrients and biota (Pineda, 1994).

In Chagos, internal waves are dependent on a mixture of tidal conditions, geostrophic and near inertial currents (Read and Pollard, 2017; Hosegood *et al.,* 2019). Off the sheltered sides of seamounts Sandes and Swart, internal lee waves propagate up the shallowing flanks breaking into hydraulic jumps due to changes in the associated shear (Hosegood *et al.,* 2019). These hydraulic jumps, which are abrupt changes in height due to interaction with different fluid velocities, appear as internal bores continuing up the same plane of the seamount onto the summit where a flushing effect provides an

increase in nutrients over the top of the seamount (Pineda, 1994; Hosegood *et al*, 2019). With additional nutrients, the productivity of the seamount summit is enhanced and can attract apex predators as it becomes an optimum feeding ground for all trophic levels (Hosegood *et al*., 2019). Other studies have also shown enhanced fish aggregations and predators over seamounts and banks perhaps due to the intensified entrainment of prey or higher productivity (Kaartvedt *et al.*, 2012; Embling *et al.,* 2013). Spatial distributions of different sized zooplankton dictated by the presence of internal waves has previously been observed in the Camarinal Sill in the Strait of Gibraltar (Macías *et al.,* 2010). Further studies have also suggested that internal waves affect predator-prey encounter rates (Woodson and McManus, 2007; Scott *et al.,* 2013; Greer *et al.,* 2014) of multiple species such as pilot whales (Moore and Lien, 2007) and sharks (Hosegood *et al.*, 2019; Pineda *et al.*, 2020). Swimming within 1 km bounds of internal waves in the South China Sea, multiple short-finned pilot whales were hypothesised to feed on the increased aggregation of prey in an upwelling zone brought about by internal waves (Moore and Lien, 2007). Alternatively, the spiny dogfish (*Squalus acanthias*) was observed actively swimming downwards during periods of fast upwards currents during nonlinear internal wave activity which was hypothesised to be an avoidance behavioural response to the increased horizontal shear in the upper water column (Pineda *et al.*, 2020). Another species of shark, silvertip (*Carcharhinus albimarginatus*), appeared to take advantage of the enhanced feeding opportunities by increasing its activity over the summit of Sandes seamount in the Chagos Archipelago during internal lee wave activity (Hosegood *et al*., 2019). These complex contrasting behaviours could be due to a range of factors such as the upper turbulence tolerance levels of each species, prey distribution and flow topographic interactions along with other submesoscale processes that are still to be accounted for.

1.5 Flow- topographic interactions

1.5.1 Islands and Atolls

A key feature in the Chagos Archipelago is the dynamic and varying topography with 58 islands and atolls and 86 seamounts (Yesson *et al.*, 2011). Interactions between currents and these features will likely cause dynamic mesoscale oceanographic events to occur such as the Island Mass Effect (IME; De Falco *et al.,* 2022). With islands and atolls, enhanced primary production can occur due to a combination of tidal mixing, island wakes, freshwater runoff, upwelling, internal waves and geostrophic-topographic interactions (Figure 1.3; Doty and Oguri, 1956). The IME has been identified within the Pacific (Jones 1962; Sander and Steven 1973; Le Borgne *et al.,* 1985; Martinez and Maamaatuaiahutapu 2004; Gove *et al.,* 2016), Atlantic (Hernández-Léon *et al.,* 2001; Hernández-Léon 1988), Southern (Blain *et al.,* 2001) and Indian Ocean (Sasamal, 2006; Elliot *et al.,* 2012) and can enhance productivity and biodiversity in otherwise oligotrophic oceans providing a refuge for pelagic species.

Increased turbulence and mixing have been identified around islands and atolls with the IME present (Hernández-León, 1991). Internal waves contribute to the enhanced productivity around islands and atolls due to current-topography interactions by drawing nutrients from depths to shallower regions (Gove *et al.,* 2016). Diversity hotspots have been observed across Chagos at locations such as Egmont and Salomon Atolls (Carlisle *et al.,* 2019; Harris, 2019; Andrzejaczek *et al.,* 2020). With increased abundance of reef manta rays and turbulent conditions at Egmont atoll (Harris *et al.,* 2021), it could be hypothesised that the IME could occur there causing increased turbulence. In a fine scale study, the increase in reef manta rays was linked to tidal bores and lagoon flushing increasing prey abundances however, the IME may still play a role

in enhancing productivity and prey aggregations around Egmont (Harris, 2019; Harris *et al.,* 2021). As tidal bores can be a factor of the IME, it could be hypothesised that the IME occurs around Egmont atoll with increased primary production and the retention of plankton within Egmont lagoon causing the consistant aggregations of reef manta rays. Furthermore, given the location of Egmont near the highly biologically diverse Great Chagos Bank (Sheppard *et al.,* 2012) oceanographic processes, such as internal waves, may occur between the two topographic features that enhances the waters around Egmont.

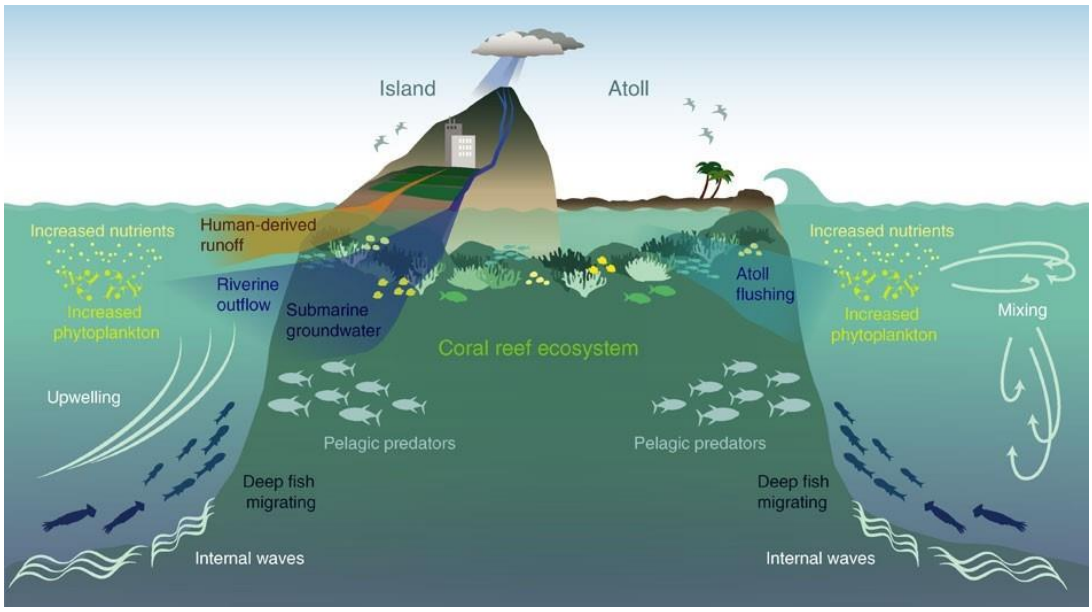

Figure 1.3: Graphic depicting the factors causing the island mass effect: tidal mixing, island wakes, freshwater runoff, upwelling, internal waves and geostrophic-topographic interactions (Gove *et al.,* 2016).

1.5.2 Seamounts

Unlike islands and atolls, seamounts deflect the current flow in an area but do not completely impede it. Defined as topographic rises they act as obstacles in the water column affecting the flow of currents (Royer, 1978; White *et al.,* 2007; Yesson *et al.*, 2011; Yesson *et al.,* 2020) and providing a sheltered enriched habitat for deeper pelagic species (Vianello *et al.,* 2020). Many species choose seamounts as nursery grounds due

to increased productivity brought about by oceanographic processes that can incite upwelling under certain conditions (Millineau and Mills, 1997; Clark *et al.*, 2010; Rowden *et al.,* 2010). There are two working hypotheses about how the aggregation and retention of biota occurs over seamounts: internal wave hypothesis and the Taylor column hypothesis. The internal wave hypothesis has already been discussed within this review, but not directly applied to seamounts. Within global oceans it is predicted that only 1% of internal waves are generated from seamounts (Zhang *et al.*, 2017), though this is likely an underestimate based on recent studies on seamount abundance and internal waves (Hosegood *et al.,* 2019; Yesson *et al.,* 2020). Internal waves were first identified in the Chagos Archipelago in 2015 resulting in an increase of apex predators such as silvertip sharks (Hosegood *et al.,* 2019) and other shark species (Tickler *et al.,* 2017) aggregating over the seamount. Other studies have also linked an increase in sharks, whales (Pitcher *et al.,* 2007) and tuna (Koldewey *et al.*, 2010) with turbulent water over seamounts. Alternatively, the Taylor column hypothesis relies on the steady flow of background currents over large seamounts. This stimulates the regional ecosystem by drawing nutrients towards the surface and trapping them within an eddy over the seamount summit promoting the growth of phytoplankton which attracts zooplankton and fish schools around the summit (Taylor, 1923; Hogg, 1973; Huppert, 1975; Huppert and Bryan, 1976; Pitcher and Bulman, 2007; White *et al.,* 2007; Lavelle and Mohn, 2010). The trapped eddy, also known as a Taylor cap, can form in stratified and unstratified conditions although the shape and position of the Taylor cap varies between the two (Chapman and Haidvogel, 1992). Taylor caps can be either temporary or permanent depending on the dimensions of the seamount and parameters of the current flow (Chapman and Haidvogel, 1992). Evidence of Taylor caps forming over seamounts has been identified in observations of increased chlorophyll-a

concentrations over seamounts in the Pacific Ocean (Genin and Boehlert, 1985; Dower *et al.,* 1992; Dower, 1994; Freeland, 1994; Comeau *et al.,* 1995). These high concentrations were only observed over a few of the total seamounts surveyed suggesting that, if a Taylor column was the mechanism retaining the high chlorophyll concentrations, then the dimensions of the seamount and the current regime play a key role in determining the formation of a Taylor column. These increases in chlorophyll concentrations over seamounts can enhance the primary productivity of a region, however there is evidence that the enhanced productivity does not directly benefit zooplankton species with lower zooplankton biomass observed over seamounts with a Taylor cap (Genin *et al.*, 1994; Dower and Mackas, 1996). Hence, fish and other predators are less likely to benefit from the presence of a Taylor column over a seamount compared with nutrients brought about by the presence of internal waves. A study at Coral Seamount in the southern Indian Ocean observed an increase in planktonic biomass along with the internal tides (Read and Pollard, 2017). Although there was little evidence of enhanced biodiversity in the higher trophic levels the authors agreed that the internal tides were more likely to have a role increasing plankton abundances rather than Taylor columns (Read and Pollard, 2017). Another weakness of the Taylor column hypothesis is the depth at which one can form. To promote primary productivity, it must occur within the photic zone. Without this, micronekton and larger species are unlikely to benefit from Taylor columns so other mechanisms are required to obtain food around seamounts.

With 86 known seamounts with different dimensions in Chagos, it is likely that Taylor columns could form. However, when high amounts of biomass at all trophic levels are identified over seamounts then the internal wave theorem seems the most likely to

occur (e.g., Hosegood *et al.,* 2019). Oceanographic measurements of currents both over the summit and flanks of seamounts could aid a greater understanding of flow-topographic interactions. A study predicted internal tides were causing the anticyclonic flow above a seamount and not Taylor columns, as background and topography induced currents were difficult to differentiate from each other (Nobel and Mullineaux, 1989; Kunze and Toole, 1997). This adds further evidence to the need to acquire joint fine-scale and regional oceanographic measurements to decipher the differences between currents and biota retaining hypotheses. Whether internal waves or Taylor columns form or a combination of both, physical oceanographic processes play a key role in the spatiotemporal distribution of biota (Genin, 2004; Shank, 2010).

One other prominent mechanism for increased biological aggregations is seamount trapping which does not depend on oceanographic processes but zooplankton and fish behaviour. It relies on the process of DVM undertaken by many micronekton species that descend at dawn from the upper surface layers but get trapped on the summit of seamounts (Genin, 2004; Martin and Christiansen, 2009; Clark *et al.*, 2010; Cascão *et al.,* 2019). As light increases in the water column trapped prey are easily visible to predators and with the amplified current flow observed over seamount summits predator prey encounter rates are increased (Genin, 2004; Clark *et al.*, 2010; Cascão *et al.,* 2019). Also known as topographic enhancement, this mechanism relies on two factors occurring: a topographic blockage and a trophic enhancement (McClain, 2007; Letessier *et al.*, 2016). This mechanism is of great benefit to apex predators who can benefit from the diurnal process with a regular, predictable food supply and can use the “feed rest” hypothesis where they reduce their locomotive energy expenditure and wait for prey to come to them (Genin, 2004). Within the Chagos Archipelago, seamounts act as the topographic

blockages enhancing both silvertip sharks and tuna abundances (Koldewey *et al.*, 2010; Tickler *et al.,* 2017; Hosegood *et al.*, 2019). However, for smaller fish species they become both prey for the apex predators, and predators of the trapped zooplankton, which is where behavioural processes such as schooling play a pivotal role in the survival of these organisms. Furthermore, this mechanism, coupled with oceanographic processes, can promote higher species diversity and productivity around seamounts providing as oasis of food and shelter in an otherwise oligotrophic ocean (Morato *et al.,* 2010).

The three mechanisms detailed above are only a few of the possibilities that cause the aggregation of biota during flow-topographic interactions through retention, nutrient enrichment, and increased prey concentrations (Genin, 2004; Bakun, 2006; Pitcher and Bulman, 2007). Whether retention processes are initiated through Taylor caps, internal waves, or seamounts, they all stimulate the increased advection of nutrients from deeper waters enhancing biological aggregations over seamounts. This can increase the concentrations of both nutrients and hence biota over a seamount promoting productivity and biodiversity.

1.6 Acoustic tools for detecting biological aggregations

Discussing the theoretical oceanographic drivers of pelagic biota or the responses of biota within a controlled experiment is easier than determining the in-situ responses of pelagic biota in the open ocean. Multiple factors that cannot be controlled or easily measured, influence biological aggregations in the open ocean in comparison to controlled laboratory experiments. However, methods to quantify the response of pelagic biota to oceanographic drivers have been developed with underwater acoustics a leading tool. Fisheries acoustics makes use of the properties of sound propagation

(scattering) to detect targets in the water column using echosounders (Simmonds and MacLennan, 2005). There are 4 generic categories that echosounders fall into based on the transmission of sound: single beam, split beam, dual beam and multibeam. Single beam echosounders transmit sound in a single pulse detecting the range of targets from the sound source. No angular information is recorded so the direction and behaviours of targets cannot be ascertained. Split, dual and multibeam echosounders all allow for angular resolution providing more detailed information on pelagic targets to be gathered. Targets within an acoustic pulse provide stronger responses if they are located on the acoustic axis which is the centre of the acoustic pulse where the most energy and maximum sensitivity occurs. To account for the range of the target from the transducers, time-varied gain (TVG) is applied ensuring that wherever targets are located in the beam, targets of the same size produce the same echo return. When detecting biological targets, the shape of the acoustic beam is called the beam pattern. Whilst you have the most energy on the acoustic axis of this beam some energy is distributed outside the main beam- into what is known as sidelobes. When the beam is being received these sidelobes can interfere and add noise to the dataset degrading the quality of data (Hamel, 2020).

1.6.1 Capabilities of fisheries acoustics

When the underwater targets are biological, it is important to understand the detection limitations of echosounders. Single beam echosounders cannot provide angular information, so the direction and orientation of the target is unknown. The position of the target within the beam is also unknown therefore, whether a small target is on the acoustic axis or a large target is on the edge of the beam then the backscattering signal received for both would be similar (Simmonds and MacLennan, 2005). Dual and split

beam echosounders provide information on the location of the target within the beam although the mechanisms behind this differ. As in the name, dual beam echosounders emit two pulses with different beam widths with the known ratio between the two beams used to estimate the position of the target (Ona, 1999). Split beams provide precise target locations by dividing the beam into 4 sections and comparing the phase differences between each section. From these comparisons, directivity, target strength and target speed can be gathered (Arrhenius *et al.,* 2000, Torgersen and Kaartvedt 2001). Biological scatterers are measured using Volume backscattering strength (S_V) or target strength (TS). If TS measurements are determined, then the echosounder must be calibrated which is the procedure of ensuring that the detected values are verified against known scattering values (Foote, 1987; Demer *et al.*, 2015).

Echosounders comprise of narrowband and wideband varieties which determines the range of frequencies in the emitted signal (Simmonds and MacLennan, 2005). Narrowband, or continuous wave, signals are a narrow range of frequencies around the target frequency whereas broadband signals produce a wider range of frequencies through frequency modulation. The advantage of broadband is the increased information received due to the multiple responses of the target at different frequencies contained in the signal. Although more complicated and expensive the extra information on targets is beneficial with echosounder models such as the wideband Simrad EK80 now taking over from the narrowband EK60 in becoming the industry standard for fisheries surveys (Demer *et al.,* 2017).

1.6.2 Acoustic detection of biological aggregations

Fish are commonly detected with acoustics due to the presence of the swimbladder. This gas-filled bladder reflects the sound pulse leaving a unique signal that with the

correct echosounder allows physiological features of the fish to be determined (Foote, 1980). There is a high amount of variation in the return signals from fish due to the shape of the swim bladder which varies between species and through the behaviour and orientation of the fish (MacLennan *et al.* 1990; Ona, 1990). Swimbladders are absent in cartilaginous fish, but stomach contents, gonads, fat content, skeleton, flesh, and pressure all contribute to target strength measurements allowing the detection of all fish species (Love, 1971; Ona, 1990). Plankton can also be detected with acoustic instruments with the backscattering strength associated with these targets dependant on the density, size and echosounder frequency (Greenlaw, 1979). Larger zooplankton groups such as species of krill (McQuinn, Dion and St. Pierre, 2013; Kang *et al.,* 2020; Cutter *et al.,* 2022; Salmerón *et al.,* 2023), squid (Goss *et al.,* 2001) and jellyfish (Brierley *et al.,* 2001; Colombo, Mianzan and Madirolas, 2003) have been well studied acoustically. Underwater acoustics is not limited to biological scatterers as bubbles, sediment, and other debris also reflect acoustic signals. In regions of higher turbulence, more bubbles or sediment resuspension occurs producing noise in the dataset (Watkins and Brierley, 1996; Mair, 2008). Determining whether acoustic scatterers are biological or not requires independent validation techniques. These techniques include, but are not limited to, video, trawling, net sampling, grab samples, aerial, and diver surveys (INFOMAR, 2008).

1.6.3 Application of acoustics for ecological surveys

Fisheries acoustics has a long history of studies conducted to look at the aggregations of fish and plankton (Tungate, 1958; Richardson *et al.,* 1959; Mitson and Wood, 1962). Commonly used in stock assessments, echosounders are useful identifiers of commercially important fish species (e.g. Misund, 1997; Toresen *et al.,* 1998; Domokos,

2021). More recently, acoustic methods have been applied to ecological surveys which focus on the drivers of the aggregations and behavioural responses such as the impacts of underwater artificial structures (e.g. Williamson *et al.,* 2019; Huang *et al.,* 2021), predator-prey interactions (e.g. Lawrence *et al.,* 2016; Cox *et al.,* 2023) and oceanographic drivers (e.g. Embling *et al.,* 2013; Fennell and Rose, 2015). Fisheries echosounders can also detect oceanographic processes in the water column due to the aggregation of scatterers associated with these features (Genin, 2004) such as the deep scattering layer (Mair, 2005; Hazen and Johnson, 2010), hydraulic jumps (Dorrell *et al.,* 2016) and internal waves (Embling *et al.,* 2013; Flood *et al.,* 2016). Using biological aggregations as a proxy for physical processes demonstrates an unique ability to collect a large quantity of data spanning multiple disciplines. With the continued development of fisheries echosounders the resolution of scatterers that can be detected in the water column will be improved.

1.7 Conclusions, future directions and thesis aims

Within this chapter, topics considering the pelagic realm, interactions between biota and oceanographic drivers and the detection of these processes have been reviewed. By considering regional and mesoscale oceanographic processes affecting biota within the Chagos Archipelago, it is evident that negative climatic and sea surface events can be amplified when multiple regional events occur such as the IOD, ENSO and MJO. Mesoscale events within Chagos are usually dictated by flow-topographic interactions which have linked biological aggregations to internal waves at specific locations. By looking at features that act as topographic blockages, multiple hypothesises about the oceanographic mechanisms causing the aggregation of biota around islands, atolls and seamounts can be derived. The evidence suggests that within Chagos, internal waves

are likely to be an important mechanism for the retention of biota over seamounts along with the behavioural mechanism of seamount trapping. This review provides an overview of the complicated dynamic links between pelagic biota behaviour and oceanographic processes in the Chagos Archipelago.

1.7.1 Future directions

This review has identified multiple gaps in the field of knowledge: (1) the structure of the pelagic food web in the Indian Ocean; (2) how both regional and mesoscale oceanographic events interact in the Indian Ocean; and (3) the effects oceanographic processes and topographic interactions have on the behaviour of pelagic biota. Although this study has focussed on the region of Chagos, it has drawn on many global studies to fill gaps in the field of knowledge. There is significant importance in researching this highly protected region which benefits over 76 threatened species that migrate and live in its waters (Sheppard *et al.,* 2013). Conservation is at the forefront of the MPA but without truly understanding the bio-physical processes that occur within the waters, and on land, it is difficult to measure the effectiveness of those strategies.

As discussed, the pelagic realm is a vast multi-dimensional area full of diverse species. Within the Indian Ocean this study is not the first to highlight the limited knowledge of the biological processes and topographic features in the ocean (Visser *et al.,* 2015). Within literature, spatial patterns in the Indian Ocean are usually described as compass bearings: either northern, eastern, southern or western (e.g., Chakravorty *et al.,* 2014; Dunne *et al.,* 2012; Hermes and Reason, 2008; Vianello *et al.,* 2020). However, there are few studies that make links between geographical locations. Some examples of studies that have achieved this include tagging surveys from sharks (Tickler *et al.,* 2019; Jacoby *et al.,* 2020), turtles (Hays *et al.,* 2014; Esteban *et al.,* 2018) and mantas (Harris, 2019;

Harris *et al.,* 2021). These studies have shown migration patterns of species between different geographic regions in the Indian Ocean. Therefore, a regional understanding of the pelagic food web supported by oceanographic processes is required. Sitting between Indian Ocean regions, the Chagos Archipelago provides a refuge in an otherwise oligotrophic ocean, providing rich feeding grounds for a diverse range of species. Its central location in the Indian Ocean means that it is accessible to many migrating species throughout the wider ocean. Further to this, information about how migratory species affect and interact with prey aggregations in Chagos is lacking. By investigating these questions, connections between the pelagic food web in the Indian Ocean regions and the role of the Archipelago for supporting large migrating species can be elucidated. Given the conservation concern of many migratory species, and their lack of protection outside of the MPA, this understanding is crucial for informing future conservation strategies.

To gain a full understanding of the role of climate-driven processes such as the monsoon, IOD, MJO, and ENSO, long-term datasets are required. Without long term meteorological and oceanographic datasets over large spatial scale (such as the entire Indian Ocean) it is difficult to understand the connections between ocean-climatic events. Remote sensing techniques have become an advantageous tool in many studies, such as those looking at the island mass effect however, cloud cover and image resolution can be an issue with the data (Sasamal 2006; Elliot *et al., 2012*). It is evident that submesoscale events must be considered when examining climatic events on regional oceanography and that a full understanding of processes cannot be achieved when solely focussing on a broader approach (Bakun, 2006). For example, a study discovered that during an El Niño event in the Pacific Ocean, naturally occurring internal

waves propagated cooler water across reefs which reduced the effect of coral beaching (Wyatt *et al.,* 2019). This process shows that submesoscale oceanographic processes can provide a beneficial effect on shallower reef regions around islands and atolls, supporting the reef ecosystems and pelagic organisms dependent on them. A submesoscale understanding of the oceanography in an ocean basin is currently unfeasible due to the size, cost and timescale of a project of that magnitude. An alternative solution would be to consider smaller, more manageable locations such as the Chagos Archipelago where submesoscale processes could be defined and act as a template for the rest of the Indian Ocean. By focussing on a small pristine region that is known to be a biodiversity hotspot after 10 years of MPA status (reviewed by Hays *et al*., 2020), then a greater understanding of the regional oceanographic processes can be achieved. Deriving the submesoscale patterns of oceanographic processes in an area relatively free from human impacts removes most of the anthropogenic issues from the results and focuses on the biological and physical interactions in the Chagos Archipelago.

1.7.2 Conclusions and thesis aims

If the meso and submesoscale oceanographic events in Chagos can be resolved, then work can begin on deciphering how and why biota is aggregated over seamounts and around atolls. Questions on whether biological aggregations are driven by biological behaviours, oceanographic processes, or a combination of the two can be answered. The distinction between the two will be difficult to define as many behaviours described in this review are a combination of bio-physical interactions. However, the benefits of identifying the different behavioural mechanisms of biological aggregations within Chagos would allow specific spatial and temporal conservation strategies to target certain species and topographic features. The aim of refining conservation strategies

would be to reduce the costs and time associated with running a large MPA. If effective and efficient strategies can be imposed, then it would help support the longevity of the Chagos Archipelago MPA. Furthermore, it could aid in the long-term monitoring of climate change within the region. By studying how the climate driven oceanography changes in relation to the regions productivity and biodiversity, then a baseline understanding of the effects of climate change can help inform conservation policy. By understanding these climate driven changes around Chagos, the area could be used as a template to help inform global conservation strategies for other regions with similar environmental and biological properties. For a project this size to happen it would rely on multi-disciplinary global action which would have positive ramifications for MPAs around the world.

There is a vital need to build upon information gained throughout the 50 years of research already conducted in the Chagos Archipelago. Oceanographic drivers determine biota movements and aggregations. When coupled with topographic features, such as seamounts, dynamic processes can occur which can have significant foraging benefits for apex predators. By determining the behaviour of pelagic biota from plankton through fish to top predators, an understanding of the ecosystem dynamics can be gained. The Chagos Archipelago, in its pristine state, has the potential to act as a conservation template for other marine systems around the world as the interdisciplinary dynamics from physical oceanographic processes to biological behaviours are linked together.

This thesis aims to combine oceanographic and biological results collected with acoustic instruments around topographic features to determine the fine scale distributions of pelagic biota. With surveys conducted around a seamount and atoll the behavioural

changes of both fish and plankton distributions will also be considered. The studies within this thesis focus on the Chagos Archipelago with **Chapter 2** exploring the spatial distributions of schooling fish around Sandes seamount in relation to oceanographic processes. Understanding why biodiversity increases around seamounts is key for improved conservation methods with linkages between biological aggregations and physical drivers significant.

Chapter 3 moves away from seamounts and focusses on Egmont Atoll in the Chagos Archipelago. A comparison of multiple sites sampled in different seasons elucidates continuous physical drivers of pelagic fish schools but varying behavioural responses due to bathymetric features around the atoll. This chapter informs on the management of coastal waters and how important oceanographic and hydrographic measurements are.

The final analysis in **chapter 4** returns to Sandes seamount, but this time focuses on the zooplankton composition. A detailed review of the limitations of sampling zooplankton distributions acoustically is conducted and compared to in-situ samples. This work supports Chapter 2 showing how the zooplankton distribution over Sandes varies from schooling fish distribution. The first deep water (>20 m) plankton samples are presented in this chapter filling knowledge gaps about the role zooplankton play in supporting fish communities around seamounts.

The results from each chapter have implications for conservation and spatial management of marine sites which are discussed fully in **Chapter 5.** Here the results are synthesised and discussed in the context of the whole Chagos Archipelago and the global applications of the results to other oceanic seamounts and atolls. Limitations of the studies are also considered with suggestions for methodological advancements made.

Chapter 2: Fish responses to regional and sub-mesoscale flow-topographic interactions over Sandes seamount in the Chagos Archipelago

2. 1 Abstract

Enhanced biodiversity has often been observed around seamounts globally, but the effect of climatic events, such as the Indian Ocean Dipole (IOD), on biological aggregations is not clearly understood. In this study, both broad and fine-scale oceanographic drivers of pelagic fish distribution and behaviour over a tropical seamount were investigated. Concurrent fisheries acoustics and vessel-based oceanography data were collected over a bowtie shaped transect at Sandes Seamount, Chagos Archipelago that was repeatedly surveyed over 25 hours on two occasions in November 2019 and March 2022. This allowed an exploration of how fish distributions and behaviour varied due to oceanographic processes. Fish school behaviour and distributions were extracted and modelled with oceanographic variables using Generalised Linear Models with Generalised Estimating Equations. During 2019 an anomalously strong positive IOD event was recorded, whilst 2022 saw a moderately negative IOD event. During the positive IOD event, fish schools were located deeper in the water column and showed a preference for turbulent south-westward currents. An 8 °C variation in water temperature in the upper 150 m of the water column was observed between the two IOD events influencing the spatial distribution of schools. Higher counts of biological aggregations over the seamount summit was also observed when internal wave activity was present during the negative IOD phase. Flow-topographic interactions likely caused the generation of internal waves which

transported colder water from depth to the summit of the seamount where increased abundances of schooling fish were located. Combined with strong oceanic currents this enhanced the foraging success rate of schooling fish. The results presented here suggest that oceanographic processes play a significant role in aggregating fish over tropical seamounts supporting higher biological aggregations at these topographic features. Changes in the oceanographic regime brought about by climatic events may affect the future abundances, distributions and behaviours of biota requiring consistent monitoring of oceanic fish populations around seamounts.

2.2 Introduction

Ocean biodiversity is a central topic with multiple regions identified globally as biological hotspots. These hotspots are often located in regions with varying topography, such as seamounts. Seamounts, which can be described as underwater mountains, have summits located beneath the ocean surface (Pitcher *et al*., 2007). They vary in shape and size, but one common feature is the biological enhancement of the waters around the seamount compared to non-seamount areas (Pitcher *et al*., 2007). Due to the increase in biodiversity in these regions, seamounts make optimum study sites to investigate the biological processes that occur there. However, with over 30,000 seamounts identified globally very few have been studied (Yesson *et al*., 2011; Yesson *et al*., 2020). Furthermore, due to the depths of some seamounts and their locations in remote oceans, research in these isolated regions can be logistically challenging (Pitcher *et al*., 2007). However, one consistent result from multiple global studies of seamounts is that they are key sites for promoting biodiversity and provide a refuge from oceanic currents and an abundance of food for both migrating and indigenous species (summarised in

Pitcher *et al.,* 2007). This makes them important areas for conservation due to both the abundance and diversity of biota concentrated in these regions.

Seamounts have been mapped within the Chagos Archipelago Marine Protected Area (MPA), a remote site in the central Indian Ocean (Figure 2.1). Within the MPA, 86 seamounts, 58 islands and atolls and multiple banks have been identified (Hays *et al*., 2020). Flow-topographic interactions with these features happen on multiple scales affecting biodiversity in the region. Broad scale ocean-atmospheric events, such as the Indian Ocean Dipole (IOD), occur across the Indian Ocean affecting the climate and varying sea surface temperatures (SST) between the east and west Indian Ocean (Saji and Yamagata, 2003a; Marchant *et al.,* 2007; Sheppard *et al.,* 2012). During a positive IOD event, decreased rainfall and cooler SST occur over the eastern Indian Ocean while increased rainfall and warm SST are observed in the western Indian Ocean (Marchant *et al.,* 2007). These climatic events switch during a negative IOD (Sheppard *et al.,* 2012). If coupled with other climatic events such as the El Niño Southern Oscillation (ENSO) or Madden-Julian Oscillation (MJO), stronger sea surface temperature anomalies and wind speeds can be observed (Saji and Yamagata, 2003a; Meyers *et al.,* 2007; McPhaden and Nagura, 2014). These regional processes change temperature and currents in the Indian Ocean, but the compounded effect of localised and regional oceanographic drivers around seamounts on pelagic biota is largely unknown.

Knowledge of the importance of oceanographic processes around seamounts is partially understood (Mejía-Mercado *et al*., 2019) with many studies suggesting links between flow-topographic interactions causing higher abundances of pelagic fish (Hubbs, 1959; Roden, 1987; Klimley and Butler, 1988; Dower and Brodeur, 2004; Johnson *et al*., 2004; Croll *et al*., 2005; Klimley *et al*., 2005; Morato *et al*., 2010a; Young *et al*., 2015; Richert *et*

al., 2017). A combination of topographic and oceanographic conditions promote and support a wide range of biota with processes such as seamount trapping, Taylor columns and internal waves (Genin, 2004; Roger, 2018). Seamount trapping occurs on the downward movement of diel vertical migration (DVM) undertaken by many micronekton species who descend on top of the seamount becoming trapped on the summit (Genin, 2004; Martin and Christiansen, 2009; Clark *et al*., 2010; Cascão *et al*., 2019). As light increases in the water column, they can be visually identified becoming targets for larger predator species (Genin, 2004; Clark *et al*., 2010; Cascão *et al*., 2019). For example, within the Chagos Archipelago, large numbers of silvertip sharks and tuna have been observed during daylight hours over the summit of Sandes seamount (Koldewey *et al*., 2010; Tickler *et al*., 2017; Hosegood *et al*., 2019).

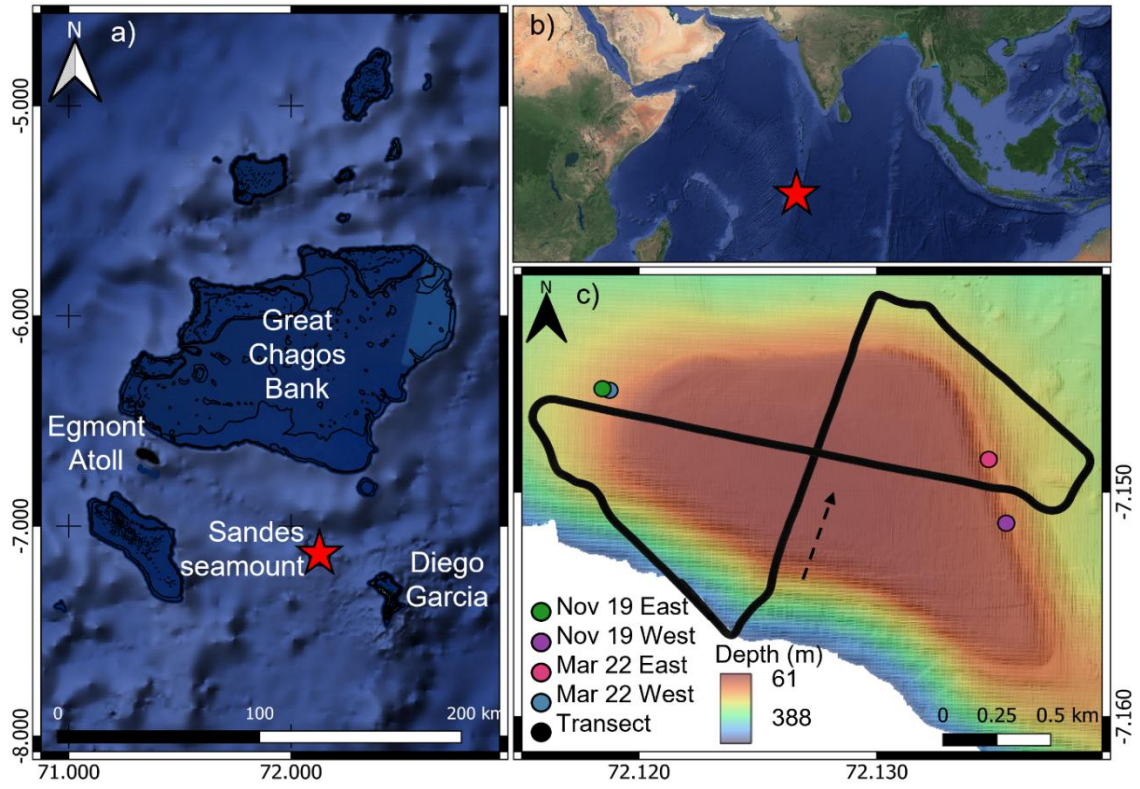

Figure 2.1: Map of a) the Chagos Archipelago with the red star indicting the location of Sandes seamount in b) a contextual Indian Ocean scale map (Google, 2023), and c) multibeam bathymetry of Sandes seamount overlaid with the bowtie survey route and direction. The coloured circles represent the locations of oceanographic moorings.

Oceanographic processes around seamounts can aid the flow of nutrients and planktonic species boosting productivity (Pineda, 1994; Lavelle and Mohn, 2010). Two processes are thought to be essential for the retention and aggregation of biota around seamounts: internal waves and Taylor columns. Internal waves are undulations within the water column that slowly propagate at amplitudes of 5-50 m between density layers caused by changing topography, tides, and turbidity currents (Pond and Pickard, 1983; Johnston and Merrifield, 2003; Trujilo and Thurman, 2007; Hughes Clarke, 2017). The propagation and breaking of internal waves can transport, suspend, and mix nutrients and planktonic species, in turn supporting the phytoplankton community, zooplankton and higher trophic levels (Eriksen, 1982; Genin *et al*., 1986; Eriksen 1991; Mohn and Beckmann, 2002a; Mohn and Beckmann, 2002b; Genin, 2004). Internal waves have been identified in the Chagos Archipelago over Sandes seamount with concurrent observations of increased silvertip sharks (Hosegood *et al*., 2019) and other shark species (Tickler *et al*., 2017). This combination of internal waves and increased abundances of pelagic species over seamounts has also been recorded in other locations with sharks, whales (Morato *et al*., 2010) and tuna (Koldewey *et al*., 2010).

The Taylor column hypothesis is the theory that a steady flow of background currents occur over large seamounts creating an eddy over the seamount summit (Taylor, 1923). This draws and traps nutrients on the summit promoting the growth of phytoplankton, attracting zooplankton and larger species (Taylor, 1923; Hogg, 1973; Huppert, 1975; Huppert and Bryan, 1976; Pitcher and Bulman, 2007; White *et al*., 2007; Lavelle and Mohn, 2010). Evidence of the formation of Taylor columns can be seen by enhanced chlorophyll-a concentrations over seamount summits although it must be noted that the dimensions and currents around a seamount play a pivotal role in whether a Taylor

column may form (Genin and Boehlert, 1985; Dower *et al*., 1992; Dower, 1994; Freeland, 1994; Comeau *et al*., 1995).

Oceanographic processes around seamounts are thought to be key in influencing fish behaviour and distributions, especially in regions such as the oligotrophic Indian Ocean, where seamounts provide refuge to biota from the sparse open ocean. If seamount summits are located in the photic or epipelagic zone (0-200 m) then an increase in biological processes may be observed due to the phytoplankton community within the upper water column (Pitcher *et al*., 2007). Seamounts can also provide shelter for biota from high magnitude oceanic currents and nursery grounds for smaller pelagic fish species (Millineau and Mills, 1997; Clark *et al*., 2010; Rowden *et al*., 2010). Pelagic organisms are commonly identified around seamounts, where it is hypothesised that fish can exploit the currents and benefit from the shelter and enhanced productivity around these topographical features (Genin and Dower, 2007; Clark *et al*., 2010). Behaviourally, pelagic fish are found to form large schools around seamounts to optimise their locomotive ability. Fish usually school when foraging for food, as more eyes can help find prey (many eyes hypothesis), especially in oligotrophic oceans where food is scarce (Lack, 1954; Ward *et al.,* 2011). Once a food source is located, then additional fish may merge with the school due to imitation behaviour until the food source expires or there is another reason to stop feeding, such as a predator attack (Pavlov and Kasumyan, 2000). Evidence of schooling fish around topographic features is not limited to seamounts. Elsewhere, they have been associated with tropical and temperate bank environments where internal wave processes and tidal conditions have acted as significant drivers in the spatial and temporal distribution of fish and plankton (Embling *et al*., 2013; Greer *et al*., 2014). Schooling enables fish to swim in a greater range of

current magnitudes and conditions due to the hydrodynamic advantage to individual fish (Belyaev and Zuev, 1969). Different school shapes can also reduce the energy expenditure of fish as tighter, more compact schools with smaller vertical and horizontal spacing reduce energy expenditure (Partridge, 1980; Abrahams and Colgan, 1985).

There are four areas within seamount ecology that are understudied (Richert *et al*., 2017). These areas are 1) the causation of biological enhancement, 2) the scale of oceanographic processes interacting with seamounts, 3) species connectivity between seamounts and 4) the effects of ecosystem management on stakeholders (Richert *et al*., 2017). This paper looks to address biological enhancements and partially explore the processes interacting with seamounts. This study focusses on the geographical region of Sandes seamount in the Chagos Archipelago (Figure 1) and over 2 surveys investigates abiotic drivers of fish school aggregations and fish schooling behaviour between them. By collecting both in-situ physical oceanographic and fish acoustic measurements over fine spatiotemporal scales, this study provides an insight into the physical drivers of pelagic fish over the seamount. Within a broader perspective, this research will aid conservation strategies in the region by identifying the drivers of biological aggregations over seamounts allowing other areas to be explored for similar relationships, whilst providing much needed information about seamount biodiversity and the importance of the seamounts in management strategies.

2.3 Methodology

2.3.1 Geographical and environmental context

The Chagos Archipelago MPA is located around 500 km south of the Maldives at the end of the Chagos-Laccadive ridge (Figure 2.1). The MPA is 640,000 km^2 and has been a strict

no-take zone since 2010 (Koldewey *et al*., 2010). This remote region consists of 58 islands and atolls along with 86 known seamounts (Hays *et al*., 2020). One of these seamounts, Sandes, is located west of Diego Garcia (Figure 2.1). With a summit at 60 m depth and steep sloping flanks descending to a maximum depth of over 2000 m, Sandes is classified as a narrow, steep seamount (Hosegood *et al*., 2019). During 2019, when the first survey was conducted, an anomalously strong ocean-atmospheric event called the Indian Ocean Dipole (IOD) occurred which affected the wind field and sea surface temperatures in the Indian Ocean (Du *et al.,* 2020). The IOD caused the deepening of the thermocline to below 100 m depth which was a departure from previous studies (Hosegood et al, 2019) and observations from a cruise in March 2022 where the thermocline was observed between 50 and 70 m depth. Both surveys were conducted during calm conditions with winds less than 7 m s^{-1}.

2.3.2 Fisheries acoustic data collection

A Simrad ES70 fisheries single beam echosounder with a combined 38/200 kHz transducer was pole mounted for the duration of two 25-hour surveys between 22nd and 24th November 2019 and 22nd to 23rd March 2022 aboard the *MV Tethys Supporter*. A survey route over Sandes (Figure 2.1c), in the shape of a bowtie, was designed to optimise the collection of spatial data to gain an understanding of the distribution of pelagic biota over the seamount. The bowtie survey route took approximately 1 hour per repeat allowing 31 and 23 repeat transects respectively for the November 2019 and March 2022 survey. For both frequencies, a pulse length of 1.024 ms was applied with the range set to 500 m with maximum ping rate mode enabled. A power output of 1000 W was used for the 38 kHz transducer and 200 W for the 200 kHz transducer.

Ancillary sensors included Global Navigational Satellite System (GNSS) data input from the on-board Applanix POS MV and heading data providing an accurate measurement of location and time in UTC (see Figure A1 in appendix A). Data were acquired using Simrad ES70 software which recorded and stored files with the UTC timestamp and position/ heading from the GNSS data. Due to the Simrad acquisition software only recording time from the laptop, the internal clock was regularly synced to the GNSS time to avoid any time lag between the datasets. The ES70 was powered using a 12 V battery independent of the main ships power supply to minimise electrical interference and noise.

2.3.3 Oceanographic data collection

Simultaneous current measurements were recorded alongside the ES70 using a Nortek Signature 100 kHz pole mounted ADCP. Data were synchronised to the ES70 using custom software, referred to as the ES70 Sync Software (see Figure A1 in appendix A; Williamson, 2019). This software triggered the ADCP via an ethernet switch to ping at 1 Hz mitigating the interference between both acoustic devices. The ADCP used the default settings as set by the SignatureVM software of 3 m bin sizes. The resolution of the oceanographic data was less than the ES70 however the parameters did not vary within bins allowing for a comparison between the datasets. Data were also collected using oceanographic moorings with ADCP's deployed below 90 m depth and thermistor strings with RBRsolo Temperature loggers positioned at 2 m internals over the summit and flanks of Sandes seamount (Figure 2.1). All moorings consisted of temperature sensors and an ADCP.

2.3.4 Calibration

Standard calibration procedures were followed to collect and process the ES70 calibration with two calibrations conducted to account for the different surveys (Foote,

1987; Demer *et al.*, 2015). The first calibration was conducted during a separate cruise to the Chagos Archipelago in March 2020 at Il Lubine, Egmont Atoll, where a tungsten carbide (WC) 38.1 mm diameter calibration sphere was positioned 7.7 m below the transducer. A conductivity, temperature, and depth (CTD) profile was measured during the calibration to provide information on the water properties. The data were processed using ES60adjust (CSIRO, 2016) and Echoview v.11 (Echoview Software Pty Ltd, 2020) to remove the triangular wave error sequence (TWES) and correct for transducer depth and geometry. Using the Echoview Calibration Assistant (Echoview Software Pty Ltd, 2020) the area backscattering coefficient (S_a) correction value was calculated for the 38 kHz (S_a = -0.5769 dB) and 200 kHz (S_a = -0.5316 dB) transducer and applied to the 2019 survey. A second calibration was conducted in March 2022 at the same location, following the same methodology and had a S_a correction value of -0.5218 dB and -0.3063 dB for the 38 kHz and 200 kHz transducers, respectively. This correction was applied to the March 2022 data only.

2.3.5 Fisheries acoustic data processing

ES70 data were imported into Echoview v.12.1 (Echoview Software Pty Ltd, 2021) for processing and the identification of biota. To allow a comparison between the frequencies, data below 200 m were removed due to beam attenuation and noise interference. Pre-processing of the data included applying transducer and GNSS offsets, before applying the Higginbottom background noise removal algorithm and subtracting the estimated background noise from each sample (De Robertis and Higginbottom, 2007). Impulse noise removal and transient noise removal filters were also applied to clean the data (Ryan *et al.,* 2015). Automatic bottom detection was undertaken using the inbuilt Echoview function, with the line repicked to ensure an accurate measurement of

the seabed. The surface 10 m, bottom 5 m and DVM transition times were excluded to remove uncertainty and the misidentification of fish as seafloor targets that increases in readings around these areas due to ringdown, the near-field distance, wind-induced bubble layer and interference with the seafloor (Simmonds and MacLennan, 2005). This process was applied to the volume backscattering coefficient (S_v) dataset.

For the S_v dataset, initial cleaning involved removing sections where there was clear evidence of interference from surface waves and the motion of the vessel. Data from the turns in the transect was also removed due to the addition of acoustic artefacts throughout these manoeuvres. A median 3x3 filter was used to reduce noise, which replaced each data point with the median of the surrounding points with a 5x5 dilation filter fitted over the top which applied an average to the data within set limits (Fernandes, 2000). Due to the high volume of plankton present at night, separate thresholds of – 66 dB were used for day (01:30 – 13:20 UTC) and -60 dB for night (13:20-01:30 UTC) to aid in the detection of pelagic fish although this limited diurnal comparisons of fish school count and nautical area scattering coefficient (NASC); Reid, 2000; Egerton, 2017). The SHAPE (Barange, 1994; Coetzee, 2000; Diner, 2001) school detection algorithm was applied to the data using fish school parameters chosen based on previous studies and evaluation of the data resolution: minimum total school height of 0.20 m, minimum candidate length of 2.22 m, minimum candidate height of 0.20 m, maximum vertical linking distance of 1.00 m, maximum horizontal linking distance of 8.00 m and minimum total school length of 8.00 m (Fernandes, 2009; Campanella and Taylor, 2016; Aronica *et al.,* 2019). School region data, including fish behaviours (Table 2.1; Figure 2.2), was exported in 1-minute timed bins to MATLAB v.R2019b (MathWorks,

2019) where any missing values were removed before the dataset was averaged over the entire water column.

Spatial analysis of fish schools was conducted using ArcMap GIS v.10.7 (ESRI, 2019) where data was normalised to account for survey effort between the datasets. Normalisation was conducted using the equation:

$$x_{normalised} = \frac{(x - x_{minimum})}{(x_{max} - x_{\min})}$$

where x is the school count per 1-minute bin.

Table 2.1: The fish school behavioural variables exported from Echoview calculated for both 38 kHz and 200 kHz in 1-minute bins.

Variable name	Unit	Description
S_v	dB re 1 m^{-1}	Mean volume backscattering strength.
seafloorDep	m	Mean depth of the seafloor.
perim	m	Mean perimeter of fish schools.
NASC	m^2nmi^{-2}	Mean Nautical area scattering coefficient.

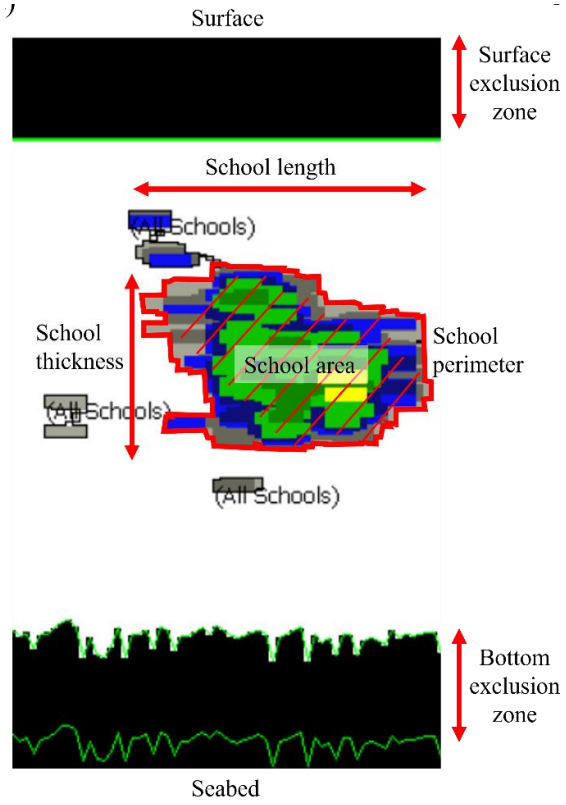

Figure 2.2: Annotated echograms depicting behavioural metrics extracted from fish schools.

2.3.6 Oceanographic data processing

A 5-point running average window along with a Hempel filter, also with a 5-point window and a one deviation maximum was applied to the raw ADCP data creating a subset of averages of the raw ADCP data representative of the full dataset before being binned into 1-minute intervals. Values of Reynolds shear, a measure of flow in turbulent waters, were derived from the binned data using the Reynolds shear stress equation:

$$S^2 = \frac{\delta u^2}{\delta z} + \frac{\delta v^2}{\delta z}$$

Where u is the east velocity component, v is the north velocity component and z is the depth. From this, a selection of variables were selected (Table 2.2) to describe the oceanographic characteristics. The variables represent a range of current magnitude, direction and shear variations which are known to affect the behaviour of fish. Within

this study, shear is used as a proxy for turbulence. Variables derived from moored data (Figure 1) included temperature, thermocline height, time of tidal cycle and horizontal current speed. All oceanographic data were cleaned and binned into three separate depth bands based on physical observations of the data which were: surface layer (0 – 50 m), summit layer (50 – 100 m) and deep layer (100 – 200 m).

Table 2.2: The environmental variables calculated and derived from the oceanographic ADCP data per 1-minute bin and a description of which analyses they are modelled in described in the statistical analysis section of the methodology.

Variable name	Unit	Description	Modelled in analyses
Time	Cyclic	Cyclic time of day.	1
upAbs	s^{-1}	Mean shear for the u component in the surface layer of the water column.	1
medAbs	s^{-1}	Mean shear for the u component in the summit layer of the water column.	1
lowAbs	s^{-1}	Mean shear for the u component in the deep layer of the water column.	1
surfU	cm s^{-1}	Mean u component in the surface layer.	1,2,3
sumU	cm s^{-1}	Mean u component in the summit layer.	1,2,3
deepU	cm s^{-1}	Mean u component in the deep layer.	1,2,3
shallowV	cm s^{-1}	Mean v component in the surface layer.	1,2,3
midV	cm s^{-1}	Mean v component in the summit layer.	1,2,3
largeV	cm s^{-1}	Mean v component in the deep layer.	1,2,3
highTemp	degrees Celsius	Mean water temperature in the surface layer, derived from either the West or East mooring depending on the vessel position.	1,2,3
avTemp	degrees Celsius	Mean water temperature in the summit layer, derived from either the West or East mooring depending on the vessel position.	1,2,3
bigTemp	degrees Celsius	Mean water temperature in the deep layer, derived from either the West or East mooring depending on the vessel position.	1,2,3
therm_depth	m	Depth of thermocline, depending based on the position of the vessel derived from either the West or East mooring.	1
TideToTideTurn	Cyclic	Time until the tide changes between ebb and flood.	1

2.3.7 Validation of acoustic data

Fishing or trawling to gather alternative evidence of acoustically detected targets was not possible in the MPA. Limited video validation of targets was undertaken during the November 2019 and March 2022 Sandes survey to reduce the impact on the acoustic survey. However, video, plankton and oceanographic (CTD) validation was undertaken during March 2022 during a separate validation survey conducted throughout the day on the 19th March 2022 between Sandes seamount and its neighbour Swart. For all data collection periods, a GoPro Hero 4 was deployed vertically into the water column to collect video data which was synchronised to the GNSS time to allow the video to be matched with the acoustic data. Video footage was analysed by visually identifying the species present in the frames and matching it with the depth and time of the CTD and ES70 data.

2.3.8 Statistical analysis

Three separate analyses were conducted for both exported day and night regions: (1) analysis of the count of fish schools per 1-minute bin in relation to oceanographic variables (Table 2); (2) analysis of the NASC of fish schools per 1-minute bin in relation to oceanographic variables and (3) analysis of the perimeter of fish schools per 1-minute bin in relation to oceanographic variables. These three analyses examined how the relative abundance (number of fish schools) and fish schooling behaviour is driven by the oceanographic variables over the seamount. NASC, a proxy for biomass, represents the behaviour of fish schools combining properties such as size and density into one parameter. Perimeter of the fish school signifies the overall size of the school, an indication of retention or aggregation processes of schooling fish. All data were used for

analysis 1, with only 38 kHz data retained for analyses 2 and 3 to ensure only fish targets were included.

All variables were explored before modelling using autocorrelation (ACF) and quartile-quartile (Q-Q) plots in R Studio V.4.3.1 (R Core Studio, 2023; Zuur *et al.,* 2010). Due to the large number of variables used a Bonferroni correction was implemented to reduce the possibility of type 1 errors. For analysis (1) a Poisson distribution was used with a Gaussian distribution used for analyses (2) and (3). A Generalised Linear Model with Generalised Estimating Equations (GLM GEE) was used to model the number of schools using the geepack library (Højsgaard *et al*., 2005; Pirotta *et al.,* 2011). The correlation structure COR AR1 accounted for temporal autocorrelation within the dataset (Pirotta *et al.,* 2011). During the survey, environmental data were collected by repeating the same spatial transect so autocorrelation was included as closely related schools could have similar behavioural movements (Garamszegi, 2016). To account for this, a fixed term was added to the model (blockid = TransectID). All terms were visualised and assessed as both linear and smooth variables before inputting into the model. Cubic *B-splines* were selected using the one-dimensional Spatially Adaptive Local Smoothing Algorithm (SALSA) which automates knot selection based on an input range (Walker *et al.,* 2010; Scott-Hayward *et al.,* 2013). The range of knots tested for each model was derived from testing the model to ensure it was not over or underfitting (Table 2.3). Each variable output from the SALSA underwent a Wald test with partial plots of all significant variables produced with the response variable scaled by the link function against the environmental variable.

Model validation was undertaken throughout all the models to ensure the optimum model, correlation structure, and variables were used throughout. An analysis of the

residuals was completed graphically comparing the Pearson residuals to the fitted values, with variables both included and excluded from the model (Hardin and Hilbe, 2003).

Table 2.3: Description of knot limits input into the one-dimensional Spatially Adaptive Local Smoothing Algorithm.

Model	Minimum knots	Maximum knots	Gap
School count ~ environmental variables	1	6	1
NASC ~ environmental variables	1	6	1
Perimeter ~ environmental variables	1	6	1

2.4 Results

2.4.1 Characteristics of the physical oceanography

Throughout November 2019 a strong positive IOD event was observed across the Indian Ocean, resulting in a decrease in sea surface temperatures, and increased strength of the wind field. This IOD phase was abnormally strong in comparison to previous events reducing the thermocline depth to 100 m over Sandes seamount (Figure 2.3). The deepening of the thermocline caused the temperature of the upper 100 m of the water column to be over 28.8 °C before decreasing to 14.1 °C at 200 m. In contrast, during the March 2022 survey, a moderate negative IOD event was detected with the thermocline shallower at a depth of approximately 50 m. Below 50 m the water temperature declined from 28.3 °C to 20.3 °C at 100 m depth making the summit of Sandes seamount 8 °C cooler than the positive IOD event in 2019 (Figure 2.3).

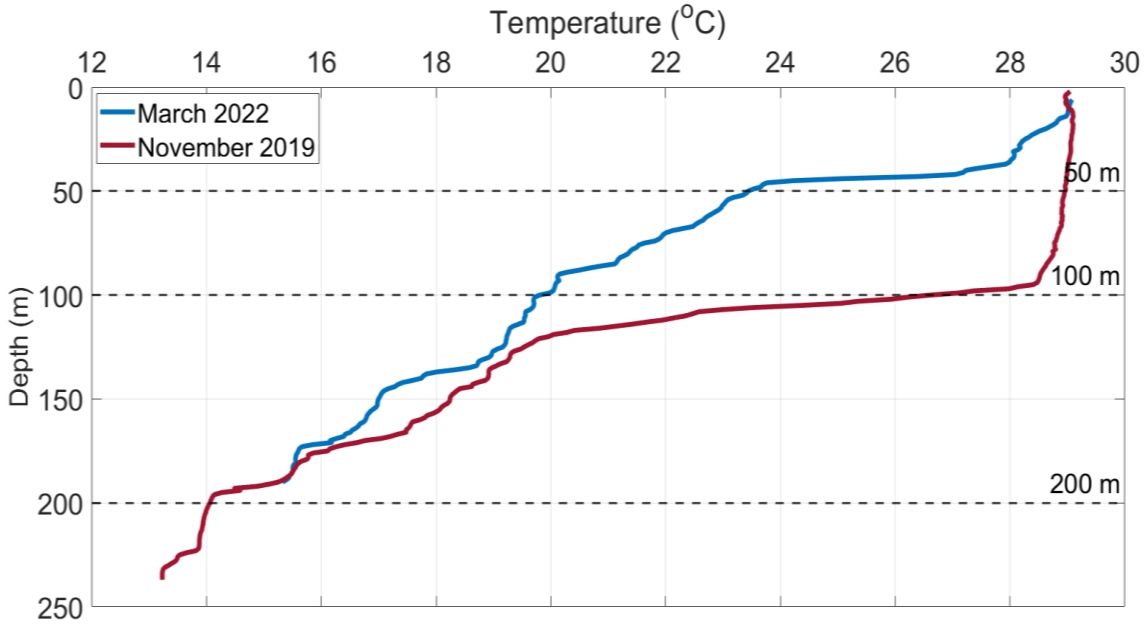

Figure 2.3: CTD profiles showing temperature with depth in March 2022 (blue) during the negative IOD event and November 2019 (red) the positive IOD event.

Internal waves with a height of approximately 15 m were observed on both the ADCP and ES70 data during negative IOD (March 2022) where the thermocline was above the summit of the seamount (Figure 2.4). Due to the deepening of the thermocline caused by the IOD event, no internal waves were observed during the Nov-19 survey period.

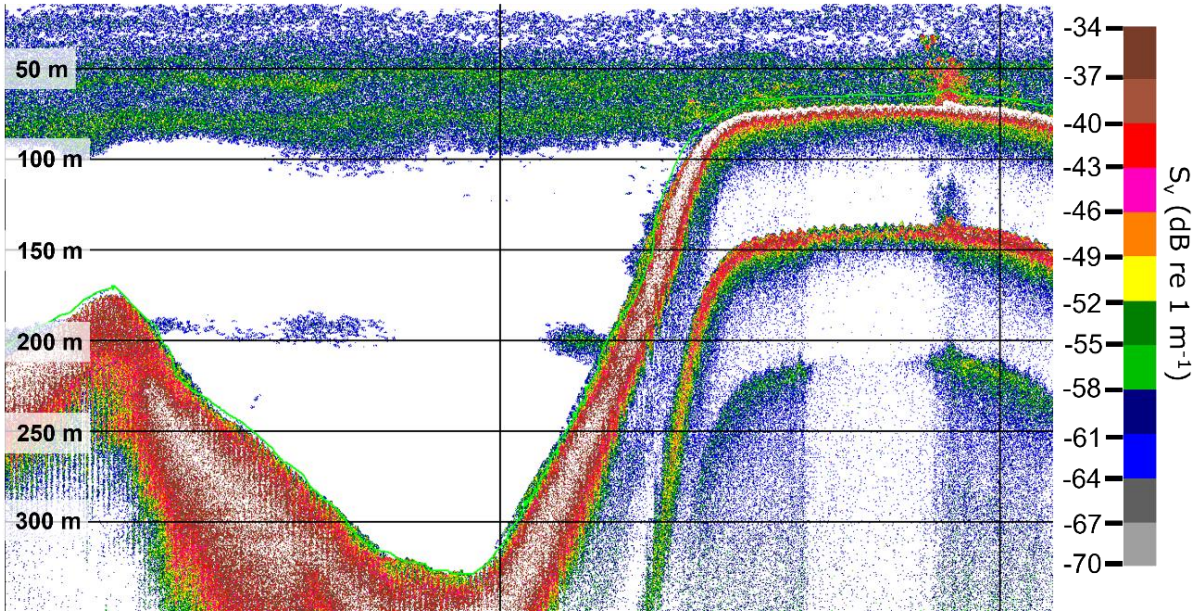

Figure 2.4: ES70 echogram at 38 kHz showing the propagation of internal waves (Green backscatter between 50 and 100 m) at the summit of Sandes during March 2020 at 38 kHz.

2.4.2 Spatial distribution of schooling fish

A total of 11,315 and 11,168 schools were identified during the positive and negative IOD surveys respectively (Table 2.4). During the positive IOD more schools were observed throughout the night (8500) than the day (2815). This pattern was also reflected during the negative IOD although comparisons between day and night periods are limited due to the different thresholds applied to the ES70 data (Table 2.4). Higher numbers of schools were identified with the 38 kHz frequency during the positive IOD (7263) however, this was inverted during the negative IOD with a higher count of 6424 fish schools recorded on the 200 kHz frequency (Table 2.4).

Table 2.4: Summary of exported fish schools from Echoview used for statistical analysis.

Survey	Effort (hours)	Total number of schools per hour	Total number of schools	Total day schools	Total night schools	Total 38 kHz schools	Total 200 kHz schools
Positive IOD (2019)	36.08	314	11315	2815	8500	7263	4052
Negative IOD (2022)	25.65	435	11168	4099	7069	4744	6424

The greatest number of fish schools per 1-minute bin (n=32) was observed during the positive IOD. These were concentrated over the north-eastern flank of Sandes seamount with low numbers observed from the fisheries echosounder along the rest of the transect (Figure 2.5). During the negative IOD event fish schools were spatially distributed over the summit of Sandes and along the flanks of the seamount (Figure 2.5).

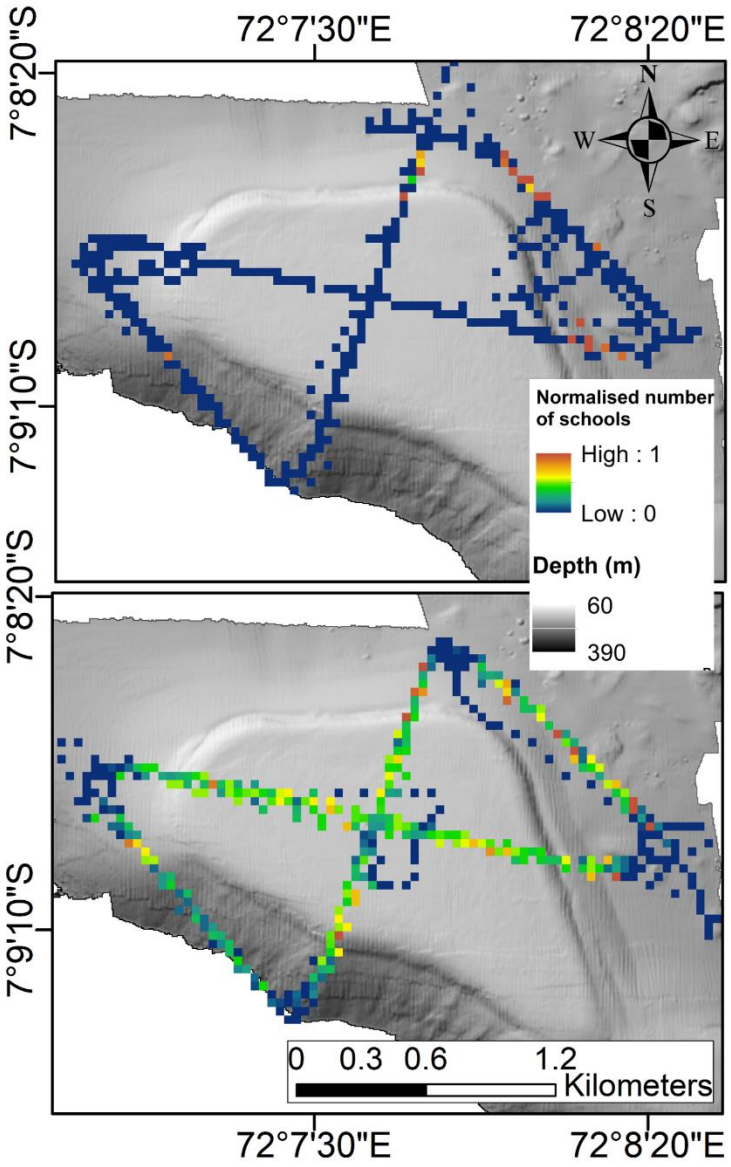

Figure 2.5: Spatial distribution of schooling with normalised values to account for survey effort of fish schools along the survey transect overlaid on multibeam bathymetry of Sandes seamount during a) the positive IOD event and b) the negative IOD event.

2.4.3 Topographical influences on schooling fish

When modelled using GLM GEEs, seafloor depth had a significant ($p<0.001$) effect on the number of fish schools (see Tables A1, A2 and A3 in appendix A for full statistical results). Similar patterns in the relationship between seafloor depth and the count of schooling fish were observed with a higher number of schools located over a seafloor depth of 130

and 160 m during the day and night respectively throughout the positive IOD (Figure 2.6). Schooling fish depths align with the thermocline depth which was approximately 100 m. The thermocline, which can also be related to the mixed layer depth, was where the deep chlorophyll-a maximum was located with a maximum value of 0.87 µg/L (Figure 2.7).

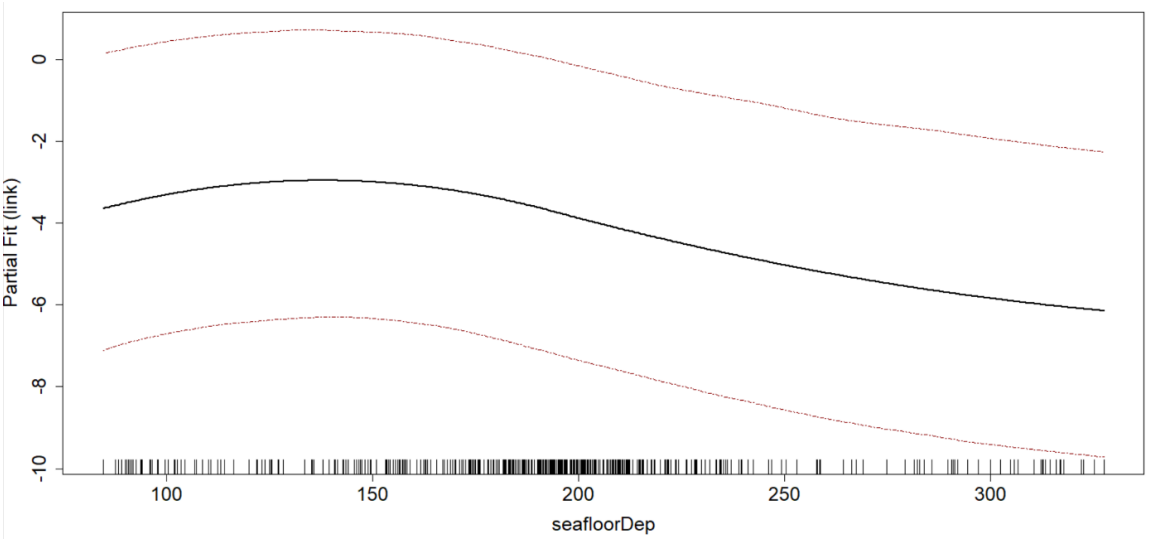

Figure 2.6: GLM GEE partial fit plot showing the response of the number of schooling fish to seafloor depth at 38 kHz during November 2019 during the day. Red dotted lines show the 95% confidence interval with a rug plot at the bottom. The units of the explanatory variables are metres.

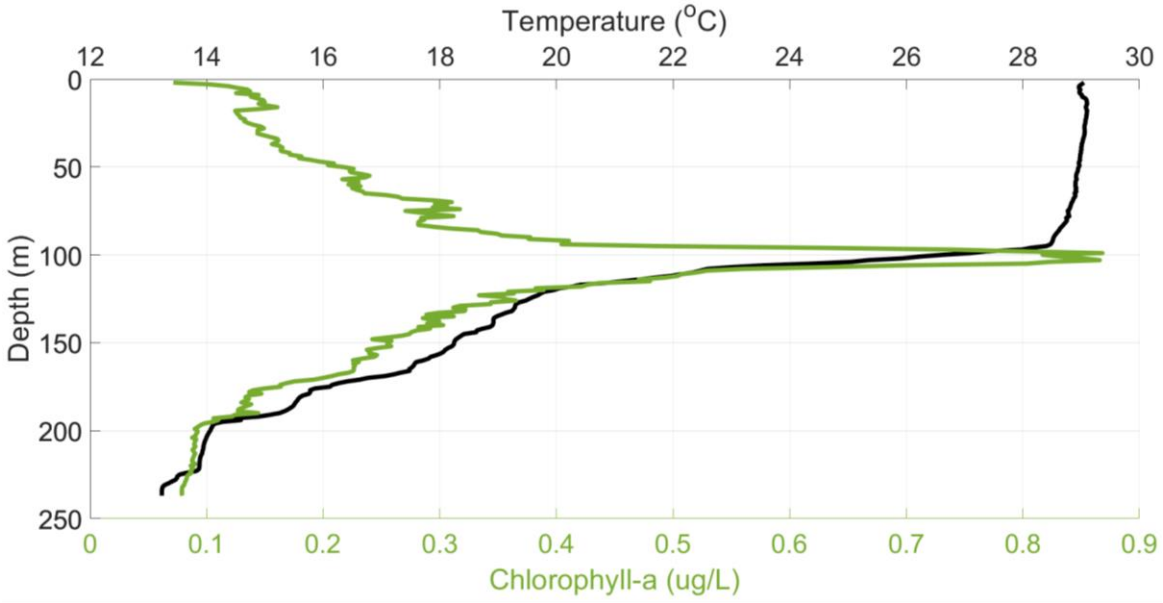

Figure 2.7: CTD profile of chlorophyll-a profile in November 2019 (green) plotted against temperature (black).

2.4.4 Environmental influences on schooling fish

The increased strength of the wind field from the positive IOD across the central Indian Ocean caused strong localised currents in the Chagos Archipelago. Both U and V components of velocity were significant ($p<0.001$) during the positive IOD event influencing the number of schooling fish. Fish schooled in relation to southwest flowing currents below 40 cm s^{-1} observed in the surface band between 0-50 m depth (Figure 2.8a). This was supported by the analysis of NASC values which also found that westward currents of 40 cm s^{-1} in the surface waters (0- 50 m) were associated with significantly higher relative biomass ($p<0.001$). At the summit of Sandes (50- 100 m) there were increased numbers of schools during weaker current magnitudes with a slight directional preference for eastward currents (Figure 2.8b). Below 100 m depth schools showed a preference for westward currents with more schooling fish present in weaker currents (Figure 2.8c).

When the IOD was in a negative mode the number of schools in the summit waters (50-100 m) increased during eastward currents less than 15 cm s^{-1}. In contrast, westward currents were favoured by schools above 50 m and below 100 m with the difference in direction linked to tidal variability which was present during the negative IOD and significant in the majority of environmental models run (see Table A1 in Appendix A) but not observed during the positive event (see Figure A2 in Appendix A).

A combination of oceanographic processes and topographic features caused shear instabilities within the water column with Reynold's shear calculated as a proxy for turbulence in the water column. Higher mean values of shear were observed during the positive IOD (Table 2.5). For both seasons the largest values of shear were detected in water below 100 m depth (Table 2.5). Between 0- 50 m, results from the positive IOD

showed a slight increase in the number of schooling fish during high shear values of 5 s^{-1} (see Figure A3 in Appendix A).

During the positive IOD event deep water temperatures had a significant ($p<0.001$) effect on the number of schools around Sandes seamount. The temperature range between the surface and 200 m depth during the positive and negative IOD was 6.6°C and 11.0°C respectively (Table 2.5).

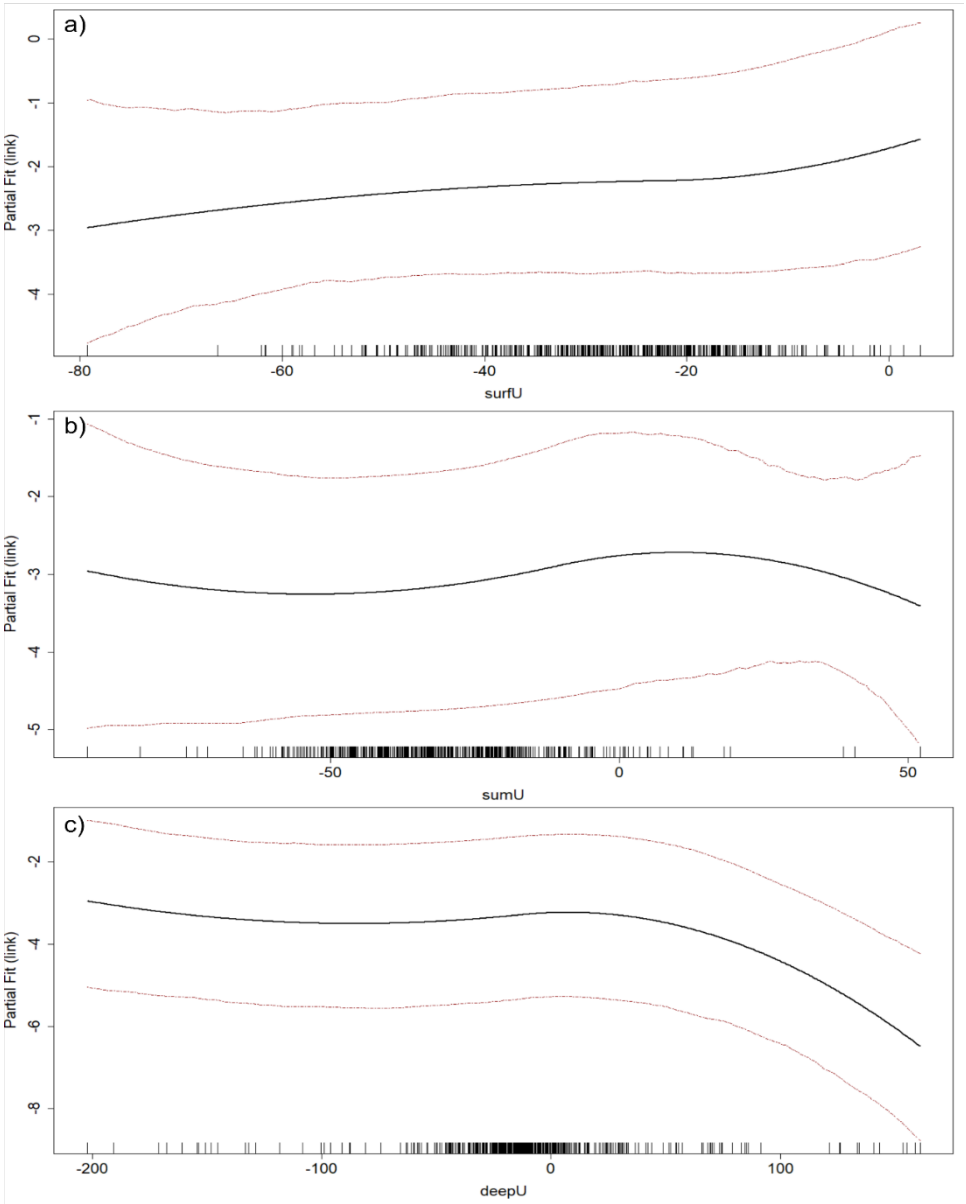

Figure 2.8: GLM GEE analysis showing the count of fish schools in response to the u velocity component (east-west) at 200 kHz during the day in November 2019. Fish responses are classified by depth band a) upper 50 m b) 50-100 m and c) 100-200 m depth. Red dotted lines show the 95% confidence interval with a rug plot at the bottom. The units of the explanatory variables are cm s^{-1}.

Table 2.5: Summary of environmental parameters at different depth bands during the two surveys.

Survey	Depth bands	Parameter (units)	u (cm s^{-1})	v (cm s^{-1})	Shear (s^{-1})	Temperature (°C)
Positive IOD (Nov-19)	Surface (0-50 m)	min	-93.45	-72.47	0.42	28.52
		mean (sd)	-35.53 (13.44)	-13.84 (9.72)	10.09 (10.25)	28.64 (0.06)
		max	3.08	45.97	86.77	28.78
	Summit (50-100 m)	min	-112.73	-85.80	0.55	28.05
		mean (sd)	-38.85 (15.21)	-11.57 (12.74)	21.56 (53.67)	28.48 (0.09)
		max	52.07	138.59	721.47	28.72
	Deep (100-200 m)	min	-202.22	-177.87	0.62	22.17
		mean (sd)	-17.94 (33.38)	-2.40 (33.68)	31.49 (62.89)	26.03 (1.75)
		max	160.90	201.32	522.48	28.27
Negative IOD (Mar-22)	Surface (0-50 m)	min	-34.97	-36.41	2.28	24.95
		mean (sd)	-2.57 (10.35)	1.66 (13.27)	4.90 (0.56)	27.15 (2.94)
		max	33.08	47.78	62.52	28.26
	Summit (50-100 m)	min	-34.77	-26.94	1.24	20.33
		mean (sd)	-1.99 (9.98)	4.79 (9.86)	5.97 (10.67)	21.73 (0.58)
		max	28.48	44.63	281.22	23.43
	Deep (100-200 m)	min	-72.93	-45.29	1.12	17.23
		mean (sd)	1.16 (12.99)	4.95 (17.22)	16.43 (21.27)	18.42 (0.52)
		max	50.722	114.636	295.195	19.94

2.4.5 Behavioural response of fish schools

The north-south velocity component was significant ($p<0.001$) during the positive IOD in explaining school perimeter with larger schools observed in southward currents between 10- 20 cm s^{-1} which occurred in all depth bands during both the day and night (Figure 2.9). This pattern was not observed when the IOD was in a negative phase. The U current velocity component and temperature were also significant in driving the NASC

and perimeter of schooling fish, but no clear patterns emerged from the data (see Tables A2 and A3 in appendix A for full statistical results).

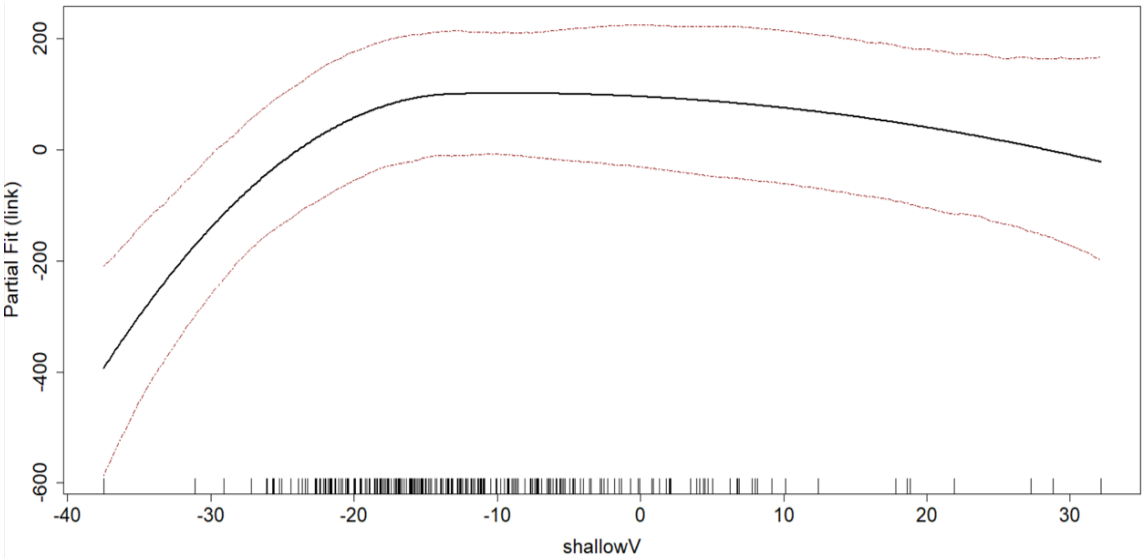

Figure 2.9: GLM GEE model output showing the perimeter of fish schools against the v velocity component in water between 0 and 50 m at 38 kHz during the day in November 2019. Red dotted lines show the 95% confidence interval with a rug plot at the bottom. The units of the explanatory variables are cm s^{-1}.

2.4.6 Validation of biological data

Throughout the two Sandes surveys, opportunistic camera drops were conducted periodically to limit influencing the acoustic survey. A total of 8 and 14 different species were identified from video footage between the positive and negative IOD respectively. During both surveys the most common species observed were bigeye trevally (*Caranx sexfasciatus*) and rainbow runners (*Elagatis bipinnulata*; Figure 2.10). From these drops a mixture of both schooling and individual fish were identified which confirmed that both were present during the surveys (Figure 2.11). Species observed ranged from predatory silver tip sharks (*Carcharhinus albimarginatus*) and barracuda (*Sphyraena barracuda*) to smaller fish such as rainbow runners (*Elagatis bipinnulata*).

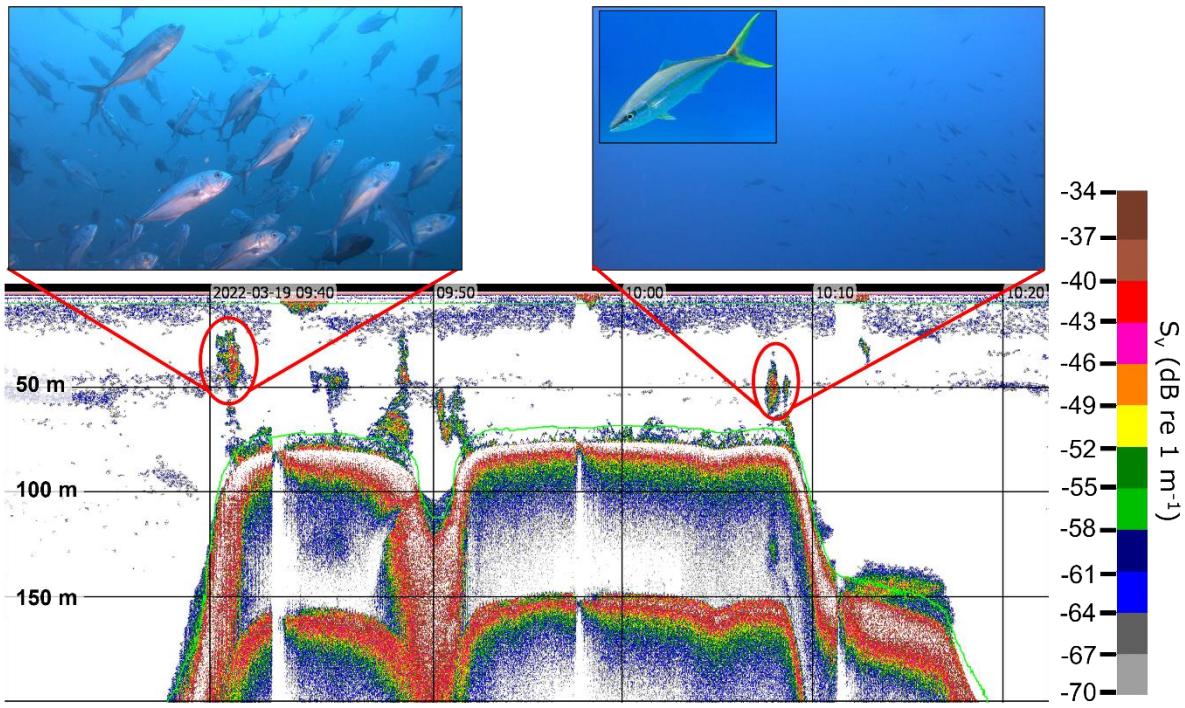

Figure 2.10: Echogram of the summit of Swart seamount (neighbour to Sandes) with examples of bigeye trevally (*Caranx sexfasciatus*; left) and rainbow runners (*Elagatis bipinnulata*; right) identified over the flanks of the seamount.

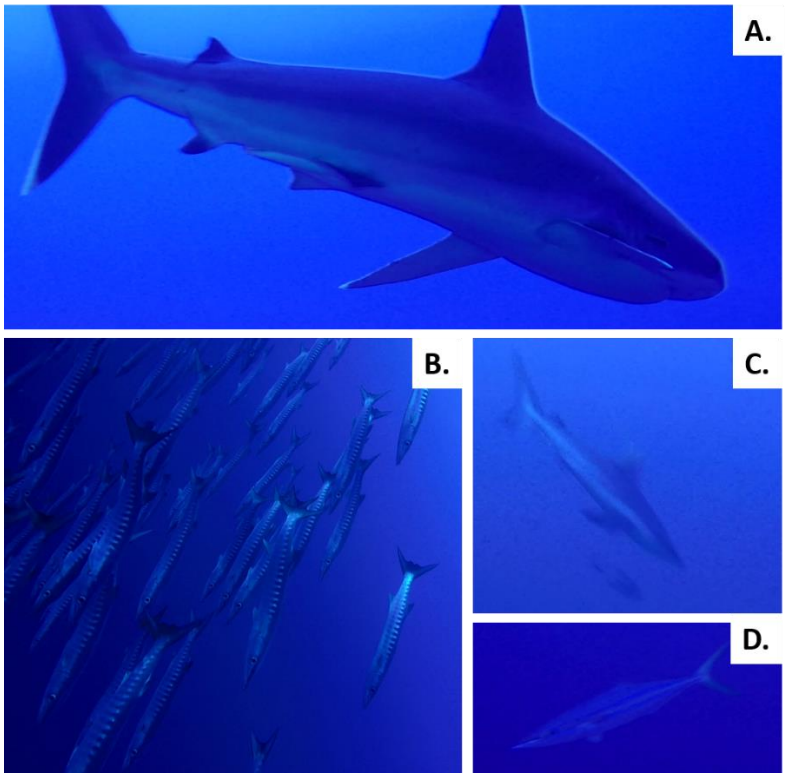

Figure 2.11: Selection of ground truthing images showing both schools and individual fish around Sandes A) Silvertip shark (*Carcharhinus albimarginatus*), B) Barracuda (*Sphyraena barracuda*), C). Grey reef shark (*Carcharhinus amblyrhynchos*) and D) Rainbow runner (*Elagatis bipinnulata*).

2.5 Discussion

This study has shown the importance of both broad and fine-scale oceanographic regimes in driving the distribution and behaviour of pelagic fish over a tropical seamount. Climatic events, such as the IOD, significantly changed the local environment altering the responses of fish. Background currents, temperature, and shear all strongly influenced the distribution and behaviour of schooling fish. When combined with flow topographic interactions and under suitable conditions internal waves were observed over Sandes.

2.5.1 Climatic effects on localised oceanographic processes

The strength of the IOD in 2019 was measured and classified as an abnormal event (Du *et al.,* 2020). The in-situ measurements in this study demonstrate the effects it had on biological organisms and the responses to it. This event forced currents over Sandes in a continuous south-westward direction, overriding any tidal variability, which is a departure from previous observations in studies conducted over the same region (Hosegood *et al.,* 2019). At the time of the positive IOD fish schools were predominantly located over the eastern flank exposed to the prevailing currents. Localised currents around Sandes measured by the ADCP showed a significant relationship between the school count and the U velocity component during the positive IOD. Increased counts of fish observed during these conditions could be due to the increased efficiency of schooling for both locomotive and foraging behaviours throughout the dominant westward current. Currents are an oceanographic mechanism that transport nutrients, plankton and other small micronekton (Castro and Huber, 2010). The increased number of fish schools on the eastern flank could suggest optimum foraging conditions transported by the currents. In particular, the increased number of schools positioned

on the exposed side of Sandes could suggest a behaviour to optimise their foraging success rate and reduce their energy expenditure using station holding. Station holding occurs in turbulent flows when fish can maintain their position and allow the advection of nutrients and prey brought with the currents to travel towards them, reducing their overall energy expenditure (Porteiro and Sutton, 2007). Many types of fish can hold station and use it to their advantage for feeding however, the strength of the current speeds dictate the type and size of fish that will benefit (Thresher, 1983; Hobson 1991). By using the seamount as a topographic blockage, nutrients and prey densities could increase on the eastern flank providing an optimum foraging site for all fish, including predators. It should also be noted that school formation cannot fully be attributed to foraging behaviours as it also has other purposes such as defence and navigation. With such a high values of NASC in one area at Sandes, the predator-prey interactions occurring here that also encourage schooling behaviour should be considered.

Schooling fish were located at greater depths (130- 160 m) during the positive IOD which also aligned with the depth of the deep chlorophyll maximum (DCM). Within the oligotrophic Indian Ocean, the DCM is vital for primary production. As phytoplankton support heterotrophs throughout the food chain, the depth schools were located at may be vital for foraging. A combination of currents causing the aggregation of prey at the DCM may provide an optimal feeding opportunity hence more schools are located off the flanks of Sandes in deeper waters.

Shear, a proxy for turbulence, can increase the hydrodynamic efficiency of fish when used successfully but it can also overwhelm fishes swimming abilities (Utne-Palm and Stiansen, 2001). Whether turbulence will have a beneficial or detrimental impact on fish depends on fish body size and the size of the velocity vortices caused by turbulence

(Utne-Palm and Stiansen, 2001; Hockley *et al*., 2014). If the velocity vortex is greater than the body size of the fish, then it will negatively affect its balance. This can reduce foraging capabilities by adversely impacting their locomotive ability (Utne-Palm and Stiansen, 2001; Lupandin, 2005). However, if the velocity vortex is smaller than the body size of the fish then it can be actively exploited to provide increased momentum when swimming (Webb, 1989). Over Sandes, during the positive IOD the number of schools increased with enhanced shear suggesting schooling behaviour was utilised to overcome any negative impacts of turbulence. Due to model limitations the behaviour of schools in relation to shear was not analysed so whether larger schools dispersed into more smaller schools or there was an increase in the number of schooling fish is not known. Enhanced shear may have been observed during this period due to the increased current strengths brought about by the positive IOD causing higher turbulence from flow-topographic interactions with Sandes. For some fish, enhanced turbulence in the water column can diminish their swimming ability. Experiments conducted with cod (*Gadus morhua*), showed they displayed a preference for specific turbulent conditions, if these conditions were not met it had detrimental effects to their swimming ability (Gerstner, 1998; Webb, 1998). This has further been hypothesised with other fish species, such as the spiny dogfish (*Squalus acanthias*) where shear affected the swimming response with the sharks moving against the currents to avoid regions of maximum shear (Pineda *et al*., 2020). This may explain why more schools are observed as shear increases over Sandes as individual fish, such as rainbow runners identified in the video footage data, may suffer in highly turbulent conditions.

2.5.2 Fish responses to temperature

As ectotherms, temperature affects the physiology, metabolism, and behaviour of fish who can tolerate temperature variations within specific species-related bands (Clarke and Johnston, 1999; Alfonso *et al.,* 2020; Volkoff *et al.,* 2020). Sustained abnormal temperatures affect the stress response of fish leading to both positive and negative effects (Alfonso *et al.*, 2020). Fish respond to high heat stress using mechanisms such as behavioural thermoregulating which is the movement of fish from a high heat stress environment to one more tolerable (Reynolds and Casterlin, 1979; Johnson and Kelsch, 1998; Habary *et al.*, 2012; Khan and Herbert, 2012). Often this is the movement of fish deeper in the water column however, results from Sandes seamount show that during the positive IOD the upper 100 m of water column were of a uniform temperature requiring a large vertical migration for fish to colder waters. The extreme IOD event began its early stages in March 2019 before maturing in September 2019 with the effects of increased water temperatures lasting for many months (Du *et al.,* 2020; Zhang and Du, 2021). Modelled upper temperature limits of species such as rainbow runners (*Elagatis bipinnulata*), barracuda (*Sphyraena barracuda*), grey reef shark (*Carcharhinus amblyrhynchos*) and silvertip sharks (*Carcharhinus albimarginatus*) are between 28.8 and 29 °C which at the time of the positive IOD was the temperature of the upper 100 m of the water column hence would have added significant stress to species not just around Sandes but within the central Indian Ocean (Kaschner *et al*, 2019). Between the positive and negative IOD events there was a temperature difference of 8°C between 50 and 100 m depth which is an intense heating event. With the duration, intensity and exposure to high temperatures affecting the overall heat stress on fish (Volkoff *et al.,*

2020) it would be plausible to consider that fish around Sandes seamount may have endured heat stress during the positive IOD.

Throughout the weaker IOD there were oceanographic processes that are advantageous to fish, such as internal waves. During the negative IOD internal waves were observed propagating over the flanks of Sandes seamount. Internal waves have been observed in previous research conducted at Sandes in 2015 where a combination of tidal conditions, geostrophic and near inertial currents caused the generation of internal waves (Hosegood *et al*, 2019). It has been suggested that internal waves promoted the aggregation of fish schools through the transport of nutrients up the flanks of the seamount onto the summit enhancing the productivity of the seamount attracting apex predators such as silvertip sharks (*Carcharhinus albimarginatus*) (Hosegood *et al*, 2019). From this study, higher numbers of schooling fish were identified over the summit of Sandes throughout the duration of the survey when internal wave activity was present flushing colder water onto the summit. Internal waves transport cold water to the summit of Sandes providing a flushing mechanism allowing fish to endure warmer surface temperatures (Robinson, unpublished data).

More extreme positive IOD events are likely to occur with a warming climate. When coupled with other ocean-atmospheric events in the Indian Ocean, such as the El Niño Southern Oscillation, the effects may be amplified (Cai *et al.*, 2014; Freund *et al.,* 2020; Zhang and Du, 2021). If these events suppress internal wave action and upwelling, there will be minimal relief in the surface waters for fish against abnormally high temperatures. When compounded with other stressors such as hypoxia and acidification, factors that are affecting the oceans globally, we may see species distributions change or new species

adaptations to acclimatise to new levels of stress, but these will likely be at the compromise of other features (Alfonso *et al.*, 2020).

2.5.3 Biological behaviours

The advantage of surveying in two different years allowed a comparison of the regional physical oceanographic regime, in particular, the effect of the IOD on the behaviour and spatial distributions of pelagic fish. However, a drawback of sampling over different time periods may have been unaccounted biological drivers of fish school distributions and behaviours, such as migrations and spawning events. Whilst both surveys were conducted within the Northeast monsoon season, the positive IOD occurred at the beginning of the period whilst the negative IOD survey was conducted at the end of the northeast monsoon period which could affect the composition and abundance of pelagic fish in the region. From the video validation undertaken at Sandes, many mixed species schools were observed with similar species being observed between the two surveys. Due to shortcomings in the validation method, it is likely the full composition of biota over Sandes seamount was not captured due to vessel-avoidance and low sampling effort. The abundance of biota between seasons may have also changed as migrating species were present in the validation footage. Research conducted on the movements of Silvertip sharks in Chagos using satellite tags found that all tagged individuals stayed within the MPA demonstrating that some migratory species have higher residence times within the MPA than has been documented in other open ocean environments (Carlisle *et al.,* 2019). Higher residency times within the Chagos MPA was also observed for silky sharks, sailfish, and yellowfin tuna (Carlisle *et al.,* 2019). This indicates that the migratory patterns of pelagic fish within the Chagos Archipelago are still largely unknown and vary

from populations found in other oceans hence no effect of biological drivers on pelagic biota can be drawn from this study.

Similarly, to migration patterns, observations of spawning events of Indian Ocean fish are absent. Spawning is a biological behaviour that can occur around seamounts (Pitcher *et al.,* 2007) with species such as rainbow runners (*Elagatis bipinnulata*) and bigeye trevally (*Caranx sexfasciatus*) forming large aggregations when this occurs (Pinheiro *et al.,* 2011; Madgett *et al.,* 2022). Research conducted on rainbow runners in the Atlantic Ocean have found they spawn between January and May (Pinheiro *et al.,* 2011). Within the Indo-Pacific Ocean they have been described as year-round spawners with peaks in March (Yesaki, 1979). Without more specific information we cannot comment on the effect of spawning aggregations on the surveys conducted in this study as the spawning behaviour of species observed is not known within the Chagos Archipelago and there is evidence of spatial variability between different populations globally.

Biological behaviours such as migration and spawning would have affected the composition and abundance of pelagic fish at Sandes seamount. Without knowledge of these biological traits the effect of sampling at two different periods cannot be quantified however, with high residency periods of fish observed within the MPA we believe our results are still valid and that the differences in the quantity and spatial variability in schools observed between the two survey periods was most likely driven by the IOD.

2.6 Conclusion

Increased biodiversity has often been recorded around seamounts with multiple mechanisms enhancing the amount of biota such as seamount trapping, feed-rest

hypothesis, concentration of prey and availability of prey (Genin, 2004; Rogers, 2018). Although diversity was not addressed within this body of work, this study emphasises the importance of the concentration and retention of prey brought about by oceanographic currents. Without the presence of the seamount, extreme conditions generated by ocean-atmospheric events may be less tolerable to schooling fish. Flow-topographic interactions around Sandes generate internal waves, aggregate nutrients, and prey, and provide shelter for schooling fish. This provides an advantage to schooling fish from a range of oceanic stressors such as currents, shear, and temperature.

This study undertakes a unique multi-disciplinary approach to investigate both broad and sub-mesoscale oceanographic drivers of spatial fish distributions over Sandes seamount. By recording concurrent oceanographic and fisheries acoustic data, significant physical drivers of fish behaviour were identified. Strong south-westward currents, enhanced by the positive IOD, dictated the location of schooling fish to the eastern flank of Sandes seamount. Whereas a reduction of current strength during the negative IOD saw a wider distribution of schools over the summit and flanks of Sandes. The strength of the currents also affected shear instabilities within the water column with more schools occurring during higher levels of turbulence. Temperature was another factor affecting schooling fish during the abnormal IOD with a homogenous water temperature in the upper 100 m of the water column. The responses of fish to these environmental factors suggest they undertake specific foraging and locomotive behaviours such as station holding, many eyes hypothesis and locomotive efficiency to increase their survival around the seamount. Fish utilise positive flow-topographic interactions, such as the generation of internal waves, and the aggregation of nutrients and prey caused by the topographic blockage in the current flow. Sandes seamount is already included in the

Chagos Archipelago MPA allowing the exclusion of anthropogenic activities from this study. With more extreme climatic events predicted to occur at higher rates in the future, the unique distribution of schooling fish in relation to oceanographic regimes should be further considered when implementing new MPAs and spatial management plans globally.

Chapter 3: Tidal and topographical influences on fish distributions and behaviour around a tropical coral atoll

3.1 Abstract

The Chagos Archipelago Marine Protected Area (MPA) protects 640,000 km^2 of ocean incorporating numerous seamounts, islands, and atolls. This large-scale MPA aims to enhance biodiversity within the region by prohibiting anthropogenic activities, such as fishing, protecting an area that is home to a variety of threatened and endangered species. It is important to understand the oceanographic drivers of high diversity and biota to inform the management of the MPA. Within this study, the fine-scale oceanographic processes that promote pelagic aggregations and biodiversity in the MPA were investigated. With a focus on pelagic fish distributions at two sites around Egmont Atoll, multiple *in situ* variables were measured over repeated transects covering variable topography for 24-hour periods using acoustic instruments. A Simrad ES70 fisheries echosounder with a combined 38/200 kHz transducer was synchronised with a Nortek Signature 100 kHz Acoustic Doppler Current Profiler to collect information on pelagic biota and current flow data throughout the water column, respectively. Tidal dynamics were numerically modelled using MITgcm and validated with in-situ data. Data were analysed using Generalised Linear Models with Generalised Estimating Equations (GLM-GEE) to test if oceanographic and environmental parameters were driving the distribution, abundance, and behaviour of schooling fish around Egmont atoll. The depth of the thermocline between the two surveys varied by 60 m eliciting different responses from schooling fish due to flow topographic interactions. At one survey site biological aggregations were primarily located over two canyons with near vertical walls

descending to 400 m. Fine-scale model simulations of upward vertical current velocities visually correlated with the distribution of schooling fish from acoustic data over these regions. The abundance of schooling fish increased with in-situ peak tidal flow measurements of 0.4 ms^{-1} likely due to the higher current velocities observed in the area. During the ebb tide, the outflow of Egmont lagoon increased the number of biological aggregations similar to results seen in other studies in the region. This multidisciplinary approach identifies fine-scale oceanographic drivers of fish distributions and behaviour that promote biological aggregations and biodiversity around tropical atolls. Comprehending the environmental drivers of biota will allow us to determine the spatial variability of pelagic fish which is key for informing spatial management plans for current and future MPAs.

3.2 Introduction

Ecosystem based management (EBM) is a holistic approach to large scale conservation and management areas (Curtin and Prellezo, 2010). EBM considers the complex links between socio-economic stakeholders and the need for ecological protection on ecosystems. With such a comprehensive scheme recognising both anthropogenic and natural interactions within an ecosystem it is believed that the long-term protection will be effective and beneficial to all stakeholders. This management technique has been gaining popularity with an increase in the number of studies considering the role of environmental conditions on biota. This is prominent in the field of active acoustics, an important tool for elucidating how pelagic ecosystems function (Benoit-Bird and Lawson, 2016). However, balancing the criteria and achieving the desired protections under an EBM scheme has been described as logistically challenging due to the high number of stakeholders and sectors that need to be considered (Ruckelshaus *et al.,* 2008; Link and

Browman, 2017). The advantage of this management technique is the enhanced protection of the pelagic realm and the consideration of temporal changes brought about by oceanographic processes such as tides. Biota respond to oceanographic processes, but the behaviours exhibited can change over space and time if environmental conditions alter. By adopting an approach that protects a whole ecosystem, it accounts for spatial variability in pelagic species distributions brought about by oceanographic conditions.

Within the EBM approach Marine Protected Areas (MPAs) form an ecological tool that strives to protect and conserve nature, often with various restrictions on destructive and disruptive activities. Many MPAs have been designated without implementing a full EBM approach which often makes them insufficient when considering an ecosystem approach as mechanisms driving species diversity, biomass and aggregations need to be understood (Halpern *et al.,* 2010). A crucial part of this is elucidating the local and regional oceanographic drivers of biological aggregations and biodiversity. Protecting large spatial scales of water is useful as it incorporates a greater area where oceanographic process can interact with biological aggregations. Very large marine protected areas (VLMPA) are those MPAs greater than 100,000 km^2 which are likely to be particularly beneficial for mobile species, although long term data sets (>15 years) do not yet exist (Koldewey *et al.,* 2010). VLMPAs can be found globally although overall MPAs (VLMPAs together with smaller MPAs) currently protect only 8% of the global ocean (UNEP-WCMC and IUCN, 2023). Many of these sites are located around islands where flow topographic interactions regularly occur but many are undocumented (Hays *et al.,* 2020). The Chagos Archipelago MPA, located in the central Indian Ocean (Figure 3.1) covers 640,000 km^2 of ocean, and is classed as one of the largest VLMPAs in the

world (Hays *et al*., 2020). Within the MPA, 58 islands and atolls are located including Egmont atoll (11 x 4.5 km) on the western edge of the Archipelago near Great Chagos Bank. The MPA was created in 2010 as a no-take zone and has been described as a pristine marine environment with minimal anthropogenic disturbances due to its remote location (Readman *et al*., 2013). The Chagos Archipelago is home to a diverse range of pelagic species (Sheppard, 1999; Hays *et al*., 2020) with some atolls, such as Egmont, identified as aggregation sites for species such as reef manta rays (*Manta alfedi*) which are classified as vulnerable on the IUCN red list (Harris *et al.,* 2021; IUCN, 2023). Studies at Egmont Atoll have linked pelagic biomass to oceanographic processes such as tidal movements and internal waves however these processes are still not fully understood largely due to the size of the Chagos Archipelago with makes monitoring and policing the VLMPA expensive and logistically challenging (Sheehan et al., 2019; Harris *et al.,* 2021). If the oceanographic drivers of the spatiotemporal distribution of pelagic biomass can be determined, then more specific and efficient protections can be implemented over large spatial scales.

Linking physical and biological drivers to the spatiotemporal distribution and behaviour of pelagic organisms is complex. The complexity of this issue is intensified when topographic features such as islands, seamounts and banks impede or interact with current flow (Lavelle and Mohn, 2015; Borland *et al.,* 2021; De Falco *et al.,* 2022). Interactions between currents and physical features can initiate unique oceanographic processes affecting the spatiotemporal distribution and behaviour of pelagic fish (Embling *et al.,* 2013). Fish behaviour is affected by oceanographic conditions such as current speeds (Belyaev and Zuev, 1969), turbulence (Hockley *et al*., 2014) and temperature changes (Clarke & Johnston, 1999; Alfonso 2020; Volkoff *et al.,* 2020). The

combination of these properties create features such as thermoclines and scattering layers through stratification. Thermoclines are a transitional layer between different water temperatures. The interaction of a thermocline with bathymetric features, such as atolls, is important due to the generation of physical processes such as cold-water flushing (Shea and Broenkow, 1982; Walter and Phelan 2016), internal tides (Sharples *et al.,* 2009) and vertical advection (Williams and Follows, 2011). Within coastal seas, turbulent entrainment is responsible for the input of nutrients into the euphotic zone enhancing plankton populations and providing foraging sites for predator species (Estrada and Berdalet, 1997). When combined with chemical and nutrient inputs from land run-off and seabirds, enhanced primary, and secondary productivity are observed which support pelagic fish (Graham *et al.,* 2018; Benkwitt *et al.,* 2020). These processes are vital in oligotrophic waters where topographic features have been identified as biological hotspots (Worm *et al.,* 2003; Hosegood *et al.,* 2019; Harris *et al.,* 2021).

Variability in fish distributions can arise from physical processes, diel differences, and tidal variations (Brierley, 2014). Diel vertical migration (DVM) is commonly triggered by light affecting the vertical distribution of zooplankton and fish; in-turn affecting predator-prey interactions (Brierley, 2014). The tidal-coupling hypothesis, the link between tidal hydrodynamic movements, plankton, and fish (Zamon, 2003) in nearshore environments has been shown to be important in determining the movements and behaviours of pelagic fish and predator-prey interactions (Dänhardt and Becker, 2011; Benoit-Bird *et al.,* 2019). High current velocities resulting from semi-diurnal tidal flows, can be detrimental to the locomotive ability of fish although the impact of increased current speeds depends on fish size and physiological abilities (Williamson *et al.,* 2019). Negative effects of high current velocities on fish include reduced energy levels and swimming

speeds (Williamson *et al.,* 2019). Over a longer time period, spring-neap tidal cycles affect the behaviour of fish with increased observations of schooling fish during high amplitude internal waves throughout a spring tide (Embling *et al.,* 2013). Currents associated with tides can transport nutrients, plankton and other small micronekton (Castro and Huber, 2010). Under ideal conditions, if the current flow is impeded by an island an accumulation of nutrients and plankton can aggregate creating foraging hotspots that support forage fish and apex predators- known as the Island Mass Effect (Doty and Oguri, 1956). Within these aggregations, schooling may be used as a foraging mechanism to increase the foraging success rate of fish through the many eyes hypothesis (Lack, 1954; Ward *et al.,* 2011) and imitation behaviour (Pavlov and Kasumyan, 2000). Schooling can also be used for predator avoidance, locomotive efficiency, and reproduction (Belyaev and Zuev, 1969). This study aims to determine physical drivers of fish aggregations around Egmont Atoll to help understand the role the atoll plays in supporting pelagic species within the wider oceanographic context. In-situ data collected from two survey sites with contrasting conditions are considered to understand changes in the distribution and behaviour of schooling fish. Understanding mechanisms driving pelagic biota will inform MPA management from a holistic EBM approach. Recognising flow topography interactions and their role in driving biodiversity hotspots are vital for optimising the efficiency of MPAs.

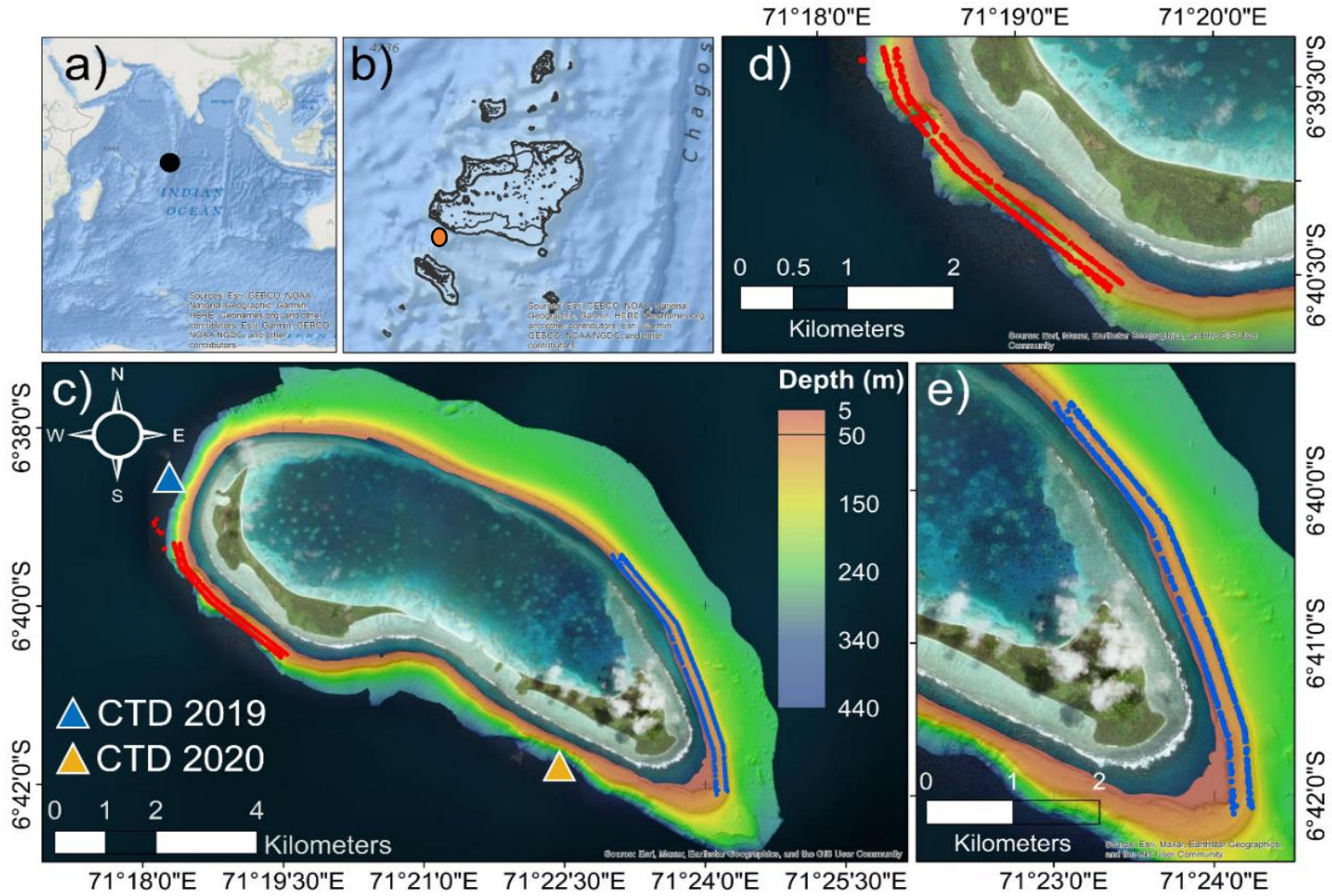

Figure 3.1: Map of Egmont Atoll with multibeam bathymetry overlaid on satellite imagery with CTD and acoustic sampling locations (c) showing its geographical location in a) the Indian Ocean and b) Chagos Archipelago (orange circle). The location of survey 1 (d) is shown in red with survey 2 (e) transect shown in blue.

3.3 Methodology

3.3.1 Survey area

Two surveys were conducted around Egmont Atoll, a coral atoll consisting of 9 small islands linked via a sand bank, in the Chagos Archipelago aboard MV *Tethys Supporter* (Figure 3.1). The first, conducted over a 36-hour period between the 27th and 29th November 2019 was undertaken in the Ile Sipaille region of Egmont Atoll (Figure 3.1d). The second, conducted over 24 hours between the 11th and 12th March 2020 at the south-eastern tip (Figure 3.1e). Herein the surveys will be referred to as Survey 1 (November 2019) and Survey 2 (March 2020). The study site of survey 1 is located to the Northwest of Egmont atoll and at the time of the November 2019 survey was on the lee side of the atoll to the prevailing westward current which is usual for the south-easterly monsoon (Figure 3.1d; Robinson *et al.,* unpublished). The topography at Ile Sipaille is characterised by steep underwater cliffs starting approximately 500 m from the shoreline and descending from 70 m to depths of over 400 m within 1 km of the shoreline. The transect covered a range of depths from shallower regions at 70 m to deeper areas with a maximum depth of 400 m. During March 2020 a site south of Manta Alley, near the lagoon, was investigated with a focus on the 50 and 100 m depth contours (Figure 3.1e).

Tides around Egmont Atoll are described as mixed and asymmetric (Figure 3.2; Robinson *et al.,* 2023). On a regional scale, oceanographic processes around the atoll may be influenced by the Indian Ocean Dipole (IOD) and Madden-Julian Oscillation (MJO) which are regional based ocean-atmospheric events affecting the wind field and sea surface temperatures across the Indian Ocean.

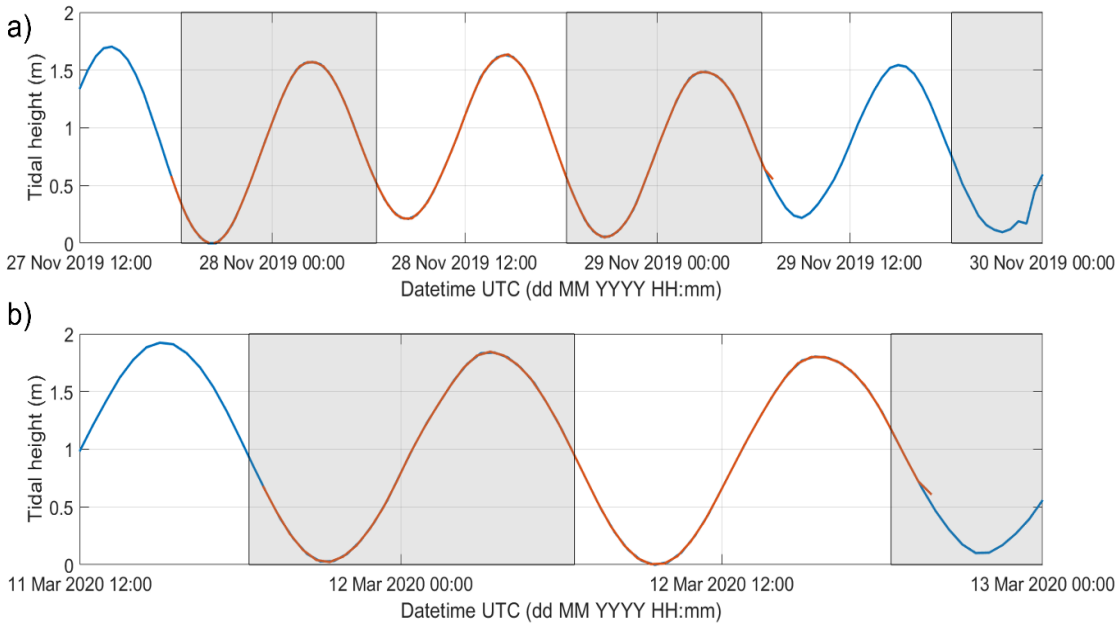

Figure 3.2: Tidal height (blue) of a) survey 1 in November 2019 (orange) and b) survey 2 in March 2020 (orange) with the grey boxes representing night in UTC.

3.3.2 Data collection

A pair of transect lines was sampled continuously throughout the survey period with each iteration requiring approximately one hour to complete. Synchronised pole mounted fisheries acoustics and acoustic doppler current profiler (ADCP) data were collected using a Simrad single beam ES70 combined 38/200kHz transducer and Nortek Signature 100 kHz ADCP. ES70 and ADCP data were collected and timestamped in UTC. Custom software allowed synchronisation of the ES70 and ADCP, triggering the ADCP to ping at 1 Hz in between ES70 pings reducing interference between the two acoustic devices (Williamson, 2019). Acoustic settings were kept consistent, throughout both surveys (Table 3.1). Both ES70 frequencies had a vertical resolution of 0.2 m while the 38 kHz and 200 kHz had a horizontal resolution of 1.85 m and 2.2 m respectively due to the beamwidth of the acoustic pulse. Global navigation satellite system (GNSS) data were collected and matched to the acoustic data using a Nortek GNSS unit providing accurate position data. To reduce noise in the data the ES70 was powered externally to the ship using independent batteries.

Validation of acoustic data was conducted during both surveys at opportunistic times to verify that biological interpretations of acoustic data were correct. Using a GoPro Hero 4 attached to a CTD, video data were collected throughout the water column and analysed by visually identifying species present and matching it with the time and depth of the CTD and ES70 data.

Table 3.1: Acoustic settings for the ES70 for each survey.

Survey Name	Survey Number	Frequency settings					
		38 kHz			200 kHz		
		Pulse length (ms)	Ping mode	Power (W)	Pulse length (ms)	Ping mode	Power (W)
November 2019	1	0.512	Maximum	1000	1.024	Maximum	200
March 2020	2	0.512	Maximum	1000	1.024	Maximum	200

3.3.3 Acoustic calibration

Standard calibration procedures were followed for the ES70 calibration (Demer *et al.*, 2015; Foote, 1987). The same calibration offsets were applied to both datasets due to no calibration being undertaken in 2019. During March 2020 at Il Lubine, Egmont Atoll a tungsten carbide (WC) 38.1 mm diameter calibration sphere was positioned 7.7 m below the transducer. A conductivity, temperature, and depth (CTD) profile was undertaken during the calibration to provide the sea temperature and salinity data required. The data were processed using ES60adjust (CSIRO, 2016) and Echoview v.11 (Echoview Software Pty Ltd, 2020) to remove the triangular wave error sequence (TWES) and correct for transducer depth and geometry. Using the Echoview Calibration Assistant the

area backscattering coefficient (Sa) correction value was calculated for the 38 kHz (S_a = -0.5769 dB) and 200 kHz (S_a = -0.5316 dB) transducer.

3.3.4 Hydrodynamic numerical model

Tidal dynamics were numerically modelled around Egmont atoll using the nonlinear nonhydrostatic Massachusetts Institute of Technology general circulation model (MITgcm; Adcroft *et al.,* 2023). Model resolution was 5 and 25 m in the vertical and horizontal planes respectively. Bathymetry at Egmont Atoll was collected in-situ with a multibeam echosounder in 2019 to depths of 400m with greater depths interpolated to match GEBCO bathymetry. Simulation of the model was run over 16 days allowing for a spin-up of one day and then 15 days of data prediction applying Orlinski-type boundary conditions to exclude the reflection of barotropic waves. Comparison of TPXO inverse tidal model predictions (Egbert *et al.,* 2002) and in-situ ADCP data showed comparable tidal harmonics which were applied to the model using a methodology by Vlasenko and Stashchuk (2021).

3.3.5 ES70 Data Processing

Data were processed in Echoview V12.1 (Echoview Software Pty Ltd, 2021) by importing and correcting the profiles using the calibration factors obtained during the calibration. Offsets between the transducer, GNSS system and pole mount were added in reference to the vessel. The surface 15 m and bottom 5 m of data were removed from analysis due to the increased presence of noise and interference associated with these regions (Simmonds and MacLennan, 2005). When visually comparing the data, it was noticed that artifacts were introduced during the turns on the transect, therefore, all turn data was removed from further analysis.

Noise reduction of the data was undertaken using Echoview's background noise removal, transient noise filter and impulse noise filter (De Robertis and Higginbottom, 2007; Ryan *et al.,* 2015). Data were split into day and night periods to account for changes in the mean volume backscattering strength (S_v) due to diel vertical migration (DVM). Day periods were set as between 06:30 to 18:20 (UTC+5) and night periods set to 18:20 to 06:30 (UTC+5) based on nocturnal DVM movements. Thresholds of -66 dB and -63 dB for the day and night respectively were applied to remove plankton and the presence of sediment on the echogram although this restricted comparisons between day and night periods throughout the surveys. A median 3x3 filter and 5x5 dilation filter were applied allowing better detection of schools using the inbuilt fish school detection algorithm SHAPES (Barange, 1994; Coetzee, 2000; Diner, 2001) which was applied to the data using the minimum fish school size parameters based on the resolution of the data and previous studies (Aronica *et al.,* 2019; Campanella and Taylor, 2016; Fernandes, 2009). These parameters were: minimum total school height of 0.20 m, minimum candidate length of 2.22 m, minimum candidate height of 0.20 m, maximum vertical linking distance of 1.00 m, maximum horizontal linking distance of 8.00 m and minimum total school length of 8.00 m. Variables were exported in 1-minute timed bins to MATLAB R2021a (Table 3.2; MathWorks, 2022) where the dataset were cleaned and averaged over the entire water column within each 1-minute bin.

Table 3.2: The fish school behavioural variables exported from Echoview per 1-minute ensembles.

Variable name	Unit	Description
S_v	dB re 1 m^{-1}	Mean of volume backscattering strength.
NASC	m^2nmi^{-2}	Mean of nautical area scattering coefficient.
perim	m	Mean perimeter of fish schools.

3.3.6 Oceanographic data

Upon reviewing the ADCP data, the November 2019 collection period only lasted for 20.5 hours due to technical issues. Current velocities were recorded as eastward and northward components, U and V, respectively. Raw data comprised of single ping ensembles with a ping rate of 0.5 Hz that were subsequently cleaned with a median filter to remove anomalous spikes and smoothed with a running average filter before being averaged into 1-minute bins to match that of the ES70 data (Table 3.3). Using the averaged ADCP data values vertical shear was derived using the equation:

$$S^2 = \frac{\delta u^2}{\delta z} + \frac{\delta v^2}{\delta z}$$

Where, u is the east velocity component, v is the north velocity component and z is the depth. CTD data was collected during both surveys with cleaning and smoothing applied in Matlab (Figure 3.1).

Table 3.3: The environmental variables calculated and derived from the ADCP and oceanographic moorings data per 1-minute ensembles.

Variable name	Unit	Description
Time	Cyclic	Cyclic time of day.
TimetoTideTurn	Cyclic	Cyclic time between high and low tides.
AbsShear	s^{-1}	Absolute shear over the entire water column.
U	cm s^{-1}	U component of velocity.
V	cm s^{-1}	V component of velocity.
SeafloorDep	m	Maximum depth of the seafloor below the vessel.

3.3.7 Data Analysis

Three biological response variables were selected to be tested against oceanographic explanatory variables to model the distribution and behaviour of schooling fish at both sites at Egmont Atoll. Separate analyses were conducted for each survey testing (1) the

number, (2) nautical area scattering coefficient (NASC) and (3) perimeter of fish schools per 1-minute bin in relation to oceanographic variables. These variables were chosen to represent the distribution and behaviour of schooling fish with NASC used as a proxy for relative biomass and perimeter incorporating both the x and y dimensions of the fish school size. Separate models were created for day and night periods due to the different thresholds set which accounted for differences in backscatter due to DVM.

Using only the 38 kHz frequency, which is optimal for identifying fish schools, data were tested for zero inflation, heteroscedasticity, normality, and autocorrelation in R V.4.3.1 (R Core Studio, 2023; Zuur *et al.,* 2010). Due to high levels of autocorrelation Generalised Linear Models with Generalised Estimating Equations (GLM GEE) were chosen using the geepack library in R (Højsgaard *et al*., 2005; Pirotta *et al.,* 2011). A Poisson distribution was used for analysis (1) with a Gaussian distribution applied to the behavioural analyses (2) and (3). The COR AR1 correlation structure was chosen to account for temporal autocorrelation in the data (Pirotta *et al.,* 2011). To account for spatial autocorrelation a fixed term was added to the model identifying the transect number (blockid= TransectID). All variables were tested as linear and smooth with QIC scores determining their form in the model (Pan, 2001). For smooth variables cubic *B-splines* were implemented using the Spatially Adaptive Local Smoothing Algorithm (SALSA) to determine the optimum number of knots and positions for each variable (Walker *et al.,* 2010; Scott-Hayward *et al.,* 2013). The range of knots was limited to 5 for the Poisson model and 4 for the Gaussian models to reduce under or overfitting of the model. Wald's tests were used to determine significance, with partial plots produced for each variable with the response scaled by the link function. Model validation was conducted at all

stages to ensure the optimum model, correlation structure and variables were included with the final model tested through residual analysis (Hardin and Hilbe, 2002).

3.4 Results

3.4.1 Interannual changes in oceanographic regime

During survey 1 in November 2019 the IOD was in a positive phase, whilst in a negative phase during survey 2 in March 2020. The thermocline was detected at 100 m depth during survey 1 and at approximately 45 m for survey 2 (Figure 3.3). During both surveys the sea surface temperature was above 29 °C. The temperature in the water column was above 28 °C in the upper 100 m during survey 1. In comparison, only the upper 45 m was above 28 °C during survey 2.

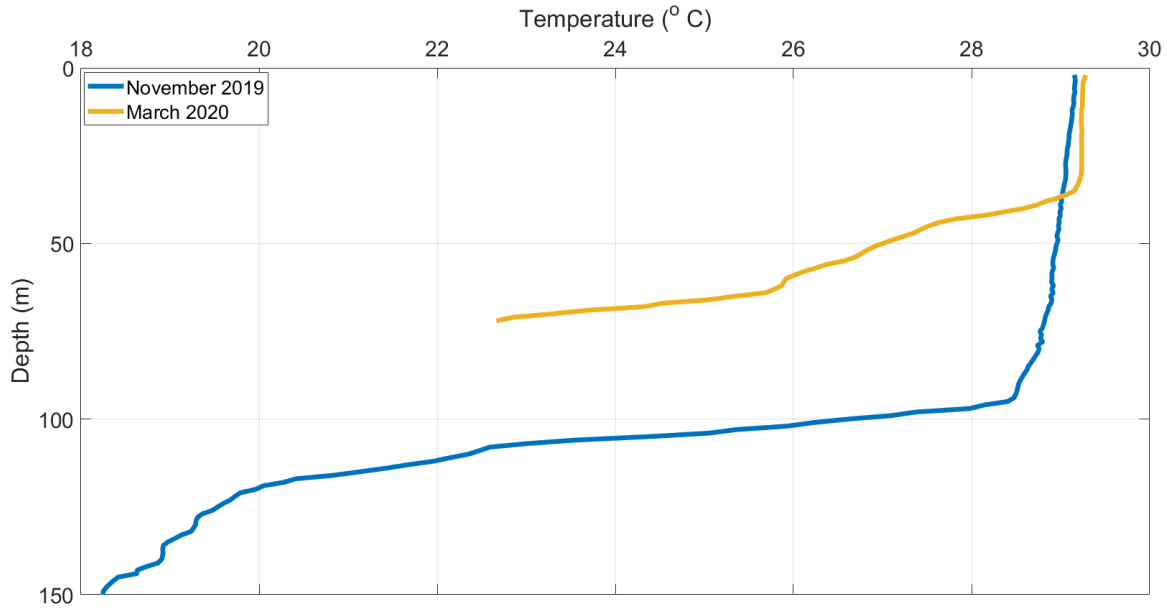

Figure 3.3: CTD profiles showing the deep thermocline during survey 1 in November 2019 (blue) and the shallower thermocline in March 2020 (yellow) during survey 2.

3.4.2 Fish school distributions

Validation of acoustic data was only undertaken during survey 1: silvertip reef sharks and snapper species were observed (see Figure B1 in appendix B). A total of 8688 and 4771 schools were identified across survey 1 and 2 respectively (Tables 3.4 and 3.5).

Throughout survey 1, 7107 schools were identified at night when the -63 dB threshold was applied with only 1581 observed during the day with a -66 dB threshold. This split was more evenly spread during survey 2 with 2743 and 2028 schools during the day and night respectively. The mean number of schools observed per one-minute bin during the day was 1.6 and 2.5 for survey 1 and 2 respectively. Mean NASC values, which relate to relative biomass were 345.7 and 41.8 for survey 1 and 2 respectively, likely showing denser schools during survey 1. The mean perimeter size of schools varied between the different surveys with the largest school sizes observed with a perimeter of 1071.9 m during the night on survey 2. A total of 12 statistical models (see appendix B for full model results) were conducted using count, NASC and perimeter size as biological response variables highlighting seafloor depth, tide, and absolute shear as the most common significant variables (Table 3.6). Whilst shear was significant on 54% of the models conducted, partial plots produced large confidence intervals limiting the graphical interpretation of this variable.

Table 3.4: Summary of exported fish schools from Echoview used for statistical analysis.

Survey	Effort (hours)	Total number of schools per hour	Total number of schools	Total day schools	Total night schools	Total 38 kHz schools
Survey 1	24.50	362.00	8688	1581	7107	6646
Survey 2	25.27	188.80	4771	2743	2028	2660

Table 3.5: Summary of exported fish schools at 38 kHz from Echoview used for statistical analysis showing the mean value for each response variable within each model with the standard deviation in brackets.

Survey	Time	Count (sd)	NASC (m^2nmi^{-2}) (sd)	Perimeter (m) (sd)
Egmont 24hr	Day	1.57 (1.89)	345.73 (1038.02)	825.47 (1997.51)
	Night	3.86 (4.02)	209.51 (632.12)	399.55 (1056.58)
Egmont 36hr	day	2.44 (3.04)	41.78 (122.27)	391.47 (1457.02)
	night	1.14 (1.45)	50.08 (114.55)	1071.89 (3733.69)

Table 3.6: Percentage of occasions when the explanatory variable was significantly modelled from each survey.

Survey	Number of models	Explanatory variables					
		U (%)	V (%)	AbsShear (%)	seafloorDep (%)	TimetoTideTurn (%)	Time (%)
1	12	33	58	58	83	58	42
2	12	8	42	50	58	50	33
Total	24	21	50	54	71	54	38

3.4.3 Topographic drivers of fish

Bathymetry between the surveys varied with steep gradients of up to 87° at submarine canyon sites throughout survey 1 (Figure 3.4a and b). In contrast, relatively flat and shallow bank environments with gradients of no more than 45° were observed during survey 2 (Figure 3.4c and d). The depth of the survey sites varied with a maximum depth of 440 m observed for survey 1 and 200 m for survey 2.

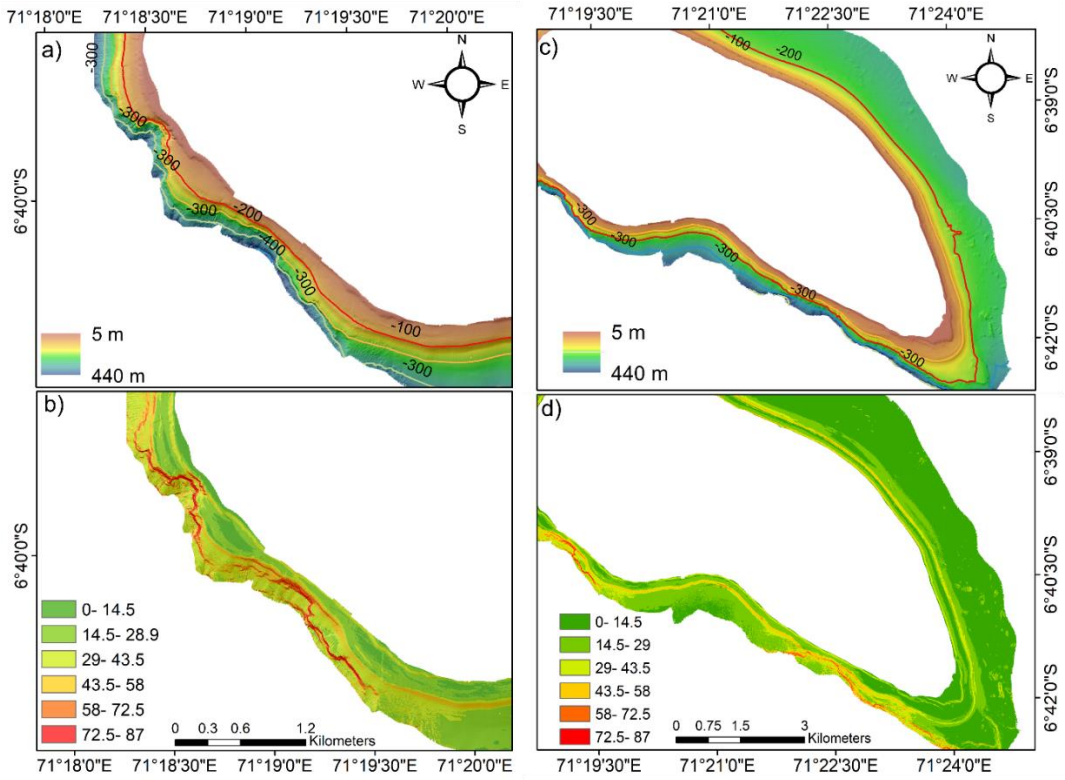

Figure 3.4: Bathymetry of Egmont Atoll showing a) multibeam bathymetry and b) derived slope (in degrees) from survey 1. c) Multibeam bathymetry and d) derived slope (in degrees) from survey 2.

Fish distributions changed in relation to water depth. Depth was significant in explaining both response variables at night ($p<0.01$) allowing a comparison of schooling behaviour between the two surveys (see Tables B1, B2 and B3 in appendix B). In survey 1, the NASC of schools decreased in shallower waters and gradually increased to a maximum when the seafloor was at 210 m depth (Figure 3.5a). In survey 2 NASC decreased with depth (Figure 3.5b). The perimeter of fish schools also mirrored this effect but with a minor peak over seafloor of a depth of 100 m during survey 2 (Table 3.5; Figure B2). Only night periods could be graphically compared as seafloor depth was not significant during the day for survey 2 (see Table B2 in appendix B).

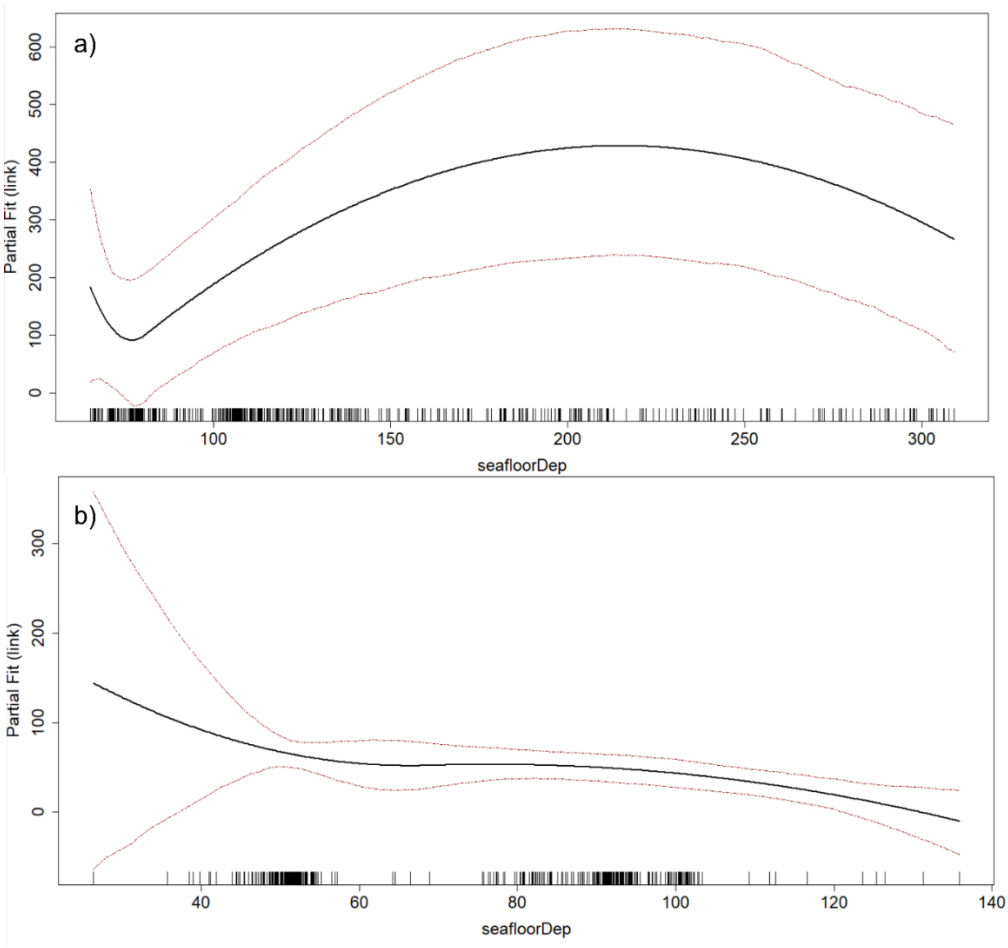

Figure 3.5: The NASC (38 kHz) fish schools at night against seafloor depth (metres) from GLM-GEE models from a) survey 1 and b) survey 2 with the red lines at 95 % confidence intervals and rug plots showing the distribution of the raw data.

Correlations between the bathymetry and fish school aggregations were observed with an increase in the number of fish schools aggregated over the canyons in survey 1 (Figure 3.6). This distribution was emphasised at night with counts of up to 17 schools identified per bin (Figures 3.6a and b). During the second survey there was no relationship between bottom depth and school presence with even distributions over both the 50 and 100 m contours (Figures 3.6c and d). However, during survey 2 higher numbers of fish schools (up to 15 per bin) were identified throughout the day compared to at night (Figures 3.6c and d).

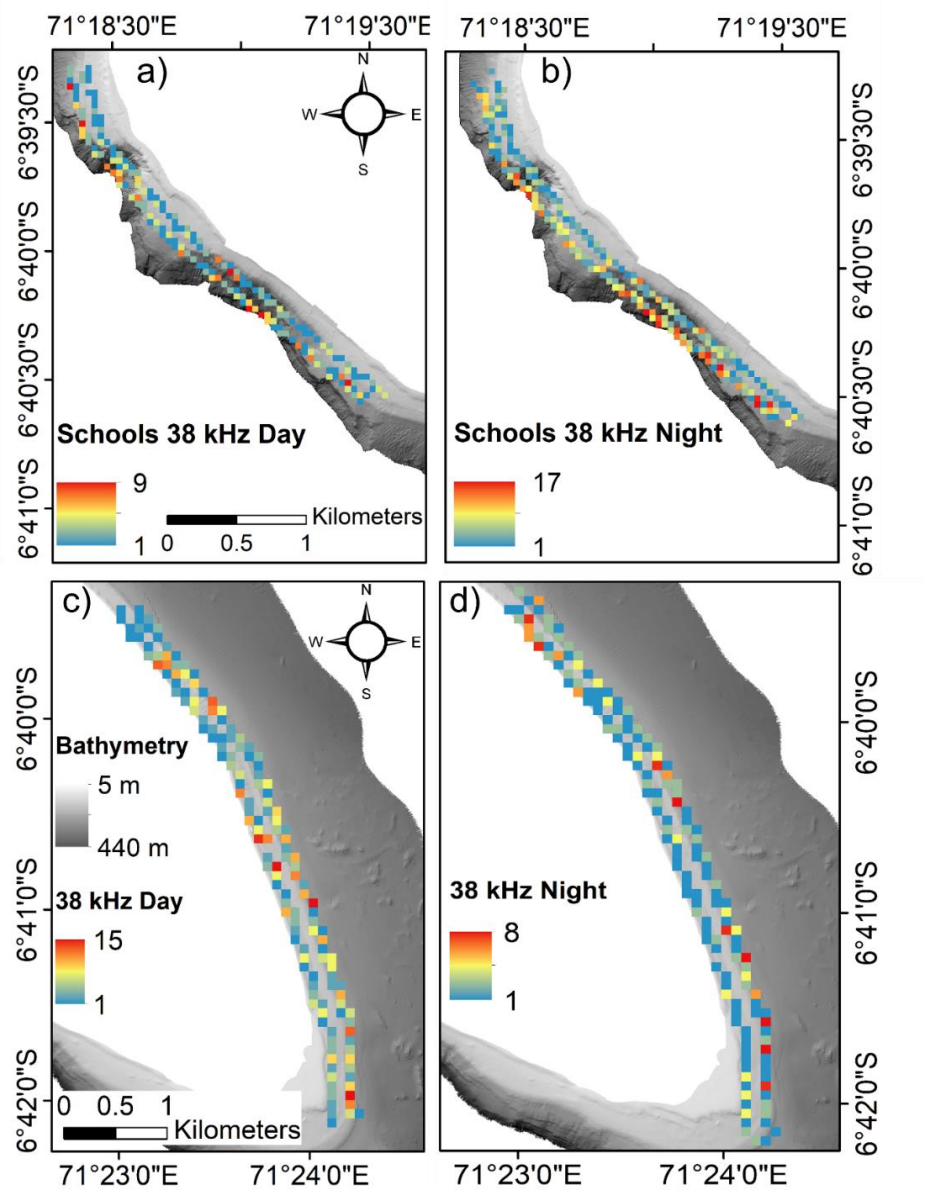

Figure 3.6: The count of fish schools identified at 38 kHz overlaid on bathymetry of Egmont Atoll during survey 1 a) day, b) night and survey 2 c) day and d) night.

3.4.4 Tidal phase influences on fish distribution

Tidal phase was the second most dominant driver of schooling fish when modelled. When investigated, tidal flows could be directly related to U and V velocity components which were significant explanatory variables for the behaviour and count of schooling fish (see Tables B1, B2 and B3 in appendix B). The U velocity component was primarily significant during survey 1 and was plotted as a tidal curve- no deviation from the central point was observed signifying there was no influence on the data from background

currents brought about by the IOD (see Figure B3 in appendix B). A tidal curve plotted against the U and V velocity components from the synchronised ADCP, showed that south-eastward currents were dominant during the flood tide throughout survey 1 (Figure 3.7). When modelled with GLM-GEEs, V was highly significant ($p<0.001$) with the number of fish schools increasing in northward currents; this direction relates to the ebb tide (Figures 3.7 and 3.9a). When the influence of the U velocity component on NASC is evaluated, an increase in U correlates with a similar increase in NASC as currents move eastward peaking at approximately 40 cm s^{-1} aligning with the timing of the flood tide (Figure 3.8).

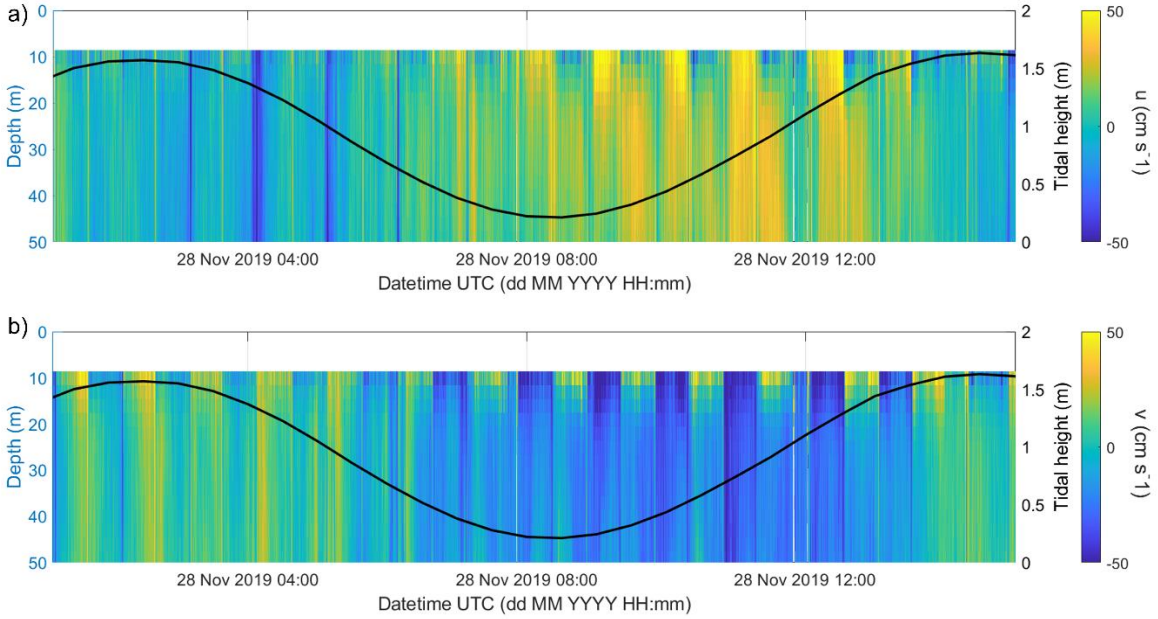

Figure 3.7: ADCP data from survey 1 showing a) U and b) V velocity component with the tidal height overlaid.

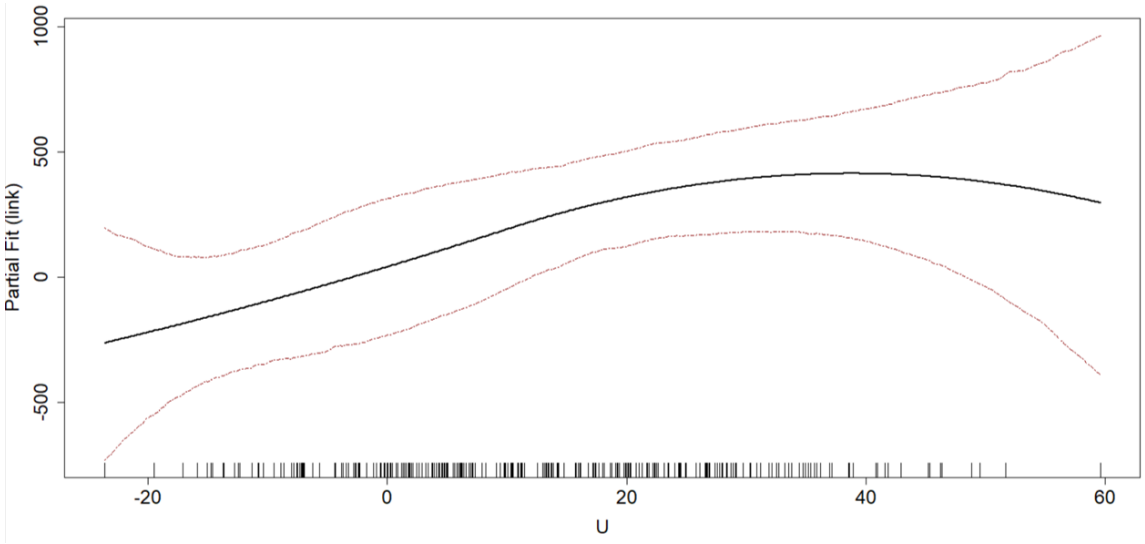

Figure 3.8: The u velocity (cm s^{-1}) component from survey 1 with the response variable of 38 kHz NASC of fish schools during the day. Red lines indicate 95 % confidence internals and rug plots show the distribution of the raw data.

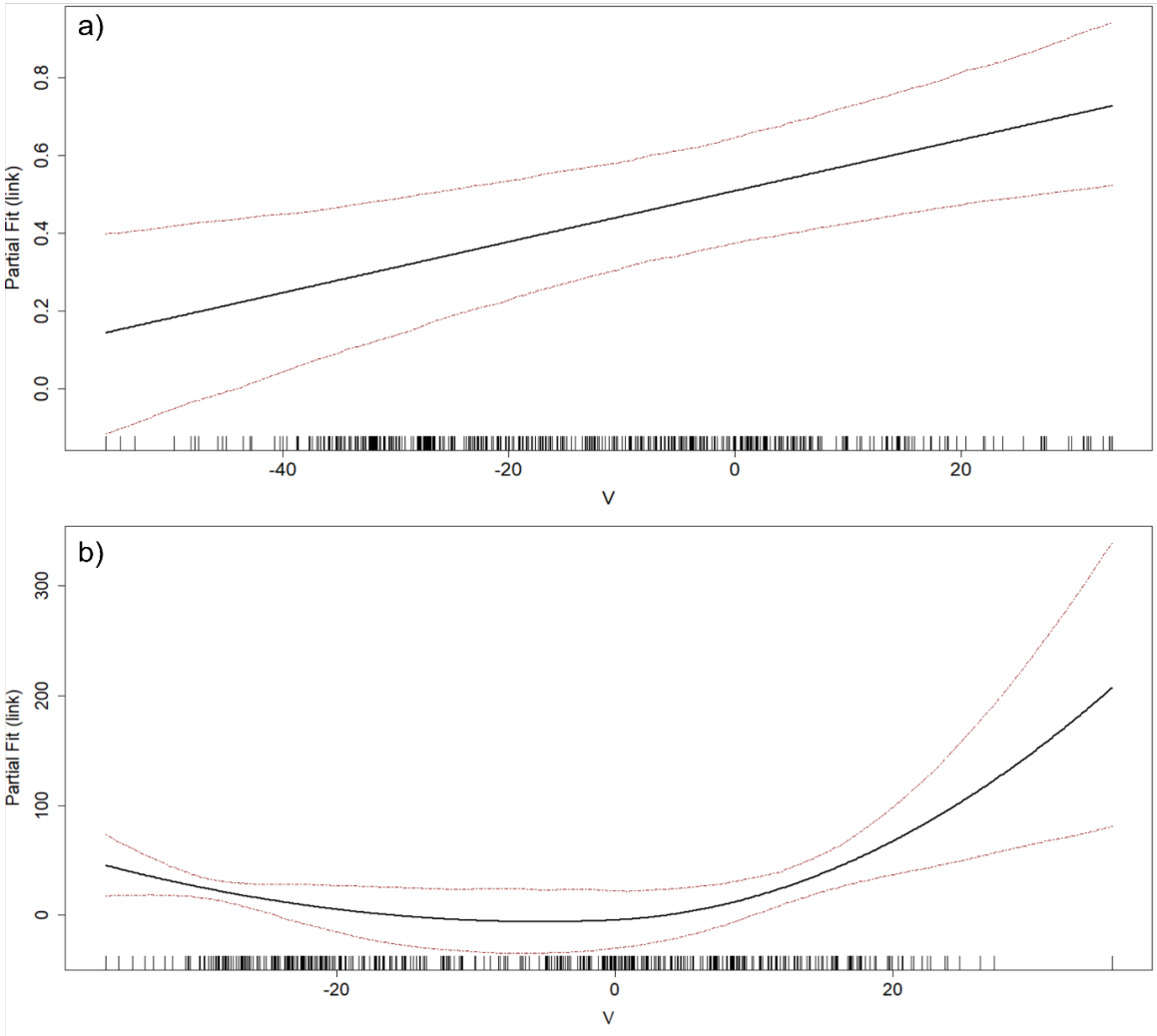

Figure 3.9: The v velocity component (cm s^{-1}) from a) survey 1 with the response variable of 38 kHz count of fish schools during the day and b) survey 2 with the response variable of 38 kHz NASC of fish schools during the day. Red lines indicate 95 % confidence internals and rug plots show the distribution of the raw data.

During survey 2, the U velocity was observed at a weaker strength and was only significant on the school count analysis at night ($p<0.05$). In contrast, the V velocity component was significant accounting for 63% of the behaviour models for survey 2. As with survey 1, the flood tide moved in a south-eastward direction throughout survey 2 (Figure 3.10). Higher NASC values was modelled to occur in northward currents above 20 cm s^{-1} during the ebb tide (Figure 3.9b).

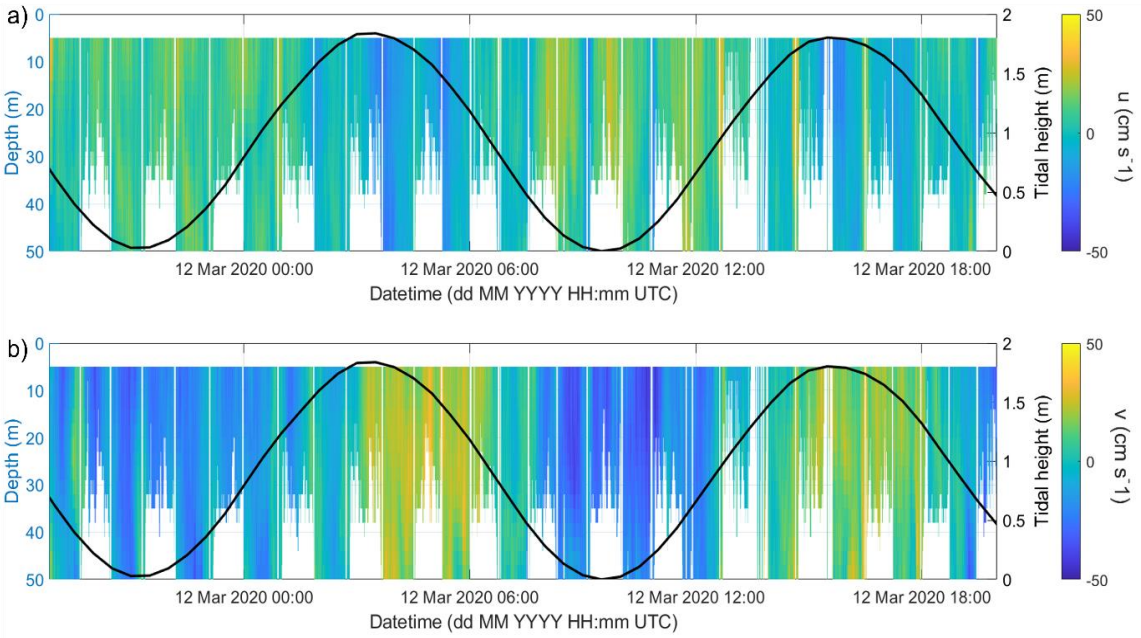

Figure 3.10: VMADCP data survey 2 showing a) u and b) v velocity component with the tidal height overlaid.

Data from the hydrodynamic model compared the sum of vertical velocities in 3 m bins throughout the water column to the distribution of schooling fish for survey 1. Net values from the water column which were either upward or downward vertical motion were identified at key sites along the transect and overlaid on top of the residual current (Figure 3.11a). These sites were located over the slopes of the canyon regions and towards the north-western tip of the transect. Visual correlations between ES70 data and MITgcm modelled data showing similar patterns in the backscatter and vertical velocities over the same sampling period (Figure 3.11b and c).

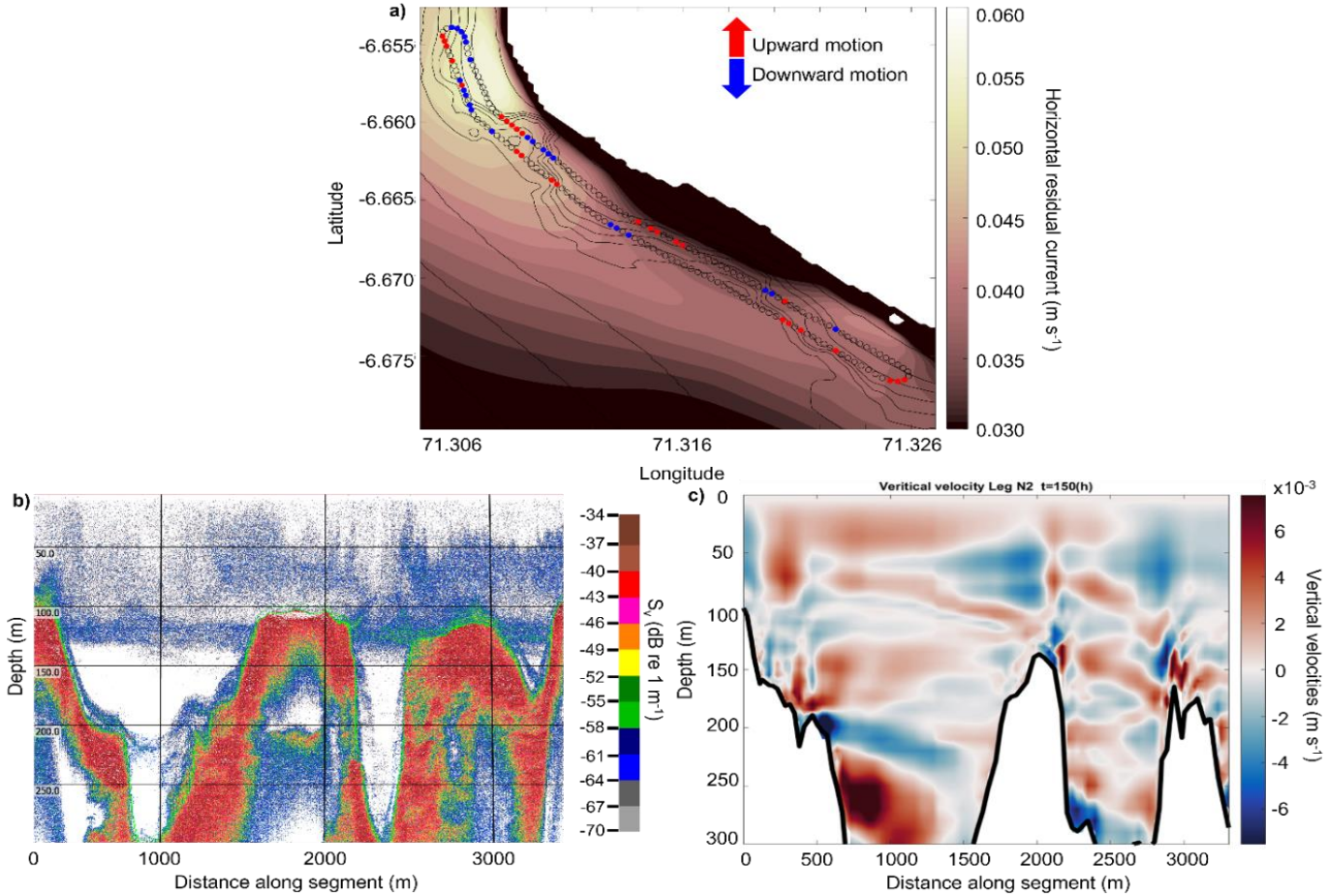

Figure 3.11: Data from the hydrodynamic model showing a) the horizontal residual current over a two-week period overlaid with U*dH/dx data along the transect of survey 1 at Egmont Atoll. Red circles represent net movement of water upwards. Blue circles show downward movement of water. B) ES70 data at 38 kHz over one transect with the bright red backscatter replicating the seafloor and c) MITgcm modelled data showing the vertical velocities over the same transect.

3.5 Discussion

Current flow around Egmont Atoll was a significant driver in the aggregation and behaviour of schooling fish throughout both surveys. The IOD was responsible for the deepening of the thermocline during survey 1 but had no effect on current magnitudes or direction around Egmont Atoll during either survey. The depth of the seafloor was significant in eliciting higher aggregations of schooling fish suggesting that the varying topography combined with currents affected the presence and behaviour of schooling fish. Whilst the tidal regime stays consistent over different seasons, schooling fish may utilise topographic features around Egmont Atoll for behavioural advantages. Although the surveys in this study were conducted at different sites, tidal dynamics were similar with south-eastward flood tides. Tidal flows increased in current strength during flood and ebb periods affecting the distributions of fish as schooling is used during high current magnitudes as a mechanism to improve locomotive efficiency (Genin, 2004). GLM-GEE modelled data presented in this study suggests increased schooling numbers during the ebb tide for both surveys. This discussion presents three reasonings for this 1) the orientation of Egmont atoll, 2) flow topographic interactions and 3) the outflow of Egmont lagoon.

Oceanic atolls act as a barricade in the current flow, deflecting currents, both regional and local, around the atoll creating sheltered environments from prevailing currents. Positioned below the northern tip of Egmont Atoll, the site of survey 1 is secluded from south-westward currents (Figure 1). From the statistical models both the east (U) and northward (V) currents were significant in driving school presence and behaviour during survey 1, but these correlate with different phases of the tide -the eastward flow relates to the flood tide and the northward flow to the ebb. Due to the location of the surveys

sites currents from certain directions are restricted due to land mass impeding the flow of currents. Both the ebb and flood tide increase current strengths in the water column which can affect the swimming ability of schooling fish (Belyaev and Zuev, 1969; Williamson *et al.,* 2019). During the flood tide on survey 1, higher NASC values were observed suggesting the increase in current strength with the flood tide either caused more fish to school or smaller schools to combine into larger schools to improve their hydrodynamic efficiency which has been observed at other tidally dominant sites (Williamson *et al.,* 2019; Couto *et al.,* 2021). However, there was no evidence from the perimeter models to support this conclusion.

Survey 2 was located on the opposite side of Egmont atoll, sheltered from north-eastward currents. Statistical GLMGEE models suggest denser and larger schools develop during northward currents throughout the ebb tide. Also occurring during the ebb tide is the outflow of the lagoon which is located at the northern end of the transect for survey 2 (Figure 3.1). Oceanic flushing of lagoons in the Chagos Archipelago has previously been studied focussing on the role of zooplankton with lower abundances of plankton found on the outer regions of lagoons except for at Egmont Atoll (Sheehan *et al.,* 2019). The southeast of Egmont was recorded to have a greater abundance of plankton which may aggregate due to the ebb tide (Sheehan et al., 2019). This is supported by oceanographic data suggesting that tidal pulses are linked to the movement of zooplankton in and out of Egmont lagoon from a study focussing on manta ray feeding sites (Harris *et al.,* 2021). This study suggested cold water bores increased zooplankton concentrations in the lagoon during the flood tide which then flow out of the lagoon during the ebb tide (Harris *et al.,* 2021). Enriched abundances of plankton may aggregate smaller forage fish and in turn create a site where larger fish occur with

schooling used to improve foraging success rates. Both studies suggest tidal movements are key drivers in zooplankton distributions with other oceanographic processes such as internal waves also suggested to cause the aggregation of plankton at the lagoon (Sheehan *et al*., 2019). This differs from the manta ray study which suggested Langmuir circulation may also transport and concentrate patches of zooplankton (Harris *et al.,* 2021). No internal waves or Langmuir circulation were identified in this study to support the retention of plankton through these mechanisms however, this study does support previous work in suggesting that tidal influences directly affect biota aggregations around Egmont Atoll. This is likely due to the survey design and locations, which was chosen due to inclement weather and sea conditions during both survey periods. Transect lines were conducted parallel to the shore, where there was adequate shelter from severe weather, but they were unsuitable for the detection of internal waves which propagate perpendicular to bathymetry. Further research is required to understand the retention processes of small plankton and prey fish as these aggregations feed into the food web driving pelagic fish distributions.

Currents around Egmont Atoll were not affected by the IOD during either survey. The IOD was in positive phase during survey 1 and a negative phase throughout survey 2 (Robinson *et al.,* 2023). The observed positive phase was abnormally strong for an independent IOD event causing increased wind strengths and a decrease in sea surface temperatures across the central Indian Ocean (Du *et al.,* 2020). In contrast, during survey 2 the background sub-inertial currents were weak relative to the tides. Due to the increased strength of the wind field across the central Indian Ocean current magnitudes increased during the positive event but no effect of the influence of the IOD on currents was detected at Egmont Atoll reflecting detailed oceanographic work conducted at the

same site (Robinson *et al.,* 2023). Why no effects of increased current strength were detected at Egmont is unknown, neighbouring topographic features and current direction may play a role. Egmont lies on the western side of the Chagos Archipelago near Great Chagos Bank which may have partially impeded or dispersed the flow of currents avoiding directly interacting with Egmont Atoll. Alternatively, Egmont Atoll may have not been affected by the wind field driven by the IOD and may reside at a high enough latitude that the extreme wind stress observed to the south of Egmont did not affect the atoll itself. There may be other reasonings behind the absence of IOD effects around Egmont Atoll but due to the lack of oceanographic measurements in this study no detailed conclusions can be made. Although currents around Egmont were unaffected, the IOD did influence the depth of the thermocline at Egmont Atoll. The IOD also affects SSTs with a positive event causing a heating event over the central Indian Ocean which was observed during survey 1 (Du *et al.,* 2020). Increased solar heating and wind strength generates surface wave induced mixing which deepens the thermocline. The thermocline was detected to be atypically deep at 100 m depth in November in comparison to previous surveys in the region and survey 2 where it was measured at approximately 45 m depth (Hosegood *et al.,* 2019; Robinson *et al.,* 2023). The deeper the thermocline the more likely flow-topographic interactions are especially at locations such as Egmont Atoll where the bathymetry varies around the atoll from steep cliffs and canyons to shallow, flat reefs.

Seafloor depth was highly significant in most models acting as a proxy for topographic features. The variable topography around Egmont atoll has been observed at other oceanic atolls (Panicker and Stafford, 2023). The presence of canyons during survey 1 with higher numbers of fish schools observed over these features suggest flow

topographic interactions may cause the retention of schools. At a depth of 100 m during survey 1, the thermocline sits as the same height as the top of the canyons (Figure 3.3). Flow topography interactions observed in other studies identify mechanisms such as cold-water flushing (Shea and Broenkow, 1982; Walter and Phelan 2016), internal tides (Robinson *et al.,* 2023) and currents (Genin, 2004) to increase the retention of biota. Cold-water flushing over canyon sites is the process of water movement over these pinnacles and shelf edges regulated by the thermocline (Shea and Broenkow, 1982; Walter and Phelan 2016). The internal tide observed at Egmont Atoll has been suggested to drive cold water flushing (Robinson *et al.,* 2023) which may support increased fish aggregations by displacing cold, deep water in shallower environments providing more optimum conditions for schooling fish or re-distributing nutrients and small prey (Walter and Phelan 2016).

Interactions between the thermocline and top of the canyons can cause turbulence when shear is strong enough to overcome stratification within the water column. This initiates both positive and detrimental effects on fish based on their size, momentum, strength, and the period of turbulence in the water column (Utne-Palm and Stiansen, 2001; Lupandin, 2005; Hockley *et al*., 2014). Current speeds have been shown to increase over abrupt topographic features enhancing biological aggregations (Genin, 2004). This occurs due to the suspension of organic matter contributing to trophic focussing which is the enhancement of aggregations of prey brought about by current flows in a topographically confined area (Genin, 2004). Vertical currents at shelf breaks have also been attributed to increased biological aggregations of both plankton and fish species (Barange 1994; Lavoie *et al.,* 2000; Genin, 2004; González-Quirós *et al.,* 2004). Many of these studies focus on the enrichment of plankton from displaced and

aggregated nutrients and it is assumed that over time this biological enrichment of areas progresses throughout the food web into pelagic fish species such as snappers and silvertip sharks which have been visually identified through cameras occurring at the same time as acoustic surveys were undertaken in this study.

Vertical advection is the transport of water to different depths enhancing biological systems. Similar to upwelling, vertical advection occurs on a smaller scale and can advect deeper nutrient rich water into the photic layer increasing biological activity (Williams and Follows, 2011). An advantage of vertical advection is that fish are not reliant on biological enrichment from primary producers. Currents aggregate food mitigating for delays between nutrients being injected and consumed by plankton and progressing through the food web to pelagic forage fish and apex predators. Around islands, vertical advection can occur due to the shallowing of the seafloor and flow-topographic interactions forcing deeper nutrient rich water to the surface (Coutis and Middleton, 1999). As nutrient rich water moves into the photic zone, primary production increases supporting organisms throughout the food web (Lavoie *et al.,* 2000; Genin, 2004; González-Quirós *et al.,* 2004). Hydrodynamically modelled vertical velocities over the canyons sites predicted strong vertical velocities driven by tidal movements causing internal wave oscillations due to flow-topographic interactions. These sites correlated with higher aggregations of fish schools suggesting a link between the localised vertical velocities and biological aggregations. Caveats of the hydrodynamic model include a simplified model of tidal forcing and no wind modulation so it is likely that the vertical velocities could be easily suppressed by oceanographic forcing and are not a consistent feature around Egmont unlike tidal movements. By being linked to internal wave oscillations, the vertical velocities have a short lifespan so cannot be related to primary

production however internal waves can aggregate prey which may enhance feeding at higher trophic levels (Garrett and Munk, 1972; Genin, 2004). Some zooplankton species also use vertical advection to ascend throughout the water column and then have the swimming capabilities to stay at the surface (Michalec *et al.,* 2017). Due to the link between regions of vertical advection and increased biological aggregations, these sites are vital to identify as they support healthy and diverse ecosystems. Within this study the interpretation of vertical velocities is limited as no in-situ data were recorded of fine-scale vertical advection due to the resolution of the ADCP.

Mechanisms such as the internal tide, vertical advection, and tidal flows have been demonstrated to drive the spatiotemporal distribution and behaviour of pelagic fish. This study contributes to the growing evidence base that a combination of tides and topography affect manta rays (*Mobula alfredi*; Harris *et al.,* 2021), zooplankton (Sheehan *et al.,* 2019) and other pelagic fish species in the Chagos Archipelago. Tidal currents and topographical features should be further considered in management plans when identifying biological hotspots around atolls and islands. This is particularly important in oligotrophic tropical waters where oceanographic processes that enhance mixing and aggregations of biota are even more important. Whilst the Chagos Archipelago is already afforded many protections such as a no-take MPA, other atolls in tropical regions are excluded from such protections. Holistic approaches to conservation measures should be considered to ensure that oceanographic drivers, topographic features, and biological behaviours are all considered in spatial planning. The use of oceanographic parameters, both of broad and fine scales, are vital when sampling biological aggregations to enhance the efficiency and efficacy of MPAs.

3.6 Conclusion

This study modelled a selection of oceanographic parameters to biological response variables to determine the physical drivers of pelagic fish schools around Egmont Atoll. Despite separate datasets from different seasons and locations around the Atoll, similar results were observed. Both topography and tide were key in determining the spatial distribution of schooling fish. Flow topography interactions affected schooling fish as steeper topography caused higher abundances of fish aggregations. Enhanced current magnitudes, brought about by tidal flows, affected the behaviour and distribution of schooling fish. The outflow of the lagoon during the ebb tide may also support biological aggregations linking this study to others in the same region. With biophysical relationships often not fully understood, this study contributes to the growing body of work presenting links between the two. This has important considerations for fishers in predicting fish distributions and understanding the spatial variability of pelagic fish for conservation sites.

Chapter 4: Spatial variations of plankton and particulate matter over Sandes seamount in the Chagos Archipelago

4.1 Abstract

Seamounts are associated with higher biodiversity and productivity with oceanographic mechanisms proposed to be driving these biological hotspots. Plankton, as the foundation of the food web, are a key component in supporting seamount ecosystems. This study investigates the mechanistic drivers of spatial variations of plankton and particulate matter over a tropical seamount. Using a Simrad ES70 at 38 and 200 kHz, acoustic data was collected over a 25-hour period at Sandes seamount in the Chagos Archipelago. Throughout the survey vertical plankton trawls were collected with a 100 µm net at 4 stations over each flank of the seamount, with physical measurements collected from oceanographic moorings and temperature-depth sensors. Plankton samples were processed using a FlowCam and individuals identified to group level and biomass density was determined through dry weight. The influence of oceanographic variables on the density and biomass of zooplankton and detritus were tested through regression analysis. This was compared to relative biomass estimates from the Nautical Area Scattering Coefficients (NASC), derived from the ES70, to establish the efficiency of the ES70 in determining plankton distributions. Zooplankton and detritus were most abundant on the eastern flank of Sandes which was shown by both in-situ and fisheries acoustic data. The most significant environmental driver of the distribution of zooplankton and detritus was the ebb tide with higher densities observed during this period. NASC and biomass density displayed similar patterns in space and time but neither varied significantly with the environmental processes modelled. Links between acoustics and plankton biomass are complex but this study elucidates some of the

environmental factors driving plankton distributions over Sandes seamount using a combination of methods. Detritus, comprising of dead plankton, is identified as a key scatterer which may be indicative of predator-prey interactions occurring over the seamount. This study provides the first evidence of zooplankton community distribution and particulate matter at Sandes seamount providing evidence of the fine-scale environmental drivers of biological aggregations supporting increased biodiversity around a productive seamount.

4.2 Introduction

Plankton are vital in supporting the oceanic food web. Phytoplankton form the foundation of the food web and are vitally important in the climate cycle as well as being food for zooplankton. Zooplankton then sustain fish communities and are a major driver of the biological carbon pump. The size of zooplankton ranges from femtoplankton from 20 µm to megaplankton at 200 cm and includes species such as jellyfish and ctenophores (Pinti *et al.,* 2023). The oceanic composition of zooplankton varies globally with higher diversity but lower biomass in the tropics and the opposite observed at the poles (Ikeda, 1985; Rombouts *et al.,* 2009; Moriarty *et al*., 2013; Drago *et al.,* 2019; Ibarbalz *et al.,* 2019; Soviadan *et al.,* 2022). Predator-prey interactions between zooplankton, phytoplankton and forage fish affect zooplankton distributions and densities locally. Zooplankton also rely on both the chemical and oceanographic environment requiring the right nutrients and oxygen concentrations which are influenced by physical drivers such as temperature and currents (Drago *et al.,* 2019).

Since the 1950s, fisheries acoustics has been an essential tool for estimating distribution, abundances, and behaviour of pelagic organisms (Tungate, 1958; Richardson *et al.,* 1959; Mitson and Wood, 1962). Mainly focussed on fish, these surveys have been refined to

provide high resolution data contributing to stock assessments and fishing quotas however anything in the water column can be a scatterer (e.g. Misund, 1997; Toresen *et al.,* 1998; Domokos, 2021). Technical advancements have led to higher resolution data resolving smaller targets in the water column however, small planktonic organisms still present a problem resulting in a lack of information on the pelagic planktonic community (Simmonds and MacLennan, 2005). Plankton are observed in most echograms as 'clouds' due to the large number of closely spaced organisms in the water column (Simmonds and MacLennan, 2005). The composition of many of these layers have not been fully resolved due to limitations in sampling small plankton species (Mair, 2008). A complication in determining scatterers is that the intensity of backscatter produced is not always directly related to the abundance of organisms so high backscatter does not necessarily equate to a high abundance of organisms (Benoit-Bird and Lawson, 2016). The acoustic signal returned from scatterers depends on physiological and behavioural responses of the organism (MacLennan *et al.* 1990b; Ona, 1990). Physiologically, if scatterers contain air bubbles or lipids then the acoustic response is likely to be stronger however gonads, bones and flesh also contribute to the acoustic response of biological matter (Love, 1971; Ona, 1990). The acoustic response of small plankton is usually dependent on the density and size of plankton and the frequency of the echosounder (Greenlaw, 1979).

Plankton are essential in supporting the marine ecosystem yet, when acoustically detected they are often filtered out of the data when the focus is on larger organisms, but they comprise important information for ecological studies. Antarctic krill *Euphausia superba*, a keystone species in the Southern Ocean, have been the focus of many studies due to their large size (Kang *et al.,* 2020; Cutter *et al.,* 2022; Salmerón *et al.,* 2023). Other

planktonic organisms studied include other species of krill (*Meganyctiphanes norvegica* and *Thysanoessa raschii*; McQuinn, Dion and St. Pierre, 2013) and gelatinous plankton (*Lychnorhiza lucerne, Iasis zonaria, Mnemiopsis leidyi* and *Aequorea* sp; Colombo, Mianzan and Madirolas, 2003) all of which are included in the larger size categories of plankton. Some studies have taken this a step further and tried to work out the multispecies composition of deep scattering layers in the North Sea (Mair *et al.,* 2005), Bay of Biscay (Peña *et al.,* 2021) and Arctic Ocean (Ingvaldsen *et al.,* 2023). The frequency response of different planktonic species has mostly been recorded at 120 kHz departing from the standard frequency of 38 kHz used to study fish (Simmonds and MacLennan, 2005). Higher resolution data at a higher frequency is required for studying plankton due to their small size.

Fisheries acoustics can identify the temporal movements of plankton through nocturnal diel vertical migration (DVM), the daily global mass migration of plankton from deep water during the day to shallow water at night (Neilson and Perry, 1990; Brodeur *et al.*, 2005b). This movement around shallow seamounts can cause seamount trapping when the summit is within the photic zone (Pitcher *et al.,* 2007). Seamount trapping occurs when zooplankton rise to the photic zone to feed and gradually get transported by currents over the summit of the seamount (Rogers, 1994; Genin, 2004; Genin and Dower, 2007). When zooplankton descend some become trapped over the seamount which acts as a topographic blockage, providing an optimum feeding site for predators (Genin, 2004). This daily cycle is likely one of the reasons why seamounts have been described as biodiversity hotspots for both benthic and pelagic organisms (Samadi *et al.,* 2006; Morato *et al.,* 2010b; Hosegood *et al.,* 2019). With over 37,000 seamounts predicated globally (Yesson *et al.,* 2020) there is a requirement to understand the fine sale dynamics

and distributions of zooplankton which is fundamental in the marine food web over these pinnacles. Net samples are an essential tool to understand the composition of plankton and to estimate densities but if combined with acoustics, larger datasets could be acquired and relationships between mean volume backscattering strength (S_v) and plankton density derived (Simmonds and MacLennan, 2005).

This study aims to validate acoustic data collected around Sandes seamount in the Chagos Archipelago using plankton net samples (Figure 4.1). The group composition of the samples are analysed and modelled against environmental variables to elucidate drivers of the distribution of zooplankton around Sandes seamount. This study provides further evidence on the importance of seamounts to pelagic organisms by understanding the biophysical drivers of the distribution of zooplankton and its effect on seamount ecology.

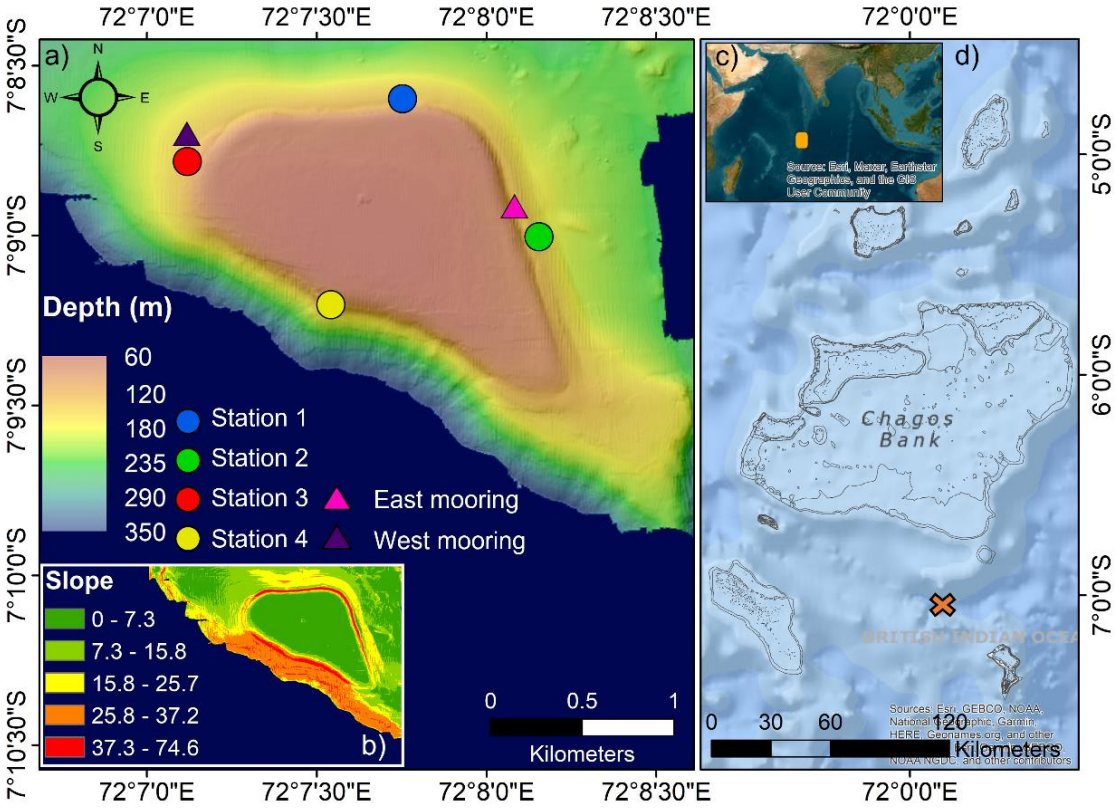

Figure 4.1: Map of a) multibeam bathymetry of Sandes seamount. Round coloured markers identify the stations where validation samples were collected, and triangular markers indicate the position of oceanographic moorings. b) Derived slope from the multibeam bathymetry in degrees. The inset map (c) depicts the location of Sandes with the context of the Indian Ocean and d) shows the Chagos Archipelago with Sandes seamount (orange cross) located in the southern part of the region.

4.3 Methodology

4.3.1 Data collection

Sandes seamount, located in the Chagos Archipelago Marine Protected Area (MPA), is classified as a shallow, steep seamount with a summit at 60 m and flanks descending to over 2000 m depth (Hosegood *et al.,* 2019). Calm sea conditions were observed throughout a 25-hour period when an acoustic survey was conducted. Using a Simrad ES70 fisheries echosounder with a combined 38/ 200 kHz transducer data were collected over Sandes seamount in a bow tie shaped transect during March 2022 aboard *MV Tethys Supporter*. Four sampling stations were situated over the flanks of the seamount which were consistently sampled with a video camera and plankton trawls (Figure 4.1).

Each station was located at the start or end of the acoustic transect lines to ensure that continuous acoustic data was collected during the sampling although for this study only on-station acoustic data was retained for the analysis. A total of 4 plankton and video samples were taken approximately 3-4 hours apart over a 24-hour period with a total of 20 samples collected equally between all 4 stations (Table 4.1).

All surveys and instruments were programmed and synchronised to Coordinated Universal Time (UTC) to allow comparisons between the validation sampling and acoustic survey. Global navigation satellite system (GNSS) data were collected and correlated to the acoustic data using a Nortek GNSS unit. To reduce noise in the data the ES70 was powered independently to the ship using DC batteries. Standard calibration procedures were followed for the acoustic data calibration completed during March 2022 with the processing completed using Echoview Calibration Assistant (Foote, 1987; Demer *et al.*, 2015; Echoview Echoview Software Pty Ltd, 2021). Area backscattering coefficient (Sa) correction values were calculated as 0.5218 dB and -0.3063 dB for the 38 and 200 kHz frequencies respectively.

Vertical plankton trawls were conducted using a weighted 102 µm, 50 cm diameter, 3:1 ratio plankton net with a GoOceanic Flowmeter. A temperature depth (TD) sensor was attached to the net to measure the physical properties experienced throughout the trawl.

Table 4.1: Metadata for plankton net trawls stating the date and timing in UTC, location based on station and transect ID with supplementary information on the tidal state, period of day and maximum depth of trawl (m). For sample ID the first value signifies the transect whilst the decimal value represents the station number, e.g. S1.1 is Transect 1, Station 1.

Sample ID	Date	Time IN (UTC)	Time OUT (UTC)	Station	Transect	Tidal State	Period of day	Max depth (m)
S1.1	17/03/2022	05:22	05:27	1	1	Flood	Day	32.8
S1.2	17/03/2022	05:55	06:00	2	1	Flood	Day	54.1
S1.3	17/03/2022	06:22	06:28	3	1	Flood	Day	72.5
S1.4	17/03/2022	06:57	07:02	4	1	Flood	Day	76.7
S2.1	17/03/2022	09:49	09:55	1	2	Ebb	Day	88.7
S2.2	17/03/2022	10:26	10:30	2	2	Ebb	Day	45.0
S2.3	17/03/2022	11:00	11:08	3	2	Ebb	Day	94.1
S2.4	17/03/2022	11:32	11:39	4	2	Ebb	Day	73.5
S3.1	17/03/2022	16:25	16:30	1	3	Flood	Night	42.8
S3.2	17/03/2022	16:57	17:01	2	3	Flood	Night	50.2
S3.3	17/03/2022	17:33	17:37	3	3	Flood	Night	48.9
S3.4	17/03/2022	16:01	16:05	4	3	Flood	Night	62.1
S4.1	17/03/2022	22:00	22:06	1	4	Ebb	Night	50.9
S4.2	17/03/2022	22:33	22:40	2	4	Ebb	Night	57.1
S4.3	17/03/2022	21:00	21:04	3	4	Ebb	Night	42.9
S4.4	17/03/2022	21:33	21:37	4	4	Ebb	Night	29.7
S5.1	18/03/2022	03:25	03:30	1	5	Ebb	Day	49.4
S5.2	18/03/2022	01:23	01:32	2	5	Ebb	Day	62.2
S5.3	18/03/2022	02:18	02:23	3	5	Ebb	Day	52.4
S5.4	18/03/2022	02:53	02:57	4	5	Ebb	Day	32.7

4.3.2 Acoustic processing

Data were processed in Echoview V12.1 (Echoview Software Pty Ltd, 2021) with vessel offsets and calibration factors applied. The surface 15 m and bottom 5 m of data were removed from analysis due to the increased presence of noise and interference associated with those regions (Simmonds and MacLennan, 2005). Data below 200 m was removed for the 200 kHz frequency due to the attenuation of the signal, reducing

confidence in the data. When visually inspecting the data, artifacts were observed during the turns of the transect, therefore, all turn data was removed from further analysis.

Frequencies below 100 kHz are limited for plankton identification in acoustic surveys (Simmonds and MacLennan, 2005). By only having one frequency above this the acoustic interpretation of plankton is restricted. However, the use of both frequencies within this survey allows for the removal of fish schools from the 200 kHz dataset using targets on the 38 kHz frequency. Schools were identified on the 38 kHz frequency using the SHAPES detection algorithm (Barange, 1994; Coetzee, 2000; Diner, 2001). Fish school parameters were defined as: minimum total school height of 0.20 m, minimum candidate length of 2.22 m, minimum candidate height of 0.20 m, maximum vertical linking distance of 3.00 m, maximum horizontal linking distance of 8.00 m and minimum total school length of 8.00 m. Schools were isolated and masked from the 200 kHz frequency data allowing only plankton to remain. A threshold of -90 dB was applied to encompass the range of zooplankton observed. On-station acoustic data were exported by cells in 1 m by 5-minute bins for further analysis. Nautical Area Scattering Coefficient (NASC), a proxy for biomass, was measured at each of the 20 sampling sites by taking a mean value throughout the duration and to the depth of when the plankton trawl was conducted. Due to an error in the ES70 data no NASC values could be derived at the survey stations 4.1 and 4.2.

4.3.3 Oceanographic processing

Environmental variables were used from the Temperature Depth (TD) sensor on the plankton net and from oceanographic moorings deployed over Sandes seamount (Figure 1). Two thermistor string moorings were chosen (on the eastern and western flank) to compare temperature around the seamount. These were averaged into 10 m bins over

10-minute ensembles to match the timing of the plankton trawls. Acoustic Doppler Current Profilers (ADCP) were located on two moorings on the east and west flank of Sandes seamount (Figure 1). The ADCP used default settings and a 3 m bin size which were set by the SignatureVM software. This data was averaged into 10-minutes ensembles and used to calculate the tidal regime over Sandes seamount. A freely deployed CTD profile was conducted during the survey to gain information on deep water layers. CTD data was arranged into 1-minute ensembles with sea surface temperatures removed from the dataset.

Tidal information showed a semi-diurnal tidal cycle in the region with the 25-hour survey covering two flood and ebb tides (Figure 4.2). Plankton samples were collected over all diurnal tidal cycles throughout the survey (Figure 4.2).

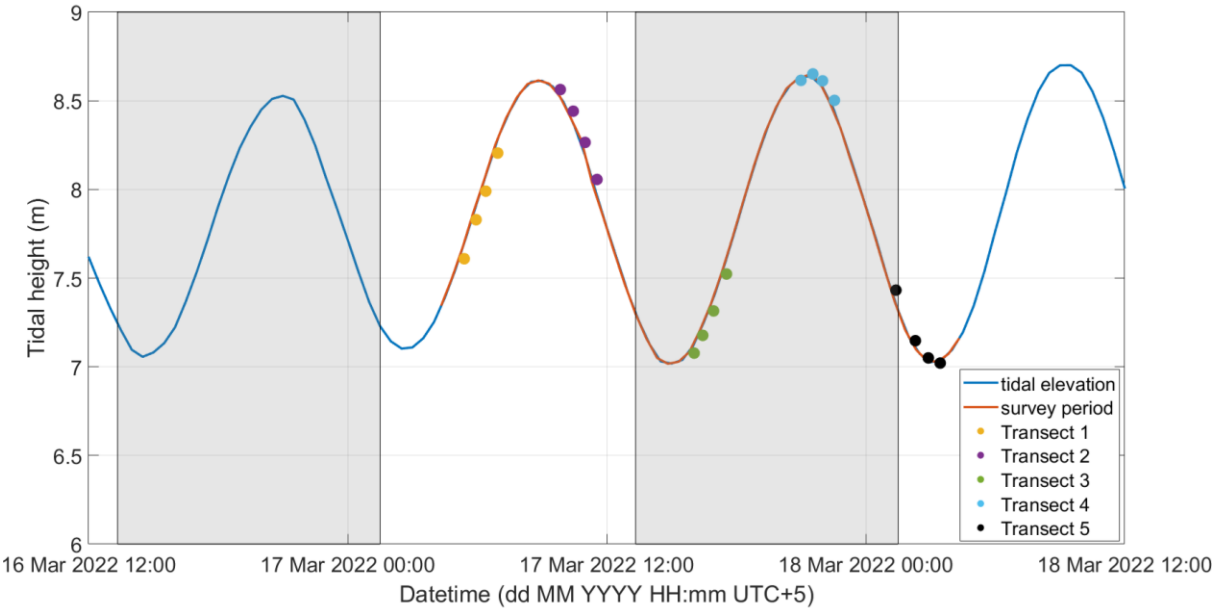

Figure 4.2: Tidal height (blue) overlaid with the duration of the acoustic survey 1 (orange) with the grey boxes representing night in local time (UTC +5). The times of the validation samples are shown with coloured circles.

4.3.4 Plankton processing

Twenty 500 ml plankton samples were collected throughout the transect covering different tidal periods and depths. The samples were split using a Folsom splitter allowing the sample to be used for two purposes 1) biomass analysis and 2) plankton identification. All samples were sieved through a 100 µm filter with the biomass density analysis sample drained completely of seawater before being placed in a drying oven at 60°C for 24 hours and weighed. To calculate the density of biomass (B; mg m^3) the following equation was used:

$$B = \frac{W}{V}$$

Where, W is the weight of the sample and V is the volume of water sampled which was calculated from the flowmeter.

Analysis of the species/group composition of the sample was conducted by preserving the sample in 10% Iodine solution (Lugol's solution) before analysing using a FlowCam VS-IVc (Yokogawa Fluid Imaging Technologies Inc) within 3 months of the survey being conducted. Samples of 5 ml were extracted and mixed using a magnetic stirrer with 100 ml of filtered seawater. The FlowCam was set to auto-imaging mode using a 2x microscopic objective and a flow rate of 10 at 25 ml/min. The extracted samples were passed through the FlowCam for 3 minutes in a 2000 mm flow cell with a 2 mm diameter producing 29,095 individual images. Images were split and imported into Ecotaxa v2.6 where specimens with a size between 100 µm and 3 mm were manually identified by a trained expert at Plymouth Marine Laboratory to the lowest operational taxonomic level (OTU; Picheral, *et al.,* 2022). Non-living samples were classified as detritus, which

included partial plankton specimens and fibres whilst living specimens were split into three groups: holoplankton, phytoplankton, and meroplankton.

Estimates of the abundance of planktonic assemblages (per m^3) were calculated for each sample using the formula:

$$Abundance = \frac{\left(\frac{n}{volume\ Imaged}\right) * \ volume\ Water}{volume\ Sampled} * \ 10^6$$

Where, n is the number of observations, volume Imaged is the volume of the subsample analysed by the FlowCam (ml). The volume Water is the total volume of the water sample (ml) and volume Sampled is the total volume of water which passed through the net measured by the flowmeter (ml). The net sample volume was multiplied by a factor of 21 to estimate the total sample volume to account for the dilution of the subsample.

4.3.5 Statistical analysis

Four response variables were identified to test against physical explanatory variables these were: zooplankton (count per m^3), NASC ($m^2 nmi^{-2}$), plankton biomass (mg m^3), and detritus (count per m^3). Four separate analyses were conducted with these response variables: 1) Generalised Additive Model (GAM) to test the relationship between the response variables and the continuous environmental variables (temperature and depth; Table 4.2); 2) Analysis of Variance (ANOVA) to test for differences in the response variables between categorical physical variable categories (Station, Transect, slope; Table 4.2); 3) Two sample T-Test to test for differences in the response variable between day and night (time) and flood and ebb (tide); 4) dissimilarity cluster analysis between 16 zooplankton groups identified from the plankton net trawls.

Generalised Additive Models (GAM) were used in R using the 'mgcv' library (Wood, 2006) with each response variable tested independently against the environmental variables. Due to the small sample size (n=20), multiple regression could not be conducted. Analysis 1 was conducted with a Gaussian distribution for all the response variables with a log transformation applied to the NASC data. Smooth variables were constrained at 3 knots to reduce overfitting (Keele, 2008). Analysis 2 used individual one-way ANOVAs to test the response variables against categorical environmental variables with a Tukey post hoc test used for statistically significant variables. Two sample T-tests were conducted on all response variables against Tide and Time.

Multivariate zooplankton assemblage composition data consisting of the lowest OTUs were log transformed to avoid overweighting dominant groups. For analysis 4, the lowest OTU groups were input into a cluster analysis using a Bray-Curtis similarity matrix in the 'clustsig' library (Whitaker and Christman, 2014). The SIMPROF routine was used to identify significant clusters with a 95% confidence level and run for 1000 permutations. Residuals and fitted values were analysed graphically with all model variables for model validation.

Table 4.2: Summary of variables used in the analyses 1,2 and 3. NASC, zooplankton, detritus and biomass were the response variables tested independently against environmental explanatory variables. The Analysis column indicates which analysis the variable was used in.

Variables	Unit	Description	Analysis
Station	N/A	Factor describing the geographic location of the plankton trawl using the Station locations in Figure 4.1.	2
Transect	N/A	Factor describing the timing of the plankton trawl based on Table 4.1.	2
Time	N/A	Factor describing the time of day (day or night).	3
Tide	N/A	Factor describing the tidal state as either flood or ebb.	3

NetDepth	m	Maximum depth reached by the plankton net.	1
NetTemp	°C	Temperature that corresponds with the maximum depth of the plankton net.	1
SurfaceTemp	°C	Surface temperature observed during plankton trawl.	1
slope	°	Slope of the seafloor where plankton trawl was conducted.	2
ThermTemp	°C	Temperature of the thermocline at 40 m depth.	1
NASC	m^2nmi^{-2}	Nautical Area Scattering Coefficient, a proxy for the density of biomass derived from the ES70.	1,2,3
Zooplankton	count per m^3	The density of zooplankton analysed in the plankton trawls.	1,2,3
Detritus	count per m^3	The density of detritus analysed in the plankton trawls.	1,2,3
Biomass	mg m^3	The density of biomass from each plankton trawl.	1,2,3

4.4 Results

4.4.1 Environmental variables

From the multibeam bathymetry, the greatest slope was identified at station 4 with a slope of 45.0° where topography increases rapidly into deep water (Figure 4.1). Stations 1 and 3 on the northern side of Sandes had the lowest slopes of between 12.8 and 17.3°. The depth of the thermocline was observed at approximately 40 m with the chlorophyll maximum located at 50 m depth (Figure 4.3a). Current direction, derived from oceanographic moorings over Sandes showed the mean flow of the upper 60 m of the water column was north-eastwards (Figure 4.3b). Temperature sensors attached to the plankton net recorded the maximum water surface temperature at 30.6 ° C. Plankton trawl depths ranged from 29.7 m to 94.1 m with a minimum temperature of 20.7 °C observed during the deepest plankton trawl (Table 4.3).

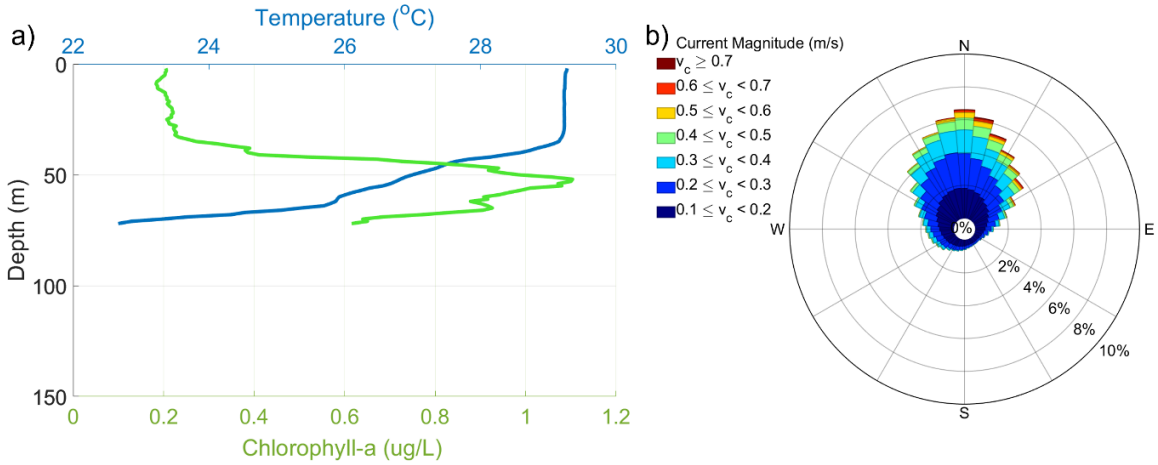

Figure 4.3: a) CTD profiles of temperature (blue) and chlorophyll (green) and b) showing a tidal rose of mean current flow in the upper 60 m of the water column around Sandes seamount.

Table 4.3: Summary of depth and temperature recorded from the TD sensor attached to the plankton net for each plankton trawl.

Sample	Continuous response variable						
	Depth (m)	Temperature (° C)					
	Maximum	Mean	Minimum	Maximum	Range	Standard deviation	
1.1	32.80	28.58	27.89	28.80	0.91	0.20	
1.2	54.10	27.91	25.24	28.84	3.60	1.09	
1.3	72.50	27.04	22.98	29.01	6.03	1.91	
1.4	76.70	27.14	22.11	29.09	6.98	1.99	
2.1	88.70	25.81	21.07	29.84	8.77	2.96	
2.2	45.00	28.52	26.72	30.57	3.85	0.50	
2.3	94.10	25.28	20.70	29.44	8.74	3.08	
2.4	73.50	25.69	21.75	29.09	7.34	2.87	
3.1	42.80	28.44	26.78	28.98	2.20	0.55	
3.2	50.20	28.25	26.07	28.98	2.91	0.81	
3.3	48.90	28.30	26.46	28.84	2.38	0.65	
3.4	62.10	27.70	24.03	28.89	4.86	1.48	
4.1	50.90	28.26	25.57	28.99	3.42	0.85	
4.2	57.10	27.43	23.08	28.88	5.80	1.80	
4.3	42.90	28.12	26.25	28.84	2.59	0.81	
4.4	29.70	28.74	28.22	29.02	0.80	0.19	
5.1	49.40	28.16	26.73	28.73	2.00	0.74	
5.2	62.20	27.39	23.22	28.69	5.47	1.41	
5.3	52.40	28.05	26.13	28.70	2.57	0.81	
5.4	32.70	28.57	27.95	28.71	0.76	0.17	

4.4.2 Composition of plankton trawls

A total of 29,095 individuals per volume were identified using the FlowCam from the 20 plankton net trawls at Sandes seamount (Figure 4.4). Of those samples, 12,746 were classified as living and 16,349 as non-living. Of the non-living samples, 7112 were identified as detritus, which was composed of 91.2 % unidentified matter and plankton parts, 8.6 % fibres and 0.2 % faeces. The remaining 8,894 samples were categorised as artefacts such as bubbles and out of focus specimens and were not retained for further analysis. From the living planktonic specimens, the nets consisted of 59.6% phytoplankton, 34.6 % holoplankton and 5.8 % meroplankton (Table 4.3). The most common species found was a phytoplankton species, *Trichodesmium* which accounted for the majority of phytoplankton recorded during the survey.

Between the different transects and stations the highest densities of phyto and zooplankton were observed on transect 2 and 4, which were carried out during an ebb tide. The highest overall density of phyto and zooplankton were recorded at station 1 throughout the survey (see Table C1 in appendix C). Throughout the surveys, station 3 had the lowest density of zooplankton whilst station 2 had the lowest density of phytoplankton.

The composition of zooplankton varied with 16 groups identified (Table 4.4). Crustacea were the most abundant group which were relatively evenly distributed between stations except for station 4 which had the lowest individual count. Within the crustacea group 'Other' (containing any specimens with Crustacea as the lowest OTU) species were the most abundant with 3036 specimens followed by copepoda with 951 specimens. Biomass density varied between stations and transects with the highest biomass recorded during Transect 3 and Station 2 (see Table C1 in appendix C).

The mean count during the day and night for detritus, which included partial plankton specimens and fibres, was 63368.3 and 80543.6 m^{-3} specimens respectively. Transect 3 had the lowest density of detritus (42,387 m^{-3}) compared to transect 2 with the most detritus specimens (113,654 m^{-3}; see Table C1 in appendix C).

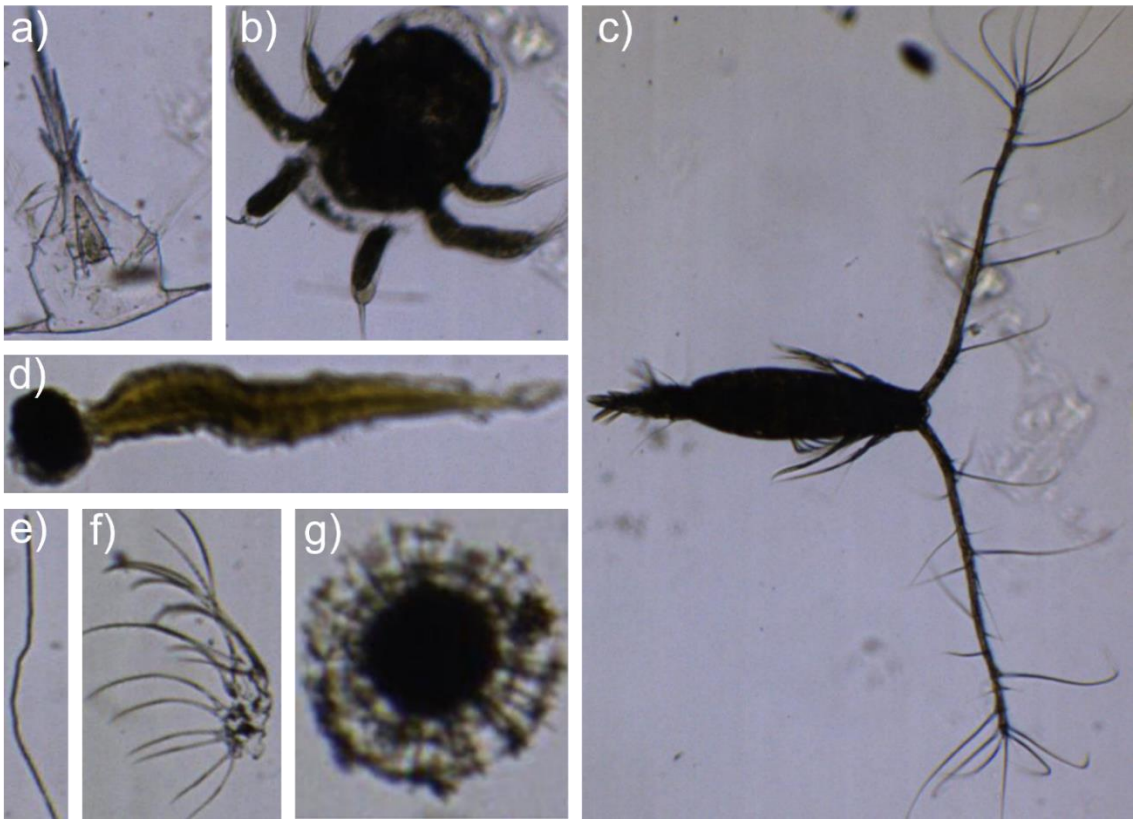

Figure 4.4: Examples of net samples identified through the Flowcam a) Cirripedia, b) copepoda nauplii c) copepod, d) Oikopleura e) fibre (detritus) f) crustacean part (detritus) and g) Radiozoa.

Table 4.4: Description of the phylum and lowest classification of all living with the cumulative count of individuals from all 20 samples.

Plankton group	Phlum	Lowest classification	Number of observations
Holoplankton	Annelidia	Polychaeta	3
	Anthropoda	Copepoda Other	951
		Copepoda nauplii	167
		Oncaea	84
		Corycaeidae	4
		Acartia	1
		Cirripedia	6
		Ostracoda	9

		Crustacean other	3036
	Bryzoa	Bryzoa	3
	Retaria	Foraminifera	3
	Chordata	*Oikopleura*	134
	Ciliophora	*Tintinnidiidae*	6
	Nematoda	Nematodes	1
Phytoplankton	Gyrista	*Coscinodiscus*	64
		Chaetoceros	77
		Planktoniella sol	23
		Pleurosigma	30
		Probisca truncata	4
		Pseudo-nitzschia sp.	*145*
		Rhizosolenia	50
		Triceratium	1
		Diatoms	3
	Cyanobacteria	*Trichodesmium*	6568
	Myzozoa	*Amphisonia*	33
		Ceratium	164
		Neoceratium	69
		Ornithocercus	5
		Dinoflagellate cysts	366
Meroplankton	Unknown	Other	736

4.4.3 Echosounder backscatter estimates

Data from the ES70 showed nocturnal DVM patterns in the backscatter during sunset and sunrise where the vertical migration of plankton occurs (See Figure C1 in appendix). Visually, backscattering values corresponded with plankton net abundances with higher backscattering values observed at Station 2 (Figure 4.5b). Throughout many of the trawls only small amounts of backscatter was observed (Figure 4.5a, c and d).

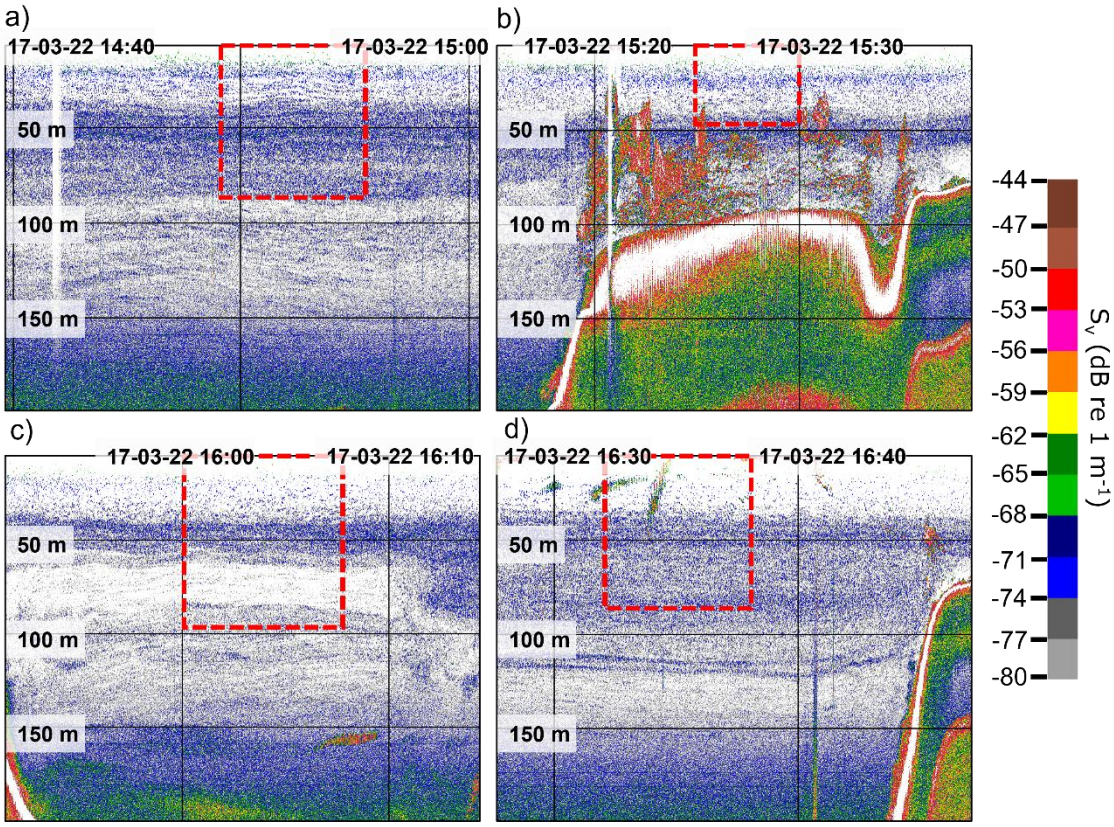

Figure 4.5: Echograms from the ES70 at 200 kHz taken during Transect 2 at a) Station 1, b) station 2, c) station 3 and d) station 4 showing the S_v at different times over Sandes seamount. Red squares indicate the time and depth of the plankton trawl. Time is in local time (UTC +5).

4.4.4 Statistical analysis

Tide and Transect were significant in explaining the response variables however, no other variables were determined to be significant from analyses 1,2 and 3 (see Table C2 in Appendix C). The densities of zooplankton and detritus were significant ($p<0.05$) when modelled against tidal phase using a two-factor t-test (Table 4.4). Zooplankton densities were almost twice as high during the ebb tide (M= 53510, SD= 6439) compared to the flood (M= 28243, SD= 4096) tide ($t(18)= 2.01$, $p= 0.009$ (Figure 4.6). Detritus densities also showed a significant difference ($t(18)= 2.41$, $p=0.027$) between the tidal phases with 68 % higher densities during an ebb tide (M= 84768, SD= 9971) compared to the flood tide (M= 50591, SD= 8763).

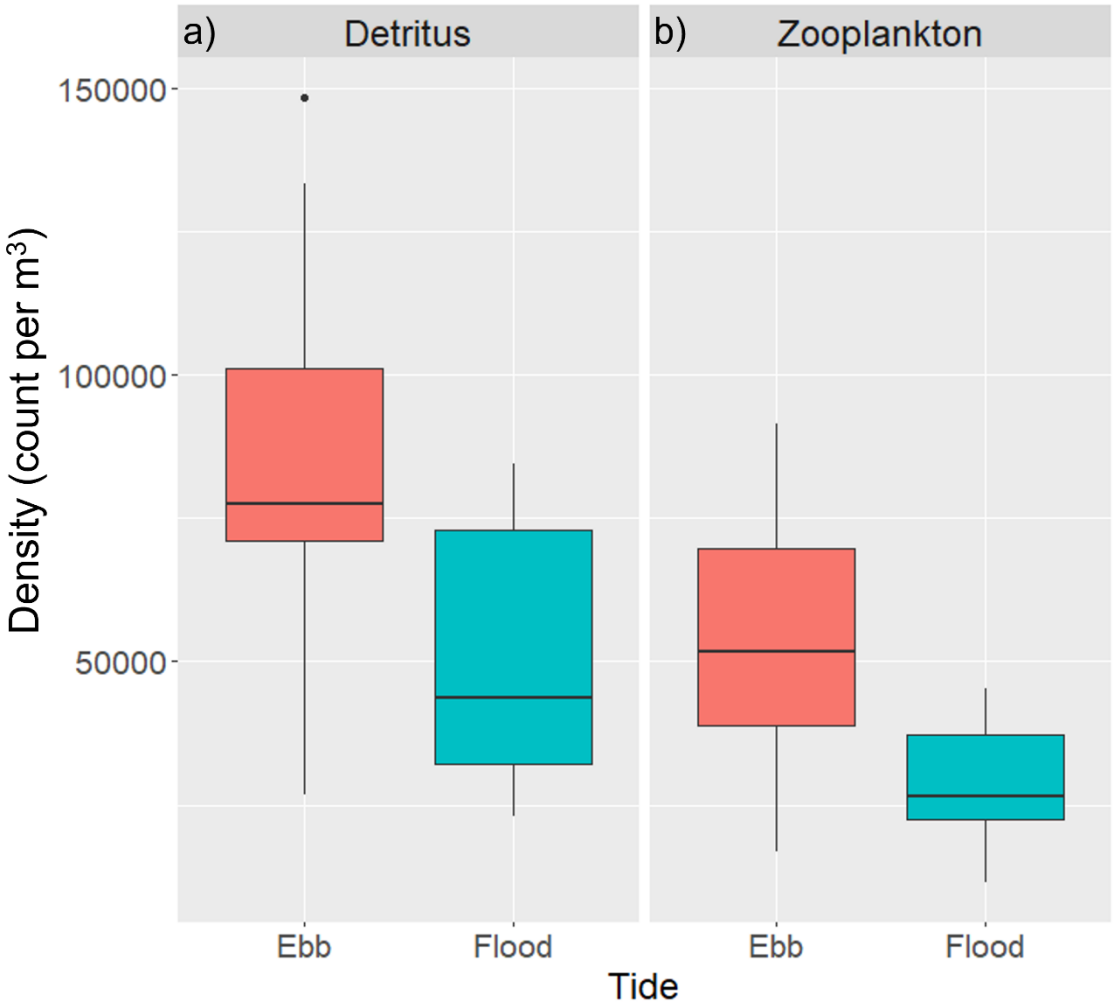

Figure 4.6: Boxplot of a) detritus and b) zooplankton densities (m^{-3}) variations with tidal phase.

A one-way ANOVA revealed that there was a significance difference in the density of detritus between transects ($F(4, 15)= 3.75$, $p=0.03$). Tukey's HSD Test for multiple comparisons found the mean density of detritus was 2.6 times higher in transect 4 than 3 ($p=0.02$, 95% C.I.= [10756.15, 131776.35] and that overall transect 4 had the highest density of detritus when compared to all other transects (Figure 4.7). There were no other significant differences found between any of the other transects.

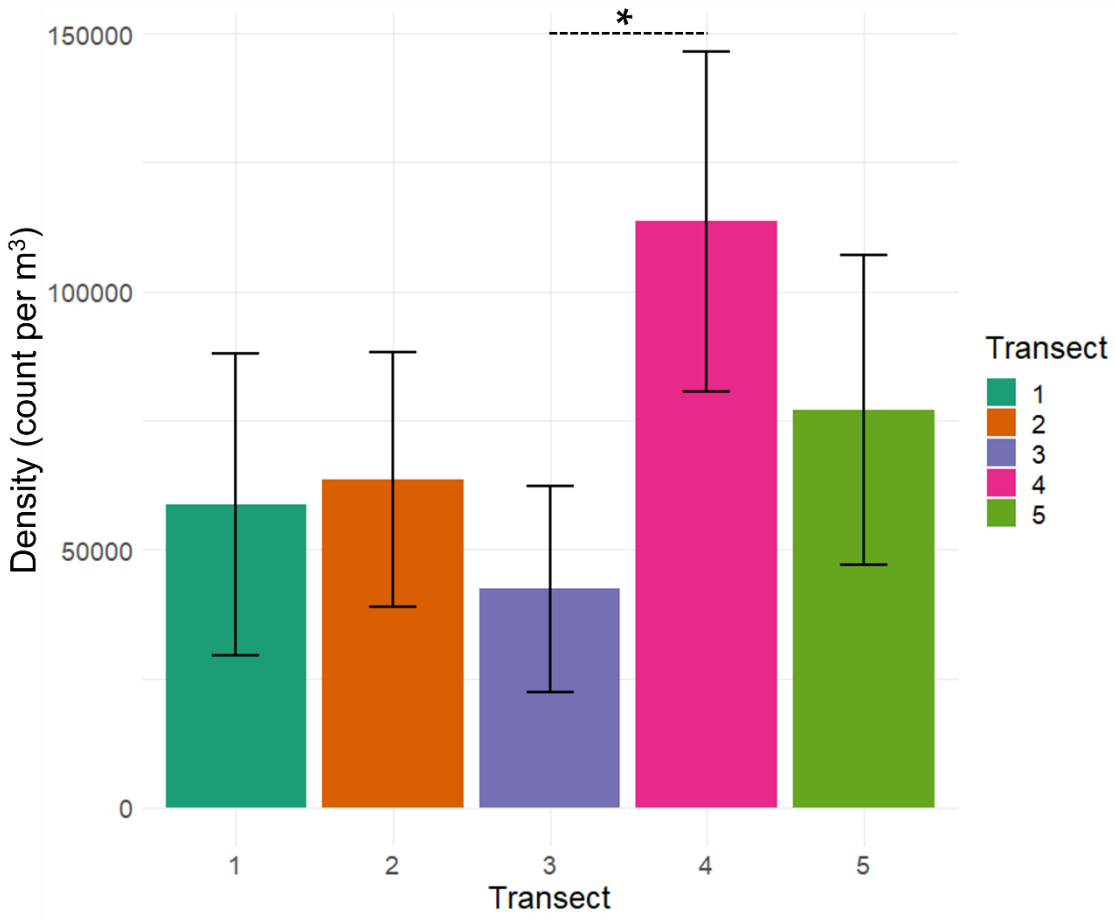

Figure 4.7: Mean density of detritus (m^{-3}) between transect numbers, where error bars show the standard deviation. Transects 3 and 4 are modelled to be significantly different ($p<0.05$).

Significant differences were observed in zooplankton community structure in samples 1.1, 2.4 when compared to the rest of the samples, the other samples did not have significantly different zooplankton communities (Figure 4.8). Within sample 2.4 (2nd transect at site 4) a total of 420 zooplankton specimens were recorded with 99.3% broadly identified as Crustacea and the remaining 0.7% as Copepoda nauplii and *Oikopleura*. Sample 1.1 was conducted on the first transect at station 1 where only 33 specimens were recorded, so this sample had the lowest count of zooplankton of all the

samples which may explain its dissimilarity to the other samples. This sample comprised of 93 % Crustacea with the remaining 7 % consisting of *Oikopleura* and *Actinopterygii.*

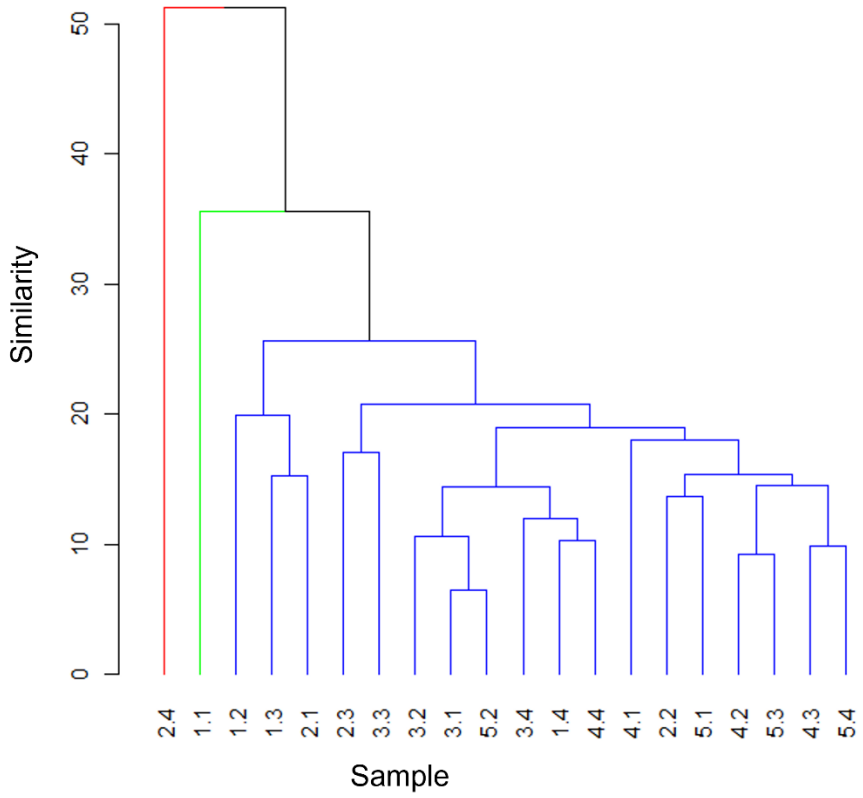

Figure 4.8: Dissimilarity cluster between 16 zooplankton groups identified to the lowest taxonomic operational unit and the sample site e.g., 2.4 represents Transect 2, Station 4. Colour differences represent dissimilar clusters.

4.5 Discussion

A combination of in-situ and fisheries acoustics techniques were undertaken to determine the spatial distribution of plankton over Sandes seamount. Similar conclusions were observed between the two techniques however some key differences were detected which were likely driven by species composition and oceanographic processes. The highest planktonic biomass, NASC, zooplankton and detritus densities were observed over the eastern flank of Sandes varying with tide and transect (a proxy

for both tide and time of day). Some studies have found an increase in zooplankton densities over seamounts which have been attributed to upwelling bringing about increased primary production (Fedosova, 1974; Genin and Boehlert, 1985; Rogers, 2018). Whereas other studies have shown a reduction in zooplankton abundance over seamounts due to the displacement of zooplankton by currents over the seamount summit and enhanced predation (Nellen, 1973; Genin *et al.,* 1994; Dower and Mackas, 1996; Haury *et al*., 2000; Martin and Christiansen, 2009; Rogers, 2018). This discussion provides a first insight into the environmental drivers of the distribution of plankton around Sandes seamount and an exploration into the capabilities of different sampling methods to determine plankton abundances. Understanding the distributions and behaviours of zooplankton, a major driver of the biological carbon pump and which sustain fish communities is essential when trying to elucidate why these regions are so biodiverse.

4.5.1 Tidal influences on plankton

Plankton distributions are often driven by current movements (Genin, 2004; Pitcher *et al*., 2007) with currents around Sandes described as complex and turbulent (Hosegood *et al.,* 2019; Robinson *et al.,* unpublished data). These flows act as both retention and dispersal mechanism for plankton. Strong surface flows could cause the displacement of plankton from Sandes however processes such as DVM can act as retaining mechanisms for zooplankton if the currents move in opposite directions over the seamount (Valle-Levinson *et al.,* 2004). Strong currents can also increase sediment resuspension and increase the amount of non-biological matter within the water column (Genin, 2004). Throughout the survey the mean current direction was predominantly northwards with a small element of eastward movement so plankton and detritus transported with the

currents would have encountered stations 2 and 4 first before being redispersed around the seamount. The north-eastern flank of Sandes was less exposed to the current regime likely providing a less turbulent environment for plankton to aggregate.

The highest densities of detritus were found on transect 4 (night, ebb tide), and the lowest on transect 3 (night, flood tide). Although not significantly different this pattern was also observed during the day between transect 1 (day, flood tide) and 2 (day, ebb tide). The variable transect acted as a proxy for both tidal state and time of day however, the data shows a clear pattern of higher densities during the ebb tide. Tidal flows have been shown to aggregate biota around topographic features such as seamounts due to flow topographic interactions (Genin, 2004; Read and Pollard, 2017). Both current strength and direction may play a role in aggregating plankton causing the significant difference between tidal states. The current direction of the ebb tide could not be determined within this study however, the direction and strength of this current causes higher densities of zooplankton and detritus. This may be due to flow-topographic interactions that are initiated when the current interacts with seamount in a certain direction. Oceanographic processes driven by tidal forcing have previously been observed over Sandes seamount with internal tides, which are internal waves propagating at a tidal frequency, identified as key features affecting biota (Hosegood *et al.,* 2019). Although not modelled within this study, the internal tide could be driving the spatiotemporal distributions and entrainment of zooplankton on the north-eastern flank of Sandes. Further research is required on the tidal variability around Sandes to determine its impact on plankton and particulate matter.

4.5.2 Diurnal influences on plankton and detritus

Diurnal differences may have played a role in the density of detritus with both significant differences between the two transects (Transect 3 and 4) conducted at night between the highest and lowest densities of detritus. In combination with the tides, this suggests that both flow-topographic interactions and illumination within the water column play a vital role in aggregating particulate matter over Sandes seamount. DVM could be a driver of increased detritus densities overnight however with both the highest and lowest detritus densities observed during this period, another factor, such as tidal phase may initiate a greater response in detritus densities than day/ night variations. Non-significant results for diurnal explanatory variables may be due to net avoidance of some species, small sample size and sampling bias as the trawls were not conducted at a consistent depth.

DVM movements can be related to the process of seamount trapping which relies on higher densities of zooplankton over the seamount summit at dawn becoming impeded from descending due to the topographic blockage of the seamount therefore becoming trapped on the seamount summit (Genin, 2004). This increased density of zooplankton increases predator-prey interactions over the seamount- a mechanism that has been suggested to occur over Sandes seamount (Hosegood *et al.,* 2019). Evidence of this may be visible with the detritus samples collected in this survey which contained partial plankton specimens and fibres. The lowest densities of detritus were observed during transect 3 which was conducted during the night (21:00- 22:30 UTC+5). Lower densities of detritus during this time suggests that predation on plankton may be limited. However, as the night progressed (transect 4; 02:00- 03:30 UTC+5) the highest density of detritus throughout the survey was observed which could indicate an increase in

foraging of zooplankton at this time. When illumination increased in the water column (Transect 5; 06:23- 08:25) the density of detritus decreased but was still higher than densities observed prior to the upward DVM migration. This may be due to fish feeding on the increased densities of zooplankton trapped over the summit of Sandes. Whilst this result cannot be directly linked to seamount trapping due to the short period of the survey and missing observations directly over the seamount summit, the detritus densities suggest an increase in predator-prey interactions overnight.

4.5.3 Influence of temperature on plankton

No significant relationship was determined between zooplankton densities or biomass and temperature within this study which is a departure from other global studies. Temperature is known to affect the metabolic rates of zooplankton (Heinle, 1969; Hirst and Bunker, 2003) with relationships between temperature and oxygen concentrations used to describe zooplankton size structure and abundances globally (Brandão *et al.,* 2021). Trends from these studies have shown that copepod abundance decreases with temperature (Brandão *et al.,* 2021; Campbell *et al.*, 2021). However, other studies have seen contrasting results suggesting that the trends observed may vary between species and may not be directly linked to the size of zooplankton (Brandão *et al.,* 2021; Davies, Beckley, and Richardson, 2022). The non-significant results in this study suggest that local variations in plankton and detritus densities are driven more by tidal, diurnal and predation factors. Sampling factors such as the small sample size, species composition and no depth specific sampling conducted to confirm the vertical distribution of plankton may have also limited the statistical analysis of these results.

4.5.4 Comparison of sampling techniques

The spatial distributions predicted by the in-situ and fisheries acoustics datasets show some positive correlation. Although not a complete match between the datasets the eastern flank is identified as the area with the highest biomass measurements and NASC. There are increased densities of zooplankton, phytoplankton, and detritus at station 1 and high values of biomass and NASC values at station 2, both on the eastern flank of the seamount. There is more ambiguity in the values of the lowest abundances with results divided between stations 1, 2 and 3. These differences may be due to species composition, oceanographic drivers, and turbidity within the water column.

Biomass and NASC showed no significant relationships to environmental variables however visual similarities in the S_v and plankton trawls could be observed. By only isolating the mean NASC at the plankton trawl locations the data was severely limited in its interpretation due to the limited number of samples. Furthermore, the effect of scatterers at the thermocline may have been reduced by averaging over the entire depth of the plankton trawl. The processing method of the ES70 data may have also affected the comparison of the NASC and in-situ datasets. By using the SHAPES school detection algorithm to remove schools from the 200 kHz data, gaps that contained no data were left within the dataset lowering the mean backscatter within the plankton trawl locations. However, due to the small sample periods the effect of this would have been minimal. Furthermore, strong single targets which were smaller than the minimal detection size used by the SHAPES algorithm would not have been removed and could have increased the NASC estimates. Prior and post analysis echograms were visually scrutinized to ensure that the processing techniques had minimal effects on the backscatter observed during the periods of the plankton trawls. Had a larger dataset

been analysed an average of the surrounding backscatter would have been interpolated for the 'no data gaps' generated by the removal of fish schools.

With both the NASC and biomass data collection methods no differentiation between biological scatterers or matter in the water column is made. The ES70 detects scatterers of biological matter but also of non-living samples which could be bubbles, sediment, or detritus, such as fibres. The acoustic return from a scatterer depends on the acoustic properties of the sound pulse, the transmission of the pulse throughout the water column and the physical properties of the target (Simmonds and MacLennan, 2005). Three discrete anatomical classes were proposed when studying plankton acoustically categorising samples as fluid-like, hard elastic shelled or gas bearing (Stanton *et al.,* 1994; Stanton *et al.,* 1996). Therefore, the plankton abundances estimated through NASC values are likely to be overinflated due to the inclusion of non-living specimens with no representation made of the backscattering properties of those specimens. Similarly, small sediment particles would have been retained in the biomass analysis samples despite initial filtering. This combination of living and non-living samples may have affected the ability to detect specific environmental drivers of the samples. Despite these limitations, the visual correlation between the two datasets was a positive result which would likely be enhanced with a higher number of plankton trawls.

4.5.5 Composition of plankton

Crustacea was the most dominant zooplankton group over Sandes likely a result of copepod composition which was similar to other studies conducted in the Indian Ocean finding a higher abundance of cyclopoids (McKinnon *et al.*, 2008; Cedras and Gibbons, 2021; Davies, Beckley and Richardson 2022). In comparison to worldwide studies, warmer, less productive oceanic waters tend to have lower abundances of copepods

which are a source of nutrition for predatory fish (Brandão *et al.,* 2021). The consumption of a specific quantity and species of copepods has been shown to increase the survival rate of larval mandarin fish (*Synchiropus splendidus*; Zeng *et al.,* 2018). Therefore, the composition and abundance of copepods around Sandes seamount may be important in supporting the larval fish community which is often higher around seamounts due to the protection that the topographic features provide from currents and turbulence (Pitcher *et al.,* 2007). Copepod abundance also directly influences the stock size of fish. When higher abundances of copepods are available then increased stocks of fish such as the Atlantic mackerel (*Scomber scpmbrus*) have been identified (Ringuette *et al.,* 2002). Therefore, copepods are likely the main source of nutrition supporting fish stocks over Sandes seamount with changes to copepod abundances influencing the abundance and composition at all levels of the trophic food web. For phytoplankton, *Trichodesmium* were most abundant and have been associated with seasonal blooms in the Indian Ocean (Carpenter and Capone, 1992). *Trichodesmium* are commonly found in areas with low nutrients such as the oligotrophic Indian Ocean and their contributions to the nitrogen cycle is of global importance (Capone *et al.,* 1997). More value could have been gained from this data by identifying plankton groups to lower taxonomic levels and is recommended for future studies.

4.6 Conclusion

Using a combination of methods this study looked to identify the spatial distribution of zooplankton around Sandes seamount. Due to limitations with the acoustic frequencies available and sampling method, the acoustic identification of plankton was constrained, however positive correlations between NASC and in-situ samples was observed. To the best of our knowledge, this study reports on the first deep (>20 m) water plankton

samples undertaken at Sandes seamount providing information on the composition and density of zooplankton around a remote seamount. Ambiguity between the spatial distributions from the different sampling techniques likely came from the inclusion of detritus in the acoustic and biomass analysis. With higher detritus located on the eastern flank of Sandes this could be due to current movements causing the aggregation of detritus and higher backscatter (NASC) in the water column potentially due to turbulence caused by flow-topographic interactions and tidal movements. These results provide an insight into the fine scale drivers of zooplankton and provides evidence for the predator-prey interactions caused by nocturnal DVM movements. This is important to monitor in oligotrophic regions, such as Sandes, that are data deficient regarding zooplankton composition, so this study contributes to the gap in knowledge elucidating fine scale variabilities in plankton distributions (Davies, Beckley, and Richardson, 2022). Using multiple methods, this study has discussed the issues presented when sampling zooplankton acoustically and the importance of in-situ sampling to provide a clearer understanding of the trophic links promoting high biodiversity at Sandes seamount. Although single beam echosounders are not commonly used for plankton ecological surveys, they do have the ability to determine the spatial distribution of scatterers in the water column. Zooplankton play a critical role in the biological carbon pump and sustain fish communities- by understanding their distribution and behaviour around seamounts this study contributes to the global understanding of the importance of seamounts.

Chapter 5: General discussion

Throughout multiple studies this thesis has identified and quantified pelagic biota around varying topographic features in the Chagos Archipelago in relation to oceanographic processes. By sampling pelagic fish, plankton and oceanographic variables, relationships between the physical drivers and biological aggregations were elucidated providing the most detailed understanding of the distribution and behaviour of pelagic biota around Sandes seamount and Egmont Atoll to date (Table 5.1). The Chagos Archipelago Marine Protected Area (MPA) is a no-take zone with minimal anthropogenic disturbances (Readman *et al*., 2013). These protections provide a study site where scientific conclusions can be related to natural responses without significant direct pressures from fishing, many types of pollution, and other anthropogenic conflicts. Unless within protected regions, seamounts have no specific protections in the high seas yet are often identified as hotspots for biological aggregations (Worm *et al.,* 2003; Morato *et al.,* 2010; Dubroca *et al.,* 2014; Marsac *et al.,* 2020). Evidencing the oceanographic mechanisms that occur around seamounts emphasising the biological value of these features is highly important for future marine planning strategies. The spatial variability of pelagic fish is important to understand due to the trophic links they support and the commercial value of many species. Around atolls the oceanographic drivers of pelagic biota vary from that of seamounts, but the significance of their distributions is just as important for both conservation and fisheries purposes. This final chapter summarises the thesis and discusses recommendations for future conservation and sampling opportunities tying together the results from each chapter and synthesising the novel results in respect to future opportunities.

Table 5.1: Summary of data collection times, locations, methods and key finding in each analysis chapter.

Thesis chapter	Survey location	Data collection time	Methods used	Key finding
2	Sandes seamount	November 2019 March 2022	• ES70 • ADCP • Oceanographic moorings • Camera validation	The basin scale Indian Ocean Dipole (IOD) underpins the response of schooling fish around Sandes seamount through the modulation of the surface mixed layer depth.
3	Egmont Atoll	November 2019 March 2020	• ES70 • ADCP • Oceanographic moorings • Hydrodynamic model • Camera validation	Topography and tide are prominent factors in determining the spatial distribution of schooling fish around Egmont Atoll between different seasons and sampling locations.
4	Sandes seamount	March 2022	• ES70 • Plankton net • Camera validation	First insight into the composition of plankton at Sandes seamount with evidence of higher plankton densities during the ebb tide.

5.1 Synthesis

Using a fisheries echosounder synchronised with an acoustic Doppler current profiler (ADCP), concurrent measurements of the biological and physical composition of the water column were collected over a range of locations and periods of time (Table 5.1). **Chapter 2** focussed on Sandes seamount which has previously been described as a 'biodiversity hotspot' with the study noting that it lacked fine scale concurrent biophysical observations (Hosegood *et al.,* 2019). To reduce this knowledge deficit, acoustic surveys with identical methodologies were conducted over different years.

During the first survey in November 2019 an anomalously strong regional ocean-atmospheric event occurred- the Indian Ocean Dipole (IOD)- increasing the sea surface temperatures (SST) and wind field in the Chagos Archipelago (Du *et al.,* 2020). In contrast, a negative IOD was observed in March 2022 which decreased SSTs in the region. Between the two surveys there was an 8 °C variation in water temperature in the upper 150 m of the water column. Analysis showed that the distribution of schooling fish over Sandes seamount changed between the two surveys likely due to the IOD affecting the depth of the thermocline spatially constraining fish schools to the flanks of the seamount. However, when the thermocline was above the summit of the seamount (in March 2022 with a negative IOD), flow-topographic interactions caused internal wave propagation over the seamount which may be the cause of the increased number of fish schools and the distribution of those schools over and around the seamount summit. This study highlighted that neither broad or fine-scale processes can be considered in isolation, rather it is a combination of the two which drive the distributions and behaviour of pelagic fish schools over Sandes seamount. Biota responded to the change in oceanographic conditions with behaviours well documented in the literature: likely using mechanisms such as station holding and the many eyes hypothesis (Lack, 1954; Porteiro and Sutton, 2007; Ward *et al.,* 2011). This chapter demonstrated the complexity of biophysical interactions and alluded to the need to protect these topographic features not only because they promote biodiversity but enhance fish aggregations. Climatic events have a clear impact on fish dynamics which likely links to impacts up and down the food web.

A similar approach was applied in **Chapter 3** around Egmont Atoll with a comparison of two sites surveyed in November 2019 and March 2020. Unlike seamounts, atolls and

islands completely impede current flow re-directing water around the island which establishes different oceanographic processes such as internal waves and upwelling which contribute to the island mass effect (De Falco *et al.,* 2022). The bathymetry around Egmont Atoll is varied with a lagoon, steep canyons, and shallower plains all within 1 km of the shoreline. Survey 1 was conducted over the steep canyon region with vertical walls descending to 400 m depth, where biological aggregations were primary observed over the canyons. Higher fish school abundances were also related to increased current velocities (of > 0.4 ms^{-1}) and the flood tide. At the second site, surveyed in March 2020, the ebb tide was found to significantly increase biological aggregations at the eastern end of Manta Alley. This is likely to be partly due to the presence of the lagoon as, in previous studies, higher aggregations of zooplankton and manta rays have been observed when water flowed out of the lagoon during the ebb tide (Harris *et al.,* 2019; Sheehan *et al.,* 2019). These zooplankton concentrations potentially moved with the outflow of water which fed into the food web causing higher aggregations of schooling forage fish to be observed during the acoustic survey. The background current at Egmont in 2019 (during the positive IOD) was measured to have no effect on the flow regime around the atoll suggesting that only localised flow topographic interactions drove the differences in fish distributions. This study had similar conclusions to Chapter 2 and showed the high spatial variability that occurs not only around seamounts, but also oceanic atolls.

Within the datasets collected, the effect of scatterers other than schooling fish were largely ignored however zooplankton are essential in supporting the global carbon pump and sustaining fish communities (Pinti *et al.,* 2023). A targeted study in **Chapter 4** over Sandes seamount collected plankton samples and acoustic data to understand how the

composition and abundance of planktonic scatterers within the water column varied. Tide and transect significantly affected the distribution of zooplankton and detritus around Sandes with higher densities located on the eastern flank likely linked to the current strength and direction brought about by the ebb tide. NASC, a proxy for biomass, derived from the ES70 did not respond to environmental drivers when modelled however, visual comparisons between mean backscatter and in-situ zooplankton abundances did align. This study found some similarities between the NASC and in-situ plankton samples (although not significant) when considering the spatial distribution of detritus showing some disconnect between the two methods but also that with some refinement the results could align. The category of detritus consisted of mainly parts of plankton so was used to indicate the recent high abundance of plankton before predation occurred. This chapter illuminated zooplankton distributions by collecting the first deep water plankton samples over Sandes seamount supporting Chapter 2 by providing evidence of the trophic links between schooling fish and zooplankton communities whilst highlighting the limitations of studying this group with acoustic instruments.

5.2 Recommendations for the conservation of seamount and atoll ecosystems

5.2.1 Chagos Archipelago

The Chagos Archipelago MPA has few anthropogenic threats although these are increasing yearly. Plastic pollution from major Indian Ocean sources such as the River Ganges, India (Napper *et al.,* 2021) are contributing to large amounts of marine debris washed ashore in the Chagos Archipelago (Hoare *et al.,* 2022). Another increasing threat is illegal, unreported, and unregulated (IUU) fishing which is a major issue in the Indian

Ocean (WWF, 2020). The Indian Ocean is home to many commercially important species such as tuna and swordfish and poor wages in countries surrounding the Indian Ocean is incentivising illegal fishing (WWF, 2020). Using Automated Identification System (AIS) to map the tracks of fishing vessels, the fishing effort around the Chagos Archipelago is some of the heaviest fished waters in the Indian Ocean (Kroodsma *et al.,* 2018). IUU fishing is a major global threat however, sanctuaries such as the Chagos Archipelago provide refuge to both migratory and stationary species allowing sites where anthropogenic threats are minimal (Koldewey *et al.,* 2010). Even within the Chagos Archipelago, IUU fishing still occurs with fish aggregating devices (FADs) identified by the fisheries patrol vessel which got significantly worse during Covid-19 when IUU boats could not be boarded (Collins *et al.,* 2021). This thesis demonstrates, along with many other studies, that in a heavily fished ocean, biological hotspots can thrive and support a wealth of biota when protected (Hays *et al.,* 2020). However, it's unlikely that by ringfencing parts of the ocean biodiversity hotspots like the Chagos Archipelago would be created, as it is a complex interplay of climate and oceanography interacting with variable topography that has been shown to be key. Within this study it is the topographic features within the epipelagic zone that are key to retaining high abundances of species.

The Indian Ocean is identified as an oligotrophic region with low nutrient levels making sustaining life challenging (Jena *et al.,* 2013; Jiang *et al.,* 2022). Within oligotrophic seas where nutrients are scarce then processes that provide mixing or the enhancement of nutrients play a vital role in supporting organisms. Flow topographic interactions around seamounts and atolls initiate processes such as localised upwelling and vertical advection which can increase primary production and the retention of biota over smaller

areas (Rogers, 2018). Around oceanic atolls the Island Mass Effect (IME; Doty and Oguri, 1956) has been observed in the Indian Ocean around islands in Mauritius (Elliot *et al.,* 2012) and the Maldives (Sasamal 2006; Su *et al.,* 2021) through satellite observations. Within this study, no conclusions can be determined about the IME as the in-situ sampling method did not target the larger scale current regime and processes around Egmont atoll and no satellite imagery was used. This research suggests that vertical advection over canyon sites increased the abundance of schooling fish which would in turn support larger species through trophic interactions. Increased biota is well documented over seamounts even if the underlying mechanisms are lesser known (summarised in Pitcher *et al.,* 2007). These examples show that topographic features are key to increasing and protecting high abundances of species and that by identifying these pinnacles and canyons will likely be a key starting point when determining the location of protected sites. One core issue in remote locations such as the Chagos Archipelago is the lack of high-resolution seafloor maps- without a greater understanding of ocean bathymetry, it increases the difficulty in identifying key aggregation sites that should be protected. This thesis shows the importance of both atolls and seamounts within the Chagos Archipelago for fish (and to a lesser extent plankton) and when combined with other studies shows the importance of flow-topography interactions in driving aggregations. Although the diversity of Sandes seamount and Egmont Atoll were not directly considered within this thesis as acoustics do not provide this level of detail, the consensus of research conducted globally around topographic features have linked both seamounts and atolls to increased diversity (Morato *et al.,* 2010a; Dubroca *et al.,* 2013). This indicates that locations such as the Chagos Archipelago are important to protect with its high diversity and remote location providing a refuge in the wider oligotrophic Indian Ocean.

5.2.2 Global applications

In a recent study over 37,000 seamounts were predicted globally based on seafloor bathymetry data (Yesson *et al.,* 2020). Seamounts tend to have higher volumes of biomass over the summit and flanks in comparison to the open ocean which was termed the 'seamount effect' (Dower and Mackas, 1996). Many seamounts, banks and atolls have already been identified as biodiversity hotspots with increased aggregations of tuna (Morato *et al.,* 2010a; Dubroca *et al.,* 2013), cephalopods (Laptikhovsky *et al.,* 2017) and sharks over these features (Worm *et al.,* 2003; Hosegood *et al.,* 2019). This thesis provides further evidence that topographic features are fundamentally natural fish aggregating devices, and that policy to increase protections globally- over atolls and seamounts should be considered. Some seamounts are protected within large scale MPAs such as the Chagos Archipelago, but there is no legislation specifically protecting seamounts in the high seas. A recent breakthrough may rectify this with the Biodiversity Beyond National Jurisdiction (BBNJ) treaty which supports the protection of 30% of the high seas by 2030 (United Nations General Assembly, 2023). Although this treaty does not specifically target seamounts, with such prevalent global coverage of these underwater features it is highly likely that many seamounts will benefit from the BBNJ protections supporting high biodiversity.

5.2.3 Sampling methods

Single beam echosounders are affordable alternatives to split beam echosounders being able to detect the presence and absence of biota but are limited when describing species, biomass, and individual targets (Simmonds and MacLennan, 2005). Within this study oceanographic drivers of pelagic fish schools were elucidated providing invaluable information that can support conservation efforts around the world. A focus was put on

schooling fish instead of individual fish due to the higher levels of certainty in school identification associated with single beam echosounders (Simmonds and MacLennan, 2005). The discrimination of biological targets was tested in Chapter 4 when determining the distribution of zooplankton. As discussed, the analysis of plankton with acoustics is limited due to the range resolution of instruments and using a single beam echosounder limits the interpretation of acoustic data to mainly spatial distributions of plankton and fish. Understanding the drivers behind the spatial distributions of plankton is a key starting point in a data deficient region. By understanding the foundation of the food chain, the information can be linked to higher trophic levels where data is also lacking. An example of this is the marine cetacean distribution, which is largely unknown in the Indian Ocean, so it is important to understand the distribution of zooplankton not just for forage fish but marine mammals too (de Boer *et al.,* 2002; Anderson *et al.,* 2020; Letessier *et al.,* 2022). Using a split beam echosounder, such as a Simrad EK60 or EK80, would have improved this study allowing a greater discrimination of targets and the directionality of schooling and individual fish to be determined. Higher resolution data produced from split beam echosounders would have provided further information on how current magnitudes affect biota and if behaviours such as station holding were occurring as split beam echosounders can provide more detailed information on how fish move throughout the beam. This thesis shows how affordable systems such as the ES70 can contribute a large volume of information and if limitations are understood biological inferences can be made. The ES70 can determine the spatial distributions of schooling fish, however individual targets and behaviours are difficult, if not impossible to conclusively determine. In the future, split or multibeam sampling methods, along with more frequencies, would be beneficial in determining the behaviour of the organisms by providing information of the directivity

and speed of the targets (Arrhenius *et al.,* 2000, Torgersen and Kaartvedt 2001). ADCP's are also being developed to collect concurrent backscatter and current data. A combination of the two would allow joint biophysical data to be collected which would be invaluable for multidisciplinary studies.

Validation of the fisheries acoustics data was limited as trawl surveys, the main quantifier of species composition (Fernandes *et al.,* 2002) were not permitted as the Chagos Archipelago is a no-take zone. Instead, a combination of drop cameras and plankton nets were used to validate acoustic targets. This simple cost-effective method involving a frame, Temperature Depth (TD) sensor and GoPro is easily replicated. An emerging validation tool is eDNA which is a sample of the genetic material in the water column and through metabarcoding can detect organisms in the water column through skin cells and excrement validating acoustic detections (Ficetola *et al.,* 2008). eDNA within the water column is estimated to last between days to weeks depending on environmental and microbial conditions (Barnes *et al.,* 2014; Rees *et al.,* 2014; Thomsen and Willerslev, 2015) although seawater may reduce these times significantly (Dell'Anno and Corinaldesi, 2004). A fine scale study comparing acoustic DVM signals to eDNA samples observed some species mirroring DVM changes showing the potential for fine temporal scale changes to be captured with eDNA (Easson *et al.,* 2020). Another study found the method in which eDNA was analysed and collected determined the significance of correlations between eDNA and echo intensity (Jo *et al.,* 2017). eDNA has the potential to be an alternative validation tool to study the biological composition of the water column which would assist the reliability of acoustic surveys. Further studies comparing the backscatter and biological compositions need to be conducted to understand the limitations of acoustics and eDNA comparisons.

Many acoustic studies target specific species, and this is driven by a need to quantify fish stocks (Starr and Thorne, 1998; Fernandes *et al.,* 2002; Doray *et al.,* 2021). However, a holistic approach such as capturing all species also has its advantages. From this research many mixed species schools were identified which would have complicated individual species identification techniques with acoustics. This study has only considered mixed schools due to the acoustic limitations of single beam echosounders and the lack of frequencies. Most studies that identify fish species use 4-5 frequencies and compare the frequency response of the target to determine the species however target strength measurements must be known prior to these surveys so they are usually only conducted on commercially important species (Simmonds and MacLennan, 2005). Fisheries acoustics have been identified as a useful data collection tool in ecosystem-based Management (EBM) allowing biophysical interactions in the marine environment to be protected alongside socio-economic factors (Trenkel *et al.,* 2011). Species specific information is vitally important but understanding ecosystem dynamics may help improve the efficacy of implemented conservation strategies. If ecosystem-scale dynamics are determined which can be achieved with acoustic and oceanographic equipment, then this provides a greater resource to marine governing bodies to aid in decision making. Fisheries acoustics can provide a large volume of information on the seafloor bathymetry, water column scatterers and can even use these scatterers as a proxy for oceanographic processes (Embling *et al.,* 2013). CTDs, temperature sensors and ADCPs are rapidly being simplified and advertised to the recreational market. Although some of these models may limit sampling rates or resolution it allows entry level oceanographic data which may identify vital biophysical interactions. Inclusion of more oceanographic variables have been shown to be advantageous on numerous studies including mesophotic corals (Diaz *et al.,* unpublished), manta rays (Harris *et al.,* 2021)

and pelagic fish (e.g. Embling *et al.,* 2013; Pineda *et al., 2020*). The examples listed show that biophysical interactions are complex and by adding additional oceanographic sensors to surveys it will provide a more in-depth understanding allowing more targeted research on specific regions. Many of the tools required for a holistic ecosystem approach are already available and can be applied to projects in an affordable way. The key is drawing both biological and physical interests together and promoting the joint benefits from combining methodologies and observations.

5.3 Oceanographic influences on pelagic aggregations

5.3.1 Regional oceanographic influences: Indian Ocean Dipole

The effect of the IOD on currents was only directly observed over Sandes seamount. Strong current magnitudes recorded over Sandes seamount in 2019 were not observed on the western flank of Egmont during the same timeframe. The reasons behind this are as yet unknown however suggestions for this are based on the positioning of Egmont in relation to other topographic features in the Chagos Archipelago and the direction of the current flow. Egmont atoll is located to the west of Great Chagos Bank which sits at the centre of the archipelago within shallower water. Similar to seamounts, banks can partially inhibit current flow dispersing the currents around Great Chagos Bank so that they do not directly interact with Egmont atoll. Another possible reason is the location of the first Egmont survey on the lee side of the island where the IOD currents may not have influenced however Robinson *et al.* (2023) does not support this suggestion as oceanographic moorings located on the eastern side of Egmont also recorded insufficient evidence of a background current. The advantage of only tidal related currents affecting biota at Egmont is the predictability of them allowing biota to have a continuous pattern of behaviour and not have to withstand adverse current magnitudes

or directions which may be detrimental to their behavioural patterns. The tidal-coupling hypothesis has been evidenced in studies around the world aiding foraging efficiency and predator-prey capture rates (Zamon, 2003; Benjamins *et al.,* 2015; Waggitt *et al.,* 2016; Williamson *et al,* 2019). By understanding tidal drivers of biota then aggregations of prey can be predicted. Outside of the Chagos Archipelago MPA this would allow time-specific protections to be implemented such as fishing exclusions during certain tidal phases to reduce the bycatch of apex predators foraging on commercially important schooling fish species. One limitation to the predictability of the tidal cycle is climatic drivers. If climatic drivers affect the strength or direction of the tidal regime, then extreme changes in distributions, abundances and behaviours of fish may be observed. Within this study a strong positive IOD event was observed, if combined with the El Nino Southern Oscillation (ENSO) then SST would likely be further amplified and the impacts on biological aggregations could be even stronger (Saji and Yamagata, 2003a; Saji and Yamagata, 2003b; Meyers *et al.,* 2007; Sheppard *et al.,* 2012; McPhaden and Nagura, 2014).

5.3.2 Regional oceanographic influences: Thermocline

A thermocline indicates a transition between warmer surface waters and cooler deeper waters. The depth and strength of the thermocline changes seasonally and is generated by the formation of distinct water layers with different densities. The IOD affects SSTs causing heating and cooling effects in different regions of the ocean depending on whether a positive or negative IOD event is occurring (Du *et al.,* 2020).

The deepening of the surface mixed layer was observed over Sandes in 2019 which caused higher temperatures in the upper 100 m of the water column which was due to increased strength of the easterly wind field generating surface wave induced mixing and

deepening the thermocline. A deep thermocline of approximately 100 m depth was observed at Sandes and Egmont in 2019 during the positive IOD event. Unlike Sandes, no evidence of enhanced current magnitudes due to the IOD event were measured at Egmont however, the thermocline was at the same depth at both sites showing that the IOD still affected the SSTs at both sites even if current magnitudes were different. The thermocline depth ties the two topographic features together and although it may not elicit the same responses in fish– it does show that fish schools respond to the thermocline depth affecting their distributions and behaviours. For example, if Egmont was sampled in March 2022 the thermocline at Ile des Rats would not have interacted with the tops of the canyons as the depth was approximately 40 m (the same as Sandes). Although the effect it had on schooling fish is unknown, it would be reasonable to suggest that it differs from 2019 and would be similar to interactions observed at Sandes in 2022 where it was suggested that internal waves were generated and propagated on to the seamount summit due to interactions between the surface mixed layer and the seamount. At Egmont internal waves may be generated and break over the canyons on the western side leading to even higher abundances of biota above these features due to the constant input of prey and nutrients transported by internal waves. This suggests that conservation measures should be adaptable and flexible so that key conservation sites where there is higher species diversity and abundances can be identified within the Chagos Archipelago. This would allow for focussed fisheries patrol vessel efforts which would be both time efficient and cost effective as there is currently only one patrol vessel assigned to the Chagos Archipelago.

An example of where adaptable large scale conservation measures would be beneficial within the Indian Ocean is Hanifaru Bay in the Baa Atoll UNESCO Biosphere Reserve,

Maldives. High volumes of zooplankton, driven by currents, aggregate in the bay attracting whale sharks and manta rays (Murray, 2013). Hanifaru Area MPA covers 11.6 km^2 compared to the total area of Baa Atoll at approximately 1200 km^2 (Ocean Country Partnership Programme, 2023). Within Baa Atoll there are 75 islands and 9 MPAs of similar sizes to Hanifaru. These areas have been chosen due to the presence of specific marine, terrestrial and mangrove ecosystems along with specific species (UNESCO, 2019). Due to climatic drivers, oceanographic conditions are changing (IPCC, 2023) and small scale MPAs, such as Hanifaru, may not be able to provide long-term protection to species if behaviours or aggregation sites of pelagic fish change. This thesis advocates for larger protected areas over varying topography so should spatial distributions of biota change with the physical drivers then biological aggregations would still have legal protections within a VLMPA.

The movement of fish due to environmental pressures is well documented with oxygen (e.g. Campana *et al.,* 2011; Domenici *et al.,* 2017; Klevjer *et al.*, 2016; Annasawmy *et al.,* 2018), currents (e.g. Warhaft, 1997; Liao, 2007; Porteiro and Sutton, 2007), light (e.g. Badcock and Merrett, 1967; Neilson and Perry, 1990; Brodeur *et al.*, 2005; Cascão *et al.*, 2019) and temperature (e.g. Reynolds and Casterlin, 1979; Johnson and Kelsch, 1998; Clarke and Johnston, 1999; Habary *et al.*, 2012; Khan and Herbert, 2012; Alfonso 2020; Volkoff *et al.,* 2020) all recognised to affect the distributions and behaviour of pelagic fish. Within a VLMPA anthropogenic pressures, such as fishing, are reduced however, outside of areas with conservation strategies multiple pressures contribute to increased stress on an ecosystem. The effect of multiple pressures on an ecosystem is well studied but whether bottom-up or top-down mechanisms control the trophodynamics of an ecosystem is contested (Young *et al.,* 2015). This study supports the former mechanism

with oceanographic drivers influencing plankton although, singular fish which are more likely to be predators were not measured in this study.

The effect of fishing versus environmental pressures is largely unknown so if a region only has small MPAs and a large fishing pressure, the behaviour of fish in response to these pressures are unknown. The trade-off between environmental and fishing pressures on the response of fish requires further study. Higher fish biomass was identified within MPAs in the Philippines even when typhoons impacted some sites suggesting that anthropogenic protections are more important than environmental (McClure *et al.,* 2020). However, if fishing pressure is added on top of multiple environmental pressures, then the responses of fish may be harder to predict. If the processes behind fish movements are understood, then there is the potential for better predictability of food stocks.

This study advocates for the continued creation of VLMPAs using the Chagos Archipelago as an example. There is conflicting literature on the benefits of VLMPAs with many of the criticisms already addressed (reviewed in O'Leary *et al.,* 2018). The main critiques of VLMPAs come from the inability to govern and manage such large sites although positive measures have been observed with unmanned aerial vehicles and AIS used as tools to monitor IUU fishing (O'Leary *et al.,* 2018; Relano *et al.,* 2021). A further drawback is the view that MPAs may be a political measure- this is a prominent issue with the Chagos Archipelago MPA due to different claims on the region (De Santo *et al.,* 2011). Despite the drawbacks, enhanced biodiversity and the protection of migratory species are some of the benefits of VLMPAs when the correct planning procedures are followed and sufficient budget is designated to the project (Relano *et al.,* 2021).

5.3.3 Fine scale physical dynamics

This study supports the idea that internal waves could be used as a driver for schooling fish over seamounts as previously suggested by Hosegood *et al* (2019). Evidence of internal waves are presented in this study but were not as clear as echograms observed in similar surveys (e.g., Embling *et al.,* 2013; Pineda *et al.*, 2020). An alternative theorem for the increased aggregation of schooling fish over seamounts is the Taylor column hypothesis where a steady flow of currents over a seamount draws nutrients towards the surface and traps them within an eddy (Taylor, 1923; Hogg, 1973; Huppert, 1975; Huppert and Bryan, 1976; White *et al.,* 2007; Pitcher and Bulman, 2007; Lavelle and Mohn, 2010). Over Cross seamount in the Indian Ocean a Taylor column was identified with the hypothesis that it retained zooplankton over the seamount enhancing biomass (Domokos, 2022). Due to the strength of the currents, the conditions for a Taylor column were not observed over Sandes during this study. An increase in biological aggregations was observed over Sandes in March 2022 when the shallow thermocline interacted with the seamount summit creating higher internal wave generation. Although no clear evidence of this was observed in the acoustic data, the increase in biota does suggest that some oceanographic mechanisms occur supporting increased aggregations. Evidence from another study sampling six seamounts in the Indian Ocean found internal waves influencing the oceanographic regime around the seamounts with little evidence of Taylor columns (Read and Pollard, 2017). Seamount morphology plays a key role in determining the oceanographic processes that occur and the retention of pelagic biomass (White *et al., 2007*; Lavelle and Mohn, 2010). Understanding seamount morphology and incorporating oceanographic variables into models would be valuable

for future research as it is thought that shallower seamounts are key for holding higher abundances of biota (Morato *et al.,* 2008).

5.4 Final conclusions

5.4.1 Contribution to knowledge and future work

This thesis has characterised the fine scale distributions of pelagic fish in relation to oceanographic drivers to determine how spatiotemporal variation drives distribution and behaviours. This is important when understanding the spatial variability of pelagic fish and plankton for conservation measures and in understanding why biodiversity is often increased around seamounts and oceanic atolls. A detailed understanding of how climatic events change oceanographic conditions and the effect on pelagic fish is key for informing marine spatial planning to ensure that there are provisions in place for future climate scenarios.

Much of this thesis focussed on elucidating patterns in the distribution of pelagic fish and zooplankton around Sandes seamount. Undertaking fine-scale biophysical sampling allowed the first in-situ evidence of the IOD affecting pelagic fish within the Chagos Archipelago. With large temperature and current variations between the two different IOD phases the productivity around Sandes changed dramatically with schooling fish less prominent over the summit of Sandes during the positive IOD event. The differences observed have significant management implications as they show that small scale protections may not be enough if pelagic fish change their behaviours when under environmental stress. Dynamic protections that can adapt to climate variability would be essential to the protection of pelagic fish in the Indian Ocean as the IOD is not the only ocean-atmospheric event. ENSO also affects the oceanographic regime of the Indian

Ocean with the effects observed across the Indian and Pacific oceans (Talley *et al.,* 2011; Sheppard *et al.,* 2012).

Further work is required to understand the behavioural changes of pelagic fish in response to oceanographic drivers. Upgrading acoustic systems from single to split or multibeam would allow information on the directionality of pelagic fish to be ascertained (Simmonds and MacLennan, 2005). Understanding the behaviour and distribution of individual fish would elucidate trophic interactions with a particular focus on higher level predator-prey interactions such as sharks. This would allow targeted conservation strategies for specific species or trophic levels by timing patrol boat efforts to specific aggregation times or when certain behavioural traits are occurring. If disruptive activities such as military trials, which can cause a significant amount of noise pollution, are taking place then knowledge of biological aggregations and their spatiotemporal variations could be applied to mitigate the impacts of anthropogenic activities. At the other end of the trophic web, higher resolution data on plankton distributions would be attained through upgrading the acoustic systems. By understanding the characteristics of each trophic level and the interactions between them holistic management plans, such as EBM, could be implemented ensuring protections for all parts of the seamount ecosystem. Validation techniques were limited in this study as trawling was prohibited within the MPA. Video and plankton net sampling methods were conducted but these methods could have been improved. The use of sizing lasers on the cameras would have allowed quantification of fish sizes permitting comparisons between the acoustic data. Towed pelagic video systems would have been beneficial to compare acoustic observations and biota with successful designs already in operation (Sheehan *et al.,* 2013). Higher repeats of zooplankton samples would have aided in further

understanding the distributions of zooplankton around Sandes. Although repeat surveys allowed the direct comparison of results between years- alterations of the transect lines away from the seamount would have been beneficial allowing an investigation into the 'seamount effect' (Dower and Mackas, 1996). Surveying fish and plankton distributions on and away from the seamount would have allowed quantification of the biological enhancement that Sandes seamount provides (e.g., Morato *et al.,* 2010a; Campanella *et al.,* 2021).

Temporal variations were inconclusive due to the short survey periods. Longer acoustic surveys- particularly over spring-neap tidal cycles may have shown better insights of the drivers of pelagic biota. For example, the effects of internal waves on biological aggregations were not definitively identified with the fisheries echosounder even though they were observed on oceanographic moorings (Robinson *et al.,* 2023). With a longer survey duration, periods of stronger internal wave generation and the long-term effect on biota may have been captured.

This thesis focuses on Egmont Atoll producing the first comparisons of bathymetric features and tidal flows on pelagic fish in the area. A canyon site was identified as a key feature with flow-topographic interactions likely causing the aggregations of fish. The outflow of the lagoon on the ebb tide linked to higher counts of schooling fish supporting studies with similar conclusions (Harris *et al.,* 2021; Sheehan *et al.,* 2019). Due to weather conditions the sample sites between years could not be repeated although this did provide an insight into how varying bathymetry affects fish distributions. Considerations within methodologies should be made to ensure that data can be collected all around an atoll or island regardless of the weather conditions as repeated surveys under different conditions would show how fish respond to alterations of the

thermocline depth and water temperature. Tides around Egmont are mixed and variable complicating comparisons between tidal movements and biological aggregations (Robinson *et al.,* 2023). Future work understanding the tidal constituents would be beneficial to model the distributions of fish highlighting the need for more fine scale in-situ observations.

Future work could test the viability of translating these results to other seamounts and atolls globally. Many studies have identified shallow seamounts and atolls as biodiversity hotspots, so the results found in this thesis are not exclusive to the Chagos Archipelago (summarised in Pitcher *et al*., 2007 and Rogers, 2018). The effect of the IOD was likely similar on many seamounts in the central Indian Ocean and by expanding this study to regions outside the MPA the effect of fishing on pelagic fish populations can be understood. Suitable sites for the continuation of this work would be looking at links between the Seychelles and Chagos Archipelago as tagging studies have identified corridors between the sites of species such as sharks (Curnick *et al.,* 2020a), and turtles (Hays *et al.,* 2020; Mortimer *et al.,* 2020). If apex predators are moving between sites, then looking at the composition of prey would be beneficial in understanding these migration behaviours and predator-prey interactions. A particular site in the Seychelles, an island called D'Arros may also be suitable as it is a designated MPA and a hotspot for multiple species of sharks (Filmalter *et al.,* 2013: Lea *et al.,* 2016). For seamounts, the Southwest Indian Ridge would be an optimum comparison site as work has already been conducted on six seamounts resolving the oceanographic regimes (Read and Pollard, 2017). Micronekton communities around seamounts were found to have complex relationships with physical processes similar to the results at Sandes seamount

(Annasawmy *et al.,* 2020). This supports the need to study seamounts globally and consider the biophysical interactions of multiple species.

The work presented here provides a novel insight into the physical drivers of pelagic fish and zooplankton around topographic features and how climatic drivers impact these distributions. Protecting the marine environment is essential with progress towards global participation evidenced with the BBNJ treaty. Conservation measures will only be effective if implemented based on robust scientific evidence elucidating the drivers of the distribution and behaviour of biological aggregations. With continued research around seamounts and atolls, the multifaceted physical mechanisms that drive marine communities can be understood to provide and predict the optimum protections for marine species ensuring that all aspects of the trophic web are sustainably supported.

Appendix A

The following figures and tables accompany Chapter 2:

Table A1: Summary of model for analysis 1 the number of fish schools per 1-minute bin in relation to oceanographic variables. Modelled with GLM GEE's with a poisson response. Only variables significant within the final model have been reported.

				Day					Night				
Frequency	Survey	Response variable	Explanatory variable	n	Df	X2	P(>|Chi|)	p	n	Df	X2	P(>|Chi|)	p
38 kHz	Nov-19	count	seafloorDep	461	3	186.45	<0.001	***	801	3	265.91	<0.001	***
			surfU		-	-	-	-		-	-	-	-
			sumU		-	-	-	-		-	-	-	-
			deepU		-	-	-	-		4	278.90	<0.001	***
			shallowV		3	26.66	<0.001	***		3	19.11	<0.001	***
			midV		3	21.12	<0.001	***		-	-	-	-
			largeV		3	16.05	<0.01	**		3	32.94	<0.001	***
			upAbs		3	65.88	<0.001	***		3	17.46	<0.001	***
			medAbs		3	17.12	<0.001	***		-	-	-	-
			lowAbs		-	-	-	-		-	-	-	-
			highTemp		-	-	-	-		-	-	-	-
			avTemp		5	94.35	<0.001	***		-	-	-	-
			bigTemp		-	-	-	-		3	12.69	<0.01	**
			thermDepth		-	-	-	-		-	-	-	-
			TimetoTideTurn		5	121.58	<0.001	***		-	-	-	-
			chagosTime		5	48.68	<0.001	***		-	-	-	-
200 kHz	Nov-19	count	seafloorDep	454	3	121.37	<0.001	***	802	3	39.90	<0.001	***
			surfU		3	12.59	<0.01	**		3	29.69	<0.001	***
			sumU		3	33.07	<0.001	***		-	-	-	-
			deepU		3	30.84	<0.001	***		-	-	-	-

			shallowV		-	-	-	-		3	12.47	<0.01	**
			midV		-	-	-	-		-	-	-	-
			largeV		-	-	-	-		3	14.66	<0.01	**
			upAbs		3	181.08	<0.001	***		-	-	-	-
			medAbs		3	22.26	<0.001	***		-	-	-	-
			lowAbs		-	-	-	-		-	-	-	-
			highTemp		-	-	-	-		-	-	-	-
			avTemp		-	-	-	-		-	-	-	-
			bigTemp		3	117.07	<0.001	***		-	-	-	-
			thermDepth		3	41.51	<0.001	***		-	-	-	-
			TimetoTideTurn		-	-	-	-		-	-	-	-
			chagosTime		-	-	-	-		-	-	-	-
38 kHz	Mar-22	count	seafloorDep	512	4	34.99	<0.001	***	501	3	46.66	<0.001	***
			surfU		-	-				-	-	-	-
			sumU		4	27.62	<0.001	***		3	13.82	<0.001	**
			deepU		-	-	-	-		3	28.35	<0.001	***
			shallowV		-	-	-	-		-	-	-	-
			midV		-	-	-	-		-	-	-	-
			largeV		-	-	-	-		3	26.88	<0.001	***
			upAbs		-	-	-	-		-	-	-	-
			medAbs		-	-	-	-		-	-	-	-
			lowAbs		-	-	-	-		-	-	-	-
			highTemp		-	-	-	-		-	-	-	-
			avTemp		-	-	-	-		3	24.37	<0.001	***
			bigTemp		-	-	-	-		1	11.76	<0.001	***
			thermDepth		-	-	-	-		3	9.91	<0.05	*
			TimetoTideTurn		6	303.65	<0.001	***		1	9.71	<0.01	**
			chagosTime		3	20.23	<0.001	***		-	-	-	-

			seafloorDep		-	-	-	-		4	65.75	<0.001	***
			surfU		-	-	-	-		3	25.95	<0.001	***
			sumU		-	-	-	-		3	14.42	<0.01	**
			deepU		3	17.32	<0.001	***		3	15.54	<0.01	**
			shallowV		-	-	-	-		-	-	-	-
			midV		3	27.05	<0.001	***		-	-	-	-
			largeV		-	-	-	-		-	-	-	-
200 kHz	Mar-22	count	upAbs	263	1	44.38	<0.001	***	335	-	-	-	-
			medAbs		3	29.14	<0.001	***		-	-	-	-
			lowAbs		-	-	-	-		-	-	-	-
			highTemp		-	-	-	-		-	-	-	-
			avTemp		-	-	-	-		3	18.61	<0.001	***
			bigTemp		3	29.70	<0.001	***		-	-	-	-
			thermDepth		-	-	-	-		-	-	-	-
			TimetoTideTurn		1	7.54	<0.01	**		-	-	-	-
			chagosTime		-	-	-	-		3	27.26	<0.001	***

Table A2: Summary of model for analysis 2 the NASC of fish schools per 1-minute bin in relation to oceanographic variables. Modelled with GLM GEE's with a gaussian response. Only variables significant within the final model have been reported.

				Day					Night				
Frequency	Survey	Response variable	Explanatory variable	n	Df	X2	P(>|Chi|)	p	n	Df	X2	P(>|Chi|)	p
38 kHz	Nov-19	NASC	seafloorDep	261	-	-	-	-	576	3	28.65	<0.001	***
			surfU		3	13.55	<0.01	**		3	18.30	0.00038	***
			sumU		-	-	-	-		3	11.90	<0.01	**
			deepU		-	-	-	-		-	-	-	-
			shallowV		-	-	-	-		-	-	-	-
			midV		-	-	-	-		3	11.80	<0.01	**
			largeV		-	-	-	-		-	-	-	-
			upAbs		-	-	-	-		-	-	-	-
			medAbs		-	-	-	-		-	-	-	-
			lowAbs		-	-	-	-		-	-	-	-
			highTemp		5	94.24	<0.001	***		-	-	-	-
			avTemp		-	-	-	-		-	-	-	-
			bigTemp		-	-	-	-		-	-	-	-
			thermDepth		-	-	-	-		-	-	-	-
38 kHz	Mar-22	count	seafloorDep	290	-	-	-	-	371	-	-	-	-
			surfU		-	-	-	-		-	-	-	-
			sumU		3	10.69	<0.05	*		-	-	-	-
			deepU		-	-	-	-		-	-	-	-
			shallowV		-	-	-	-		-	-	-	-
			midV		-	-	-	-		-	-	-	-
			largeV		-	-	-	-		-	-	-	-
			upAbs		-	-	-	-		-	-	-	-
			medAbs		-	-	-	-		-	-	-	-

	lowAbs		-	-	-	-		-	-	-	-
	highTemp		-	-	-	-		-	-	-	-
	avTemp		3	62.67	<0.001	***		-	-	-	-
	bigTemp		-	-	-	-		-	-	-	-
	thermDepth		-	-	-	-		-	-	-	-

Table A3: Summary of model for analysis 3 the perimeter of fish schools per 1-minute bin in relation to oceanographic variables. Modelled with GLM GEE's with a gaussian response. Only variables significant within the final model have been reported.

				Day					Night				
Frequency	Survey	Response variable	Explanatory variable	n	Df	X2	P(>|Chi|)	*p*	n	Df	X2	P(>|Chi|)	*p*
38 kHz	Nov-19	Perimeter	seafloorDep	261	-	-	-	-	576	-	-	-	-
			surfU		-	-	-	-		-	-	-	-
			sumU		-	-	-	-		-	-	-	-
			deepU		4	121.18	<0.001	***		3	265.06	<0.001	***
			shallowV		3	33.77	<0.001	***		3	15.48	<0.01	**
			midV		-	-	-	-		-	-	-	-
			largeV		-	-	-	-		3	20.60	<0.001	***
			upAbs		-	-	-	-		-	-	-	-
			medAbs		-	-	-	-		-	-	-	-
			lowAbs		-	-	-	-		-	-	-	-
			highTemp		6	31.46	<0.001	***		6	34.73	<0.001	***
			avTemp		6	28.52	<0.001	***		-	-	-	-
			bigTemp		-	-	-	-		3	21.77	<0.001	***
			thermDepth		-	-	-	-		-	-	-	-
38 kHz	Mar-22	count	seafloorDep	290	-	-	-	-	371	-	-	-	-
			surfU		-	-	-	-		-	-	-	-
			sumU		-	-	-	-		3	12.62	<0.01	**
			deepU		-	-	-	-		-	-	-	-
			shallowV		3	22.87	<0.001	***		-	-	-	-
			midV		-	-	-	-		-	-	-	-
			largeV		3	12.29	<0.01	**		-	-	-	-
			upAbs		-	-	-	-		-	-	-	-
			medAbs		-	-	-	-		-	-	-	-

	lowAbs	-	-	-	-	-	-	-	-
	highTemp	-	-	-	-	3	29.10	<0.001	***
	avTemp	-	-	-	-	-	-	-	-
	bigTemp	-	-	-	-	-	-	-	-
	thermDepth	-	-	-	-	-	-	-	-

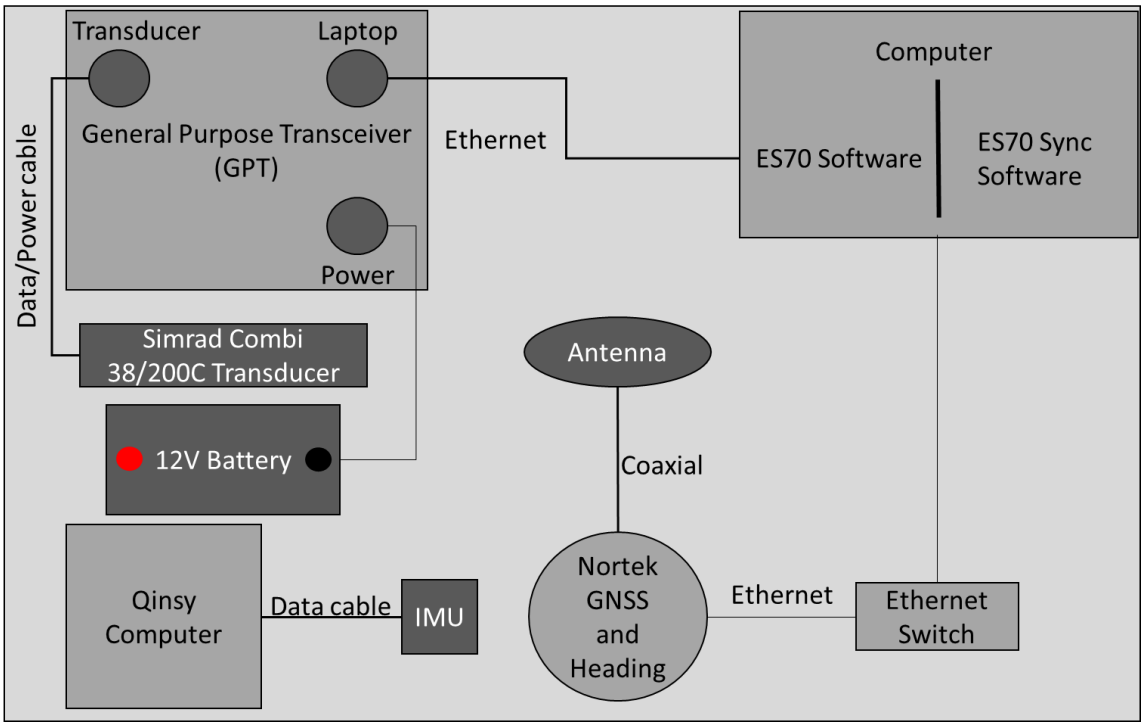

Figure A1: Cable diagram for the mobilisation of the Simrad ES70 during the survey.

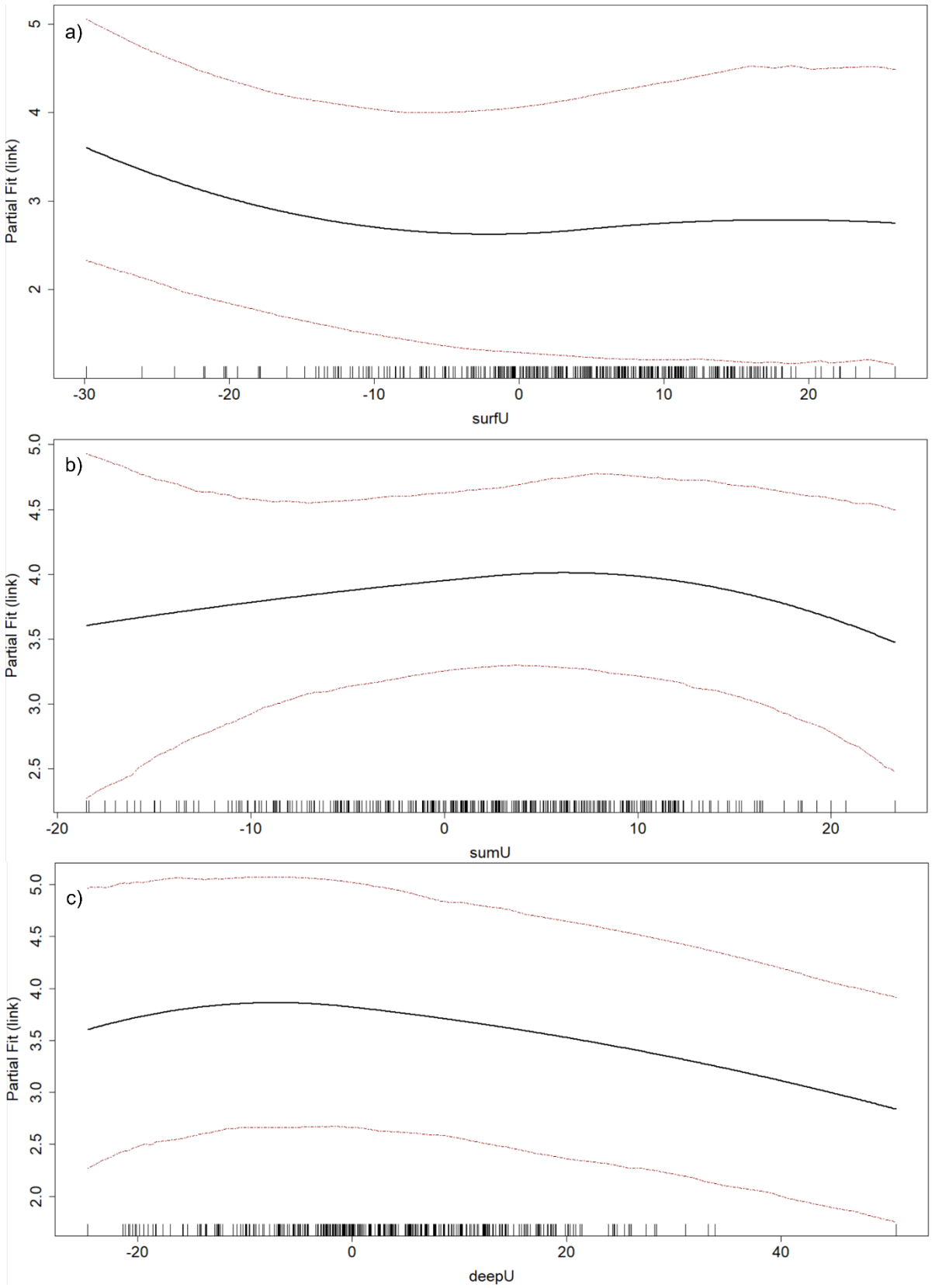

Figure A2: GLM GEE analysis showing the fish count in response to the u velocity component (east-west) at 200 kHz during night time in March 2022 (negative IOD). Fish responses are classified by depth band a) upper 50 m b) 50-100 m and c) 100-200 m depth. The units of the explanatory variables are cm s^{-1}. Red dotted lines show the 95% confidence interval with a rug plot at the bottom.

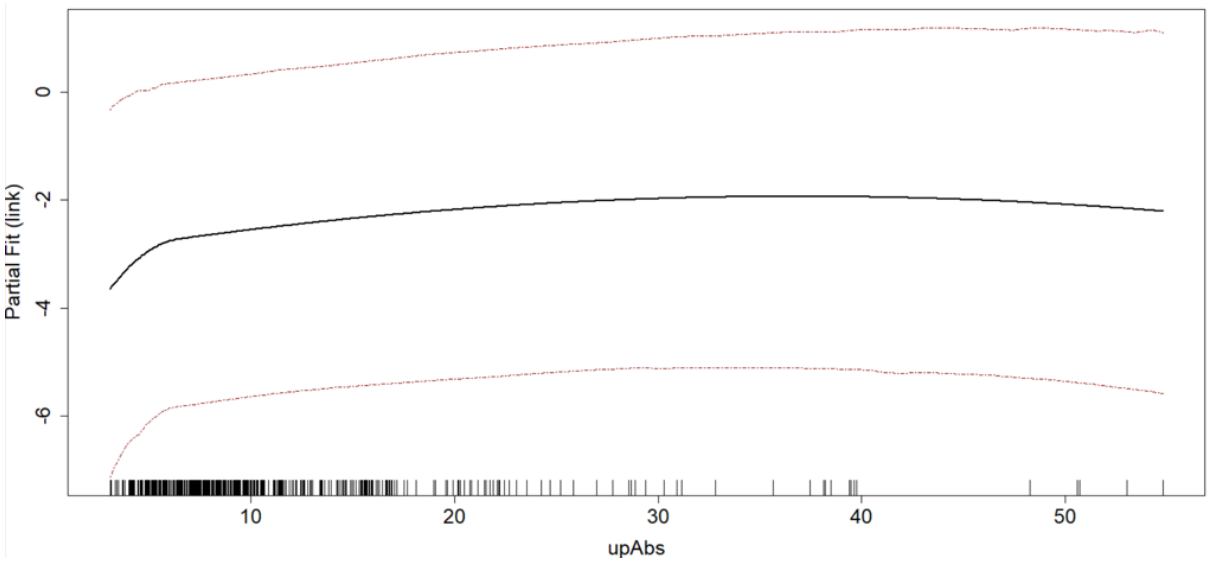

Figure A3: GLM GEE analysis showing the fish count in response to shear in the upper 50 m of the water column at 38 kHz during the day time in November 2019 (positive IOD). The unit of the explanatory variable is s^{-1}. Red dotted lines show the 95% confidence interval with a rug plot at the bottom.

Appendix B

The following figures and tables accompany Chapter 3:

Table B1: Summary of model for analysis 1 the number of fish schools per 1-minute bin in relation to oceanographic variables. Modelled with GLM GEE's with a poisson response. Only variables significant within the final model have been reported.

				Day					Night				
Frequency	Survey	Response variable	Explanatory variable	n	Df	X2	P(>|Chi|)	p	n	Df	X2	P(>|Chi|)	p
38 kHz	Nov-19	count	seafloorDep	476	-	-	-	-	649	3	58.40	<0.001	***
			u		-	-	-	-		3	32.16	<0.001	***
			v		-	-	-	-		-	-	-	-
			AbsShear		1	10.11	<0.01	**		-	-	-	-
			TimetoTideTurn		-	-	-	-		3	9.17	<0.05	*
			Time		-	-	-	-		-	-	-	-
38 kHz	Mar-20	count	seafloorDep	680	3	42.50	<0.001	***	788	3	23.07	<0.001	***
			u		-	-	-	-		3	9.13	<0.05	*
			v		-	-	-	-		-	-	-	-
			AbsShear		-	-	-	-		-	-	-	-
			TimetoTideTurn		-	-	-	-		-	-	-	-
			Time		3	43.52	<0.001	***		-	-	-	-

Table B2: Summary of model for analysis 2 the NASC of fish schools per 1-minute bin in relation to oceanographic variables. Modelled with GLM GEE's with a gaussian response. Only variables significant within the final model have been reported.

				Day					Night				
Frequency	Survey	Response variable	Explanatory variable	n	Df	X2	P(>|Chi|)	p	n	Df	X2	P(>|Chi|)	p
38 kHz	Nov-19	NASC	seafloorDep	280	3	61.77	<0.001	***	530	3	27.92	<0.001	***
			u		3	15.03	<0.01	**		-			
			v		-	-	-	-		-			
			AbsShear		-	-	-	-		3	8.97	<0.05	*
			TimetoTideTurn		3	19.24	<0.001	***		-			
			Time		-	-	-	-		3	16.89	<0.001	***
38 kHz	Mar-20	NASC	seafloorDep	452	-	-	-	-	384	3	16.64	<0.001	***
			u		-	-	-	-		-	-	-	-
			v		3	15.46	<0.01	**		-	-	-	-
			AbsShear		-	-	-	-		-	-	-	-
			TimetoTideTurn		3	15.83	<0.01	**		-	-	-	-
			Time		-	-	-	-		-	-	-	-

Table B3: Summary of model for analysis 3 the perimeter of fish schools per 1-minute bin in relation to oceanographic variables. Modelled with GLM GEE's with a gaussian response. Only variables significant within the final model have been reported.

				Day					Night				
Frequency	Survey	Response variable	Explanatory variable	n	Df	X2	P(>|Chi|)	p	n	Df	X2	P(>|Chi|)	p
38 kHz	Nov-19	perim	seafloorDep	280	-	-	-	-	530	4	76.38	<0.001	***
			u		-	-	-	-		-	-	-	-
			v		-	-	-	-		3	9.26	<0.05	*
			AbsShear		-	-	-	-		3	14.31	<0.01	**
			TimetoTideTurn		3	22.54	<0.001	***		-	-	-	-
			Time		3	88.48	<0.001	***		-	-	-	-
38 kHz	Mar-20	perim	seafloorDep	452	-	-	-	-	384	3	18.97	<0.001	***
			u		-	-	-	-		-	-	-	-
			v		3	16.76	<0.001	***		-	-	-	-
			AbsShear		-	-	-	-		-	-	-	-
			TimetoTideTurn		3	18.86	<0.001	***		-	-	-	-
			Time		-	-	-	-		-	-	-	-

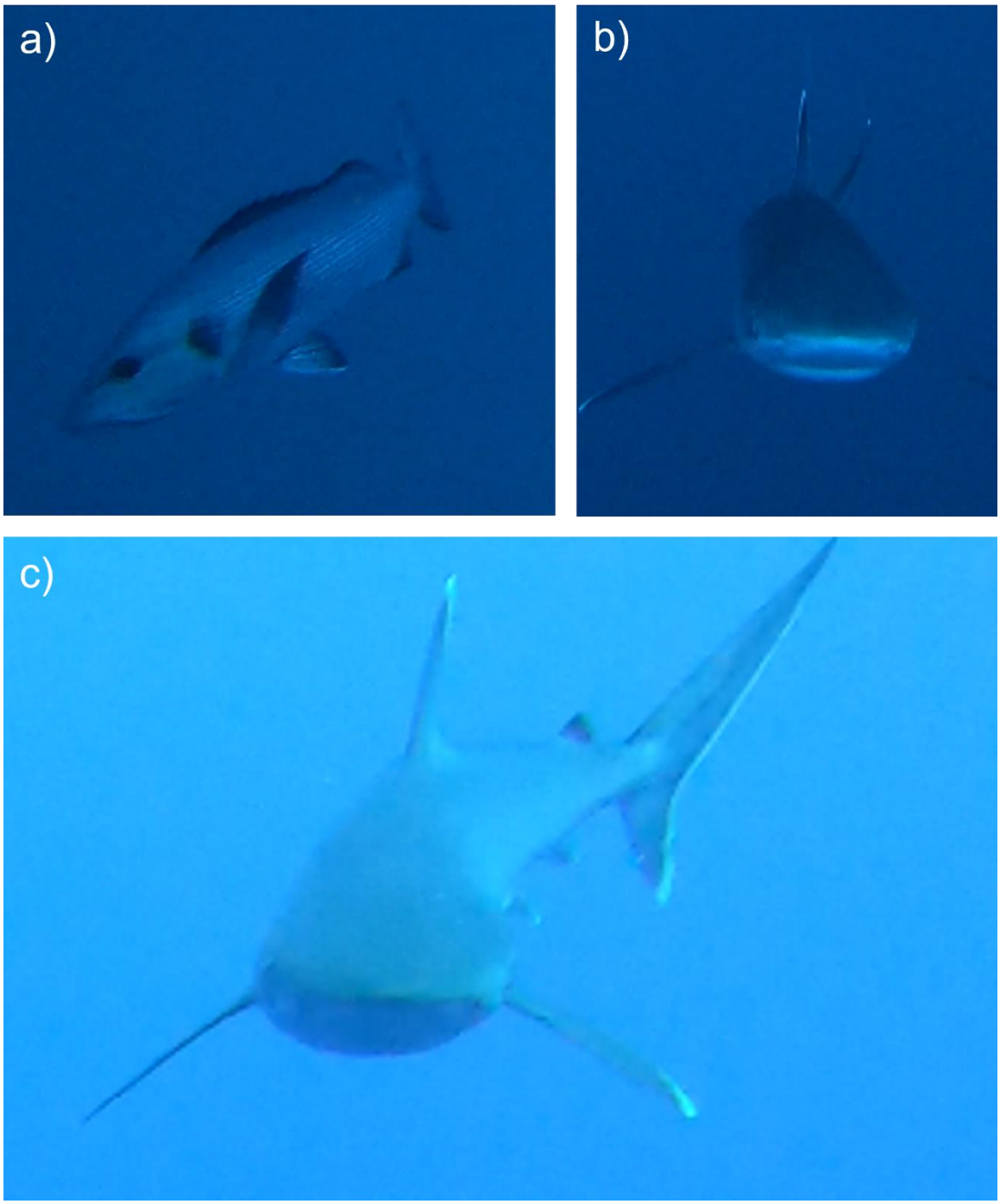

Figure B1: Still images taken from the video validation of acoustic data taken during survey 1 showing a) snapper spp, b and c) silvertip reef shark (*Carcharhinus albimarginatus*).

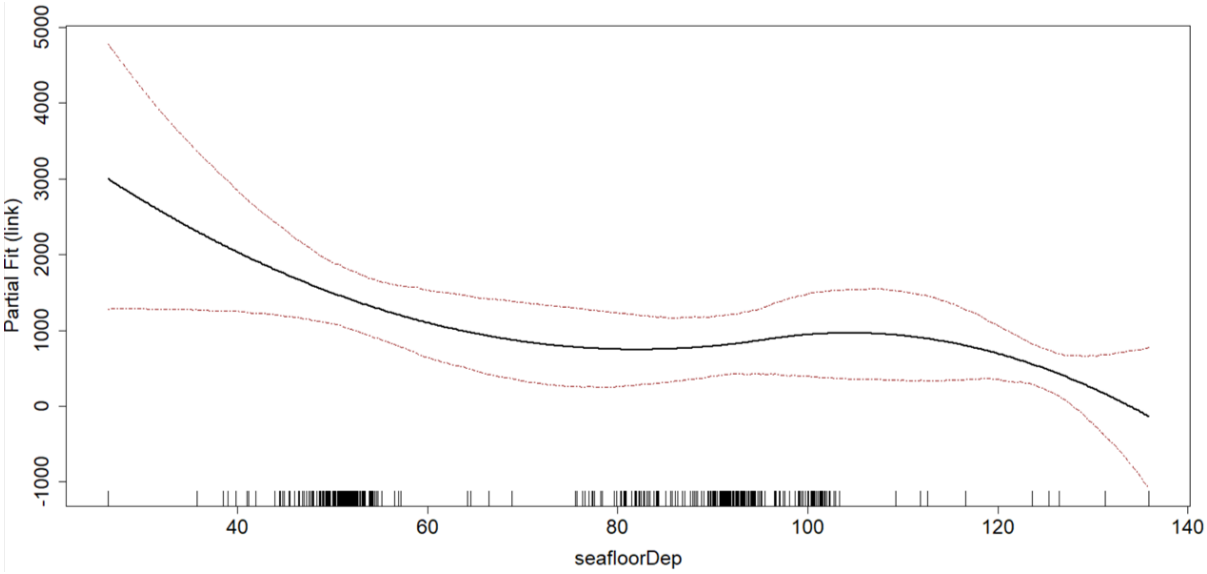

Figure B2: The perimeter response of 38 kHz fish schools at night against seafloor depth from GLMGEE models from survey 2 with the red lines at 95 % confidence internals and rug plot showing the distribution of the raw data. The unit of the explanatory variable is metres.

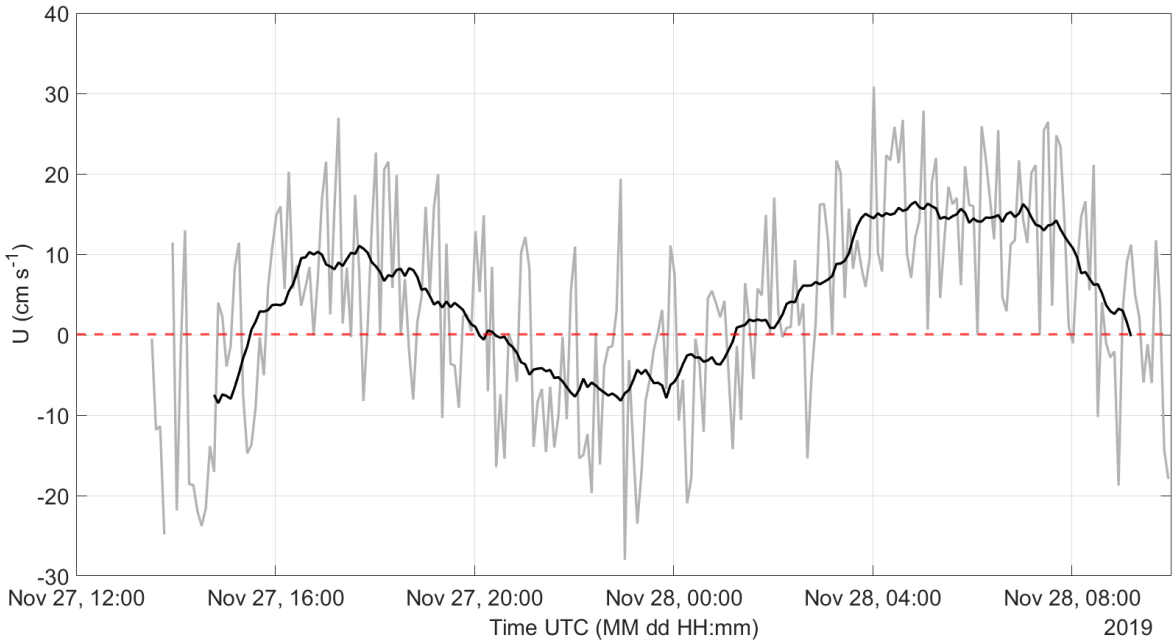

Figure B3: The U component (cm s^{-1}) collected by the ADCP showing the raw output (grey) over time with a time averaged mean (black) replicating a tidal curve. The orange line at U=0 shows that the U velocity data was not shifted so no background currents influenced the data.

Appendix C

The following figures and tables accompany Chapter 4:

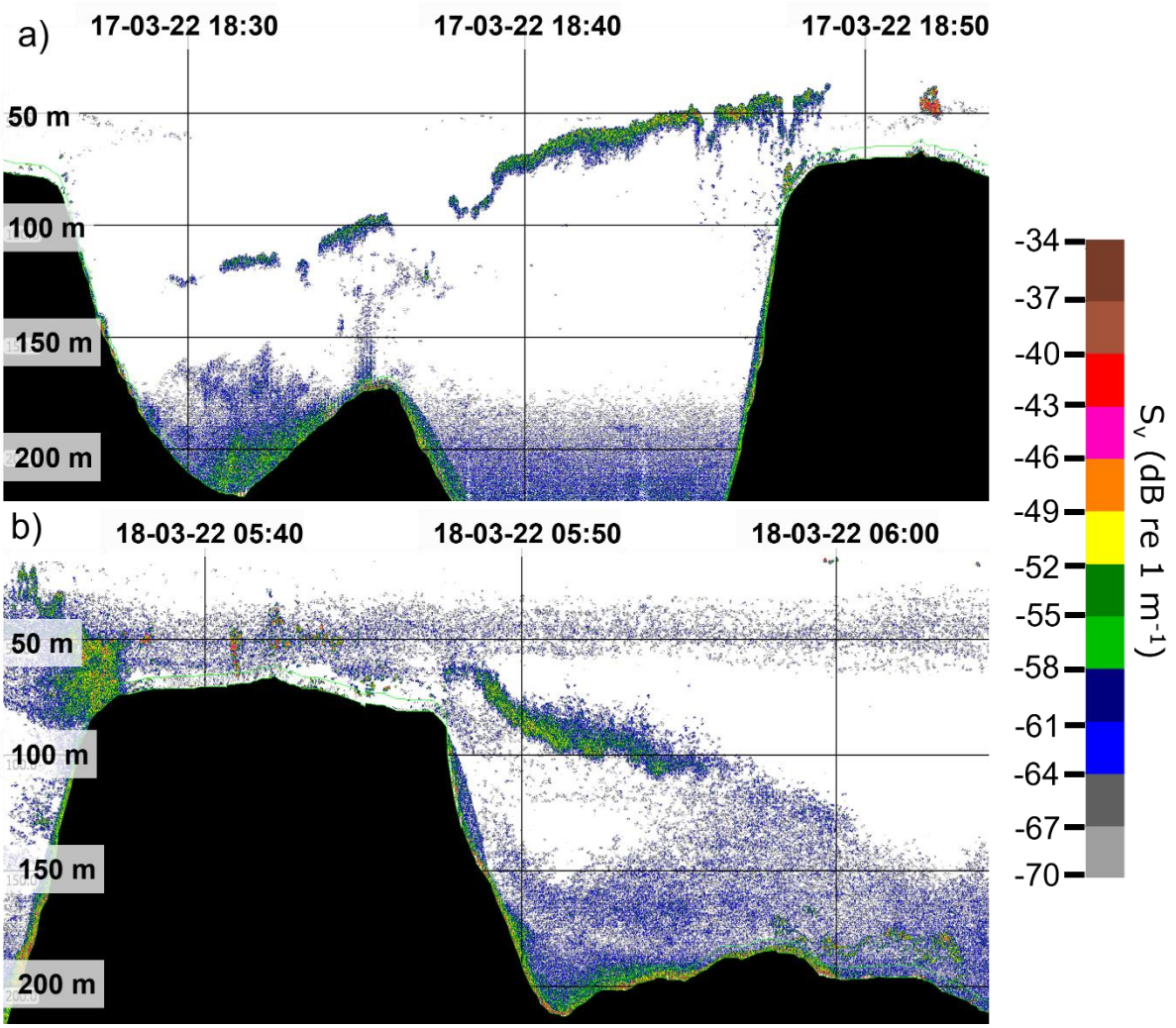

Figure C1: Echograms from the ES70 at 200 kHz showing S_v of a) the ascent and b) the descent of DVM over Sandes seamount in local time (UTC+5).

Table C1: Abundances of phytoplankton, zooplankton and detritus per transect and station (m^3). Mean estimates of biomass and NASC per station and transect.

Site	Variable	Phytoplankton abundance (m^3)	Zooplankton abundance (m^3)	Detritus abundance (m^3)	Biomass (mg m^3)	NASC (m^2nmi^{-2})
Transect	1	58795.6	30155.3	58795.6	4.8	30.4
	2	63616.6	45770.1	63616.6	3.7	112.8
	3	42387.3	26329.8	42387.3	5.2	228.5
	4	113653.5	62440.7	113653.5	4.6	24.5
	5	77032.8	52318.4	77032.8	5.4	248.8
Station	1	83178.5	51647.7	83178.5	4.8	13.4
	2	74810.1	45062.5	74810.1	5.2	266.9
	3	49864.0	38146.4	49864.0	4.1	23.0
	4	76536.1	38754.8	76536.1	4.8	258.9
Time	Day	63404.9	40230.9	63368.3	4.6	141.6
	Night	79203.4	47279.6	80543.6	4.9	139.0

Table C2: Summary of response and explanatory variables modelled with the associated p-values and significant variables from all 4 analyses.

Response variable	Explanatory variable	p-value	Significance
Zooplankton	NetDepth	0.772	-
	NetTemp	0.944	-
	SurfaceTemp	0.633	-
	ThermTemp	0.918	-
	Station	0.785	-
	Transect	0.122	-
	Slope	0.948	-
	Time	0.500	-
	Tide	0.009	***
Detritus	NetDepth	0.345	-
	NetTemp	0.555	-
	SurfaceTemp	0.998	-
	ThermTemp	0.916	-
	Station	0.481	-
	Transect	0.026	*
	Slope	0.481	-
	Time	0.284	-
	Tide	0.027	*
Biomass	NetDepth	0.113	-
	NetTemp	0.175	-
	SurfaceTemp	0.395	-

	ThermTemp	0.565	-
	Station	0.811	-
	Transect	0.692	-
	Slope	0.811	-
	Time	0.732	-
	Tide	0.582	-
NASC	NetDepth	0.074	-
	NetTemp	0.063	-
	SurfaceTemp	0.090	-
	ThermTemp	0.589	-
	Station	0.153	-
	Transect	0.757	-
	Slope	0.153	-
	Time	0.845	-
	Tide	0.887	-

References

Abrahams, M.V. and Colgan, P.W. (1985) 'Risk of predation, hydrodynamic efficiency and their influence on school structure', *Environmental Biology of Fishes*, *13*, pp.195-202.

Accad, Y. and Pekeris, C.L. (1978) 'Solution of tidal equations for M2 and S2 tides in the world ocean from a knowledge of the tidal potential alone', *Philos. Trans. R. Soc. A*, 290, pp.235-266.

Adcroft,A., Campin, J.M., Doddridge, E., Dutkiewicz, S., Evangelinos, C., Ferreira, D., Follows, M., Forget, G., Fox-Kemper, B., Heimbach, P., Hill, C., Hill, E., Hill, H., Jahn, O., Klymak, J., Losch, M., Marshall, J., Maze, G., Mazloff, M., Menemenlis, D., Molod, A. and Scott, J. (2023) *MITgcm Documentation.* Available at: https://buildmedia.readthedocs.org/media/pdf/mitgcm/latest/mitgcm.pdf (Accessed: 26th August 2023).

Alfonso, S., Gesto, M. and Sadoul, B. (2020) 'Temperature increase and its effects on fish stress physiology in the context of global warming', *Journal of Fish Biology*, 98(6), pp. 1496–1508. Available at: 10.1111/jfb.14599.

Ame, J.M., Halloy, J., Rivault, C., Detrain, C. and Deneubourg, J.L. (2006) 'Collegial decision making based on social amplification leads to optimal group formation', *Proc. Natl. Acad. Sci. U.S.A.*, 103(15), pp. 5835–5840.

Anderson, R.C., Herrera, M., Ilangakoon, A.D., Koya, K.M., Moazzam, M., Mustika, P.L. and Sutaria, D.N. (2020) 'Cetacean bycatch in Indian Ocean tuna gillnet fisheries', *Endangered Species Research*, 41, pp. 39–53. Available at: https://doi.org/10.3354/esr01008.

Andrzejaczek, S., Chapple, T.K., Curnick, D.J., Carlisle, A.B., Castleton, M., Jacoby, D.M.P., Peel, L.R., Schallert, R.J., Tickler, D.M. and Block, B.A. (2020) 'Individual variation in residency and regional movements of reef manta rays *Mobula alfredi* in a large marine protected area', *Mar. Ecol. Prog. Ser.,* 639, pp. 137–153.

Annasawmy, P., Cherel, Y., Romanov, E.V., Loc'h, F., Ménard, F., Ternon, J.F. and Marsac, F. (2020) 'Stable isotope patterns of mesopelagic communities over two shallow seamounts of the south-western Indian Ocean', *Deep Sea Research Part II: Topical Studies in Oceanography,* 176:104804.

Annasawmy, P., Ternon, J.F., Marsac, F., Cherel, Y., Béhagle, N., Roudaut, G., Lebourges-Dhaussy, A., Demarcq, H., Moloney, C.L., Jaquemet, S. and Ménard, F. (2018) 'Micronekton diel migration, community composition and trophic position within two biogeochemical provinces of the South West Indian Ocean: Insight from acoustics and stable isotopes', *Deep-Sea Research Part I*, 138, pp.85-97.

Aronica, S., Fontana, I., Giacalone, G., Bosco, G.L., Rizzo, R., Mazzola, S., Basilone, G., Ferreri, R., Genovese, S., Barra, M. and Bonanno, A. (2019) 'Identifying small pelagic Mediterranean fish schools from acoustic and environmental data using optimized artificial neural networks', *Ecological Informatics*, 50, pp.149-161. Available at: 10.1016/j.ecoinf.2018.12.007.

Arrhenius, F., Benneheij, B.J.A.M., Rudstam, L.G. and Boisclair, D. (2000) 'Can stationary bottom split-beam hydroacoustics be used to measure fish swimming speed in situ?', *Fisheries Research*, 45(1), pp. 31-41. Available at: https://doi.org/10.1016/S0165-7836(99)00102-2.

Ateweberhan, M., Feary, D.A., Keshavmurthy, S., Chen, A., Schleyer, M.H. and Sheppard, C.R.C. (2013) 'Climate change impacts on coral reefs: Synergies with local effects, possibilities for acclimation and management implications', *Marine Pollution Bulletin,* 74, pp. 526-539.

Badcock, J. and Merrett, N.R. (1967) 'Midwater fishes in the eastern North Atlantic—I. Vertical distribution and associated biology in 30°N, 23°W, with developmental notes on certain myctophids', *Progress in Oceanography*, 7(1), pp.3-58.

Bakun, A. (2006) 'Fronts and eddies as key structures in the habitat of marine fish larvae: opportunity, adaptive response and competitive advantage', *Sci. Mar.,* 70, pp. 105–122.

Barange, M. (1994) 'Acoustic identification, classification and structure of biological patchiness on the edge of the Aghulas Bank and its relation to frontal features', *South African Journal of marine science*, 14(1), pp.333-347.

Barnes, M.A., Turner, C.R., Jerde, C.L., Renshaw, M.A., Chadderton, W.L. and Lodge, D.M. (2014) 'Environmental conditions influence eDNA persistence in aquatic systems', *Environmental Science and Technology,* 48, pp. 1819-1827.

Belyaev, V.V. and Zuev, G.V. (1969) 'The Hydrodynamic Hypothesis of Fish Schooling', *Journal of Ichthyology*, 9(4), pp. 716–725.

Benkwitt, C.E, Wilson, S.K. and Graham, N.A.J. (2020) 'Biodiversity increases ecosystem functions despite multiple stressors on coral reefs', *Nature Ecology & Evolution,* 4(7), pp. 919-926.

Benjamins, S., Dale, A.C., Hastie, G.D., Waggitt, J.J., Lea, M., Scott, B.E. and Wilson, B. (2015) 'Confusion reigns? A review of marine megafauna interactions with tidal-stream environments', *Oceanography and Marine Biology,* 53, pp.1-54.

Benoit-Bird, K.J. and Lawson, G.L. (2016) 'Ecological Insights from Pelagic Habitats Acquired Using Active Acoustic Techniques', *Annual Review of Marine Science*, 8, pp. 463–490. Available at: https://doi.org/10.1146/annurev-marine-122414-034001.

Benoit-Bird, K.J., Waluk, C.M. and Ryan, J.P. (2019) 'Forage Species Swarm in Response to Coastal Upwelling', *Geophysical Research Letters*, 46(3), pp. 1537–1546. Available at: https://doi.org/10.1029/2018GL081603.

Bianchi, D. and Mislan, K.A.S. (2015) 'Global patterns of diel vertical migration times and velocities from acoustic data', *Limnology and Oceanography*, 61, pp. 353-364.

Blain, S., Tréguer, P., Belviso, S., Bucciarelli, E., Denis, M., Desabre, S., Fiala, M., Jézéquel, V.M., Le Fèvre, J., Mayzaud, P., Marty, J.C. and Razouls, S. (2001) 'A biogeochemical study of the island mass effect in the context of the iron hypothesis: Kerguelen Islands, Southern Ocean', *Deep-Sea. Res.* I., 48, pp. 163-187.

Boer, M. de, Baldwin, R., Burton, C.L., Eyre, E., Jenner, K.C., Jenner, M.N., Keith, S., McCabe, K., Parsons, E.C., Peddemors, V., Rosenbaum, H., Rudolph, P. and Simmonds, M.P. (2002) *Cetaceans in the Indian Ocean Sanctuary: A Review,* Whale and Dolphin Conservation Society.
Bollens, S.M. and Frost, B.W. (1989) 'Predator-induced diet vertical migration in a planktonic copepod', *Journal of Plankton Research*, 11(5), pp. 1047-1065.

Borland, H.P., Gilby, B.L., Henderson, C.J., Leon, J.X., Schlacher, T.A., Connolly, R.M., Pittman, S.J., Sheaves, M. and Olds, A.D. (2021) 'The influence of seafloor terrain on fish and fisheries: A global synthesis', *Fish and Fisheries*, 22(4), pp. 707–734. Available at: https://doi.org/10.1111/faf.12546.

Braga, E. S., Chiozzini, V.G. and Berbel, G.B.B. (2018) 'Oligotrophic water conditions associated with organic matter regeneration support life and indicate pollution on the western side of Fernando de Noronha Island - NE, Brazil (3°S)', *Brazilian Journal of Oceanography*, *66*(1), pp. 73-90.

Brandão, M.C., Benedetti, F., Martini, S., Soviadan, Y.D., Irisson, J.O., Romagnan, J.B., Elineau, A., Desnos, C., Jalabert, L., Freire, A.S., Picheral, M., Guidi, L., Gorsky, G., Bowler, C., Karp-Boss, L., Henry, N., de Vargas, C., Sullivan, M.B., Acinas, S.G., Babin, M., Bork, P., Boss, E., Bowler, C., Cochrane, G., de Vargas, C., Gorsky, G., Guidi, L., Grimsley, N., Hingamp, P., Iudicone, D., Jaillon, O., Kandels, S., Karp-Boss, L., Karsenti, E., Not, F., Ogata, H., Poulton, N., Pesant, S., Raes, J., Sardet, C., Speich, S., Stemmann, L., Sullivan, M.B., Sunagawa, S., Wincker, P., Stemmann, L. and Lombard, F. (2021) 'Macroscale patterns of oceanic zooplankton composition and size structure', *Scientific Reports*, 11(1), pp. 1–19. Available at: https://doi.org/10.1038/s41598-021-94615-5.

Brierley, A.S. (2014) 'Diel vertical migration', *Current Biology*, 24(22), pp. 1074-1076.

Brierley, A.S., Axelsen, B.E., Buecher, E., Sparks, C.A.J., Boyer, H. and Gibbons, M. J. (2001) 'Acoustic observations of jellyfish in the Nambian Benguela', *Marine Ecology Progress Series*, 210, pp. 55-66.

Brodeur, R.D., Fisher, J.P., Emmett, R.L., Morgan, C.A. and Casillas, E. (2005b) 'Species composition and community structure of pelagic nekton off Oregon and Washington under variable oceanographic conditions', *Marine Ecology Progress Series*, 298, pp. 41–57. Available at: https://doi.org/10.3354/meps298041.

Brodeur, R.D., Seki, M.P., Pakhomov, E.A. and Suntsov, A.V. (2005a) *Micronekton - What are they and why are they important?* Available at: https://www.nwfsc.noaa.gov/assets/2/106_02092005_154400_micronekton.pdf (Accessed: 20 January 2020).

Cai, L.N., Xu, L.L., Tang, D.L., Shao, W.Z., Liu, Y., Zuo, J.C. and Ji, Q.Y. (2020) 'The effects of ocean temperature gradients on bigeye tuna (*Thunnus obesus*) distribution in the equatorial eastern Pacific Ocean', *Advances in Space Research*, 65(12), pp. 2749–2760. Available at: https://doi.org/10.1016/j.asr.2020.03.030.

Campana, S. E., Dorey, A., Fowler, M., Joyce, W., Wang, Z. L., Wright, D., and Yashayaev, I. (2011) 'Migration pathways, behavioural thermoregulation and overwintering grounds of blue sharks in the Northwest Atlantic', *PLoS One,* 6(2). Available at: https://doi.org/10.1371/journal.pone.0016854.

Campanella, F. and Taylor, J.C. (2016) 'Investigating acoustic diversity of fish aggregations in coral reef ecosystems from multifrequency fishery sonar surveys', *Fisheries Research*, *181*, pp.63-76.

Campanella, F., Collins, M.A., Young, E.F., Laptikhovsky, V., Whomersley, P. and van der Kooij, J. (2021) 'First Insight of Meso- and Bentho-Pelagic Fish Dynamics Around Remote Seamounts in the South Atlantic Ocean', *Frontiers in Marine Science*, 8. Available at: https://doi.org/10.3389/fmars.2021.663278.

Campbell, M.D., Schoeman, D.S., Venables, W., Abu-Alhaija, R., Batten, S.D., Chiba, S., Coman, F., Davies, C.H., Edwards, M., Eriksen, R.S., Everett, J.D., Fukai, Y., Fukuchi, M., Esquivel Garrote, O., Hosie, G., Huggett, J.A., Johns, D.G., Kitchener, J.A., Koubbi, P., McEnnulty, F.R., Muxagata, E., Ostle, C., Robinson, K. V., Slotwinski, A., Swadling, K.M., Takahashi, K.T., Tonks, M., Uribe-Palomino, J., Verheye, H.M., Wilson, W.H., Worship, M.M., Yamaguchi, A., Zhang, W. and Richardson, A.J. (2021)

'Testing Bergmann's rule in marine copepods', *Ecography*, 44(9), pp. 1283–1295. Available at: https://doi.org/10.1111/ecog.05545.

Capone, D.G., Zehr, J.P., Paerl, H.W., Bergman, B. and Carpenter, E.J. (1997) 'Trichodesmium, a Globally Significant Marine Cyanobacterium', *Science,* 276, pp. 1221- 1229.

Carlisle, A.B., Tickler, D., Dale, J.J., Ferretti, F., Curnick, D.J., Chapple, T.K., Schallert, R.J., Castleton, M. and Block, B.A. (2019) 'Estimating space use of mobile fishes in a large Marine Protected Area with methodological considerations in acoustic array design', *Front. Mar. Sci.,* 6:256. Doi: 10.3389/fmars.2019.00256.

Carpenter, E. J., and Capone, D. G. (1992) 'Nitrogen fixation in Trichodesmium blooms', in Carpenter, E.J., Capone, D.G., Rueter, J.G. (eds.) *Marine pelagic cyanobacteria: Trichodesmium and other diazotrophs*. Springer, pp. 211-217.

Cascão, I., Domokos, R., Lammers, M.O., Santos, R.S. and Silva, M.A. (2019) 'Seamount effects on the diel vertical migration and spatial structure of micronekton', *Progress in Oceanography*, 175, pp. 1–13. Available at: https://doi.org/10.1016/j.pocean.2019.03.008.
Castro, P. and Huber, M.E. (2010) *Marine Biology.* Eighth Edition. New York: McGraw-Hill.

Cedras, R.B. and Gibbons, M.J. (2021) 'Latitudinal changes in copepod assemblages across the South West Indian Ridge', *Deep-Sea Research Part II: Topical Studies in Oceanography*, 193, p. 104963. Available at: https://doi.org/10.1016/j.dsr2.2021.104963.

Chakravorty, S., Gnanaseelan, C., Chowdary, J.S. and Luo, J. (2014) 'Relative role of El Niño and IOD forcing on the southern tropical Indian Ocean Rossby waves', *Journal of Geophysical Research: Oceans*, 119, pp. 5105-5122.

Chapman, D.C. and Haidvogel, D.B. (1992) 'Formation of Talyor caps over a tall isolated seamount in a stratified ocean', *Geophys. Astrophys. Fluid. Dyn.,* 64, pp. 31-65.

Clark, M.R., Rowden, A.A., Schlacher, T., Williams, A., Consalvey, M., Stocks, K.I., Rogers, A.D., O'Hara, T.D., White, M., Shank, T.M. and Hall-Spencer, J.M. (2010) 'The Ecology of Seamounts: Structure, Function and Human Impacts', *Annu. Rev. Mar. Sci*, 2, pp. 253-278. Available at: 10.1146/annurev-marine-120308- 081109.

Clarke, A. and Johnston N.M. (1999) 'Scaling of metabolic rate with body mass and temperature in teleost fish', *Journal of Animal Ecology,* 68, pp. 893-905.

Coetzee, J. (2000) 'Use of a shoal analysis and patch estimation system (SHAPES) to characterise sardine schools', *Aquatic Living Resources*, 13(1), pp. 1-10.

Collins, C., Nuno, A., Broderick, A., Curnick, D.J., de Vos, A., Franklin, T., Jacoby, D.M.P., Mees, C., Moir-Clark, J., Pearce, J. and Letessier, T.B. (2021) 'Understanding Persistent Non-compliance in a Remote, Large-Scale Marine Protected Area', *Frontiers in Marine Science*, 8, pp. 1–13. Available at: https://doi.org/10.3389/fmars.2021.650276.

Colombo, G., Mianzan, H. and Madirolas, A. (2003) 'Acoustic characterization of gelatinous-plankton aggregations: Four case studies from the Argentine continental shelf', *ICES Journal of Marine Science*, 60(3), pp. 650–657. Available at: https://doi.org/10.1016/S1054-3139(03)00051-1.

Comeau, L. A., Vézina, A.F., Bourgeois, M. and Juniper, S.K. (1995) 'Relationship between phytoplankton production and the physical structure of the water column near Cobb Seamount,

northeast Pacific', *Deep-Sea Research Part I*, 42(6), pp. 993–1005. Doi: 10.1016/0967-0637(95)00050-G.

Coutis, P.F. and Middleton, J.H. (1999) 'Flow-topography interaction in the vicinity of an isolated, deep ocean island', *Deep-Sea Research Part I: Oceanographic Research Papers*, 46(9), pp. 1633–1652. Available at: https://doi.org/10.1016/S0967-0637(99)00007-2.
Couto, A., Williamson, B.J., Cornulier, T., Fernandes, P.G., Fraser, S., Chapman, J.D., Davies, I.M. and Scott, B.E. (2021) 'Tidal streams, fish, and seabirds: Understanding the linkages between mobile predators, prey, and hydrodynamics', *Ecosphere*, 13(5), pp. 1–13. Available at: https://doi.org/10.1002/ecs2.4080.

Cox, M.J., Smith, A.J.R., Brierley, A.S., Potts, J.M., Wotherspoon, S. and Terauds, A. (2023) 'Scientific echosounder data provide a predator's view of Antarctic krill (Euphausia superba)', *Scientific Data*, 10(1), pp. 1–8. Available at: https://doi.org/10.1038/s41597-023-02187-y.

Croll, D. A. *et al.* (2005) 'From wind to whales: Trophic links in a coastal upwelling system', *Marine Ecology Progress Series*, 289, pp. 117–130. Available at: 10.3354/meps289117.

CSIRO (2016) ES60adjust [Computer program]. Available at: https://github.com/gavinmacaulay/calibration-code (Accessed: 13 December 2020).

Curnick, D.J., Andrzejaczek, S., Jacoby, D.M.P., Coffey, D.M., Carlisle, A.B., Chapple, T.K., Ferretti, F., Schallert, R.J., White, T., Block, B.A., Koldewey, H.J. and Collen, B. (2020a) 'Behavior and Ecology of Silky Sharks Around the Chagos Archipelago and Evidence of Indian Ocean Wide Movement', *Frontiers in Marine Science*, 7, pp. 1–18. Available at: https://doi.org/10.3389/fmars.2020.596619.

Curnick, D.J., Collen, B., Koldewey, H.J., Jones, K.E., Kemp, K.M. and Ferretti, F. (2020b) 'Interactions Between a Large Marine Protected Area, Pelagic Tuna and Associated Fisheries', *Frontiers in Marine Science*, 7, pp. 1–12. Available at: https://doi.org/10.3389/fmars.2020.00318.

Curtin, R. and Prellezo, R. (2010) 'Understanding marine ecosystem based management: A literature review', *Marine Policy*, 34(5), pp. 821–830. Available at: https://doi.org/10.1016/j.marpol.2010.01.003.

Cutter, G.R., Reiss, C.S., Nylund, S. and Watters, G.M. (2022) 'Antarctic Krill Biomass and Flux Measured Using Wideband Echosounders and Acoustic Doppler Current Profilers on Submerged Moorings', *Frontiers in Marine Science*, 9, pp. 1–23. Available at: https://doi.org/10.3389/fmars.2022.784469.

Dänhardt, A. and Becker, P.H. (2011) 'Herring and Sprat Abundance Indices Predict Chick Growth and Reproductive Performance o Common Terns Breeding in the Wadden Sea', *Ecosystems,* 14, pp. 791-803.

Davies, C.H., Beckley, L.E. and Richardson, A.J. (2022) 'Copepods and mixotrophic Rhizaria dominate zooplankton abundances in the oligotrophic Indian Ocean', *Deep-Sea Research Part II: Topical Studies in Oceanography*, 202. Available at: https://doi.org/10.1016/j.dsr2.2022.105136.

De Falco, C., Desbiolles, F., Bracco, A. and Pasquero, C. (2022) 'Island Mass Effect: A review of oceanic physical processes', *Frontiers of Marine Science,* 9:894860. Doi: 10.3389/fmars.2022.894860.

De Robertis, A. and Higginbottom, I. (2007) 'A post-processing technique for estimation of signal-to-noise ratio and removal of echosounder background noise', *ICES Journal of Marine Science*, 64, pp. 1282-1291.

De Santo, E.M., Jones, P.J.S. and Miller, A.M.M. (2011) 'Fortress conservation at sea: A commentary on the Chagos marine protected area', *Marine Policy*, 35(2), pp. 258–260. Available at: https://doi.org/10.1016/j.marpol.2010.09.004.

Dell'Anno, A., and Corinaldesi, C. (2004) 'Degradation and turnover of extracellular DNA in marine sediments: Ecological and methodological considerations', *Applied and Environmental Microbiology* 70(7), pp. 4384–4386.

Demer, D.A., Berger, L., Bernasconi, M., Bethke, E., Boswell, K., Chu, D., Domokos, R., Dunford, A., Fassler, S., Gauthier, S. and Hufnagle, L.T. (2015) *Calibration of acoustic instruments.* ICES Cooperative Research Report No. 326. Available at: http://dx.doi.org/10.25607/OBP-185 (Accessed: 20 May 2020).

DeMott, C.A., Klingaman, N.P. and Woolnough, S.J. (2015) 'Atmosphere-ocean coupled processes in the Madden-Julian oscillation', *Rev. Geophys.,* 53, pp. 1099-1154.

determinants of fish target strength. *Rapp. P.-v. Reun. Cons. Int. Explor. Mer* 189, pp.245–53.

Diner, N. (2001) 'Correction on school geometry and density: approach based on acoustic image simulation', *Aquatic Living Resources*, 14(4), pp. 211-222.

Domenici, P., Steffensen, J.F, and Marras, S. (2017) 'The effect of hypoxia on fish schooling', *Phil. Trans. R. Soc. B*., 372: 20160236.

Domokos, R. (2021) 'On the development of acoustic descriptors for semi-demersal fish identification to support monitoring stocks', *ICES Journal of Marine Science*, 78(3), pp. 1117–1130. Available at: https://doi.org/10.1093/icesjms/fsaa232.

Domokos, R. (2022) 'Seamount effects on micronekton at a subtropical central Pacific seamount', *Deep-Sea Research Part I: Oceanographic Research Papers*, 186. Available at: https://doi.org/10.1016/j.dsr.2022.103829.

Doray, M., Boyra, G., and van der Kooij, J. (2021) *ICES Survey Protocols – Manual for acoustic surveys coordinated under ICES Working Group on Acoustic and Egg Surveys for Small Pelagic Fish (WGACEGG).* 1st Edition. ICES Techniques in Marine Environmental Sciences Vol. 64. 100 pp. Available at: https://doi. org/10.17895/ices.pub.7462

Dorrell, R.M., Peakall, J., Sumner, E.J., Parsons, D.R., Darby, S.E., Wynn, R.B., Özsoy, E. and Tezcan. D. (2016) 'Flow dynamics and mixing processes in hydraulic jump arrays: Implications for channel-lobe transition zones', *Marine Geology,* 381, pp. 181-193.

Doty, M.S. and Oguri, M. (1956) 'The island mass effect', *J Int Coun Expl Sea,* 22, pp. 33-37.

Dower, J. F. and Brodeur, R. D. (2004) 'The role of biophysical coupling in concentrating marine organisms around shallow topographies', *Journal of Marine Systems*, 50(1–2), pp. 1–2. Available at: 10.1016/j.jmarsys.2004.04.002.

Dower, J., Freeland, H. and Juniper, K. (1992) 'A strong biological response to oceanic flow past Cobb Seamount', *Deep Sea Research Part A. Oceanographic Research Papers*, 39(7-8), pp.1139-1145.

Dower, J.F. (1994) *Biological consequences of current-topography interactions at Cobb Seamount.* (Doctoral dissertation). University of Victoria. Available at: https://dspace.library.uvic.ca/handle/1828/9691 (Accessed: 14 August 2022).

Dower, J.F. and Mackas, D.L. (1996) '"Seamount effects" in the zooplankton community near Cobb Seamount', *Deep-Sea Research Part I: Oceanographic Research Papers*, 43(6), pp. 837–858. Available at: https://doi.org/10.1016/0967-0637(96)00040-4.

Drago, L., Panaïotis, T., Irisson, J.O., Babin, M., Biard, T., Carlotti, F., Coppola, L., Guidi, L., Hauss, H., Karp-Boss, L., Lombard, F., McDonnell, A.M.P., Picheral, M., Rogge, A., Waite, A.M., Stemmann, L. and Kiko, R. (2022) 'Global Distribution of Zooplankton Biomass Estimated by In Situ Imaging and Machine Learning', *Frontiers of Marine Science*, 9. Available at: https://doi.org/10.3389/fmars.2022.894372.

Du, Y., Zhang, Y., Zhang, L.Y., Tozuka, T., Ng, B. and Cai, W. (2020) 'Thermocline Warming Induced Extreme Indian Ocean Dipole in 2019', *Geophysical Research Letters*, 47(18), pp. 1–10. Available at: https://doi.org/10.1029/2020GL090079.

Dubroca, L., Chassot, E., Floch, L., Demarcq, H., Assan, C. and de Molina, D. (2012) 'Seamounts and tuna fisheries: tuna hotspots or fishermen habits?', *Inter-sessional meeting of the tropical tuna species group*, pp.2087-2102.

Dunne, R.P., Barbosa, S.M. and Woodworth, P.L. (2012) 'Contemporary Sea level in the Chagos Archipelago, central Indian Ocean', *Global and Planetary Change*, 82-83, pp. 25-37.

Dunne, R.P., Polunin, N.V.C., Sand, P.H. and Johnson, M.L. (2014) 'The Creation of the Chagos Marine Protected Area: A Fisheries Perspective', in Johnson, M.L. and Sandell, J. (ed.) *Advances in Marine Biology, Vol 69*. Oxford: Academic Press, pp. 79-127.

Duvel, J.P. and Vialard, J. (2007) ' Indo-Pacific sea surface temperature perturbations associated with intraseasonal oscillations of tropical convection', *Journal of Climate,*20, pp. 3056-3082. Doi: 10.1175/JCLI4144.1.

Easson, C.G., Boswell, K.M., Tucker, N., Warren, J.D. and Lopez, J. V. (2020) 'Combined eDNA and Acoustic Analysis Reflects Diel Vertical Migration of Mixed Consortia in the Gulf of Mexico', *Frontiers in Marine Science*, 7, pp. 1–13. Available at: https://doi.org/10.3389/fmars.2020.00552.

Echoview Software Pty Ltd (2020). *Echoview* (Version 11) [Computer program] Available at: https://www.echoview.com (Accessed: 29 September 2020).

Echoview Software Pty Ltd (2021). *Echoview* (Version 12.1) [Computer program] Available at: https://www.echoview.com (Accessed: 21 January 2022).

Egbert, G. D., and Erofeeva, S.Y. (2002) 'Efficient inverse modeling of barotropic ocean tides', *Journal of Atmospheric and Oceanic Technology*, 19(2), pp.183-204.

Egerton, J.P., Al-Ansi, M., Abdallah, M., Walton, M., Hayes, J., Turner, J., Erisman, B., Al-Maslamani, I., Mohannadi, M. and Le Vay, L. (2018) 'Hydroacoustics to examine fish association with shallow offshore habitats in the Arabian Gulf', *Fisheries Research*, 199, pp. 127–136. Available at: https://doi.org/10.1016/j.fishres.2017.12.002.

Elliot, J., Patterson, M. and Gleiber, M. (2012) 'Detecting 'Island Mass Effect' through remote sensing', *Proceedings of the 12th International Coral Reef Symposium,* Cairns: Australia, 9-13 July.

Embling. C.B., Sharples, J., Armstrong. E., Plamer, M.R. and Scott, B.E. (2013) 'Fish behaviour in response to tidal variability and internal waves over a shelf sea bank', *Progress in Oceanography*, 117, pp.106-117. Available at: 10.1016/j.pocean.2013.06.013.

Eriksen, C.C. (1982) 'Observations of internal wave reflection off sloping bottoms', *Journal of Geophysical Research*, 87, pp. 525–538.

Eriksen, C.C. (1991) 'Observations of amplified flows atop a large seamount', *Journal of Geophysical Research*, 96, pp. 227–215.

Escalle, L., Pennino, M.G., Gaertner, D., Chavance, P., Delgado de Molina, A., Demarcq, H., Romanov, E. and Merigot, B. (2016) 'Environmental factors and megafauna spatio-temporal co-occurrence with purse-seine fisheries', *Fish. Oceanogr.,* 25, pp. 433-447.

ESRI. (2019) *ArcGIS Desktop* (Version 10.7) [Computer program] Available at: https://www.esri.com/en-us/arcgis/products/arcgis-desktop/resources. (Accessed: 16th December 2019).

Esteban, N., Mortimer, J.A. and Hays, G.C (2018) *Sea Turtle Conservation Research Diego Garcia, British Indian Ocean Territory 25 June – 18 July 2018*. Available at: https://biot.gov.io/wp-content/uploads/2018_June_BIOT_turtle_expedition_report.pdf (Accessed: 28 November 2020).

Estrada, M. and Berdalet, E. (1997) 'Phytoplankton in a turbulent world', *Scientia Marina*, 61, pp. 125–140.

Fedosova, R.A. (1974) 'Distribution of some copepod species in the vicinity of the underwater Hawaiian Ridge', *Oceanology* 14, pp. 724–727.

Fennell, S. and Rose, G. (2015) 'Oceanographic influences on Deep Scattering Layers across the North Atlantic', *Deep-Sea Research Part I: Oceanographic Research Papers*, 105, pp. 132–141. Available at: https://doi.org/10.1016/j.dsr.2015.09.002.

Fernandes, G. (2009) 'Classification trees for species identification on fish-school echotraces', *ICES Journal of Marine Science,* 66, pp. 1073-1080. Available at: 10.1093/icesjms/fsp060.

Fernandes, P.G., Brierly, A.S., Simmonds, E.J., Millard, N.W., McPhail, S.D., Armstrong, F., Stevenson, P. and Squires, M. (2000) 'Fish do not avoid survey vessels', *Nature*, *404*, pp.35-36.

Fernandes, P.G., Gerlotto, F., Holliday, D.V., Nakken, O. and Simmonds, E.J. (2002) 'Acoustic applications in fisheries science: the ICES contribution', *ICES Marine Science Symposia*, 215, pp. 483–492.

Fernandes, L. D. D. A., Quintanilha, J., Monteiro-Ribas, W., Gonzalez-Rodriguez, E., and Coutinho, R. (2012) 'Seasonal and interannual coupling between sea surface temperature, phytoplankton and meroplankton in the subtropical south-western Atlantic Ocean', *Journal of Plankton Research*, *34*(3), pp.236-244.

Ficetola, G.F., Miaud, C., Pompanon, F. and Taberlet, P. (2008) 'Species detection using environmental DNA from water samples', *Biology Letters*, 4(4), pp. 423–425. Available at: https://doi.org/10.1098/rsbl.2008.0118.

Filmalter, J.D., Dagorn, L. and Cowley, P.D. (2013) 'Spatial behaviour and site fidelity of the sicklefin lemon shark Negaprion acutidens in a remote Indian Ocean atoll', *Marine Biology*, 160(9), pp. 2425–2436. Available at: https://doi.org/10.1007/s00227-013-2237-1.

Fish, F.E., Fegely, J.F. and Xanthopoulos, C.J. (1991) 'Burst-and-coast swimming in schooling fish (*Notemigonus crysoleucas*) with implications for energy economy', *Comp. Biochem. Physiol.*, 100(3), pp. 633-637.

Flood, B., Wells, M., Young, J. and Dunlop, E. (2016) 'Investigating the effect of the Coriolis force on internal wave dynamics and flushing of a coastal embayment', *International Symposium on Stratified Flows,* 1(1).

Florentine, A.N., Constance, D.N., Justin, A.M., Paul, A.K.J., Yao, N., Abekan, N., Konan, N. and Marie, G.A. (2019) 'Diet of *Elagatis bipinnulata* (Guoy & Gaimard, 1824) in Côte d'Ivoire (Gulf of Guinea), *European Scietific Journal,* 15(3), pp. 131- 142. Available at: https://doi.org/10.19044/esj.2019.v15n3p131.

Foote, K.G. (1980) 'Importance of the swimbladder in acoustic scattering by fish: A comparison of gadoid and mackerel target strengths', *Journal of the Acoustical Society of America,* 67(6), pp. 2084-2089.

Foote, K.G. (1987) 'Fish target strengths for use in echo integrator surveys', *The Journal of the Acoustical Society of America*, *82*(3), pp.981-987.

Freeland, H. (1994) 'Ocean circulation at and near Cobb Seamount', *Deep-Sea Research*, 41, pp. 1715–1732.

Freund, M.B., Marshall, A.G., Wheeler, M.C. and Brown, J.N. (2020) 'Central Pacific El Niño as a Precursor to Summer Drought-Breaking Rainfall Over Southeastern Australia', *Geophysical Research Letters,* 48(7). Available at: https://doi.org/10.1029/2020GL091131.

Garamszegi, L. Z. (2016) 'A simple statistical guide for the analysis of behaviour when data are constrained due to practical or ethical reasons', *Animal Behaviour*, 120, pp. 223–234. Available at: 10.1016/j.anbehav.2015.11.009.

Garrett, C. (2003) 'Internal tides and ocean mixing', *Science*, 301(5641), pp. 1858-1859. Doi: 10.1126/science.10900.

Garrett, C. and Munk, W. (1972) 'Space-Time scales of internal waves', *Geophysical Fluid Dynamics,* 3, pp. 225- 264. Available at: https://doi.org/10.1080/03091927208236082.

Genin, A. (2004) 'Bio-physical coupling in the formation of zooplankton and fish aggregations over abrupt topographies', *Journal of Marine Systems*, 50(1–2), pp. 3–20. Available at: 10.1016/j.jmarsys.2003.10.008.
Genin, A. and Boehlert, G.W. (1985) 'Dynamics of temperature and chlorophyll structures above a seamount: an oceanic experiment', *J. Mar. Res.* 43, pp. 907–924.

Genin, A. and Dower, J.F. (2007) 'Seamount plankton dynamics', in Pitcher, T.J., Morato, T., Hart, P.J.B., Clark, M.R., Haggan, N., Santos, R.S. (Eds.), *Seamounts: Ecology, Fisheries & Conservation.* Oxford: Blackwell, pp. 86–100.

Genin, A., Dayton, P.K., Lonsdale, P.F. and Spiess, F.N. (1986) 'Corals on seamount peaks provide evidence of current acceleration over deep-sea topography', *Nature*, 322, pp. 59–61.

Genin, A., Greene, C., Haury, L., Wiebe, P., Gal, G., Kaartvedt, S., Meir, E., Fey, C. and Dawson, J. (1994) 'Zooplankton patch dynamics: daily gap formation over abrupt topography', *Deep-Sea Res. I* 41, pp. 941–951.

Gerstner, C.L. (1998) 'Use of substratum ripples for flow refuging by Atlantic cod, *Gadus morhua'*, *Environmental Biology of Fishes*, *51*(4), pp.455-460.

Girard, C., Benhamou, S. and Dagorn, L. (2004) 'FAD: fish aggregating device or fish attracting device? A new analysis of yellowfin tuna movements around floating objects', *Anim. Behav,* 67, pp. 319–326.

González-Quirós, R., Pascual, A., Gomis, D. and Anadón, R. (2004) 'Influence of mesoscale physical forcing on trophic pathways and fish larvae retention in the central Cantabrian Sea', *Fisheries Oceanography*, 13(6), pp. 351–364. Available at: https://doi.org/10.1111/j.1365-2419.2004.00295.x.

Google (2019) *Google Earth Pro*. Available at: https://www.google.co.uk/intl/en_uk/earth/ (Accessed: 28 January 2020).

Goss, C., Middleton, D. and Rodhouse, P. (2001) 'Investigations of squid stocks using acoustic survey methods', *Fisheries Research,* 54(1), pp.111-121. Available at: https://doi.org/10.1016/S0165-7836(01)00375-7.

Gove, J., McManus, M., Neuheimer, A. *et al.* (2016) 'Near-island biological hotspots in barren ocean basins', *Nat Commun* 7, 10581.

Graham, N.A.J., Wilson, S.K., Carr, P., Hoey, A.S., Jennings, S. and MacNeil, M.A. (2018) 'Seabirds enhance coral reef productivity and functioning in the absence of invasive rats', *Nature,* 559(7713), pp. 250-253. Available at: https://10.1038/s41586-018-0202-3.

Greenlaw, C.F. (1979) 'Acoustical estimation of zooplankton populations', *Limnol. Oceanogr*., 24(2), pp. 226-242.

Greer, A.T., Cowen, R.K., Guigand, C.M., Hare, J.A. and Tang, D. (2014) 'The role of internal waves in larval fish interactions with potential predators and prey', *Progress in Oceanogr*aphy, 127, pp.47–61. Available at: 10.1016/j.pocean.2014.05.010.

Habary, A., Johansen, J.L., Nay, T.J., Steffensen, J.F. and Rummer, J.L. (2012) 'Adapt, move or die-how will tropical coral reef fishes cope with ocean warming?', *Global Change Biology,* 23, pp. 566-577.

Halpern, B.S., Lester, S.E. and McLeod, K.L. (2010) 'Placing marine protected areas onto the ecosystem-based management seascape', *Biological Sciences,* 107(43), pp. 18312-18317. Available at: https://doi.org/10.1073/pnas.0908503107.

Hamel, J. (2020) *Effects of transmission side lobe interference on multibeam echosounder phase ramps.* (Master's Thesis). University of New Hampshire. Available at:

https://scholars.unh.edu/cgi/viewcontent.cgi?article=2464&context=thesis. (Accessed: 12 July 2023).

Hardin, J.W. and Hilbe, J.M. (2003). *Generalized linear models and extensions*. CRC Press: Florida, USA.

Harris, J.L. (2019) *Reef manta rays, Mobula afredi, of the Chagos Archipelago: Habitat use and the effectiveness of the region's marine protected area*. MRes Thesis. University of Plymouth.

Harris, J.L., Hosegood, P., Robinson, E., Embling, C.B., Hilbourne, S. and Stevens, G.M.W. (2021) 'Fine-scale oceanographic drivers of reef manta ray (*Mobula alfredi*) visitation patterns at a feeding aggregation site', *Ecology and Evolution,* 11(9), pp. 4588-4604. Doi: https://doi.org/10.1002/ece3.7357.

Haury, L., Fey, C., Gal, G., Hobday, A. and Genin, A. (1995) 'Copepod carcasses in the ocean. I. Over seamounts', *Marine Ecology Progress Series,* 123, pp. 57–63.

Haury, L., Fey, C., Newland, C. and Genin, A. (2000) 'Zooplankton distribution around four eastern North Pacific seamounts', *Prog. Oceanogr*. 45, pp. 69–105.

Hays, G.C., Koldewey, H.J., Andrzejaczek, S., Attrill, M.J., Barley, S., Bayley, D.T.I., Benkwitt, C.E., Block, B., Schallert, R.J., Carlisle, A.B., Carr, P., Chapple, T.K., Collins, C., Diaz, C., Dunn, N., Dunbar, R.B., Eager, D.S., Engel, J., Embling, C.B., Esteban, N., Ferretti, F., Foster, N.L., Freeman, R., Gollock, M., Graham, N.A.J., Harris, J.L., Head, C.E.I., Hosegood, P., Howell, K.L., Hussey, N.E., Jacoby, D.M.P., Jones, R., Sannassy Pilly, S., Lange, I.D., Letessier, T.B., Levy, E., Lindhart, M., McDevitt-Irwin, J.M., Meekan, M., Meeuwig, J.J., Micheli, F., Mogg, A.O.M., Mortimer, J.A., Mucciarone, D.A., Nicoll, M.A., Nuno, A., Perry, C.T., Preston, S.G., Rattray, A.J., Robinson, E., Roche, R.C., Schiele, M., Sheehan, E. V., Sheppard, A., Sheppard, C., Smith, A.L., Soule, B., Spalding, M., Stevens, G.M.W., Steyaert, M., Stiffel, S., Taylor, B.M., Tickler, D., Trevail, A.M., Trueba, P., Turner, J., Votier, S., Wilson, B., Williams, G.J., Williamson, B.J., Williamson, M.J., Wood, H. and Curnick, D.J. (2020) 'A review of a decade of lessons from one of the world's largest MPAs: conservation gains and key challenges', *Marine Biology*, 167(11), pp. 1–22. Available at: https://doi.org/10.1007/s00227-020-03776-w.

Hays, G.C., Mazaris, A.D. and Schofield, G. (2014) 'Different male vs. female breeding periodicity helps mitigate offspring sex ratio skews in sea turtles', *Frontiers in Marine Science*., 1. Available at: https://doi.org/10.3389/fmars.2014.00043.

Hazen, E.L. and Johnston, D.W. (2010) 'Meridional patterns in the deep scattering layers and top predator distribution in the central equatorial Pacific', *Fisheries Oceanography*, 19(6), pp. 427–433. Available at: https://doi.org/10.1111/j.1365-2419.2010.00561.x.

He, J., Christakos, G., Cazelles, B., Wu, J. and Leng, J. (2021) 'Spatiotemporal variation of the association between sea surface temperature and chlorophyll in global ocean during 2002–2019 based on a novel WCA-BME approach', *International Journal of Applied Earth Observation and Geoinformation*, 105, p. 102620. Available at: https://doi.org/10.1016/j.jag.2021.102620.

Heinle, D.R. (1969) 'Temperature and zooplankton', *Chesapeake Science*, 10(3-4), pp.186-209.

Hermes, J.C. and Reason, C.J.C. (2008) 'Annual cycle of the South Indian Ocean (Seychelles-Chagos) thermocline ridge in a regional ocean model', *Journal of Geophysical Research: Oceans*, 113(C4), pp. 1-10.

Hernández-Léon, S. (1988) 'Gradients of mesozooplankton biomass and ETS activity in the wind-shear area as evidence of an island mass effect in the Canary Island waters', *J. Plank. Res.,* 10(6) pp. 1141- 1154.

Hernández-León, S. (1991) 'Accumulation of mesozooplankton in a wake area as a causative mechanism of the "island-mass effect"', *Mar. Biol.* 109, pp. 141–147.

Hernández-Léon, S., Almeida, C., Gómez, M., Torres, S., Montero, I. and Portillo-Hahnefeld, A. (2001) 'Zooplankton biomass and indices of feeding and metabolism in island-generated eddies around Gran Canaria', *J. Mar. Sys.,* 30, pp. 51-66.

Hirst, A.G. and Bunker, A.J. (2003) 'Fecundity of marine planktonic copepods: Global rates and patterns in relation to chlorophyll a, temperature and body weight', *Limnology and Oceanography*, 48(5), pp. 1988–2010. Available at: https://doi.org/10.3354/meps279161.

Hoare, V., Atchison Balmond, N., Hays, G.C., Jones, R., Koldewey, H., Laloë, J.O., Levy, E., Llewellyn, F., Morrall, H. and Esteban, N. (2022) 'Spatial variation of plastic debris on important turtle nesting beaches of the remote Chagos Archipelago, Indian Ocean', *Marine Pollution Bulletin*, 181(July). Available at: https://doi.org/10.1016/j.marpolbul.2022.113868.

Hobson, E. S. (1991) 'Trophic Relationships of Fishes Specialized to Feed on Zooplankters above Coral Reefs', *The Ecology of Fishes on Coral Reefs*, pp. 69–95. Available at: 10.1016/b978-0-08-092551-6.50009-x.

Hockley, F.A., Wilson, C.A.M.E., Brew, A. and Cable, J. (2014) 'Fish responses to flow velocity and turbulence in relation to size, sex and parasite load', *Journal of the Royal Society Interface*, 11(91). Available at: https://doi.org/10.1098/rsif.2013.0814.

Hogg, N.G. (1973) 'On the stratified Taylor column', *J. Fluid Mech.* 58, pp. 517–537.

Højsgaard, S., Halekoh, U., and Yan, J. (2005) 'The R Package geepack for Generalized Estimating Equations', *Journal of Statistical Software*, *15*(2), pp. 1–11. Available at: https://doi.org/10.18637/jss.v015.i02

Hosegood, P.J., Nimmo-Smith, W.A.M., Proud, R., Adams, K. and Brierley, A.S. (2019) 'Internal lee waves and baroclinic bores over a tropical seamount shark 'hot-spot'', *Progress in Oceanography*, 172, pp. 34-50.

Howell, P. and Simpson, D. (1994) 'Abundance of marine resources in relation to dissolved oxygen in Long Island Sound', *Estuaries,* 17, pp. 394–402.

Huang, T.C., Lu, H.J., Lin, J.R., Sun, S.H., Yen, K.W. and Chen, J.Y. (2021) 'Evaluating the fish aggregation effect of wind turbine facilities by using scientific echo sounder in Nanlong wind farm area, western Taiwan', *Journal of Marine Science and Technology (Taiwan)*, 29(2), pp. 228–238. Available at: https://doi.org/10.51400/2709-6998.1084.

Hubbs, C.L. (1959) 'Initial discoveries of fish faunas on seamounts and offshore banks in the eastern Pacific', *Pac Sci*.,13(4), pp.311-316.

Hughes Clarke, J.E. (2017) 'Coherent refraction "noise" in multibeam data due to oceanographic turbulence', *United States Hydrographic Conference*, Galveston, Texas, 20-23 March. Available at: https://scholars.unh.edu/ccom/1372/ (Accessed: 17 December 2019).

Huppert, H.E. (1975) ‘Some remarks on the initiation of inertial Taylor columns’, *J. Fluid Mech.,* 67, pp. 397–412.

Huppert, H.E. and Bryan, K. (1976) ‘Topographically generated eddies’, *Deep-Sea Res*., 23, pp. 655–679.

Hutchinson, G.E. (1967) *A Treatise on Limnology, Introduction to Lake Biology and the Limnoplankton,* New York: Wiley. Volume II.

Ibarbalz, F.M., Henry, N., Brandão, M.C., Martini, S., Busseni, G., Byrne, H., Coelho, L.P., Endo, H., Gasol, J.M., Gregory, A.C., Mahé, F., Rigonato, J., Royo-Llonch, M., Salazar, G., Sanz-Sáez, I., Scalco, E., Soviadan, D., Zayed, A.A., Zingone, A., Labadie, K., Ferland, J., Marec, C., Kandels, S., Picheral, M., Dimier, C., Poulain, J., Pisarev, S., Carmichael, M., Pesant, S., Acinas, S.G., Babin, M., Bork, P., Boss, E., Bowler, C., Cochrane, G., de Vargas, C., Follows, M., Gorsky, G., Grimsley, N., Guidi, L., Hingamp, P., Iudicone, D., Jaillon, O., Karp-Boss, L., Karsenti, E., Not, F., Ogata, H., Poulton, N., Raes, J., Sardet, C., Speich, S., Stemmann, L., Sullivan, M.B., Sunagawa, S., Wincker, P., Pelletier, E., Bopp, L., Lombard, F. and Zinger, L. (2019) ‘Global Trends in Marine Plankton Diversity across Kingdoms of Life’, *Cell*, 179(5), pp. 1084-1097.e21. Available at: https://doi.org/10.1016/j.cell.2019.10.008.

Ikeda, T. (1985) ‘Metabolic Rates of Epipelagic Marine Zooplankton as a Function of Body Mass and Temperature’, *Mar. Biol.* 85, pp. 1–11. Available at: https://doi.org//10.1007/BF00396409.

INFOMAR (2008) Ground truthing and sampling strategy. Available at: https://www.infomar.ie/sites/default/files/pdfs/INFOMAR%20Ground_Truthing_and_Sampling_Strategy.pdf.

Ingvaldsen, R.B., Eriksen, E., Gjøsæter, H., Engås, A., Schuppe, B.K., Assmann, K.M., Cannaby, H., Dalpadado, P. and Bluhm, B.A. (2023) ‘Under-ice observations by trawls and multi-frequency acoustics in the Central Arctic Ocean reveals abundance and composition of pelagic fauna’, *Scientific Reports*, 13(1), pp. 1–15. Available at: https://doi.org/10.1038/s41598-023-27957-x.

IPCC (2023) *Climate Change 2023: Synthesis Report*. Contribution of Working Groups I, II and III to the Sixth Assessment Report of the Intergovernmental Panel on Climate Change. Geneva, Switzerland, pp. 1-34, Available at: https://doi.org/10.59327/IPCC/AR6-9789291691647.001.

IUCN (2023) *The IUCN Red List of Threatened Species.* Available at: https://www.iucnredlist.org/ (Accessed: 16 June 2023).

Izumo, T., Masson, S., Vialard, J., de Boyer Montegut, C., Behera, S.K., Madec, G., Takahashi, K. and Yamagata, T. (2010) ‘Low and high frequency Madden-Julian oscillations in austral summer: Interannual variations’, *Clim. Dyn.,* 35, pp. 669–683.

Jacoby, D.M.P., Ferretti, F., Freeman, R., Carlisle, A.B., Chapple, T.K., Curnick, D.J., Dale, J.J., Schallert, R.J., Tickler, D.M. and Block, B.A. (2020) ‘Shark movement strategies influence poaching risk and can guide enforcement decisions in a large, remote Marine Protected Area’, *Journal of Applied Ecology*, 57(9), pp. 1782–1792. Available at: https://doi.org/10.1111/1365-2664.13654.

Jayakumar, A., Vialard, J., Lengaigne, M., Gnanaseelan, C., McCreary, J.P. and Praveen Kumar, B. (2011) ‘Processes controlling the surface temperature signature of the Madden-Julian Oscillation in the thermocline ridge of the Indian Ocean’, *Clim. Dyn.,* 37, pp. 2217-2234.

Jena, B., Sahu, S., Avinash, K. and Swain, D. (2013) ‘Observation of oligotrophic gyre variability in the south Indian Ocean: Environmental forcing and biological response’, *Deep-Sea Research Part I:*

Oceanographic Research Papers, 80, pp. 1–10. Available at: https://doi.org/10.1016/j.dsr.2013.06.002.

Jiang, S., Hashihama, F., Masumoto, Y., Liu, H., Ogawa, H. and Saito, H. (2022) 'Phytoplankton dynamics as a response to physical events in the oligotrophic Eastern Indian Ocean', *Progress in Oceanography*, 203. Available at: https://doi.org/10.1016/j.pocean.2022.102784.

Jo, T., Murakami, H., Masuda, R., Sakata, M.K., Yamamoto, S. and Minamoto, T. (2017) 'Rapid degradation of longer DNA fragments enables the improved estimation of distribution and biomass using environmental DNA', *Molecular Ecology Resources*, 17(6), pp. e25–e33. Available at: https://doi.org/10.1111/1755-0998.12685.

Johnson, J.A. and Kelsch, S.W. (1998) 'Effects of evolutionary thermal environment on temperature-preference relationships in fishes', *Environmental Biology of fishes*, *53*, pp.447-458.

Johnson, T.B., Hoff, M.H., Trebitz, A.S., Bronte, C.R., Corru, T.D., Kitchell, J.F, Lozano, S.J., Mason, D.M., Scharold, J.V., Schram, S.T. and Schreiner, D.R. (2004) 'Spatial patterns in assemblage structures of pelagic forage fish and zooplankton in Western Lake Superior', *J. Great Lakes Res.,* 30(1), pp. 395-406.

Johnston, T.M. and Merrifield, M.A. (2003) 'Internal tide scattering at seamounts, ridges and islands', *Journal of Geophysical Research*, 108(C6).

Jones, C., Carvalho, L.M.V., Higgins, R.W., Waliser, D.E. and Schemm, J.K.E. (2004) 'Climatology of tropical intraseasonal convective anomalies: 1979–2002', *J. Clim*., 17, pp. 523–539.

Jones, E.C. (1962) 'Evidence of an island effect upon the standing crop of zooplankton near the Marquesas islands, central Pacific', *J. Cons. Int. Expl. Mer.,* 27(3), pp. 223-231.

Kaartvedt, S., Klevjer, T.A. and Aksnes, D.L. (2012) 'Internal wave-mediated shading causes frequent vertical migrations in fishes', *Marine Ecology Progress Series*, 452, pp. 1-10.

Kang, M., Fajaryanti, R., Son, W., Kim, J.H. and La, H.S. (2020) 'Acoustic Detection of Krill Scattering Layer in the Terra Nova Bay Polynya, Antarctica', *Frontiers in Marine Science*, 7, pp. 1–14. Available at: https://doi.org/10.3389/fmars.2020.584550.

Kaschner, K., Kesner-Reyes, K., Garilao, C., Segschneider, J., Rius-Barile, J. Rees, T. and Froese, R. (2019) AquaMaps: Predicted range maps for aquatic species. Available at: https://www.aquamaps.org.

Keele, L.J. (2008) *Semiparametric Regression for the Social Sciences.* Chichester: John Wiley & Sons.

Khan, J.R. and Herbert, N.A. (2012) 'The behavioural thermal preference of the common triplefin (*Forsterygion lapillum*) tracks aerobic scope optima at the upper thermal limit of its distribution', *Journal of Thermal Biology*, *37*(2), pp.118-124.

Kiladis, G.N., Straub, K.H. and Haertel, P.T. (2005) 'Zonal and Vertical Structure of the Madden-Julian Oscillation', *J. Atmos. Sci*., 62, pp. 2790- 2809.

Klevjer, T.A., Irigoien, X., Røstad, A., Fraile-Nuez, E., Benítez-Barrios. and Kaartvedt, S. (2016) 'Large scale patterns in vertical distribution and behaviour of mesopelagic scattering layers', *Sci Rep*, 6(19873).

Klimley, A. P., Richert, J. E., and Jorgensen, S. J. (2005) 'The Home of Blue Water Fish: Rather than singly inhabiting the trackless ocean, pelagic fish species travel together in groups, which migrate between hidden, productive oases', *American Scientist*, *93*(1), pp. 42–49. Available at: http://www.jstor.org/stable/27858513.

Klimley, A.P., Butler, S.B., Nelson, D.R. and Stull., A.T. (1988) 'Diel movements of scalloped hammerhead sharks, *Sphyrna lewini* Griffith and Smith, to and from a seamount in the Gulf of California', *Journal of Fish Biology,* 33, pp. 751-761. Available at: https://doi.org/10.1111/j.1095-8649.1988.tb05520.x

Koldewey, H.J., Curnick, D., Harding, S., Harrison, L.R. and Gollock, M. (2010) 'Potential benefits to fisheries and biodiversity of the Chagos Archipelago/British Indian Ocean Territory as a no-take marine reserve', *Marine Pollution Bulletin*, 60, pp. 1906-1915. Available at: 10.1016/j.marpolbul.2010.10.002.

Kroodsma, D.A., Mayorga, J., Hochberg, T., Miller, N.A., Boerder, K., Ferretti, F., Wilson, A., Bergman, B., White, T.D., Block, B.A., Woods, P., Sullivan, B., Costello, C. and Worm, B. (2018) 'Tracking the global footpint of fisheries', *Science*, 305, pp. 904–908. Available at: http://www.ncbi.nlm.nih.gov/pubmed/29472481.

Kumar, P. S., Pillai, G. N. and Manjusha, U. (2014) 'El Nino Southern Oscillation (ENSO) impact on tuna fisheries in Indian Ocean', *SpringerPlus,* 3(591).

Kunze, E. and Toole, J.M. (1997) 'Tidally Driven Vorticity, Diurnal Shear and Turbulence atop Fieberling Seamount', *J. Phys. Oceanogr., 27(12), pp. 2663-2693.*

Lack, D. (1954) *The Natural Regulation of Animal Numbers.* London: Oxford University Press.

Laptikhovsky, V., Boersch-Supan, P., Bolstad, K., Kemp, K., Letessier, T. and Rogers, A.D. (2017) 'Cephalopods of the Southwest Indian OceanRidge: A hotspot of biological diversity and absence of endemism', *Deep-Sea Research Part II: Topical Studies in Oceanography*, 136, pp. 98–107. Available at: https://doi.org/10.1016/j.dsr2.2015.07.002.

Lavelle and Mohn (2015) 'Motion, Commotion and Biophysical Connections at Deep Ocean Seamounts', *Oceanography*, 23(1), pp. 90–103.
Lavelle, J. and Mohn, C. (2010) 'Motion, commotion, and biophysical connections at deep ocean seamounts', *Oceanography,* 23, pp. 90–103.

Lavoie, D., Simard, Y. and Saucier, F.J. (2000) 'Aggregation and dispersion of krill at channel heads and shelf edges: the dynamics in the Saguenay - St. Lawrence Marine Park', *Canadian Journal of Fisheries and Aquatic Sciences*, 57(9), pp. 1853–1869. Available at: https://doi.org/10.1139/cjfas-57-9-1853.

Lawrence, J.M., Armstrong, E., Gordon, J., Lusseau, S.M. and Fernandes, P.G. (2016) 'Passive and active, predator and prey: using acoustics to study interactions between cetaceans and forage fish', *ICES Journal of Marine Science,* 73(8), pp. 2075-2084. Available at: https://doi.org/10.1093/icesjms/fsw013.

Le Borgne, R., Dandonneau, Y. and Lemasson, L. (1985) 'The problem of the island mass effect on chlorophyll-and zooplankton standing crops around Mare (Loyalty Islands) and New Caledonia', *Bull. Mar. Sci ,* 37(2), pp. 450-459.

Lea, J.S.E., Humphries, N.E., von Brandis, R.G., Clarke, C.R. and Sims, D.W. (2016) 'Acoustic telemetry and network analysis reveal the space use of multiple reef predators and enhance marine protected area design', *Proc. R. Soc. B,* 283. Available at: http://dx.doi.org/10.1098/rspb.2016.0717.

Letessier, T.B., Cox, M.J., Meeuwig, J.J., Boersch-Supan, P.H. and Brierley, A.S. (2016) 'Enhanced pelagic biomass around coral atolls*', Marine Ecology Progress Series*, 546, pp. 271-276.

Letessier, T.B., Mannocci, L., Goodwin, B., Embling, C., de Vos, A., Anderson, R.C., Ingram, S.N., Rogan, A. and Turvey, S.T. (2022) 'Contrasting ecological information content in whaling archives with modern cetacean surveys for conservation planning and identification of historical distribution changes', *Conservation Biology*, 37(3), pp. 1–15. Available at: https://doi.org/10.1111/cobi.14043.

Liao, J.C. (2007) 'A review of fish swimming mechanics and behaviour in altered flows', *Phil. Trans. R. Soc. B*, 362, pp. 1973-1993.

Link, J.S. and Browman, H.I. (2017) 'Operationalizing and implementing ecosystem-based management', *ICES Journal of Marine Science*, 74(1), pp. 379–381. Available at: https://doi.org/10.1093/icesjms/fsw247.

Lupandin, A.I. (2005) 'Effect of flow turbulence on swimming speed of fish', *Biology Bulletin*, *32*, pp.461-466.

Macías, D., Somavilla, R., González-Gordillo, J.I. and Echevarría, F. (2010) 'Physical control of zooplankton distribution at the Strait of Gibraltar during an episode of internal wave generation', *Marine Ecology Progress Series*, 408, pp. 79-95.

MacLennan, D.N., Magurran, A.E., Pitcher, T.J. and Hollingworth, C.E. (1990) Behavioural
Madden, R.A., and Julian, P.R. (1972) 'Description of global-scale circulation cells in the tropics with a 40–50 day period', *J. Atmos. Sci*., 29, pp. 1109–1123.

Madgett, A.S., Harvey, E.S., Driessen, D., Schramm, K.D., Fullwood, L.A.F., Songploy, S., Kettratad, J., Sitaworawet, P., Chaiyakul, S., Elsdon, T.S. and Marnane, M.J. (2022) 'Spawning aggregation of bigeye trevally, *Caranx sexfasciatus,* highlights the ecological importance of oil and gas platforms', *Estuarine, Coastal and Shelf Science*, 276, p. 108024. Available at: https://doi.org/10.1016/j.ecss.2022.108024.

Mair, A. (2008) *Investigation into a prominent 38 kHz scattering layer in the North Sea.* (PhD thesis). University of St. Andrews. Available at: https://research-repository.st-andrews.ac.uk/bitstream/handle/10023/490/AngusMairPhDThesis.pdf?isAllowed=y&sequence=7.

Mair, A., Fernandes, P.G., Lebourges-Dhaussy, A. and Brierley, A.S. (2005) 'An investigation into the zooplankton composition of a prominent 38-kHz scattering layer in the North Sea', *Journal of Plankton Research,* 27(7), pp. 623-633. Available at: https://doi.org/10.1093/plankt/fbi035.

Marchant, R., Mumbi, C., Behera, S. and Yamagata, T. (2006) 'The Indian Ocean dipole - the unsung driver of climatic variability in East Africa', *African Journal of Ecology,* 45(1), pp.4-16. Available at: 10.1111/j.1365-2028.2006.00707.x.

Marsac, F. and Demarcq, H. (2016) *Outline of climate and oceano- graphic conditions in the Indian Ocean, an update to mid-2016. Submitted to 18th Working Party on Tropical Tunas (WPTT18),* IOTC-2016-WPTT18-09.

Marsac, F., Annasawmy, P., Noyon, M., Demarcq, H., Soria, M., Rabearisoa, N., Bach, P., Cherel, Y., Grelet, J. and Romanov, E. (2020) 'Seamount effect on circulation and distribution of ocean taxa in the vicinity of La Pérouse, a shallow seamount in the southwestern Indian Ocean', *Deep-Sea Research Part II: Topical Studies in Oceanography*, 176. Available at: https://doi.org/10.1016/j.dsr2.2020.104806.

Martin, B. and Christiansen, B. (2009) 'Distribution of zooplankton biomass at three sea- mounts in the NE Atlantic', *Deep-Sea Res. Part II: Topical Stud. Oceanogr*. 56 (25), pp. 2671–2682.

Martinez, E. and Maamaatuaiahutapu, K. (2004) 'Island mass effect in the Marquesas Islands: time variation', *Geophy. Res. Lett.,* 31(L18307).

MathWorks (2019) *Matlab* (R2019b) [Computer program]. Available at: https://uk.mathworks.com/products/matlab.html (Accessed: 13 December 2020).

MathWorks (2022) *Matlab* (R2022a) [Computer program]. Available at: https://uk.mathworks.com/products/matlab.html (Accessed: 02 April 2022).

McClain, C.R. (2007) 'Seamounts: identity crisis or split personality?', *Journal of Biogeography*, 34, pp. 2001-2008.

McClure, E.C., Sievers, K.T., Abesamis, R.A., Hoey, A.S., Alcala, A.C. and Russ, G.R. (2020) 'Higher fish biomass inside than outside marine protected areas despite typhoon impacts in a complex reefscape', *Biological Conservation*, 241. Available at: https://doi.org/10.1016/j.biocon.2019.108354.

McKinnon, A.D., Duggan, S., Carleton, J.H. and Böttger-Schnack, R. (2008) 'Summer planktonic copepod communities of Australia's North West Cape (Indian Ocean) during the 1997-99 El Niño/La Niña', *Journal of Plankton Research*, 30(7), pp. 839–855. Available at: https://doi.org/10.1093/plankt/fbn043.

McPhaden, M. J. and M. Nagura. (2014) 'Indian Ocean Dipole interpreted in terms of Recharge Oscillator theory', *Climate Dynamics*, 42, pp. 1569-1586. Available at: 10.1007/s00382-013-1765-1.

McQuinn, I, H., Dion, M. and St. Pierre, J.F. (2013) 'The acoustic multifrequency classification of two sympatric euphausiid species (*Meganyctiphanes norvegica* and *Thysanoessa raschii*), with empirical and SDWBA model validation', *ICES Journal of Marine Science*, 70(3), pp. 636–649. Available at: https://doi.org/10.1093/icesjms/fst004.

Mejía-Mercado, B. E., Mundy, B. and Baco, A. R. (2019) 'Variation in the structure of the deep-sea fish assemblages on Necker Island, Northwestern Hawaiian Islands', *Deep-Sea Research Part I: Oceanographic Research Papers*, 152(103086). Available at: 10.1016/j.dsr.2019.103086.

Meyers, G., McIntosh, P., Pigot, L. and Pook, M. (2007) 'The years of El Niño, La Niña, and interactions with the tropical Indian Ocean', *Journal of Climate*, 20, pp. 2872–2880. Available at: 10.1175/JCLI4152.1.

Michalec, F.G., Fouxon, I., Souissi, S. and Holzner, M. (2017) 'Zooplankton can actively adjust their motility to turbulent flow', *Biological Sciences,* 114(52), E11199-E11207. Available at: https://doi.org/10.1073/pnas.1708888114.

Miller, C.B. and Wheeler, P.A. (2012) *Biological Oceanography*. 2nd edn. Sussex: Wiley.

Millineau, L.S. and Mills, S.W. (1997) 'A test of the larval retention hypothesis in seamount-generated flows', *Deep Sea Research Part I*, 44(5), pp. 745-770.

Misund, O.A. (1997) 'Underwater acoustics in marine fisheries and fisheries research', *Review in Fish Biology and Fisheries,* 7, pp. 1-34.

Mitson, R.B. and Wood, R.J. (1962) 'An automatic method of counting fish echoes', *J. Cons.* 26, pp. 281-291.

Mohn, C. and Beckmann, A. (2002a) 'The upper ocean circulation at Great Meteor Seamount. Part I: structure of density and flow fields', *Ocean Dynamics*, 52, pp. 179–193.

Mohn, C. and Beckmann, A. (2002b) 'Numerical studies on flow amplification at an isolated shelf break bank, with application to Porcupine Bank', *Continental Shelf Research,* 22, pp. 1325–1338.

Moore, S.E. and Lien, R. (2007) 'Pilot whales follow internal solitary waves in the South China Sea', *Marine Mammal Science,* 23(1), pp. 193-196.

Morato, T., Hoyle, S.D., Allain, V. and Nicol, S.J. (2010a) 'Seamounts are hotspots of pelagic biodiversity in the open ocean', *Proc. Natl. Acad. Sci,* 107(21), pp. 9707-9711.

Morato, T., Pitcher, T.J., Clark, M.R., Menezes, G., Tempera, F., Porteiro, F., Giacomello, E. and Santos, R.S. (2010b) 'Can we protect seamounts for research? A call for conservation', *Oceanography*, 23(1), pp. 190–199. Available at: https://doi.org/10.5670/oceanog.2010.71.

Morato, T., Varkey, D.A., Damaso, C., Machete, M., Santos, M., Prieto, R., Santos, R.S. and Pitcher, T.J. (2008) 'Evidence of a seamount effect on aggregating visitors', *Marine Ecology Progress Series*, 357, pp. 23–32. Available at: https://doi.org/10.3354/meps07269.

Moriarty, R., Buitenhuis, E.T. and Le Quéré, C. (2013) 'Distribution of known macrozooplankton abundance and biomass in the global ocean', *Earth System Science Data*, 5(2), pp. 241–257. Available at: https://doi.org/10.5194/essd-5-241-2013.

Mortimer, J.A., Esteban, N., Guzman, A.N. and Hays, G.C. (2020) 'Estimates of marine turtle nesting populations in the south-west Indian Ocean indicate the importance of the Chagos Archipelago', *Oryx*, 54(3), pp. 332–343. Available at: https://doi.org/10.1017/S0030605319001108.

Murray, A. (2013) *A study of the social interactions of Manta Rays in the Baa Atoll, Maldives.* Available at: https://www.cms.int/sharks/en/publication/study-social-interactions-manta-rays-baa-atoll-maldives. (Accessed: 18th July 2023).

Napper, I.E., Baroth, A., Barrett, A.C., Bhola, S., Chowdhury, G.W., Davies, B.F.R., Duncan, E.M., Kumar, S., Nelms, S.E., Hasan Niloy, M.N., Nishat, B., Maddalene, T., Thompson, R.C. and Koldewey, H. (2021) 'The abundance and characteristics of microplastics in surface water in the transboundary Ganges River', *Environmental Pollution*, 274, p. 116348. Available at: https://doi.org/10.1016/j.envpol.2020.116348.

Neilson, J.D. and Perry, R.I. (1990) 'Diel vertical migrations of marine fishes: an obligate or facultative process?', *Advances in marine biology*, 26, pp. 115-168.

Nellen, W. (1973) 'Untersuchungen zur Verteilung von Fischlarven und Plankton im Gebiet der Grosen Meteorbank', *Meteor Forschung*, 13, pp. 47–69.

NOAA (2018) *Where is the highest tide?* Available at: https://oceanservice.noaa.gov/facts/highesttide.html (Accessed: 28 November 2020).

Nobel, M. and Mullineaux, L.S. (1989) 'Internal tidal currents over the summit of cross seamount', *Deep Sea Res. Part I Oceanogr. Res. Pap.,* 36(12), pp. 1791-1802.

Noda, T., Fujioka, K., Fukuda, H., Mitamura. H., Ichikawa, K. and Arai, N. (2016) 'The influence of body size on the intermittent locomotion of a pelagic schooling fish', *Proc. Royal Soc. B,* 283.

O'Leary, B.C., Ban, N.C., Fernandez, M., Friedlander, A.M., García-Borboroglu, P., Golbuu, Y., Guidetti, P., Harris, J.M., Hawkins, J.P., Langlois, T., McCauley, D.J., Pikitch, E.K., Richmond, R.H. and Roberts, C.M. (2018) 'Addressing Criticisms of Large-Scale Marine Protected Areas', *BioScience*, 68(5), pp. 359–370. Available at: https://doi.org/10.1093/biosci/biy021.

Ocean Country Partnership Programme (2023) *Report of Protected Area Management Effectiveness Evaluations for the three sites in the Maldives.* Available at: https://data.jncc.gov.uk/data/97819c0b-2bce-4cf6-a1fe-7d98138ce919/ocpp-maldives-pame-report-final.pdf (Accessed: 6th July 2023).

Ona, E. (1990) 'Physiological factors causing natural variations in acoustic target strength of fish', *Journal of the Marine Biological Association of the United Kingdom,* 70(1), pp.107-127.

Ona, E. (1999) *Methodology for target strength measurements.* ICES Cooperative Research Report, No. 235.

Pan, W. (2001) 'Akaike's Information Criterion in Generalized Estimating Equations', *Biometrics,* 57, pp. 120-125. Available at: https://doi.org/10.1111/j.0006-341X.2001.00120.x

Panicker, D. and Stafford, K.M. (2023) 'Temporal variability of a soundscape near a mid-oceanic atoll in the northern Indian ocean', *Progress in Oceanography*, 214(September 2022), p. 103033. Available at: https://doi.org/10.1016/j.pocean.2023.103033.

Partridge, B.L. (1980) 'The Effect of School Size on the Structure and Dynamics of Minnow School', *Anim. Behav.,* 28(1), pp. 68–77.

Pauly, D., Christensen, V., Guénette, S., Pitcher, T.J., Sumaila, U.R., Walters, C.J., Watson, R and Zeller, D. (2002) 'Towards sustainability in world fisheries', *Nature,* 418, pp. 689–695.

Pavlov, D.S. and Kasumyam, A.O. (2000) 'Patterns and Mechanisms of Schooling Behavior in Fish: A Review', *Journal of Ichthyology,* 40(2), pp. 163 –231.

Pecuchet, L., Törnroos, A. and Lindegren, M. (2016) 'Patterns and drivers of fish community assembly in a large marine ecosystem', *Marine Ecology Progress Series*, 546, pp. 239–248. Available at: https://doi.org/10.3354/meps11613.

Peña, M., Munuera-Fernández, I., Nogueira, E. and González-Quirós, R. (2021) 'First recording of a bathypelagic deep scattering layer in the Bay of Biscay', *Progress in Oceanography*, 198(May). Available at: https://doi.org/10.1016/j.pocean.2021.102669.

Pfeiffer, M. and Dullo, W.C. (2006) 'Monsoon-induced cooling if the western equatorial Indian Ocean as recorded in coral oxygen isotope records from the Seychelles covering the period of 1840-1994 AD', *Quaternary Science Reviews*, 25, pp. 993-1009.

Phleger, C.F. (1998) 'Buoyancy in Marine Fishes: Direct and Indirect Role of Lipids', *American Zoologist*, 38(2), pp. 321–330.

Picheral, M., Coln, S. & Irisson, J. (2022) *EcoTaxa, a tool for the taxonomic classification of images.* [Online] Available at: http://ecotaxa.obs-vlfr.fr [Accessed 2022].

Pickard, G.L. and Emery, W.J. (1990) *Descriptive Physical Oceanography: an introduction*. Oxford: Butterworth-Heinemann.

Pineda, J. (1994) 'Internal tidal bores in the nearshore: Warm-water fronts, seaward gravity currents and the onshore transport of neustonic larvae', *Journal of Marine Research*, 52, pp. 427-458.

Pineda, J. *et al.* (2020) 'Response of small sharks to nonlinear internal waves', *Limnology and Oceanography*, 65(4), pp. 707–716. Available at: 10.1002/lno.11341.

Pinheiro, P., Hazin, F., Travassos, P., Oliveira, P., Carvalho, F. and Rêgo, M. (2011) 'The reproductive biology of the rainbow runner, caught in the São Pedro and São Paulo Archipelago .', *Brazilian Journal of Biology*, 71(1), pp. 99–106.

Pinti, J., Jónasdóttir, S.H., Record, N.R. and Visser, A.W. (2023) 'The global contribution of seasonally migrating copepods to the biological carbon pump', *Limnology and Oceanography*, (68), pp. 1147–1160. Available at: https://doi.org/10.1002/lno.12335.

Pirotta, E., Matthiopoulos, J., MacKenzie, M., Scott-Hayward, L. and Rendell, L. (2011) 'Modelling sperm whale habitat preference: a novel approach combining transect and follow data', *Marine Ecology Progress Series*, 436, pp. 257-272. Available at: 10.3354/meps09236.

Pitcher, T.J. (1983) 'Heuristic definitions of fish shoaling behaviour', *Animal Behaviour,* 31(2), pp. 611-613.

Pitcher, T.J. (1998) 'Shoaling and Schooling in Fishes', in Greenberg, G. and Hararway, M.M. (eds) *Comparative Psychology: A Handbook*. New York: Garland, pp. 748- 760.

Pitcher, T.J. and Bulman, C. (2007) 'Raiding the larder: a quantitative evaluation framework and trophic signature for seamount food webs', in Pitcher, T.J., Morato, T., Hart, P.J.B., Clark, M.R., Haggan. N. and Santos, R.S. *Seamounts: Ecology, Fisheries and Conservation*. Oxford: Blackwell Publishing, pp. 282–295.

Pitcher, T.J., Morato, T., Hart, P.J.B., Clark, M.R., Haggan, N. and Santos, R.S. (2007) *Seamounts: Ecology, Fisheries & Conservation*, *Seamounts: Ecology, Fisheries & Conservation*. Available at: https://doi.org/10.1002/9780470691953.

Pond, S. and Pickard, G.L. (1983) *Introductory Dynamical Oceanography*. Oxford: Pergamon Press Ltd.

Porteiro, F.M. and Sutton, T. (2007) 'Midwater fish assemblages and seamounts', in Pitcher, T.J., Morato, T., Hart, P.J.B., Clark, M.R., Haggan. N. and Santos, R.S. *Seamounts: Ecology, Fisheries and Conservation*. Oxford: Blackwell Publishing, pp. 101- 116.

Pugh, D. T., and Rayner, R. F. (1981). 'The tidal regimes of three indian ocean atolls and some ecological implications', *Estuar. Coast. Shelf Sci.* 13, pp. 389–407. Doi: 10.1016/S0302-3524(81)80036-9.

R Core Team (2019). R: A language and environment for statistical computing. R Foundation for Statistical Computing [Computer program]. (Version 1.2.1335) Vienna, Austria: R Core Team. 2019. Available at: https://www.R-project.org/.

R Core Team (2023). R Studio[Computer program]. (Version 4.3.1). Available at: https://www.R-project.org/.

Rasmussen, A.S. and Arnason, U. (1999) 'Molecular studies suggest that cartilaginous fishes have a terminal position in the piscine tree', *Proceedings of the National Academy of Sciences.,* 96(5), pp. 2177-2182.

Read, J. and Pollard, R. (2017) 'An introduction to the physical oceanography of six seamounts in the southwest Indian Ocean', *Deep-Sea Research II,* 136, pp. 44-58.

Readman, J.W., DeLuna, F., Ebinghaus, R., Guzman, A., Price, A.R.G., Readman, E.E., Sheppard, A.L.S., Sleight, V.A., Sturm, R., Thompson, R.C., Tonkin, A., Wolschke, H., Wright, R.J. and Sheppard, C.R.C. (2013) 'Contaminants, Pollution and Potential Anthropogenic Impacts in Chagos/BIOT', in Sheppard, C.R.C. (ed.) *Coral Reefs of the United Kingdom Overseas Territories*. Netherlands: Springer, pp. 283-298.

Rees, H.C., Maddison, B.C., Middleditch, D.J., Patmore, J.R.M. and Gough, K.C. (2014) 'The detection of aquatic animal species using environmental DNA - a review of eDNA as a survey tool in ecology', *Journal of Applied Ecology*, 51(5), pp. 1450–1459. Available at: https://doi.org/10.1111/1365-2664.12306.

Reid, D. (2000) *Report on echo trace classification*. ICES Cooperative Research Report No. 238. Available at: http://www.ices.dk/sites/pub/Publication%20Reports/Cooperative%20Research%20Report%20(CRR)/CRR238.pdf (Accessed: 13 December 2020).

Relano, V., Palomares, M.L.D. and Pauly, D. (2021) 'Comparing the performance of four very large marine protected areas with different levels of protection', *Sustainability*, 13(17). Available at: https://doi.org/10.3390/su13179572.

Reynolds, W.W. and Casterlin, M.E. (1979) 'Thermoregulatory behavior of brown trout, *Salmo trutta'*, *Hydrobiologia*, *62*, pp.79-80.

Richardson, I.D., Cushing, D.H., Harden Jones, F.R., Beverton, R.J. and Blacker, R.W. (1959) 'Echo sounding experiments in the Barents Sea', *Fishery Investigations,* 22, pp. 1-57.

Richardson, A.J., Downes, K.J., Nolan, E.T., Brickle, P., Brown, J., Weber, N. and Weber, S.B. (2018) 'Residency and reproductive status of yellowfin tuna in a proposed large-scale pelagic marine protected area', *Aquatic Conservation: Marine and Freshwater Ecosystems*, 28(6), pp. 1308–1316. Available at: https://doi.org/10.1002/aqc.2936.

Richert, J. and Klimley A, P. (2017) 'The Importance of Pinnacles and Seamounts to Pelagic Fishes and Fisheries off the Southern Baja California Peninsula', *Oceanography & Fisheries Open access Journal*, 4(2). Available at: 10.19080/ofoaj.2017.04.555634.

Ringuette, M., Castonguay, M., Runge, J.A., and Grégoire, F. (2002) 'Atlantic mackerel (*Scomber scombrus*) recruitment fluctuations in relation to copepod production and juvenile growth', *Can. J. Fish. Aquat. Sci.,* 59, pp. 165-175.

Robert, M., Dagorn, L., Lopez. J., Moreno, G. and Deneubourg, J.L. (2013) 'Does social behavior influence the dynamics of aggregations formed by tropical tunas around floating objects? An experimental approach', *J. Exp. Mar. Biol. Ecol.,* 440, pp. 238-243.

Robinson, E., Hosegood, P, Bolton, A. (2023). 'Dynamical oceanographic processes impact on reef manta ray behaviour: Extreme Indian Ocean Dipole influence on local internal wave dynamics at a remote tropical atoll', *Progress in Oceanography,* 103129.

Robinson, J., New, A.L., Popova, E.E., Srokosz, M.A. and Yool, A. (2017) 'Far-field connectivity of the UK's four largest marine protected areas: Four of a kind?', *Earth's Future*, 5, pp. 475- 494.

Robinson. E. (2023) [Sandes oceanography]. Unpublished data.

Roden, G.I. (1987) 'Effect of seamounts and seamount chains on ocean circulation and thermohaline structure', *Seamounts, islands, and atolls*, *43*, pp.335-354.

Rogers, A. D. (2018) 'The Biology of Seamounts: 25 Years on', *Advances in Marine Biology*, 79, pp. 137–224. Available at: 10.1016/bs.amb.2018.06.001.

Rombouts, I., Beaugrand, G., Ibaňez, F., Gasparini, S., Chiba, S., and Legendre, L. (2009) 'Global Latitudinal Variations in Marine Copepod Diversity and Environmental Factors', *Proc.R. Soc.B.: Biol.Sci*, 276, pp. 3053–3062. Available at: https://doi.org/10.1098/rspb.2009.0742.

Rowden, A.A., Dower, J.F., Schlacher, T.A., Consalvey, M. and Clark, M.R. (2010) 'Paradigms in seamount ecology: fact, fiction and future', *Marine Ecology*, 31, pp. 226-241.

Royer, T.C. (1978) 'Ocean eddies generated by seamounts in the North Pacific', *Science,* 199, pp. 1063–1064.

Ruckelshaus, M., Klinger, T., Knowlton, N. and DeMaster, D.P. (2008) 'Marine ecosystem-based management in practice: Scientific and governance challenges', *BioScience*, 58(1), pp. 53–63. Available at: https://doi.org/10.1641/B580110.

Ryan, T. and Kloser, R. (2004) *Quantification and correction of a systematic error in Simrad ES60 Echosounders*. Available at: http://courses.washington.edu/fish538/resources/Ryan_Kloser_2004_ES60_Error.pdf (Accessed: 14 December 2020).

Ryan, T.E., Downie, R.A., Kloser, R.J., Keith, G. (2015) 'Reducing bias due to noise and attenuation in open-ocean echo integration data', *ICES Journal of Marine Science*, 72(8), pp.2482-2493.

Ryther, J. H., Hall, J. R., Pease, A. K., Bakun, A. and Jones, M. M. (1966) 'Primary organic production in relation to the chemistry and hydrography of the western Indian Ocean', *Limnol. Oceanogr.,* 11, pp. 371–380.

Saji, N. H. and Yamagata, T. (2003a) 'Structure of SST and surface wind variability during Indian Ocean Dipole mode events: COADS observations', *Journal of Climate*, 16(16), pp. 2735–2751. Available at: https://doi.org/10.3354/cr025151.

Saji, N.H. and Yamagata, T. (2003b) 'Possible impacts of Indian Ocean Dipole mode events on global climate', *Climate Research,* 25, pp. 151-169.

Sala, E., Aburto-Oropeza, O., Paredes, G. and Thompson, G. (2003) 'Spawning aggregations and reproductive behavior of reef fishes in the Gulf of California', *Bulletin of Marine Science*, 72(1), pp. 103–121.

Salmerón, N., Belle, S., Cruz, F.S., Alegria, N., Finger, J.V.G., Corá, D.H., Petry, M.V., Hernández, C., Cárdenas, C.A. and Krüger, L. (2023) 'Contrasting environmental conditions precluded lower availability of Antarctic krill affecting breeding chinstrap penguins in the Antarctic Peninsula', *Scientific Reports*, 13(1), pp. 1–9. Available at: https://doi.org/10.1038/s41598-023-32352-7.

Samadi, S., Bottan, L., Macpherson, E., De Forges, B.R. and Boisselier, M.C. (2006) 'Seamount endemism questioned by the geographic distribution and population genetic structure of marine invertebrates', *Marine Biology*, 149(6), pp. 1463–1475. Available at: https://doi.org/10.1007/s00227-006-0306-4.

Sander, F., and Steven, D.M. (1973) 'Organic productivity of inshore and offshore waters of Barbados: a study of the island mass effect', *Bull Mar Sci,* 23, pp. 771-792.

Sasamal, S.K. (2006) 'Island mass effect around the Maldives during the winter months of 2003 and 2004', *Int J. Rem. Sens.,* 27(22), pp. 5087-5093.

Scales, K.L., Miller, P.I., Embling, C.B., Ingram, S.N., Enrico, P. and Votier, S.C. (2014) 'Mesoscale fronts as foraging habitats: composite front mapping reveals oceanographic drivers of habitat use for a pelagic seabird', *J. R. Soc. Interface.,* 11:20140679.

Schott, F.A. and McCreary Jr. J.P. (2001) 'The monsoon circulation of the Indian Ocean', *Progress in Oceanography,* 51, pp. 1-123.

Scott, B.E., Webb, A., Palmer, M.R., Embling, C.B. and Sharples, J. (2013) 'Fine scale bio-physical oceanographic characteristics predict the foraging occurrence of contrasting seabird species; Gannet (*Morus bassanus*) and storm petrel (*Hydrobates pelagicus*), *Progress in Oceanography*, 117, pp.118-129.

Scott-Hayward, L. A. S., Mackenzie, M.L, Donovan, C.R., Walker, C.G. and Ashe, E. (2013) 'Complex Region Spatial Smoother (CReSS)', *Journal of Computational and Graphical Statistics*, 23(2), pp. 340-360. Available at: https://doi.org/10.1080/10618600.2012.762920.

Shank, T.M. (2010) 'Seamounts: deep-ocean laboratories of faunal connectivity, evolution, and endemism', *Oceanography*, 23(1), pp. 108-122.

Shankar, D., Vinayachandran, P.N. and Unnikrishnan, A.S. (2002) 'The monsoon currents in the north Indian Ocean', *Progress in Oceanography*, 52, pp. 63-120.

Sharples, J., Moore, C.M., Hickman, A.E., Holligan, P.M., Tweddle, J.F., Palmer, M.R. and Simpson, J.H. (2009) 'Internal tidal mixing as a control on continental margin ecosystems', *Geophysical Research Letters*, 36, pp. 1–8. Available at: https://doi.org/10.1029/2009GL040683.1.

Shea, R.E. and Broenkow, W.W. (1982) 'The role of internal tides in the nutrient enrichment of Monterey Bay, California', Estuar. Coast. Shelf Sci. 15, pp. 57–66. Available at: http: //dx.doi.org/10.1016/0272-7714(82)90036-1.

Sheehan, E. V., Hosegood, P., Game, C.A., Attrill, M.J., Tickler, D., Wootton, M., Johns, D.G. and Meeuwig, J.J. (2019) 'The effect of deep oceanic flushing on water properties and ecosystem functioning within atolls in the British Indian ocean territory', *Frontiers in Marine Science*, 6, pp. 1–13. Available at: https://doi.org/10.3389/fmars.2019.00512.

Sheehan, E. V., Stevens, T.F., Gall, S.C., Cousens, S.L. and Attrill, M.J. (2013) 'Recovery of a temperate reef assemblage in a marine protected area following the exclusion of towed demersal fishing', *PLoS ONE*, 8(12), pp. 1–12. Available at: https://doi.org/10.1371/journal.pone.0083883.

Sheppard, C. R., Ateweberhan, M., Bowen, B. W., Carr, P., Chen, C. A., Clubbe, C., Craig, M. T., Ebinghaus, R., Eble, J., Fitzsimmons, N., Gaither, M. R., Gan, C. H., Gollock, M., Guzman, N., Graham, N. A., Harris, A., Jones, R., Keshavmurthy, S., Koldewey, H., Lundin, C. G., Yesson, C. (2012) 'Reefs and islands of the Chagos Archipelago, Indian Ocean: why it is the world's largest no-take marine protected area', *Aquatic conservation: marine and freshwater ecosystems*, *22*(2), pp. 232–261. https://doi.org/10.1002/aqc.1248

Sheppard, C.R.C., Bowen, B.W., Chen, A.C., Craig, M.T., Eble, J., Fitzsimmons, N., Gan, C., Gaither, M.R., Gollock, M., Keshavmurthy, S., Koldewey, H., Mortimer, J.A., Obura, D., Pfeiffer, M., Rogers, A.D., Sheppard, A.L.S., Vogler, C., Wörheide, G., Yang, M. and Yesson, C. (2013) 'British Indian Ocean Territory (the Chagos Archipelago): Setting, Connections and the Marine Protected Area', in Sheppard, C.R.C. (ed.) *Coral Reefs of the United Kingdom Overseas Territories*. Netherlands: Springer, pp. 223- 240.

Sheppard, C.R.C., Seaward, M.R.D., Klaus, R. and Topp, J.M. (1999) 'The Chagos Archipelago: an introduction', in Sheppard, C.R.C. and Seaward, M.R.D. *Ecology of the Chagos Archipelago*. Great Britain: Westbury Academic & Scientific Publishing.

Simmonds, J. and MacLennan, D. (2005) *Fisheries Acoustics: theory and practice.* 2nd edn. Oxford: Blackwell Science Ltd.

Soviadan, Y.D., Benedetti, F., Brandão, M.C., Ayata, S.D., Irisson, J.O., Jamet, J.L., Kiko, R., Lombard, F., Gnandi, K. and Stemmann, L. (2022) 'Patterns of mesozooplankton community composition and vertical fluxes in the global ocean', *Progress in Oceanography*, 200. Available at: https://doi.org/10.1016/j.pocean.2021.102717.

Stanton, T.K., Chu, D. and Wiebe, P.H. (1996) 'Acoustic scattering characteristics of several zooplankton groups', *ICES Journal of Marine Science,* 53, pp. 289–302.

Stanton, T.K., Wiebe, P.H., Chu, D., Benfield, M., Scanlon, L., Martin, L. and Eastwood, R.L. (1994) 'On acoustic estimates of zooplankton biomass', *ICES Journal of Marine Science,* 51, pp. 505–512.

Starr, R.M. and Thorne, R.E. (1988) 'Acoustic assessment of squid stocks', *FAO Fisheries Technical Paper*, pp. 181–198.

Su, D., Wijeratne, S. and Pattiaratchi, C.B. (2021) 'Monsoon Influence on the Island Mass Effect Around the Maldives and Sri Lanka', *Frontiers in Marine Science*, 8, pp. 1–18. Available at: https://doi.org/10.3389/fmars.2021.645672.

Talley, L.D., Pickard, G.L., Emery, W.J. and Swift, J.H. (2011) 'Climate and the Oceans', in Talley, L.D., Pickard, G.L., Emery, W.J. and Swift, J.H. (ed.) *Descriptive Physical Oceanography*. 6th edn. Academic Press, pp. 1-36.

Taylor, G.I. (1923) 'Experiments on the motion of solid bodies in rotating fluids' *Proceedings of the Royal Society of London. Series A, Containing Papers of a Mathematical and Physical Character*, 104(725), pp.213-218.

Thomson, P.F. and Willerslev, E. (2015) 'Environmental DNA- An emerging tool in conservation for monitoring past and present biodiversity', *Biological Conservation,* 183, pp. 4-18.

Thresher, R. (1983) 'Environmental Correlates of the Distribution of Planktivorous Fishes in the One Tree Reef Lagoon', *Marine Ecology Progress Series*, 10, pp. 137–145. Available at: 10.3354/meps010137.

Tickler, D.M., Carlisle, A.B., Chapple, T.K., Curnick, D.J., Dale, J.J., Schallert, R.J. and Block, B.A. (2019) 'Potential detection of illegal fishing by passive acoustic telemetry', *Animal. Biotelemetry,* 7(1). Available at: https://doi.org/10.1186/s40317-019-0163-9.

Tickler, D.M., Letessier, T.B., Koldewey, H.J., Meeuwig, J.J. (2017) 'Drivers of abundance and spatial distribution of reef-associated sharks in an isolated atoll reef system', *PLoS ONE*, 12(e0177374).

Toresen, R., Gjøsæter, H., and de Barros, P. (1998) 'The acoustic method as used in the acoustic-abundance estimation of capelin (*Mallotus villosus* Müller) and herring (*Clupea harengus* Linné) in the Barents Sea', *Fisheries Research*, 34, pp.27–37.

Torgersen, T. and Kaartvedt, S. (2001) '*In situ* swimming behaviour of individual mesopelagic fish studies by split-beam echo target tracking', *ICES Journal of Marine Science,* 58(1), pp. 346-354. Available at: https://doi.org/10.1006/jmsc.2000.1016.

Tourre, Y.M. and White, W.B. (1995) 'ENSO signals in global upper-ocean temperature', *Journal of Physical Oceanography,* 25, pp. 1317-1332.

Trenkel, V.M., Ressler, P.H., Jech, M., Giannoulaki, M. and Taylor, C. (2011) 'Underwater acoustics for ecosystem-based management: state of the science and proposals for ecosystem indicators', 442, pp. 285–301. Available at: https://doi.org/10.3354/meps09425.

Trujilo, A.P. and Thurman, H.V. (2007) *Essentials of Oceanography*. New Jersey: Pearson Prentice Hall.

Tungate, D.S. (1958) 'Echo-sounder surveys in the autumn of 1956', *Fishery Investigations, Series 2,* 12, pp. 3–17.

UNEP-WCMC and IUCN (2023) *Protected Planet: The World Database on Protected Areas (WDPA)*. Available at: www.protectedplanet.net (Accessed: 1 August 2023).

United Nations General Assembly (2023) *Agreement under the United Nations Convention on the Law of the Sea on the conservation and sustainable use of marine biological diversity of areas beyond national jurisdiction*. Resolution A/CONF.232/2023/4. Available at: https://documents-dds-ny.un.org/doc/UNDOC/LTD/N23/177/28/PDF/N2317728.pdf?OpenElement (Accessed: 17 August 2023).

UNSECO (2019) *Baa Atoll Biosphere Reserve, Maldives*. Available at: https://en.unesco.org/biosphere/aspac/baa-atoll (Accessed: 17th July 2023).

Utne-Palm, A. C. and Stiansen, J. E. (2001) 'Effect of larval ontogeny, turbulence and light on prey attack rate and swimming activity in herring larvae', *Journal of Experimental Marine Biology and Ecology*, 268(2), pp. 147–170. Available at: 10.1016/S0022-0981(01)00383-5.

Valle-Levinson, A., Castro. L., Cáceres, M. and Pizarro, O. (2014) 'Twilight vertical migrations of zooplankton in a Chilean fjord', *Progress in Oceanography*, 129, pp. 114-124.

Valle-Levison, A., Castro, A.T., de Velasco, G.G. and Armas, G.G. (2004) 'Diurnal vertical motions over a seamount of the southern Gulf of California', *Journal of Marine Systems*, 50(1), pp.61-77. Available at: https://doi.org/10.1016/j.jmarsys.2003.09.016.

Vianello, P., Ternon,J.F., Demarcq, H., Herbette, S. and Roberts, M.J. (2020) 'Ocean currents and gradients of surface layer properties in the vicinity of the Madagascar Ridge (including seamounts) in the South West Indian Ocean', *Deep Sea Research Part II: Topical Studies in Oceanography*, 176: 104819.

Visser, A.W., Nielsen, T.G., Middelboe, M., Høyer, J.L. and Markager, S. (2015) 'Oceanography and the base of the pelagic food web in the southern Indian Ocean', *J. Plankton Res.,* 37(3), pp. 571-583.

Vlasenko, V. and Stashchuk, N. (2021) 'Setting tidal forcing for regional modelling of internal waves', *Ocean Modelling,* 160. Available at: https://doi.org/10.1016/j.ocemod.2021.101767.

Volkoff, H. and Rønnestad, I. (2020) 'Effects of temperature on feeding and digestive processes in fish', *Temperature*, 7(4), pp. 307–320. Available at: 10.1080/23328940.2020.1765950.

Waggitt, J.J., Cazenave, P., Torres, R., Williamson, B.J., Scott, B.E. (2016) 'Quantifying pursuit diving seabirds' associations with fine-scale physical features in tidal stream environments', *Journal of Applied Ecology,* 23, pp. 1653-1666.

Walker, C. G., Mackenzie, M.L., Donovan, C.R., and O'Sullivan, M.J. (2010) 'SALSA - a Spatially Adaptive Local Smoothing Algorithm', *Journal of Statistical Computation and Simulation*, 81(2), pp.179–91.

Walter, R.K. and Phelan, P.J. (2016) 'Internal bore seasonality and tidal pumping of subthermocline waters at the head of the Monterey submarine canyon', *Continental Shelf Research*, 116, pp. 42–53. Available at: https://doi.org/10.1016/j.csr.2016.01.015.

Wannamaker, C.M. and Rice, J.A. (2000) 'Effects of hypoxia on movements and behavior of selected estuarine organisms from the southeastern United States', *J. Exp. Mar. Biol. Ecol*, 249, pp. 145–163.

Ward, A.J.W., Herbert-Read, J.E., Sumpter, D.J.T. and Krause, J. (2011) 'Fast and accurate decisions through collective vigilance in fish shoals', *Proc Natl Acad Sci USA,* 108(6), pp. 2312-2315.

Warhaft, Z. (1997) *An introduction to thermal fluid engineering: The engine and the atmosphere.* Cambridge: Cambridge University Press.

Watkins, J. L. and Brierley, A.S. (1996) 'A post-processing technique to remove background noise from echo integration data', *ICES Journal of Marine Science,* 53(2), pp. 339-344. Available at: https://doi.org/10.1006/jmsc.1996.0046.

Webb, P.W. (1989) 'Station-holding by three species of benthic fishes', *Journal of Experimental Biology*, 145(1), pp.303-320.

Webber, B.G.M., Matthews, A.J., and Heywood, K.J. (2010) 'A dynamical ocean feedback mechanism for the Madden-Julian oscillation', *Q. J. R. Meteorol. Soc.,* 136, pp. 740–754.

West, J.B. (1999) 'The original presentation of Boyle's law', *Journal of Applied Physiology,* 87(4), pp. 1543- 1545.

Whitaker, D., Christman, M. and Whitaker, M.D., 2014. Package 'clustsig'. *R package*.

White, M., Bashmachnikov, I., Aristegui, J. and Martins, A. (2007) 'Physical processes and seamount productivity', in Pitcher, T.J., Morato, T., Hart, P.J.B., Clark, M.R., Haggan. N. and Santos, R.S. *Seamounts: Ecology, Fisheries and Conservation*. Oxford: Blackwell Publishing, pp. 101- 116.

Williams, R.G. and Follows, M.J. (2011) *Ocean Dynamics and the Carbon Cycle: Principles and Mechanisms.* Cambridge University Press: United Kingdom.

Williamson, B. (2019) ES70 Sync. [Computer program]

Williamson, B., Fraser, S., Williamson, L., Nikora, V. and Scott, B. (2019) 'Predictable changes in fish school characteristics due to a tidal turbine support structure', *Renewable Energy*, 141, pp. 1092–1102. Available at: https://doi.org/10.1016/j.renene.2019.04.065.

Wood, L.J., Fish, L., Laughen, J. and Pauly, D. (2008) 'Assessing progress towards global marine protection targets: shortfalls in information and action', *Oryx,* 42, pp. 340-351.

Wood, S.N., 2006. Generalized Additive Models – An Introduction with R. Chapman & Hall/CRC.

Woodson, C.B. (2018) 'The Fate and Impact of Internal waves in Nearshore Ecosystems', *Annu. Rev. Mar. Sci*, 10, pp. 421-441.

Woodson, C.B. and McManus, M.A. (2007) 'Foraging behaviour can influence dispersal of marine organisms', *Limnology and Oceanography*, 52(6), pp. 2701-2709.

Worm, B., Lotze, H.K. and Myers, R.A. (2003) 'Predator diversity hotspots in the blue ocean', *Proceedings of the National Academy of Sciences of the United States of America*, 100(17), pp. 9884–9888. Available at: https://doi.org/10.1073/pnas.1333941100.

WWF (2020) *Unregulated fishing on the high seas of the Indian Ocean*. Available at: https://wwfeu.awsassets.panda.org/downloads/wwftmt_unregulated_fishing_on_the_high_seas_of_the_indian_ocean_2020.pdf (Accessed: 17 August 2023).

Wyatt, A.S.J., Leichter, J.J., Toth, L.T., Miyajima, T., Aronson, R.B. and Nagata, T. (2019) 'Heat accumulation on coral reefs mitigated by internal waves', *Nat. Geosci.,* 13, pp. 28–34.

Wyrtki, K. (1973) 'An equatorial jet in the Indian Ocean', *Science*, 181, pp. 262–264.

Yang, C., Xu, D., Chen, Z., Wang, J., Xu, M. and Yuan, Y. (2019) 'Diel vertical migration of zooplankton and micronekton on the northern slope of the South China Sea observed by a moored ADCP', *Deep-Sea Research Part II,* 167, pp. 93-104.

Yang, C.H., Liao, G.H., Yuan, Y.C., Chen, H. and Zhu, X.H. (2013) 'The diel vertical migration of sound scatterers observed by an acoustic Doppler current profiler in the Luzon Strait from July 2009 to April 2011', *Acta Oceanologica Sinica*, 32(11), pp. 1–9.

Yesaki, M. (1979) 'Rainbow Runner: A Latent Oceanic Resource?', *Marine Fisheries Review,* 8, pp. 1-6.

Yesson, C., Clark, M.R., Taylor, M.L. and Rogers, A.D. (2011) 'The global distribution of seamounts based on 30 arc seconds bathymetry data', *Deep-Sea Research I*, 58(4), pp. 442-453. Available at: 10.1016/j.dsr.2011.02.004.

Yesson, C., Letessier, T.B., Nimmo-Smith, A., Hosegood, P.J., Brierley, A.S., Harouin, M. and Proud, R. (2020) 'Improved bathymetry leads to 4000 new seamount predictions in the global ocean', *UCL Open: Environment*, Preprint(June), pp. 1–12. Available at: https://doi.org/10.14324/111.444/000044.v1.

Young, J.W., Hunt, B.P.V., Cook, T.R., Llopiz, J.K., Hazen, E.L., Pethybridge, H.R., Ceccarelli, D., Lorrain, A., Olson, R.J., Allain, V., Menkes, C., Patterson, T., Nicol, S., Lehodey, P., Kloser, R.J., Arrizabalaga, H. and Anela Choy, C. (2015) 'The trophodynamics of marine top predators: Current knowledge, recent advances and challenges', *Deep-Sea Research Part II: Topical Studies in Oceanography*, 113, pp. 170–187. Available at: https://doi.org/10.1016/j.dsr2.2014.05.015.

Zamon, J.E. (2003) 'Mixed species aggregations feeding upon herring and sandlance schools in a nearshore archipelago depend on flooding tidal currents', *Marine Ecology Progress Series*, 261(1), pp. 243–255. Available at: https://doi.org/10.3354/meps261243.

Zeng. C., Shao, L., Ricketts. A., and Moorhead, J. (2018) 'The importance of copepods as live feed for larval rearing of the green mandarin fish *Synchiropus splendidusl', Aquaculture,* 491, pp. 65-71.

Zhang, C. (1997) 'Intraseasonal variability of the upper-ocean thermal structure observed at 0◦ and 165◦E', *J. Clim*., 10, pp. 3077–3092.

Zhang, C. (2005) 'Madden-Julian Oscillation', *Reviews of Geophysics*, 43, pp. 1-36.

Zhang, L., Buijsman, M.C., Comino, E. and Swinney, H.L. (2017) 'Internal waves generation by tidal flow over periodically and randomly distributed seamounts', *Journal of Geophysical Research: Oceans*, 112, pp. 5063-5074.

Zhang, Y. and Du, Y. (2021) 'Extreme IOD induced tropical Indian Ocean warming in 2020', *Geoscience Letters*, 8(37). Available at: https://doi.org/10.1186/s40562-021-00207-6.

Zhang. H., Ludsin, S.A., Mason, D.M., Adamack, A.T., Brandt, S.B., Zhang, X., Kimmel, D.G., Roman, M.R., and Boicourt, W.C. (2009) 'Hypoxia-driven changes in the behaviour and spatial distribution of pelagic fish and mesozooplankton in the northern Gulf of Mexico', *J. Exp. Mar. Biol. Ecol,* 381, pp. 80-91.

Zuur, A. F., Ieno, E. N. and Elphick, C. S. (2010) 'A protocol for data exploration to avoid common statistical problems', *Methods in Ecology and Evolution*, 1(1), pp. 3–14. Available at: 10.1111/j.2041-210x.2009.00001.x.